



University
of Glasgow

Hurson, Catherine Eileen (2011) *Expression and function of the atypical chemokine receptor CCX-CKR*. PhD thesis

<http://theses.gla.ac.uk/2718/>

Copyright and moral rights for this thesis are retained by the author

A copy can be downloaded for personal non-commercial research or study, without prior permission or charge

This thesis cannot be reproduced or quoted extensively from without first obtaining permission in writing from the Author

The content must not be changed in any way or sold commercially in any format or medium without the formal permission of the Author

When referring to this work, full bibliographic details including the author, title, awarding institution and date of the thesis must be given.

**Expression and Function of the Atypical Chemokine
Receptor CCX-CKR**

Catherine Eileen Hurson

A thesis submitted to the College of Medicine, Veterinary and Life Sciences,
University of Glasgow in fulfillment of the requirements for the degree of
Doctor of Philosophy

June 2011

Institute of Infection, Immunity and Inflammation
University of Glasgow
120 University Place
Glasgow
G12 8TA

Summary

The ability to clear infections and repair injury is dependent on the coordinated migration of immune cells, or leukocytes. These cells can directly destroy invading pathogens and also produce a variety of bioactive factors that promote pathogen clearance. Interactions between immune cells occur both at the site of inflammation and in specialised lymphoid organs throughout the body. The efficiency and specificity of these interactions relies on the production of a family of molecules called **chemotactic cytokines**, or chemokines, that drive leukocyte migration. Cells express specific profiles of chemokine receptors to ensure they are directed to the appropriate location to exert their immunological function. The field of chemokine biology, already complex, has been further complicated by the discovery of a subfamily of receptors, the atypical chemokine receptors. These molecules lack the ability to couple to signal transduction pathways used by the other chemokine receptors, and are proposed to act as chemokine scavengers or transport molecules.

The atypical chemokine receptor CCX-CKR was discovered more than a decade ago but its function *in vivo* remains unclear. At the beginning of my project, information about this molecule was very limited. The murine receptor binds the CC chemokines CCL19, CCL21 and CCL25, which have well-characterised and critical roles in the development and homeostasis of the immune system as well as in the immune response to infection. Thus, identification of this new receptor, which unlike classical receptors does not induce cell migration in response to ligand binding, presented some exciting possibilities as to how these processes might be regulated *in vivo*. Reports describing the pattern of expression of CCX-CKR have thus far provided only limited and sometimes contradictory information. Additionally, while *in vitro* studies from our lab have provided some important clues as to the potential role of the receptor, published *in vivo* studies were, at the time of commencing this work, limited to one report describing an unvalidated EGFP reporter knock-in transgenic mouse and a conflicting online resource detailing data generated using a LacZ reporter mouse. To understand the true function of this molecule, it is critical to know where it is expressed *in vivo* and to explore its function on these cells. In this project I set out with the aim of identifying murine tissues and cells expressing CCX-CKR, as well as examining its potential as an *in vivo* scavenger of chemokine. Related to this, I hoped to uncover any impact of deletion of CCX-CKR on lymphoid tissue cellularity and/or function, both in resting and inflamed conditions.

In chapter 3, I present data that identify lymphoid tissues and “barrier” tissues as sites of robustly detectable CCX-CKR mRNA expression. I describe how I have established a

novel fluorescent chemokine tetramer-based protocol for the detection of CCL19 receptors, with emphasis on the application of this protocol to identify CCX-CKR activity on specific cell subsets. Using this method, I present evidence that some CD11b⁺ CD11c⁺ myeloid subsets in the inguinal lymph node exhibit CCX-CKR dependent internalisation of chemokine. I also describe attempts to fractionate tissues to identify cell populations responsible for the detected whole-tissue expression of CCX-CKR mRNA.

The results described in chapter 4 provide support for the hypothesis that CCX-CKR regulates levels of its ligands *in vivo*, with alterations in chemokine levels in serum and inguinal lymph nodes in the absence of CCX-CKR. I also present evidence demonstrating that deletion of the receptor can influence mRNA levels of the related receptor CCR7. Following on from this, chapter 5 details my analysis of the impact of CCX-CKR on the cellularity of various lymphoid compartments. I present evidence that CCX-CKR influences lymphocyte populations in the peritoneal cavity, with both innate-like and conventional lymphocytes significantly overrepresented in this compartment. The cellularity of the inguinal lymph node, but not the spleen, is subtly altered by deletion of the receptor. Splenic leukocyte cellularity is not affected, either in number or in localisation.

In chapter 6, I turn my attention to the possible role of CCX-CKR during the inflammatory response by examining various experimental parameters during a short-term model of induced cutaneous inflammation. This study shows that CCX-CKR deletion alters the cellularity of the myeloid compartment in the draining lymph node and again highlights myeloid subsets as displaying CCX-CKR dependent chemokine internalisation. Finally, I present preliminary data suggesting a protective effect of CCX-CKR deletion during a long-term model of inflammation-driven tumorigenesis.

Taken together, my data provide tentative support for the theory that CCX-CKR acts as a chemokine scavenger *in vivo*. They further indicate that CCX-CKR is involved in regulating cellularity of various lymphoid compartments both at rest and during induced inflammation. In chapter 7 I discuss in detail the implications of my findings in the context of work published since my project began, and highlight growing evidence to suggest a role for CCX-CKR in regulating immune function.

Table of Contents

Summary	2
Table of Contents	4
List of Tables and Figures.....	8
Acknowledgements	12
Author's Declaration.....	15
Abbreviations	16
1 Introduction	27
1.1 General Introduction	27
1.2 The immune response	27
1.3 Lymphoid tissue – development, structure and function	30
1.3.1 Primary lymphoid organs.....	31
1.3.2 Secondary lymphoid tissue	32
1.4 Chemokines.....	44
1.4.1 Systematic nomenclature	44
1.4.2 Chemokine function in vivo.....	46
1.5 Chemokine receptors.....	49
1.5.1 Signalling through GPCRs.....	50
1.5.2 Internalisation and desensitisation of chemokine receptors.....	52
1.5.3 Chemokine/receptor interactions	54
1.6 Identification and early characterisation of CCR7, CCR9 and their ligands	55
1.6.1 CCR7 identification and expression	56
1.6.2 CCL19 and CCL21 – identification, expression and interaction with CCR7 ..57	
1.6.3 Lacking CCR7 ligands – <i>plt/plt</i> mice.....	61
1.6.4 CCR9 and CCL25	62
1.7 CCR7 and CCR9 in immune system development and function.....	63
1.7.1 Thymocyte development.....	63
1.7.2 Lymphocyte migration to, within and from lymph nodes	68
1.7.3 DC migration to lymph nodes.....	73
1.7.4 Leukocyte homing to the small intestine	75
1.8 Atypical chemokine receptors.....	78
1.8.1 DARC.....	79
1.8.2 D6.....	82
1.8.3 CXCR7.....	87
1.8.4 CCRL2	89

1.8.5	Identification and preliminary characterisation of CCX-CKR	90
2	Materials and Methods	95
2.1	Animals	95
2.2	Genotyping	95
2.3	Isolation of cells from primary tissue	97
2.4	Antibodies and chemokines	98
2.5	Uptake and binding assays	99
2.6	Competition assays	99
2.7	Antibody staining	99
2.8	Flow cytometry	100
2.9	Cell sorting using the FACS Aria	100
2.10	Isolation of RNA from whole tissues	100
2.11	Isolation of RNA from single cell suspensions	101
2.12	DNase treatment of RNA	101
2.13	Synthesis of cDNA from RNA	101
2.14	Measuring relative mRNA expression by quantitative polymerase chain reaction (QPCR)	102
2.15	Preparing samples for chemokine measurement	103
2.16	Measuring chemokine concentrations by Enzyme-linked Immunosorbent Assays (ELISAs)	103
2.17	Embedding tissues for sectioning	104
2.18	Haemotoxylin and eosin staining	104
2.19	Immunofluorescent staining of frozen sections	105
2.20	Induction of skin inflammation	105
2.21	Tumorigenesis	106
2.22	Statistical analysis	106
3	Expression and activity of CCX-CKR in resting mice	107
3.1	Quantifying expression of CCX-CKR mRNA in whole tissue	107
3.2	Towards the identification of cells expressing functional CCX-CKR	109
3.2.1	Optimisation of an assay for detecting CCL19 receptor “activity”	109
3.2.2	Investigating CCX-CKR expression in the spleen	112
3.2.3	Searching for CCX-CKR expressing cells in inguinal lymph nodes	117
3.2.4	Investigating CCL19 tetramer internalisation by leukocytes in other compartments – analysis of whole blood and peritoneal lavage	119

3.3	Attempts to identify cells expressing CCX-CKR mRNA in the spleen by cell fractionation	120
3.4	Summary	122
4	Effect of CCX-CKR deletion on expression of its ligands and related receptors	146
4.1	Expression of CCR7 and CCR9 mRNA in the CCX-CKR deficient mouse	146
4.1.1	Expression of CCR7 by peritoneal cavity lavage cells is increased in the absence of CCX-CKR	148
4.2	The impact of CCX-CKR deletion on ligand expression and availability	149
4.2.1	Dysregulation of CCL19 protein in CCX-CKR deficient mice	150
4.2.2	Subtle alterations in CCL21 protein levels in CCX-CKR deficient mice	150
4.2.3	Expression of CCL19 and CCL25 mRNA	151
4.3	Summary	152
5	Effect of CCX-CKR deletion on cellularity, cell distribution and microarchitecture of resting secondary lymphoid tissues	169
5.1	Cellularity in the spleen	170
5.2	Microarchitecture of the CCX-CKR deficient spleen	170
5.3	Cellularity in the inguinal lymph nodes	171
5.4	Deletion of CCX-CKR increases lymphocyte abundance in the peritoneal cavity	172
5.5	Summary	173
6	Effect of CCX-CKR deletion on the inflammatory response.....	186
6.1	CCX-CKR in a model of cutaneous inflammation	187
6.1.1	Histology of wild-type and CCX-CKR deficient inflamed skin	187
6.1.2	Expression of CCX-CKR and related receptors in inflamed skin	188
6.1.3	No impact of CCX-CKR deletion on the draining lymph node cellularity during skin inflammation	189
6.2	CCX-CKR in a model of tumour formation	192
6.3	Summary	193
7	Discussion.....	210
7.1	Introduction	210
7.2	Expression of CCX-CKR in resting tissues	210
7.2.1	Detecting CCL19 receptors with CCL19 tetramers	211

7.2.2	Which cells express CCX-CKR in lymphoid tissues?	213
7.3	CCX-CKR influences the expression and activity of CCR7 in resting tissues.....	216
7.4	Regulation of chemokine levels in resting tissue by CCX-CKR	220
7.5	CCX-CKR influences lymph node and peritoneal cavity cellularity.....	223
7.6	CCX-CKR during the induction of cutaneous inflammation.....	225
7.7	CCX-CKR influences papilloma development during a model of inflammation- driven tumorigenesis	228
7.8	Conclusions and future directions.....	230
8	References	233

List of Tables and Figures

Chapter 1

Table 1.1: Systematic nomenclature for chemokines	45
Figure 1.1: Lymph node development	35
Figure 1.2: Structure of a lymph node	38
Figure 1.3: Lymphocyte extravasation into lymph nodes.....	39
Figure 1.4: Structure of the spleen	42
Figure 1.5: Receptor-ligand binding leads to G protein activation and downstream signalling events.....	51
Figure 1.6: CCR7 and CCR9 in thymocyte development.....	65
Figure 1.7: Chemokine-dependent lymph node organisation	73
Figure 1.8: Proposed activity of erythrocyte DARC as a buffering system for blood-borne chemokine	80

Chapter 2

Table 2.1: Primers used for genotyping	95
Table 2.2: List of fluorescently labelled antibodies used in the experiments described in this thesis.....	98
Table 2.3: Taqman® probes used for QPCR assays.....	102
Figure 2.1: Genotyping wild-type and CCX-CKR deficient mice.....	97

Chapter 3

Figure 3.1: Detection of CCX-CKR mRNA expression using a Taqman® Gene Expression Assay.....	124
Figure 3.2: Detection of CCX-CKR mRNA expression in whole tissue.....	125
Figure 3.3: Designing an assay to detect CCL19 receptors using fluorescent CCL19 tetramers.....	126
Figure 3.4: Optimisation of internalisation assay conditions.....	127
Figure 3.5: Binding and internalisation of fluorescent CCL19 tetramers is significantly reduced in the presence of CCR7 ligands	128
Figure 3.6: T and B cells in the spleen do not exhibit CCX-CKR-dependent internalisation of fluorescent CCL19 tetramers	129
Figure 3.7: Pre-incubation or co-incubation with unlabelled CCL19 does not lead to detectable CCX-CKR-dependent internalisation of fluorescent CCL19 tetramers in splenic T and B cells	130

Figure 3.8: B1 cells and marginal zone B cells in the spleen do not exhibit CCX-CKR-dependent internalisation of CCL19	131
Figure 3.9: Gating strategy to identify myeloid cells in the spleen	132
Figure 3.10: Myeloid cells in the spleen do not exhibit CCX-CKR-dependent CCL19 internalisation.....	133
Figure 3.11: Pre-incubation or co-incubation with unlabelled CCL19 does not lead to detectable CCX-CKR-dependent internalisation of fluorescent CCL19 in splenic myeloid cells	134
Figure 3.12: CD45 ⁺ and CD45 ⁻ cells in the spleen do not exhibit CCX-CKR-dependent internalisation of CCL19 with or without pre- or co-incubation with excess unlabelled CCL19	135
Figure 3.13: T and B cells in the inguinal lymph nodes do not exhibit CCX-CKR-dependent internalisation of CCL19	136
Figure 3.14: Myeloid cells within the inguinal lymph node exhibit some CCX-CKR dependent internalisation of CCL19	137
Figure 3.15: CD45 ⁻ cells in the inguinal lymph node do not exhibit CCX-CKR-dependent internalisation of CCL19.....	138
Figure 3.16: T and B cells in the blood do not exhibit CCX-CKR-dependent internalisation of CCL19.....	139
Figure 3.17: Gating of peritoneal cavity lavage cells	140
Figure 3.18: Cells isolated from peritoneal lavage do not exhibit CCX-CKR-dependent internalisation of fluorescent CCL19	141
Figure 3.19: Gating strategy for sorting cells from the spleen.....	142
Figure 3.20: Expression of CCX-CKR mRNA by sorted CD45 ⁺ cells in the spleen	143
Figure 3.21: Expression of CCX-CKR and CCR7 mRNA in disrupted spleen.....	145

Chapter 4

Figure 4.1: Expression of CCR7 mRNA in wild-type and CCX-CKR deficient lymph nodes, spleen, thymus and Peyer's patches.....	153
Figure 4.2: Expression of CCR7 mRNA in wild-type and CCX-CKR deficient skin and small intestine	154
Figure 4.3: Expression of CCR9 mRNA in wild-type and CCX-CKR deficient lymph nodes, spleen and thymus.....	155
Figure 4.4: Expression of CCR9 mRNA in wild-type and CCX-CKR deficient skin, liver, Peyer's patches and small intestine.....	156

Figure 4.5: Expression of CCR7 mRNA in wild-type and CCX-CKR deficient peritoneal lavage cells	157
Figure 4.6: Expression of CCR9 mRNA in wild-type and CCX-CKR deficient peritoneal lavage cells	158
Figure 4.7: CCL19 protein levels in wild-type and CCX-CKR deficient lymph nodes, spleen and thymus	159
Figure 4.8: CCL19 protein in wild-type and CCX-CKR deficient serum and peritoneal cavity lavage	160
Figure 4.9: CCL19 protein levels in wild-type and CCX-CKR deficient kidney, skin, brain and heart	161
Figure 4.10 CCL21 protein in wild-type and CCX-CKR deficient serum and peritoneal cavity lavage	162
Figure 4.11: CCL21 protein levels in wild-type and CCX-CKR deficient lymph nodes, spleen and thymus	163
Figure 4.12: CCL21 protein levels in wild-type and CCX-CKR deficient kidney, skin, brain and heart	164
Figure 4.13: Expression of CCL19 mRNA in wild-type and CCX-CKR deficient lymph nodes, spleen and thymus	165
Figure 4.14: Expression of CCL19 mRNA in wild-type and CCX-CKR deficient skin, liver, Peyer's patches and small intestine	166
Figure 4.15: Expression of CCL25 mRNA in wild-type and CCX-CKR deficient lymph nodes, spleen and thymus	167
Figure 4.16: Expression of CCL25 mRNA in wild-type and CCX-CKR deficient skin, liver, Peyer's patches and small intestine	168

Chapter 5

Figure 5.1: Total cell numbers retrieved from wild-type and CCX-CKR deficient spleens	174
Figure 5.2: B and T cell cellularity in the spleen	175
Figure 5.3: Proportions and numbers of B1 and marginal zone B cells in the spleen	176
Figure 5.4: Proportions and numbers of myeloid cells in the spleen	177
Figure 5.5: Area of white pulp in wild-type and CCX-CKR deficient spleens	178
Figure 5.6: Immunofluorescent staining of B and T cells in wild-type and CCX-CKR deficient spleen	179
Figure 5.7: Total cell numbers retrieved from wild-type and CCX-CKR deficient inguinal lymph nodes	180

Figure 5.8: Proportions and numbers of myeloid cells in the inguinal lymph nodes	181
Figure 5.9: B and T cell cellularity in the inguinal lymph nodes.....	182
Figure 5.10: Total cell numbers retrieved from wild-type and CCX-CKR deficient peritoneal cavity lavage	183
Figure 5.11: B and T cell cellularity in the peritoneal cavity	184
Figure 5.12: Macrophage cellularity in the peritoneal cavity	185
 Chapter 6	
Figure 6.1: Induction of skin inflammation	195
Figure 6.2: Epidermal thickness of wild-type and CCX-CKR deficient skin during TPA- induced inflammation	196
Figure 6.3: Expression of CCX-CKR in the skin during TPA-induced inflammation	197
Figure 6.4: Expression of CCR7 and CCR9 in the skin during TPA-induced inflammation	198
Figure 6.5: Total numbers retrieved from wild-type and CCX-CKR deficient draining inguinal lymph nodes during a model of skin inflammation	199
Figure 6.6: Expression of CCX-CKR in the inguinal lymph node during TPA-induced inflammation	200
Figure 6.7: Expression of CCR7 and CCR9 in the draining inguinal lymph node during TPA-induced inflammation.....	201
Figure 6.8: Proportions and numbers of B and T cells in the draining inguinal lymph node during a model of skin inflammation.....	202
Figure 6.9: Internalisation of CCL19 by wild-type and CCX-CKR deficient T and B cells in the draining lymph node in a model of skin inflammation.....	203
Figure 6.10: Proportions and numbers of myeloid cell subsets in the draining inguinal lymph node during a model of skin inflammation.....	204
Figure 6.11: Internalisation of fluorescent CCL19 by myeloid cells in the draining lymph node in a model of skin inflammation	205
Figure 6.12: Development of papillomas by wild-type and CCX-CKR deficient mice during a model of tumourigenesis.....	206
Figure 6.13: Expression of CCX-CKR in papillomas and normal adjacent skin during a model of tumourigenesis.....	207
Figure 6.14: Expression of CCR7 in papillomas and normal adjacent skin during a model of tumourigenesis	208
Figure 6.15: CCX-CKR deficient mice exhibit reduced inguinal lymph node size compared to WT following DMBA/TPA-induced papilloma formation	209

Acknowledgements

I must firstly thank my supervisor, Rob Nibbs, for his support and advice over the last few years. This thesis would not have been possible without it, so thank you. I'm really glad you persuaded me to turn to the "dark side" and do an immunology project!

I think I can honestly say through all the ups and downs, scientific and otherwise, I have never regretted the decision to embark on a PhD (or not much anyway!). This is almost entirely due to the people I've met along the way. The members, past and present, of the Nibbs group have made for a fantastic workplace, ably assisted by CRG, the rest of Level 3 and the inhabitants of Level 4. There were always plenty of people ready and willing to give advice, lend reagents, steal reagents, have a laugh, have an impromptu dance, have a cuppa, make cakes, "decorate" benches, go for a drink or generally have the craic. So thank you all, there are too many to name but you have all been fabulous in your own unique ways!

Special thanks must go to a few though, for fear of retribution. Cat and Claire, the other members of the 3Cs (a flowery pink wine appreciation society), and Elinor, my CCX-CKR partner in crime and recent lab neighbour – I would not have made it through everything in and especially outside of the lab without you. I love the three of you, more than wine, *and* potatoes! ☺ Chris, my mentor/friend/lab big brother – well done for putting up with me for so long, you get a star ★ ! Thanks for making me keep going during my first, ridiculously ambitious, experiment back at the start of my placement, and for continuing that theme throughout my time here. Rossatron and MairiClarke MairiClarke (nee Proven), my other most recent bay buddies (although MC has been there from the start!), as well as Jude and medic Laura, my original bay buddies – thanks for letting me play my (questionable) music and for putting up with all the greenery on/around Paddys Day (special thanks to our resident Gerbil for his patience with this!); You have made my time here so much fun, and managed to make work a good place to be, even when science had other ideas. Everyone in the Nibbs empire (including Rae, student Laura, Steven, Darren, Fiona, Joo, placement, masters and undergrad students (particularly Steph), those already mentioned, and anyone I've forgotten!) - thanks for putting up with my dictatorial tendencies and generally for being a good laugh and excellent workmates and friends. Honourable mention goes to Debs for dealing very well with having a mentaller as a deskmate for the last few months, Laura and Cat for not getting too pissed off that I was a permanent fixture in the office, and to KJP and Anne Donachie for excellent hugs and tea (Kenny) or booze (Anne) as required. The Aussies have a lot to live up to!

For science-related help/advice/support, there are also a variety of people who must be thanked (in no particular order, for I am not that organized, and without detail, because it becomes a novella otherwise...). My heartfelt thanks to: Elinor Anderson; Mairi Clarke; Tottenham HotsBurt; KP Dallas; Cath Wilson; Chris Hansell; Derek Gilchrist; Clare McCulloch; Ashley Gilmour; Prof Bainer and the rest of the Mowats; Colin Nixon at the Vet school; Ian Montgomery; Jim Reilly; all the staff in the CRF and JRF, but particularly Joanne Battersby; Darren and Tim, my other placement supervisors; various PIs in the department for teaching me (or trying to!) about basic immunology (especially Allan) and stats (Carl!) and answering my many many questions with patience and clarity; and everyone else I have inevitably forgotten to mention, who gave me advice, trained me in techniques, helped me troubleshoot, lent me reagents and generally made my life so much easier than it would otherwise have been! A special word of thanks goes to the Wellcome Trust, especially Bill, Darren and Olwyn, for their fantastic support throughout my PhD, and particularly in my second year. I must also especially thank Elinor, Chris and Ross for reading large chunks of my thesis and helping make it better (especially Elinor – who is getting as many mentions as I can fit in as a token of my gratitude!).

Finally, for getting me to the point where my doing a PhD was even possible! First, thanks to my family, especially my mum and dad, Mary and Pat, and all my siblings and siblings-in-law, and a special thanks to Luke, for being the cutest nephew in the world! ☺ I love you all.

To Aoife, for supporting me, making me laugh, comforting me, getting drunk with me, talking crap with me, being the best friend anyone could ask for and making it feel like we've not been apart at all even though we live in different countries. You even proofread my results chapters you nutter. Thanks too to Alan for keeping her entertained in my absence ;) To Sparky, Caroline, Jacqueline, Eileen and everyone else for getting me through uni and beyond and still being friends with me! ☺ Thanks to you all, I love you too!

To the Hughes family (including the Estibeiro, Wills and McGregor sections!), for taking me into your lives (and home!) so readily and so happily, for all the support and love you've shown, and for giving me Dave – thank you, I love you all too.

An extra special massively huge thank you and tons of love is reserved for Julie and Donal Larkin, for opening their home to me and making me a part of their family, for giving me a roof over my head for the last couple of years of my undergrad and for always making me

feel welcome. In particular to Julie, for pseudo-adopting me, making me get through my exams, making me do the very best I could, being the major reason I got the PhD place I got – so many things. I cannot begin to express how grateful I am. Thank you, so much.

Last, but by no means least, thanks to my husband (!), David Hughes. You have been so patient, supportive, funny, comforting, adorable, understanding – everything I could ever want. I can't believe I am lucky enough to have you as mine. It is unfortunate but I suppose necessary that you are clearly mental... ☺ I love you most of all.

(Elinor, what one word would you use to sum this up...?)

Author's Declaration

I declare that, except where explicit reference is made to the contribution of others, this thesis is the result of my own work and has not been submitted for any other degree at the University of Glasgow or any other institution.

Signature:

Printed name:

Abbreviations

The following abbreviations are used throughout this thesis:

AIRE	autoimmune regulator
ANOVA	analysis of variance
AP-2	adaptor protein 2
APC	allophycocyanin
APCs	antigen-presenting cells
BCR	B cell receptor
Bio	biotinylated
BM	bone marrow
BMECs	bone marrow sinusoidal endothelial cells
bp	base pair
cAMP	cyclic adenosine monophosphate
CCL	CC chemokine ligand
CCR	CC chemokine receptor
CCRL2	CC chemokine receptor-like 2
CCX-CKR	ChemoCentryx chemokine receptor
CD	cluster of differentiation
cDNA	complementary DNA
CFA	complete Freund's adjuvant

CHO	Chinese hamster ovary
CMJ	cortico-medullary junction
CMKLR-1	chemokine-like receptor 1
CRAM	chemokine receptor on activated macrophages
Ct	threshold cycle
C-terminal	carboxy terminal
CXCL	CXC chemokine ligand
CXCR	CXC chemokine receptor
CX ₃ CL	CX ₃ C chemokine ligand
CX ₃ CR	CX ₃ C chemokine receptor
Cys	cysteine
DAG	diacyl glycerol
DAMPs	danger-associated molecular patterns
DARC	Duffy antigen/receptor for chemokines
°C	degrees Celsius
DC	dendritic cell
DMBA	7,12-Dimethylbenz(a)anthracene
DN	double negative
DNA	deoxyribonucleic acid
DP	double positive

DPBS	D ulbecco's p hosphate b uffered s aline
DTH	d elayed t ype h ypersensitivity
E	e mbyronic d ay
EAE	e xperimental a utoimmune e ncephalitis
EBI1	E pstein- B arr virus i nduced r eceptor- 1 (CCR7)
EBV	E pstein- B arr virus
<i>E. coli</i>	<i>Escherichia coli</i>
EDTA	e thylene d iamine t etra a cetic a cid
e.g.	<i>exempli gratia</i>
EGFP	e nhanced G FP
ELC	E BI1- l igand c hemokine (CCL19)
ERK	e xtracellular- s ignal r egulated k inase
EST	e xpressed s equence t ag
FACS	f luorescence a ctivated c ell s orting
FAE	f ollicle- a ssociated e pithelium
FCS	f oetal c alf s erum
FDCs	f ollicular d endritic c ells
FITC	f luorescein i sothiocy a nate
FLT3	F ms- l ike T yrosine k inase 3
FLT3L	FLT3 - l igand

FRC	f ibroblastic r eticular c ell
FRET	f luorescence r esonance e nergy t ransfer
FSC	f orward s catter
GAG	g lycosaminoglycan
GAPDH	G lyceraldehyde 3- p hosphate d ehydrogenase
GC	g erminal c entre
GDP	g uanosine d iphosphate
GFP	g reen f luorescent p rotein
Glu	g lutamic acid
gMFI	g eometric m ean f luorescence i ntensity
GPCR	G -protein coupled r eceptor
GPR-9-6	G -protein coupled r eceptor 9-6 (CCR9)
GRK	G -protein coupled r eceptor k inase
GTP	g uanosine t riphosphate
h	h uman
HA	h aemagglutinin
HBSS	H anks B alanced S alt S olution
HEC	h igh e ndothelial c ell
HEK	h uman e mbryonic k idney
HEPES	4-(2- h ydroxyethyl)-1- p iperazineethanesulfonic acid

het	heterozygous
HEV	high endothelial venule
hi	high
HSCs	Haematopoietic stem cells
HSV	Herpes simplex virus
HVEM	Herpes virus entry mediator
ICAM	intercellular adhesion molecule
IC ₅₀	half-maximal inhibitory concentration
ID2	inhibitor of DNA binding 2
i.e.	<i>id est</i>
IFN	interferon
Ig	immunoglobulin
IL	interleukin
ILF	isolated lymphoid follicle
ILN	inguinal lymph node
int	intermediate
IP3	inositol triphosphate
JAK	Janus kinase
KO	knock-out
LC	Langerhans cell

Leu	leucine
LFA1	leukocyte function-associated antigen 1
LIGHT	homologous to lymphotoxins , exhibits inducible expression, and competes with HSV glycoprotein D for HVEM , a receptor expressed by T lymphocytes
LN	lymph node
LPCs	Lymphoid progenitor cells
LPS	lipopolysaccharide
LT	lymphotoxin
LT β R	LTβ receptor
LTi	lymphoid tissue inducer
m	mouse
MACS	magnetic activated cell sorting
MAdCAM1	mucosal addressin cell adhesion molecule 1
MALT	mucosa-associated lymphoid tissue
MAP	mitogen activated protein
M cells	microfold cells
MDCK	Madin-Darbin canine kidney
med	medium
MIP-3 β	macrophage inflammatory protein-3β (CCL19)
μ g	microgram

μl	microlitre
μM	micromolar
MGB	minor groove binder
MHC	major histocompatibility complex
mL	millilitre
MLN	mesenteric lymph node
mM	millimolar
MMP	matrix metalloproteinase
mRNA	messenger RNA
MZ	marginal zone
NaCl	sodium chloride
NETs	neutrophil extracellular traps
NF	nuclear factor
NFQ	non-fluorescent quencher
ng	nanogram
NK cells	natural killer cells
NK T cells	CD1d-restricted natural killer-like T cells
nM	nanomolar
NTC	no template control
ORF	open reading frame

OVA	ovalbumin
p	probability
PALS	periarteriolar lymphoid sheath
PAMPs	pathogen-associated molecular patterns
PC	phosphorylcholine
PCR	polymerase chain reaction
pDC	plasmacytoid DC
PE	phycoerythrin
PerCP	peridinin-chlorophyll-protein
pers. comm.	Personal communication
PGC	primordial germ cell
PIP2	phosphatidylinositol biphosphate
PI3K	phosphatidylinositol-3-kinase
PKA	protein kinase A
PKC	protein kinase C
<i>P. knowlesi</i>	<i>Plasmodium knowlesi</i>
PLN	peripheral lymph node
<i>plt</i>	paucity of lymph node T cells
PNAd	peripheral node addressin
PP	Peyer's patch

PRR	p attern r ecognition r eceptors
Ptx	p ertussis t oxin
QPCR	q uantitative P CR
RA	r etinoic a cid
RALDH	r etinal d ehydrogenase
RET	r earranged during t ransfection
RNA	r ibonucleic a cid
ROR γ t	r etinoic acid-related o rphan r eceptor- γ t
RPMI	R oswell P ark M emorial I nstitute
RQ	r elative q uantity
RT	r everse t ranscriptase
RT-PCR	r everse t ranscriptase p olymerase c hain r eaction
SCC	s quamous cell c arcinoma
SCM	s ubcapsular m acrophage
SCS	s ubcapsular s inus
SCZ	s ubcapsular z one
SD	s tandard d evelopment
SDF-1	s tromal d erived f actor- 1
SDS	s odium d odecyl sulphate
SED	s ubepithelial d ome

SEM	standard error of the mean
Ser	serine
siRNA	small interfering RNA
SLC	secondary lymphoid tissue chemokine (CCL21)
SLE	systemic lupus erythematosus
SP	single positive
S1P	sphingosine-1-phosphate
S1P ₁	S1P receptor 1
SSC	side scatter
STAT	signal transducer and activator of transcription
Str	streptavidin
TCA-4	thymus-derived chemotactic agent-4 (CCL21)
T _{CM}	central memory T
TCR	T cell receptor
TECK	thymus expressed chemokine
T _{EM}	effector memory T
T _{FH}	T follicular helper
T _H	T helper
TNF	tumour necrosis factor
TNFR	TNF receptor

TPA	12- <i>O</i> -tetradecanoylphorbol-13-acetate
TRAF6	TNF-receptor-associated factor 6
TRANCE	TNF-related activation induced cytokine
TRANCER	TRANCE receptor
T _{reg}	regulatory T
Tyr	tyrosine
U	units
VCAM1	vascular cell adhesion molecule 1
VEGF	vascular endothelial growth factor
WT	wild-type
XCL	XC chemokine ligand
XCR	XC chemokine receptor
x g	times gravity
XLA	X-linked agammaglobulinemia

1 Introduction

1.1 General Introduction

Throughout life, animals are constantly challenged by invaders that can parasitize or overwhelm the host in their quest for a niche to flourish within. At the same time, there are a myriad of injuries to be repaired as well as dying or dysregulated cells to be removed or developing cancerous growths to be eliminated. The host must be able to clear dead cells, repair injury, remove tumours and combat infection to remain healthy and fully functional. The ability to survive these numerous challenges requires a fully functional immune system, a complex and highly organised system of cells and organs that has evolved over time to protect the host from invasion and repair injury. Physical barriers, such as the skin and mucosa, protect the body from initial injury and infection, while mechanical reflexes like sneezing and coughing further prevent foreign organisms from adhering to and colonising the host, thereby hampering the development and spread of infection. In addition to these basic defences, the mammalian immune system has evolved to allow both immediate, low-specificity responses to invasion or injury (innate immunity) and longer term, highly specific responses to infection by foreign organisms (adaptive/acquired immunity). These adaptations allow eradication of infectious agents that circumvent the initial barriers, and then help facilitate the repair of tissue damage to the host. However, although it provides invaluable protection, the immune system has inherent flaws that can, under some circumstances, lead to pathology and even fatality. Allergic reactions, autoimmune diseases (like systemic lupus erythematosus (SLE)) and immunodeficiency syndromes (e.g. X-linked agammaglobulinemia (XLA)) are the result of dysregulated immune responses or defective or disrupted development of the immune system (Chan et al., 1999, Conley et al., 1994, Finkelman, 2010, Murphy et al., 2010). Thus, tight regulation of the immune response is critical to ensure the survival and continuing health of the host.

1.2 The immune response

The effectiveness of the immune system lies in its multifaceted approach to combating infection. By employing both the rapid but transient innate response and the slower but long-lasting adaptive response, and by linking these together through a variety of “innate-like” leukocytes and direct interaction between “innate” and “adaptive” cells, the ability to respond to infection and provide long-term protection against re-infection is

comprehensive and efficient. Indeed, there is considerable overlap between the two arms, and many cells make important contributions to both.

The rapid influx of immune cells to the site of infection that typifies the innate immune response contributes to the classic hallmarks of inflammation; *calor, dolor, rubor et tumor* (heat, pain, redness and swelling). Recognition of pathogens by inflammatory cells occurs via pattern recognition receptors (PRRs), which recognise damage- or pathogen-associated molecular patterns (DAMPs or PAMPs, respectively). Upon recognition of an invading pathogen, tissue-resident macrophages secrete cytokines and other inflammatory mediators that precipitate the rapid accumulation of innate immune cells in the infected tissue. Some of the mediators released trigger vasodilation, i.e. an increase in the diameter of surrounding blood vessels, thereby increasing the number of leukocytes in the area. The slowing of blood flow caused by blood vessel dilation, in combination with the induction of expression of adhesion molecules by endothelial cells lining the blood vessels, allows leukocytes to exit circulation and enter the infected tissue (Murphy et al., 2010). Of particular interest to this thesis are the subfamily of cytokines that induce the directed migration of leukocytes, in this case into the infected tissue. These **chemotactic cytokines**, or chemokines, comprise an extensive family of ligands that are recognised by receptors on the surface of leukocytes and trigger their migration towards the source of the chemokine.

At the site of infection various cells, both leukocytic and non-leukocytic, secrete an array of chemokines that attract an initial wave of neutrophils, closely followed by monocytes that rapidly differentiate into macrophages and DCs, with other immune cells also arriving at later stages of infection (Murphy et al., 2010). Neutrophils are highly phagocytic and granular, producing a range of antimicrobial molecules as well as various inflammatory mediators that promote recruitment of other leukocytes to the site of infection. They also produce “neutrophil extracellular traps” (NETs), which comprise extracellular fibres composed of granule proteins and chromatin that bind, neutralise and kill bacteria within the infected tissue (Brinkmann et al., 2004, Soehnlein and Lindbom, 2010). Neutrophils are typically short-lived in circulation, although cytokines produced by endothelial cells at the site of inflammation can promote their survival (Coxon et al., 1999). Cytokines produced by these cells also contribute to the activation of recruited macrophages and DCs at the inflamed site and can influence the programming of macrophages towards a pro- or anti-inflammatory phenotype depending on context (Bennouna et al., 2003, Nathan, 2006). Macrophages, too, are highly phagocytic, engulfing invading microbes and destroying them, as well as clearing dead neutrophils from the site of inflammation. They can produce a variety of bactericidal molecules, in addition to production of chemokines and other

inflammatory mediators. They can also present antigen to T cells, albeit less efficiently than DCs, thereby providing a link between innate and adaptive responses (Kalupahana et al., 2005, Murphy et al., 2010). Other granulocytes, such as eosinophils, are also involved in release of microbicidal products and clearance of infection, and are recruited in the later stages of the inflammatory response (Murphy et al., 2010).

These initial stages, characterised by vasodilation and increased “leakiness” of blood vessels, recruitment of phagocytic and granular cells, and production of anti-microbial factors, provide instant, non-specific protection against infection by pathogens. The involvement of “innate-like” lymphocytes is believed to span the period between this initial burst of activity and the subsequent, more specific adaptive response. (Bendelac et al., 2001, Lopes-Carvalho and Kearney, 2004). These “innate-like” cells, which are poorly understood but coming under increasing scrutiny, include $\gamma\delta$ T cells, CD1d-restricted natural killer-like T cells (NK T cells), B1 B cells and marginal zone (MZ) B cells. Like the archetypal innate cells described above, these innate-like lymphocytes recognise conserved patterns rather than the practically endless array of specific antigens recognised by “classical” lymphocytes, with their highly restricted T cell receptor (TCR) and B cell receptor (BCR) repertoires. Innate-like lymphocytes are typically resident in peripheral tissues, unlike classical lymphocytes that are normally found in lymph nodes and in circulation, and have specialised functions including secretion of natural antibody (in the case of innate-like B cells) and production of inflammatory cytokines (Bendelac et al., 2001). Some innate-like lymphocytes have been shown to act as antigen presenting cells (APCs), strengthening their claim to act as a link to the adaptive response (Brandes et al., 2009, Brandes et al., 2005).

The induction of the primary adaptive immune response principally involves DCs, T cells and B cells. Immature DCs patrol the body and preferentially home to the site of infection in response to inflammatory chemokine production, which they recognise through surface receptors. They become loaded with antigen and mature, altering their chemokine receptor expression profile to facilitate homing to the adjacent lymph node. There they can interact with T lymphocytes to promote pathogen specific responses such as B cell activation and the generation of effector T cells. Free antigen also drains to the lymph node where it is recognised by B cells, eventually leading to antibody production and generation of memory B cells. Activated T cells migrate to the site where their specific antigen was detected, where they combine with the innate mechanisms already in place to help shape the inflammatory response and eradicate the infection. Plasma cells migrate to the spleen and bone marrow where they reside and maintain circulating antibody titres over long

periods. Memory cells are generated to enhance the capacity for a rapid specific response should the infectious agent be encountered again. The tissues and molecules involved in the adaptive immune response are presented in greater detail below, with emphasis on the importance of chemokines and their receptors throughout the process. For a general text on the immune system see Murphy and colleagues (Murphy et al., 2010).

1.3 Lymphoid tissue – development, structure and function

The ability of the adaptive immune system to respond rapidly and specifically to infection lies in its highly organised system of lymphoid organs. Within primary lymphoid organs such as the bone marrow and thymus, immune cells are produced and develop, while secondary lymphoid organs, such as lymph nodes and spleen, have well-defined compartments that promote efficient interactions of immune cells to facilitate production of antibody-secreting cells and effector and memory lymphocytes (Campbell et al., 2003, Cyster, 2005). Mammals lacking properly developed or organised lymphoid tissue have been shown to have defective immune responses.

Lymphoid organs are important for a number of functions within the immune system. Leukocytes are produced and mature in primary lymphoid organs such as the bone marrow and thymus, with T cell development in the thymus critical for development of central tolerance. Secondary lymphoid organs, which include lymph nodes, Peyer's patches and spleen, play an important role in peripheral immune tolerance and are where adaptive immune responses are initiated. Other secondary lymphoid tissues include smaller lymphoid aggregates, such as cryptopatches and other mucosa-associated lymphoid tissue (MALT), including isolated lymphoid follicles (ILF) prominent in the intestine. The major body cavities, i.e. the pleural and peritoneal cavities, also contribute to the function of the immune system, containing substantial populations of lymphocytes that protect these sites from invasive pathogens, produce large amounts of "natural" antibody and contribute to immune responses in adjacent organs. The main lymphoid organs of direct relevance to this thesis are the spleen and peripheral lymph nodes. The lymphocyte populations of the peritoneal cavity have also been studied in detail. Therefore, I will provide a brief summary of the structure and function of primary lymphoid organs, followed by a more detailed account of the development, structure and function of secondary lymphoid tissues. I will also discuss the development and function of a major lymphocyte population in the peritoneal cavity, the innate-like B cells.

1.3.1 Primary lymphoid organs

Haematopoiesis, i.e. the generation of new blood cells, takes place in the foetal liver early in gestation and then transfers to the bone marrow (BM), with some overlap between the two in late foetal development (Lee et al., 2011, Ueno and Weissman, 2010).

Haematopoietic stem cells (HSCs), which can differentiate into each different type of blood cell, seed the BM from the foetal liver. There, cells that are involved in bone development are also believed to be involved in maintaining the HSCs that reside in the BM, and may play a role in their enduring proliferative capacity. Cultured osteoblasts (mesenchymal/stromal cells involved in bone formation) from both human and mouse produce cytokines that promote HSC proliferation *in vitro*, and *in vivo* studies have shown a link between increased osteoblast numbers and increased numbers of HSCs in BM (Calvi et al., 2003, Taichman and Emerson, 1998, Zhang et al., 2003). HSCs also interact with BM sinusoidal endothelial cells (BMECs) that express adhesion molecules such as E-selectin and vascular cell adhesion molecule 1 (VCAM1), the CXC chemokine ligand (CXCL)12 (also known as stromal derived factor-1, or SDF-1) and other cytokines.

Interaction of HSCs with stromal cells in the BM allow proliferation and differentiation of the stem cells, through stromal production of growth factors and through cell-cell contact (Avecilla et al., 2004, Rafii et al., 1997). While T cell precursors from the BM travel to the thymus to mature, B cell maturation occurs predominantly in the BM. A variety of factors involved in B cell development and believed to be produced by BM stromal cells have been identified. These include CXCL12, TNF-related activation induced cytokine (TRANCE, also called RANKL and OPGL), interleukin (IL)-7 and FLT3-ligand (FLT3L) (Dougall et al., 1999, Egawa et al., 2001, Kong et al., 1999, Namen et al., 1988, Sitnicka et al., 2003, Sitnicka et al., 2002). Interaction of B cell precursors with the BM stroma promotes immunoglobulin (Ig) gene rearrangement and proliferation, while BM stromal cells also present antigen to facilitate deletion or editing of self-reactive B cells that recognise the self-antigen (Gay et al., 1993, Hardy and Hayakawa, 2001, Tiegs et al., 1993). Mature B cells that do not recognise self-antigens are released into circulation and can traffic to various sites throughout the body, with some further maturation occurring in the spleen. A subset of B cells, the B1 B cells, develop in a way that is largely independent of the BM, and will be discussed later. Following activation of mature B cells in the periphery, resulting plasma cells can return to the bone marrow, where they can reside for at least several months, allowing maintenance of antibody levels in circulation (Hardy and Hayakawa, 2001, Manz et al., 1997).

The earliest steps of thymus development occur between embryonic day (E)10 and E13.5, with thymic/parathymic epithelial primordium expanding from the pharyngeal endoderm and growing into surrounding mesenchymal cells, likely neural crest cells. The primordium separates from the pharynx and develops into both the thymus and the parathyroid glands, which are distinguishable by E13.5 (Gill et al., 2003, Manley, 2000, Manley and Blackburn, 2003). Lymphoid progenitor cells (LPCs) can be detected in the thymus around E11.5, and are thought to cross the mesenchymal layer of the developing thymus that, at this point, lacks vasculature (Wilkinson et al., 1999). Interactions with these cells are involved in the development of the thymic epithelium, which, in the adult thymus, includes cortical, medullary and subcapsular epithelium (Boyd et al., 1993). The thymic epithelium also appears to play a role in regulating the development of LPCs within the thymus and controlled interactions between the two cell types may lead to signals that the thymus is “mature” and ready to promote thymocyte development (Manley, 2000). HSCs from the bone marrow (or, in early embryogenesis, the foetal liver) seed the thymus, losing the ability to differentiate into other cell types and becoming committed to the T cell lineage. In the adult thymus, migration into the thymus is believed to occur through post-capillary venules at the cortico-medullary junction (Gill et al., 2003, Prockop and Petrie, 2000). The signals governing the entry of HSCs into the thymus include expression of various chemokines by thymic epithelial cells (Champion et al., 1986, Liu et al., 2005, Wilkinson et al., 1999). Once within the thymus, thymocytes migrate through the cortex to the subcapsular region, where they undergo rearrangement of their TCR. They then return through the cortex to the medulla, undergoing selection to remove self-reactive T cells, and leave the thymus as mature, self-tolerant T cells (Gill et al., 2003, Smith et al., 1989). The processes involved in thymocyte development, leading to generation of functional CD4⁺ and CD8⁺ T cells, are covered in more detail later in this chapter, with particular reference to the involvement of chemokines and their receptors.

1.3.2 Secondary lymphoid tissue

The major secondary lymphoid tissues, including lymph nodes (LN), spleen and Peyer’s patches (PP), develop prenatally, while other secondary lymphoid tissue, such as cryptopatches in the intestine, develop after birth. Here, I will provide an overview of our current understanding of secondary lymphoid tissue development, highlighting the critical roles played by certain chemokines and their receptors. I will first discuss the organogenesis of LN and PP, which share a number of developmental features, and will provide a brief description of splenic development. The structure and function of LN and spleen will also be discussed. I will also briefly discuss the peritoneal cavity and the

innate-like B cells that reside there. This is relevant for some of the results described in this thesis.

1.3.2.1 Lymph node and Peyer's patch development

Development of LN has been shown to occur from E10.5 (Wigle and Oliver, 1999). The development of various distinct LN occur in a sequential manner in the mouse, with mesenteric lymph nodes (MLN) developing first, followed by, in order, brachial, axillary, inguinal and popliteal lymph nodes. PP develop subsequent to these lymph nodes (Rennert et al., 1996). A number of molecules involved in the early stages of lymph node development have been reported. In 1994, de Togni and colleagues described a role for the tumour necrosis factor (TNF) superfamily cytokine lymphotoxin (LT) in lymph node development, with $LT\alpha$ -deficient mice lacking all lymph nodes and PP (De Togni et al., 1994). Subsequently, $LT\beta$ -receptor ($LT\beta R$)^{-/-} mice were shown to similarly lack all lymph nodes and PP (Fütterer et al., 1998). While $LT\beta R$ signalling can be induced by both $LT\alpha_1\beta_2$ and LIGHT (another member of the TNF family), peripheral lymph nodes (PLN) of LIGHT-deficient mice develop normally, although MLN development appears sensitive to deletion of this ligand in combination with $LT\beta$ deletion (Scheu et al., 2002). This indicates $LT\alpha_1\beta_2$ as the main $LT\beta R$ ligand involved in LN organogenesis, with a possible role for LIGHT in MLN development.

$LT\beta R$ is expressed by stromal organiser cells, mesenchymal cells that are precursors to a variety of stromal cells found within lymphoid organs (Cupedo et al., 2004). $LT\alpha_1\beta_2$ is expressed by lymphoid tissue inducer (LTi) cells, which aggregate with stromal organiser cells to form the nascent LN (Mebius et al., 2001, van de Pavert and Mebius, 2010). Signalling through $LT\beta R$ induces the expression of adhesion molecules, including VCAM1, and of chemokines, including CXCL13, CC chemokine ligand (CCL)19 and CCL21, through nuclear factor (NF)- κB (Cuff et al., 1999, Dejardin et al., 2002). These factors are all involved in the development of LN and PP. LTi cells express integrins such as $\alpha_4\beta_1$ (which binds VCAM1) and blocking either VCAM1 or β_1 integrin inhibits PP formation (Finke et al., 2002). Deletion of CXC chemokine receptor (CXCR) 5, the receptor for CXCL13, or CXCL13 itself disrupts formation of most PLN, likely through disruption of LTi clustering, which is required for LN development. CCL21 has also been shown to be involved in development of some PLN (Ansel et al., 2000, Luther et al., 2003, Ohl et al., 2003, van de Pavert et al., 2009). LTi cells express both CXCR5 and CCR7, and deletion of both receptors (or of the ligands for both) leads to a more severe phenotype

than single deletion mutants, suggesting the two receptors and their ligands play partially overlapping roles in lymphoid tissue development (Luther et al., 2003, Ohl et al., 2003). Another important factor in development of the lymphoid tissue is connection of the forming structure to the lymphatic vasculature. This may be mediated through expression of vascular endothelial growth factor (VEGF)-C, a lymphangiogenic factor that is produced by mesenchymal cells following LT_i cell-induced LT β R signalling (Vondenhoff et al., 2009).

As one might expect from the above observations, LT_i cell development is crucial for formation of LN and PP. LT_i cells are derived from IL-7R α^+ cells from the foetal liver that can also give rise to various leukocyte subsets, including T cells, B cells and DCs (Mebius et al., 2001). They require expression of inhibitor of DNA binding 2 (ID2), which suppresses the expression of proteins that promote differentiation of the progenitor cells into B cells. In the absence of ID2, LT_i cells are not present and LNs do not form (Boos et al., 2007). LT_i cells also express the retinoic acid-related orphan receptor (ROR)- γ t, which has been shown to be required for formation of LN and PP. ROR γ t^{-/-} animals are devoid of LT_i cells and fail to develop LN or PP (Kurebayashi et al., 2000, Sun et al., 2000).

LN formation is also dependent on signalling of TRANCE through its receptor, TRANCER. Deletion of either ligand or receptor results in a complete absence of LN, although PP form normally (Kim et al., 2000, Kong et al., 1999). Deletion of TNF-receptor-associated factor 6 (TRAF6), which is involved in TRANCER signalling, also results in loss of LN formation (Naito et al., 1999). TRANCER signalling induces LT $\alpha_1\beta_2$ expression on LT_i cells, which express both TRANCE and TRANCER, providing at least one likely role for these molecules in lymphoid tissue development (Kim et al., 2000, Vondenhoff et al., 2009, Yoshida et al., 2002).

PP development, while similar to LN formation, does have some distinct features. It involves recruitment of not only LT_i cells, which are CD45⁺ IL-7R α^+ CD4⁺ CD3⁻, but also a subset of precursors that are CD45⁺ IL-7R α^- CD4⁻ CD3⁻ CD11c⁺ and that can be found distributed throughout the small intestine at E15.5. They require expression of a receptor tyrosine kinase, RET, to form the lymphoid aggregates that will develop into PP (Veiga-Fernandes et al., 2007). RET ligands, expressed in the gut, appear to induce LT $\alpha_1\beta_2$ expression, suggesting a possible explanation for the ability of PP to form in the absence of TRANCE/TRANCER signalling (Kim et al., 2000, Veiga-Fernandes et al., 2007).

A fascinating development emerging in the story of lymphoid tissue organogenesis is that of the involvement of retinoic acid (RA) and retinal dehydrogenase (RALDH) 2, and the suggestion that neuronal RA expression may be the primary signal for development of lymphoid tissues. This is believed to initiate the aggregation of stromal organiser and LTi cells and lead to the expression and interaction of the various factors described above, ultimately resulting in the formation of LN and PP. RA is required for the expression of CXCL13 by stromal organiser cells, a process that is LT-independent. The expression of CXCL13 initiates the clustering of LTi cells, with CCL21 also involved subsequent to the initiation of aggregation (van de Pavert et al., 2009). It has been suggested that neurons that lie adjacent to LN anlagen are the source of RA in this process, and indeed these cells do produce RA and CXCL13 expression can be induced in the gut following vagal nerve stimulation (van de Pavert et al., 2009). Data supporting this theory has recently been reviewed by van de Pavert and Mebius (van de Pavert and Mebius, 2010). The steps believed to be involved in LN formation are summarised in Figure 1.1.

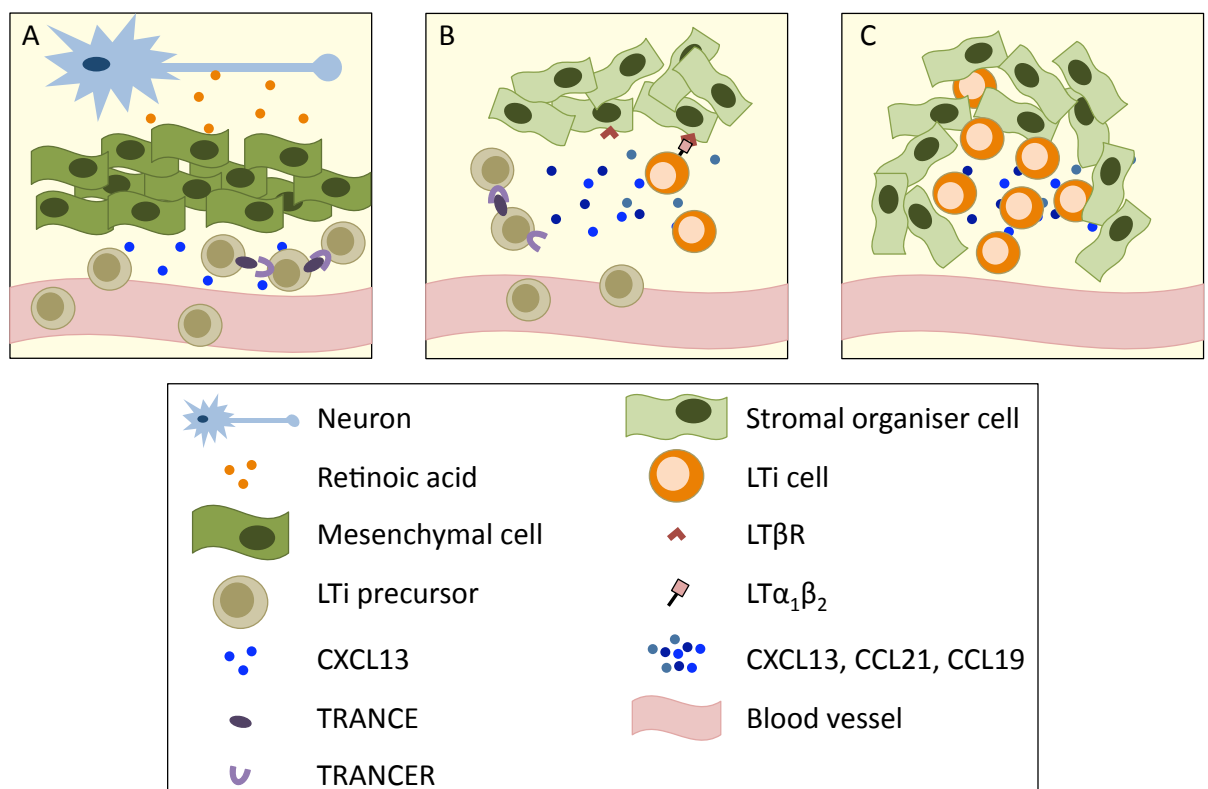


Figure 1.1: Lymph node development. (A) Mesenchymal cells are induced to express CXCL13 in response to retinoic acid (RA), possibly produced by nearby neurons. The CXCL13 is recognised by lymphoid tissue inducer (LTi) cell precursors, and it induces extravasation of these LTi precursors from the blood towards the mesenchymal cells. Clustering of the LTi precursors promotes TRANCE-induced signalling through TRANCER. (B) This signalling induces expression of lymphotoxin (LT)-α₁β₂ on the LTi precursors, which mature into LTi cells. This maturation is dependent on expression of ID2 (not shown). LTi cells interact with LTβR on stromal organiser cells (derived from mesenchymal cells) via LTα₁β₂. The stromal organiser cells then express a variety of chemokines (including CXCL13, CCL19 and CCL21) as well as adhesion molecules, including VCAM1, MAdCAM1 and ICAM1 (not shown). (C) The production of these various factors promote recruitment of more haematopoietic cells, leading to development of the mature lymph node. Figure adapted from van de Pavert and Mebius, 2010.

1.3.2.2 Spleen development

The spleen has a number of functions, including filtering the blood, removing old or damaged erythrocytes, and acting both as a site of B cell maturation and as a secondary lymphoid organ. “Transitional” B cells that migrate to the spleen from the BM mature into either classical follicular B cells that traffic around the body or innate-like marginal zone B cells that remain resident in the splenic marginal zone (Allman and Pillai, 2008). Removal of the spleen greatly increases the risk of sepsis, identifying the spleen as an important organ in fighting bacterial infections. A number of factors involved in this increased susceptibility to bacterial infection have been suggested, including defects in T cell function, impaired antibody production and loss of specialised macrophages that line the marginal zone of the spleen, allowing detection and removal of blood-borne bacteria (Brendolan et al., 2007). In asplenic mice a subset of innate-like B cells, the B1a B cells, is absent (Wardemann et al., 2002). These cells are involved in production of natural antibody, mainly IgM, as well as acting as precursors to a high proportion of IgA-producing plasma cells in the intestinal mucosa (Kroese et al., 1993, Kroese et al., 1989a). Human IgM memory B cells, which are found in the marginal zone of the spleen as well as in circulation, are generated in and/or maintained by the spleen and are absent from patients lacking the organ (Kruetzmann et al., 2003, Weller et al., 2004). The loss of these cells has been linked to defective immune responses to encapsulated bacterial pathogens and associated with the sepsis common in splenectomised patients (Kruetzmann et al., 2003).

In the mouse, the spleen begins to develop at E11.5, with mesodermal cells that express the homeobox gene *Hox11* accumulating on the dorsal region of the developing stomach, where they form a ridge of mesenchymal cells detectable at E12.5 (Roberts et al., 1994). A number of cells involved in the early development of the spleen have been identified, although specific roles for many remain unclear. For a review describing the early stages of spleen development, see Brendolan et al., 2007. Lymphoid progenitor cells can be found in the developing spleen at E12.5-13.5 (Godin et al., 1999, Mebius et al., 1997), and haematopoietic cells are readily detected at E15.5 (Sasaki and Matsumura, 1988). The mechanisms controlling the initial migration of cells to the spleen are unclear but once populated with leukocytes, similar processes to those that occur in lymph nodes and other lymphoid tissues regulate the organisation of the white pulp in the spleen (Mebius, 2003).

1.3.2.3 Structure and function of the secondary lymphoid organs

Lymphoid tissue is highly organised and structured to maximise capacity for interaction between leukocytes, allowing effective scanning of tissues for infection or injury and supporting the efficient generation of adaptive immune responses. The factors involved in organisation of lymphoid tissues are, in the main, common to LNs and splenic white pulp and include a variety of adhesion molecules and cytokines. In this section, I will describe the structure of these tissues with reference to how this influences their function. In subsequent sections, I will provide detail of how chemokines are particularly required for the appropriate organisation and function of lymphoid tissues.

Lymph nodes

Lymph nodes contain two main regions – the cortex, which holds the B cell follicles (and germinal centres, following antigen encounter) and T cell zones (in the paracortex), and the medulla, which contains a network of lymphatic sinuses through which lymphocytes exit the LN. Afferent lymph enters the LN and flows through the subcapsular sinus (SCS), which lies directly beneath the fibrous capsule of the LN, surrounding the LN parenchyma, and through trabecular sinuses (which traverse the LN parenchyma), to the medullary sinuses and out of the LN via the efferent lymphatic vessel. Naïve lymphocytes enter the LN through high endothelial venules (HEVs) that are found in the T cell zone (von Andrian and Mempel, 2003). The basic structure of the LN is shown in Figure 1.2.

To enter the LN via HEVs, lymphocytes must be directed to extravasate from the blood at the appropriate point. This involves the coordinated expression and interaction of numerous molecules on the lymphocytes and the endothelial cells of the HEVs. These molecules include integrins and selectins, chemokines and chemokine receptors, addressins and cell adhesion molecules as well as possibly glycosaminoglycans (GAGs). Lymphocytes expressing L-selectin weakly bind to endothelial cells expressing peripheral node addressin (PNAd), which causes them to roll along the endothelial cell surface, in the direction of bloodflow through the venule (Arbonés et al., 1994, Streeter et al., 1988b, Tang et al., 1998). Chemokines expressed and/or presented by the endothelial cells bind to receptors on the lymphocyte surface and induce upregulation of leukocyte function-associated antigen 1 (LFA1), an integrin that interacts with intercellular adhesion molecule (ICAM)-1 (and possibly ICAM2) on the endothelial cell surface (Andrew et al., 1998, Baekkevold et al., 2001, Hamann et al., 1988, Stein et al., 2000). This leads to firm adhesion of the lymphocyte to the endothelial cell and prompts extravasation, via either a transcellular or a paracellular route. This process is summarised in Figure 1.3.

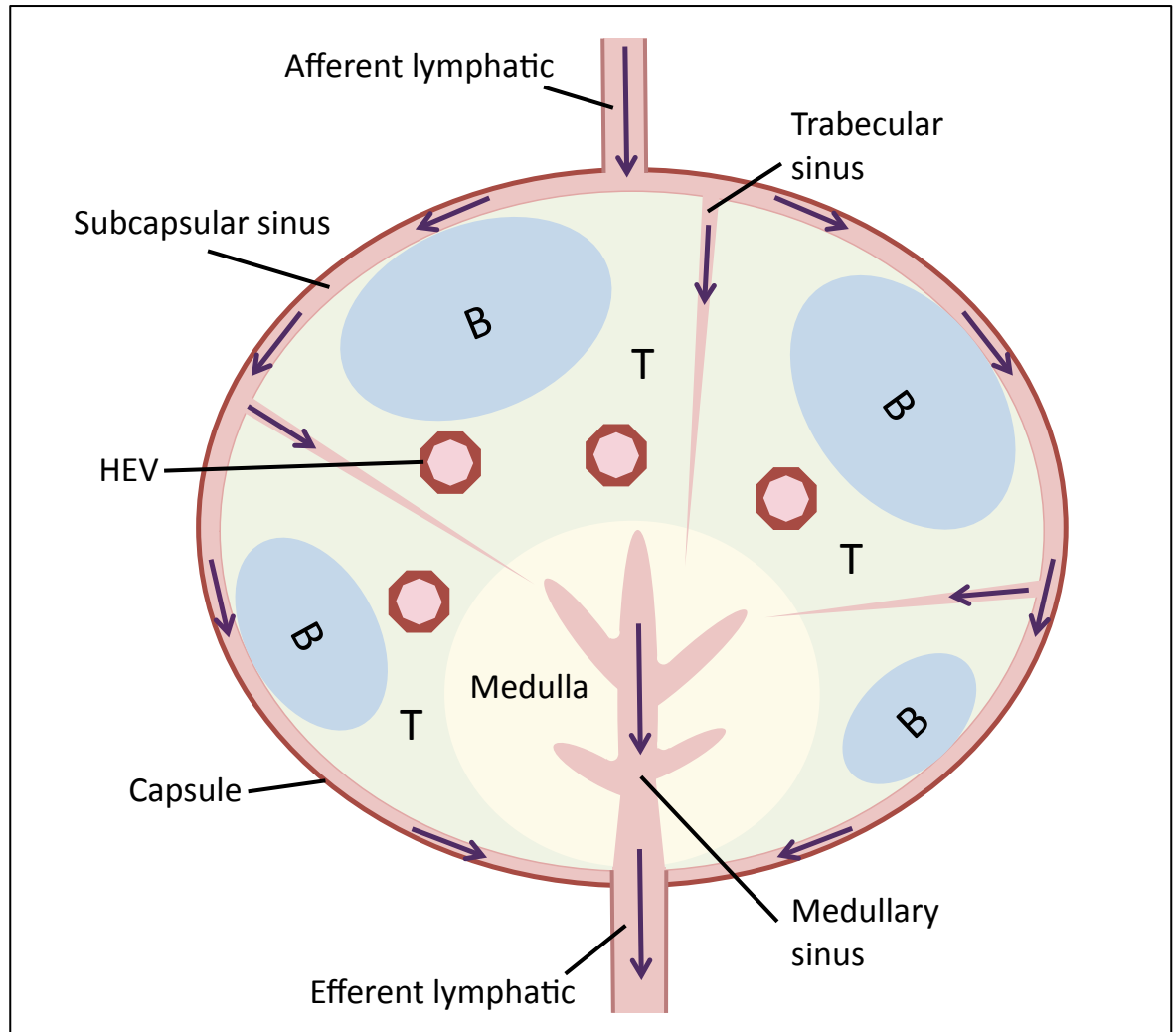


Figure 1.2: Structure of a lymph node. The LN is surrounded by a fibrous capsule, beneath which lymph flows through the subcapsular sinus, as well as through the trabecular sinuses. These connect to the medullary sinus. Direction of lymph flow from afferent (entering) to efferent (exiting) lymphatic vessels is indicated by purple arrows. B cell follicles (B) are shown in blue, surrounded by T cell zones (T) in green. High endothelial venules (HEVs), through which naïve lymphocytes enter the LN, are found in the T cell zone, as indicated. Adapted from von Andrian and Mempel, 2003.

In mucosal LNs (e.g. MLN), HEVs express mucosal addressin cell adhesion molecule 1 (MAdCAM1), which binds $\alpha_4\beta_7$ integrin expressed by naïve lymphocytes. This interaction allows for lymphocyte rolling on the HEV in the absence of L-selectin, and lymphocyte homing to MLN in L-selectin deficient mice is less disrupted than that to PLN (Arbonés et al., 1994, Bargatze et al., 1995, Berlin et al., 1993, Streeter et al., 1988a). In PP, HEVs express MAdCAM1 but not PNA_d, and homing of lymphocytes to this tissue is lost in the absence of β_7 integrin (Wagner et al., 1996). Once within the lymph node, lymphocytes rely heavily on chemokine signals to migrate to the appropriate area, as well as to allow interaction in the event of antigen encounter. A more detailed account of the role of chemokines in these processes will be provided later in this chapter.

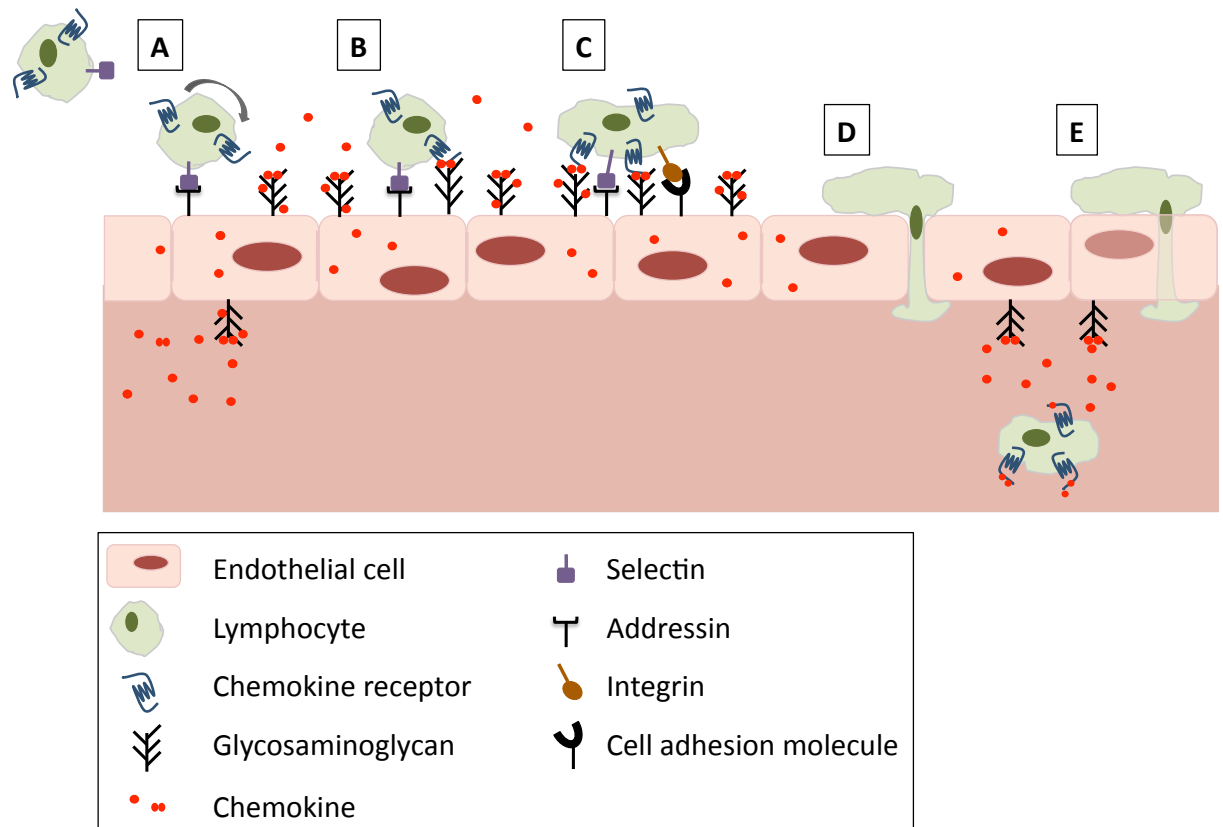


Figure 1.3: Lymphocyte extravasation into lymph nodes. Migration of lymphocytes from the blood into LNs is a multi-step process involving a number of different molecules. (A) A lymphocyte expressing selectins (e.g. L-selectin on naïve lymphocytes) and chemokine receptors initially makes contact with an addressin (e.g. peripheral node addressin, or PNA_d, on high endothelial venules (HEVs)). This slows the cells progress through the blood and causes it to “roll” along the endothelial layer. (B) The chemokine receptor comes into contact with its ligand, presented on endothelial cells by glycosaminoglycans (GAGs). GAGs may also facilitate transport of chemokine across the endothelial layer. (C) The interaction between receptor and chemokine leads to a change in conformation of surface integrins on the lymphocyte, which are then capable of binding cell adhesion molecules (e.g. intercellular adhesion molecule 1, or ICAM1). This causes firm adhesion of the lymphocyte to the endothelium. This is followed by extravasation through either (D) paracellular or (E) transcellular routes. Figure adapted from Handel et al., 2005 and Förster et al., 2008.

The other route of entry into the LN is via lymphatics, which drain interstitial fluid from tissues throughout the body. Tissue-derived DCs use this route in both steady-state and antigen-driven migration, and free antigen can also enter LNs via the lymph (Banchereau and Steinman, 1998, Lutz and Schuler, 2002, Ohl et al., 2004, Sainte-Marie and Peng, 1986, Wilson et al., 2003). Again, chemokines are heavily involved in the migration of DCs to and within LN and I will discuss this process in depth later in this Introduction. DC interaction with naïve T cells within LNs is required for induction of appropriate responses to antigen presented in the LN – for instance, activation of T cells and promotion of effector functions against invading pathogens versus induction of tolerance or anergy (where the T cell can no longer be activated) towards self-antigen (von Andrian and Mempel, 2003). DCs migrating under steady-state conditions can induce antigen-specific tolerance in T cells and are suggested to act to maintain peripheral tolerance by presenting self- or harmless antigen in the absence of costimulatory molecules (Hawiger et al., 2001,

Steinman et al., 2003, Steinman and Nussenzweig, 2002). Hawiger and colleagues showed that, in a model where DCs targeted with a DC specific antibody could induce tolerogenic T cells, the addition of an agonistic antibody for CD40 induced upregulation of CD40 and CD86 (costimulatory molecules) on the DCs and led to T cell activation (Hawiger et al., 2001). This capacity of DCs to induce peripheral tolerance complements and supplements the central tolerance induced in the thymus during T cell development, which provides wide, but incomplete, protection against autoreactivity (Bouneaud et al., 2000).

The ability of DCs to induce T cell activation and initiate adaptive immune responses is one of the central features of the immune system. Upon recognition of foreign, or “harmful”, antigen in the periphery, DCs internalise the antigen, upregulate costimulatory molecules and modify their chemokine receptor expression profile to migrate to the LN via the lymphatic system. There they enter T cell zones and present processed antigen to T cells, which become activated following recognition of their cognate antigen and interaction with co-stimulatory molecules and migrate towards the B cell follicle (Banchereau et al., 2000, Garside et al., 1998).

B cells also require antigen encounter and activation to take part in the immune response. In contrast to T cells, B cells recognise intact antigen, which enters the LN via the lymph and is presented to B cells by stromal cells called follicular dendritic cells (FDCs). As their name suggests, FDCs are found in the follicular compartment of the LN and express the chemokine CXCL13, which is involved in homing of B cells to B cell follicles (see below for more detail). They can trap and present immune complexes of complement and “free” antigen to B cells. Upon recognition and uptake of their cognate antigen, B cells alter their chemokine receptor expression profile to migrate to the boundary of the B cell follicle and T cell zone. There, B and T cells interact, with B cells presenting processed antigen to T cells and receiving activation signals that induce germinal centre formation, antibody production and proliferation (Clark and Ledbetter, 1994, Cyster et al., 2000, Garside et al., 1998).

Interestingly, recent work has demonstrated a role for macrophages that line the SCS of the LN in presenting immune complexes containing cognate antigen to B cells that reside in the B cell follicles adjacent to the SCS (Phan et al., 2007). B cells were also able to act as antigen-transporting cells, using complement receptors to collect immune complexes containing non-cognate antigen from the surface of SCS macrophages and transfer them to FDCs residing deeper within the follicle (Phan et al., 2007). This macrophage population is incompletely understood, although it has long been known to differ from classical

macrophages in its poor phagocytic capacity and ability to retain surface presentation of immune complexes over a long period (Szakal et al., 1983).

Spleen

The spleen is composed of red pulp and white pulp, with the latter comprising lymphoid tissue that is organised into B cell follicles and T cell zones reminiscent of LNs. The red pulp contains macrophages that phagocytose old erythrocytes and are involved in the recycling of iron, both from the dying erythrocytes and through scavenging of circulating haemoglobin (Mebius and Kraal, 2005). These macrophages are also involved in responding to blood-borne bacterial pathogens, in part through production of molecules that inhibit the uptake of iron by bacteria and thus limit their growth (Flo et al., 2004). Additionally, antibody-producing cells (plasmablasts and plasma cells) can be found in the red pulp. Their migration to the red pulp from the white pulp is linked to alteration in chemokine receptor expression and is believed to occur to provide rapid delivery of antibody into the bloodstream (Hargreaves et al., 2001, Mebius and Kraal, 2005).

As mentioned above, the white pulp of the spleen shares some organisational similarities with LNs. However, there are some specialised features of the splenic white pulp that are specific to this particular lymphoid tissue. The white pulp surrounds arterial vessels entering the spleen, with the T cell zone forming the periarteriolar lymphoid sheath (PALS) and B cell follicles organised near the marginal zone (MZ) of the white pulp (Figure 1.4). Lymphocytes enter from the bloodstream via the MZ, migrating into the white pulp through a layer of cells that line the marginal sinus. The MZ contains some specialised leukocyte subsets, including MZ metallophilic macrophages, which lie directly below the marginal sinus-lining cells, MZ macrophages, which are dispersed among the reticular fibroblasts of the MZ and form an outer ring of macrophages around the white pulp, and MZ B cells, which are also distributed throughout the MZ (Kang et al., 2003, Koppel et al., 2008, Martin and Kearney, 2002, Mebius and Kraal, 2005). Interactions between MZ macrophages and MZ B cells have been shown to be required for responses to some bacterial infections (Koppel et al., 2008). Leukocytes migrating to the red pulp can also be detected in the marginal zone. B cells are thought to be required for correct localisation of macrophage populations in the MZ, and chemokines involved in the organisation of B cell follicles and T cell zones are also involved in MZ organisation (Ato et al., 2004, Mebius and Kraal, 2005, Nolte et al., 2004). Additionally, sphingosine-1-phosphate (S1P), a sphingolipid involved in retention of T cells in the thymus and LN, also plays a role in B cell migration to and residence within the marginal zone, with B cells

deficient in S1P₁ (a receptor for S1P) unable to localise to the MZ (Cinamon et al., 2004, Matloubian et al., 2004).

The white pulp is largely a site of adaptive immune response generation, through processes shared with LN. However, the MZ can be involved in both innate and adaptive immune responses. MZ macrophages produce molecules that promote internalisation and degradation of bacterial pathogens (Geijtenbeek et al., 2002, Kang et al., 2004), as well as being involved in clearance of viruses (Oehen et al., 2002). MZ B cells, which have a distinct surface marker phenotype to follicular B cells, are also important in the response to blood-borne pathogens (Lopes-Carvalho and Kearney, 2004, Martin and Kearney, 2002). Upon encounter with pathogens, they can either differentiate into IgM-producing plasma cells or act as antigen-presenting cells, migrating into the white pulp where they are potent activators of CD4⁺ T cells (Attanavanich and Kearney, 2004, Martin and Kearney, 2002). These various features of specialised MZ cells may explain why splenectomised patients fail to respond effectively to many bacterial infections and require prophylactic antibiotic treatment for life (Mebius and Kraal, 2005).

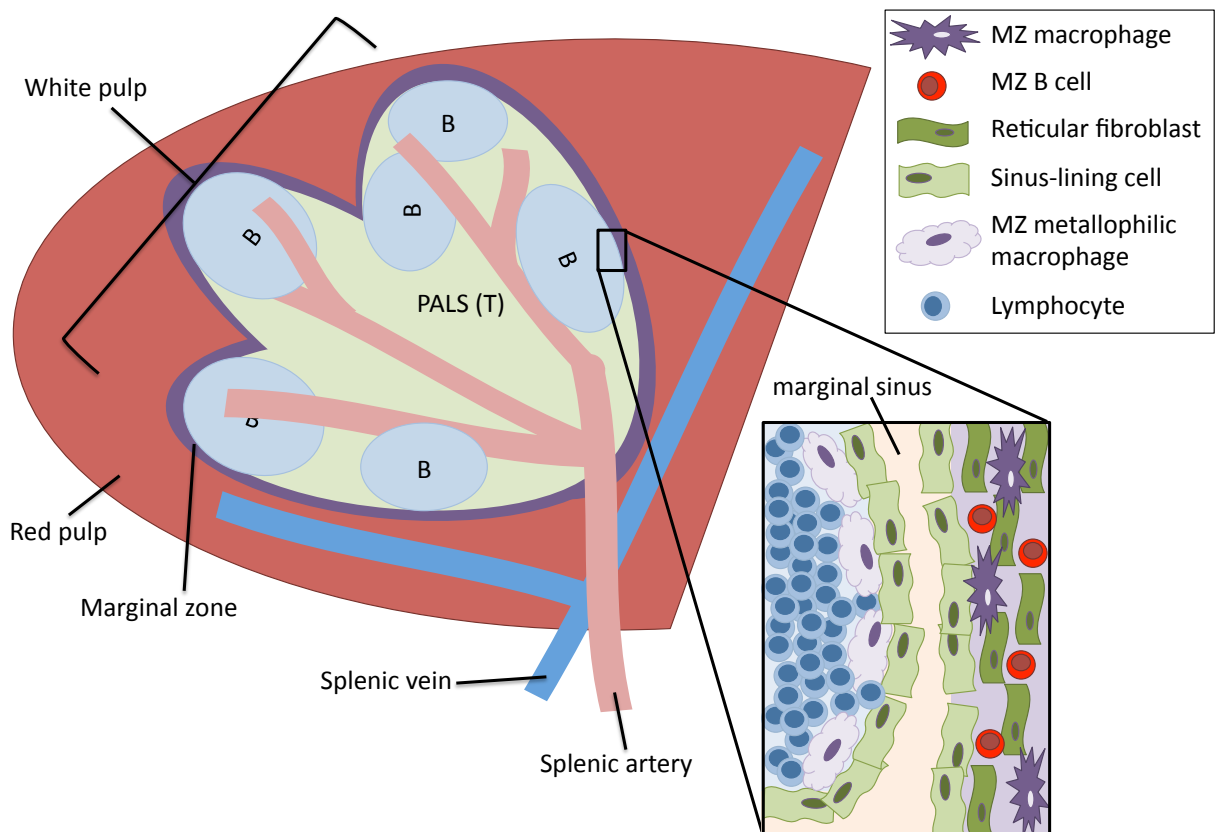


Figure 1.4: Structure of the spleen. The spleen is divided into red pulp and white pulp, as indicated. The white pulp consists of the periarteriolar lymphoid sheath (PALS; green), which contain the T cells (T) and B cell follicles (B; blue) and is surrounded by the marginal zone (MZ; purple). The marginal zone is separated from the white pulp by the marginal sinus (see inset). MZ metallophilic macrophages lie beneath sinus-lining cells in the white pulp, while MZ macrophages and MZ B cells are found interspersed between reticular fibroblasts of the marginal zone. Adapted from Mebius and Kraal, 2005.

Innate-like B cells of the peritoneal cavity

The peritoneal cavity contains a large number of leukocytes, and is home to a sizeable and heterogeneous population of innate-like B cells, the B1 B cells. Originally identified as a CD5 (Ly-1)-expressing subset of B cells, CD5⁺ B1 B cells have also been defined (B1b cells). In the peritoneal cavity, these cells, as well as the “original” B1 B subset, B1a cells, express CD11b (Hayakawa et al., 1986, Hayakawa et al., 1983, Stall et al., 1992).

However, a CD5⁺ CD11b⁻ population can also be identified in the peritoneal cavity (B1c cells). This subset may be a precursor to CD11b⁺ B1 cell subsets, as transfer experiments have shown that, in contrast to CD11b⁺ subsets, B1c cells can reconstitute both their own and B1a and B1b populations (Ghosn et al., 2008, Hastings et al., 2006a). Indeed, early experiments reported that B1 B cells are self-renewing and distinct from “classical” B2 cells, arising from distinct lineages that cannot be recapitulated in irradiated mice by transferred adult bone marrow but are reconstituted with the transfer of peritoneal cavity lavage cells or foetal or neonatal liver, spleen or bone marrow cells (Hayakawa et al., 1985). Since then, a B1 B cell precursor has been reported that is abundant in foetal liver but much less prevalent in adult bone marrow (Montecino-Rodriguez et al., 2006).

Additionally, it has been suggested that B1b cells may in fact be derived from B2 B cell precursors, rather than the proposed separate lineage of other B1 B cells (Alugupalli et al., 2004). Regardless of these differences, B1 B cells share a number of common traits, and in fact it has been suggested that residence in the peritoneal cavity may have a significant impact on the characteristics exhibited by all its B cells, with B2 cells from this site distinguishable from splenic B2 cells and exhibiting B1b-like characteristics in some settings (Berberich et al., 2007, Hastings et al., 2006b). However, recent work from our lab and others has indicated that the markers used to define “B2” cells in this work may be too restricted, as many CD11b⁻ B cells in the peritoneal cavity are more correctly defined as B1 cells according to a variety of criteria (Hansell et al., 2011b). B1 B cells can also be found in the spleen, and are rare but present in other tissues, including MLN, intestinal lamina propria and blood. However, they are distinct from those found in the peritoneal cavity and constitute a very low proportion of total lymphocytes in these compartments (Tumang et al., 2004). Unlike splenic MZ B cells, B1 B cells have been shown to be capable of recirculation throughout the body, with a demonstrated role for chemokines and their receptors in this process (Ansel et al., 2002, Ha et al., 2006).

One of the common properties of innate-like B cells is the limited diversity of their BCR repertoire. Unlike classical B2/follicular B cells predominating in spleen and LN, B1 B cells do not enter germinal centres to undergo somatic hypermutation to increase the antigen specificity of their BCR and class-switching is limited (Bendelac et al., 2001).

They recognise conserved structures in both self- and foreign antigens, such as phosphorylcholine (PC) on pathogenic bacteria, and produce antibodies that recognise apoptotic cells, presumably binding lipids that are not normally exposed on healthy cells (Bendelac et al., 2001). Like marginal zone B cells, B1 B cells express high levels of IgM, and they are believed to act as a major source of IgA-secreting plasma cells typically found in the lamina propria of the gut (Hayakawa et al., 1986, Kroese et al., 1989a, Kroese et al., 1989b). They are a major source of “natural” IgM, i.e. IgM present in serum in the absence of pathogen/foreign antigen stimulus, and can also contribute to production of “immune” IgM, i.e. IgM produced as part of an immune response (Briles et al., 1981, Ehrenstein and Notley, 2010, Haas et al., 2005). These properties have identified a role for B1 B cells, and innate-like B cells generally, in providing early protection against infection, prior to establishment of a strong adaptive immune response.

1.4 Chemokines

Chemokines are small, mainly secreted, peptides about 8-12 kDa in size that are required for the correct mobilization and migration of immune cells. They have a variety of critical roles in the immune system including development and maintenance of immune structures, transient response to infection, wound healing, etc. They are also known to play a part in a number of diseases, including a range of autoimmune diseases and cancers. Outside of their role as immune molecules, they are also required for a variety of essential functions, some of which overlap with their immunological effects. These include stem cell mobilization, development, angiogenesis and cell proliferation, survival and differentiation. Their structure is broadly similar at the tertiary level, although they can vary considerably in amino acid sequence (Allen et al., 2007, Rossi and Zlotnik, 2000).

1.4.1 Systematic nomenclature

Originally named for the properties observed when each was first discovered, the explosion in the number of defined chemokines that followed the advent of bioinformatics has required a new, standardized method of naming chemokines to avoid confusion in publication. The current system is based on the order in which the relevant gene was reported – therefore, CCL1 was the first CC chemokine gene to be cloned. Characterized by a conserved cysteine (Cys) motif based usually on 4 Cys residues, chemokines can be classified based on the arrangement of these residues in the primary sequence – thus there are four subfamilies; CXC/ α chemokines, CC/ β chemokines, XC/ γ chemokines and

CX₃C/δ chemokines (Murphy et al., 2000, Rossi and Zlotnik, 2000). Members of these families are listed in Table 1.1.

CXC chemokines have a single, non-conserved amino acid between the first two Cys residues in their Cys motif. CC chemokines, the largest of the four described chemokine subfamilies, have two adjacent Cys residues at the beginning of their Cys motif. XC chemokines, of which only two have been described, are without one of the first and third Cys residues in their motif (Kennedy et al., 1995, Yoshida et al., 1995), while CX₃CL1, the sole described member of the CX₃C chemokine subfamily, has three non-conserved amino acids between the first and second of its Cys residues (Comerford and Nibbs, 2005, Rossi and Zlotnik, 2000). The Cys residues contribute to the regularity of structure to be found in the chemokine family, as disulphide bonding between the first and third residues and second and fourth residues respectively is responsible for stabilizing the tertiary structure of the proteins (Rossi and Zlotnik, 2000).

CXC/α Chemokine Family

Systematic Nomenclature	Alternative name(s)	Receptor(s)
CXCL1	GRO α , KC	CXCR1, CXCR2
CXCL2	GRO β , MIP-2	CXCR2
CXCL3	GRO γ , DCIP-1	CXCR2
CXCL4	PF4	CXCR3B
CXCL5	ENA-78, GCP-2, LIX	CXCR2
hCXCL6	GCP-2	CXCR1, CXCR2
hCXCL7	NAP-2	CXCR2
hCXCL8	IL-8	CXCR1, CXCR2
CXCL9	Mig	CXCR3, CCR3
CXCL10	IP-10	CXCR3, CCR3
CXCL11	I-TAC	CXCR3, CXCR7, CCR3
CXCL12	SDF-1	CXCR4, CXCR7
CXCL13	BCA-1, BLC	CXCR5
CXCL14	BRAK, Bolekine	unknown
mCXCL15	Lungkine, WECHÉ	unknown
CXCL16	SCYB16, SR-PSOX	CXCR6

CC/β Chemokine Family

Systematic Nomenclature	Alternative name(s)	Receptor(s)
CCL1	I-309, TCA-3	CCR8
CCL2	MCP-1, MCAF, JE	CCR2
CCL3	MIP-1 α S, MIP-1 α	CCR1, CCR5
hCCL3L1	MIP-1 α P, MIP-1 α	CCR1, CCR3, CCR5
CCL4	MIP-1 β	CCR5
CCL5	RANTES	CCR1, CCR3, CCR5
mCCL6	C10, MRP-1	CCR1
CCL7	MCP-3, MARC	CCR1, CCR2, CCR3, CCR5
CCL8	MCP-2	CCR2, CCR3

mCCL9	MIP-1 γ , MRP-2, CCF18	CCR1
mCCL10	MIP-1 γ , MRP-2, CCF18	CCR1
CCL11	Eotaxin	CCR3, CXCR3
mCCL12	MCP-5	CCR2
hCCL13	MCP-4	CCR2, CCR3
hCCL14	HCC-1	CCR1
hCCL15	HCC-2, Lkn-1, MIP-1 δ	CCR1, CCR3
hCCL16	HCC-4, LEC, LCC-1	CCR1, CCR2, CCR5
CCL17	TARC	CCR4
hCCL18	DC-CK1, PARC	unknown
CCL19	ELC, MIP-3 β , exodus-3	CCR7
CCL20	MIP-3 α , LARC, exodus-1	CCR6
CCL21	SLC, 6Ckine, exodus-2	CCR7
CCL22	MDC, STCP-1, ABCD-1	CCR4
hCCL23	MPIF-1	CCR1
CCL24	Eotaxin-2, MPIF-2	CCR3
CCL25	TECK	CCR9
CCL26	Eotaxin-3	CCR1, CCR2, CCR3, CCR5, CX ₃ CR1
CCL27	C-TACK, PESKY, Eskine	CCR10
CCL28	MEC	CCR3, CCR10

XC/ γ Chemokine Family

Systematic Nomenclature	Alternative name(s)	Receptor(s)
XCL1	Lymphotactin, SCM-1 α	XCR1
hXCL2	SCM-1 β	XCR1

CX₃C/ δ Chemokine Family

Systematic Nomenclature	Alternative name(s)	Receptor(s)
CX ₃ CL1	Fractalkine, neurotactin	CX ₃ CR1

Table 1.1: Systematic nomenclature for chemokines. Chemokine names as per systematic nomenclature are shown, with previous/alternative name(s) and receptor(s). Chemokines present only in humans are prefixed with 'h'. Chemokines present only in mice are prefixed with 'm'. Adapted from (Murphy et al., 2000) and (Comerford and Nibbs, 2005).

1.4.2 Chemokine function in vivo

As mentioned above, chemokines have a highly conserved tertiary structure. The N terminus contains signalling and receptor binding domains, and proteolytic cleavage of the N terminus can influence the agonistic or antagonistic interaction of chemokines with their receptors (Clark-Lewis et al., 1995, Gong and Clark-Lewis, 1995, Jarnagin et al., 1999). In particular, matrix metalloproteinases (MMPs) are involved in modification of numerous chemokines, and can either cause a change from agonist to antagonist or block activity altogether (McQuibban et al., 2001, McQuibban et al., 2002, McQuibban et al., 2000, Parks et al., 2004), while CD26 proteolytic cleavage of two N-terminal residues from CCL4 influences its binding affinity for CCR1 and CCR2 but not CCR5 (Guan et al., 2004, Guan et al., 2002, Van Damme et al., 1999). Most chemokines are secreted although

CXCL16 and CX₃CL1 are expressed in a membrane-bound form, with mucin-like stalks attached to transmembrane domains anchoring them to the cell surface. These can be cleaved and shed from the cell surface through the activity of proteases, allowing them to act like other soluble chemokines (Allen et al., 2007, Garton et al., 2001, Gough et al., 2004). It is believed that, at least for CX₃CL1, the surface-anchored expression of the chemokine mediates adhesion of cells bearing the relevant chemokine receptor (Chapman et al., 2000, Haskell et al., 2000). The N terminus also contains an “N-loop” that has been highlighted as an important region for receptor binding, although other parts of the chemokine may also be required (Campanella et al., 2003, Clark-Lewis et al., 1995, Hemmerich et al., 1999, Pakianathan et al., 1997, Skelton et al., 1999).

Chemokines fall broadly into two functional groups - the constitutive or homeostatic chemokines and the inducible or inflammatory chemokines - and carry out their function through G-protein coupled receptors on the surface of immune cells (Rossi and Zlotnik, 2000). Chemokines are produced throughout the body either continuously (constitutive) or in response to stimulus such as infection or injury (inflammatory). They may be present as monomers, dimers or higher order oligomers and may form homo- or hetero-oligomeric structures, which can be required for function *in vivo* (Koenen et al., 2009, Nesmelova et al., 2008, Proudfoot et al., 2003, Thelen et al., 2010). Presentation of chemokines on cell surfaces is intrinsic to their function, particularly in promoting extravasation of leukocytes into tissue. Implicated in this presentation are the glycosaminoglycans (GAGs), which decorate the surface of most mammalian cells and have been shown to bind chemokines, as described below.

1.4.2.1 Glycosaminoglycans and chemokine presentation

The involvement of GAGs in chemokine function has been demonstrated in studies where mutagenised chemokines with disrupted GAG binding sites lack functionality *in vivo* (Proudfoot et al., 2003, Severin et al., 2010). GAGs are composed of negatively charged polysaccharide chains that can vary in composition depending on the site of expression. This variability has been suggested to contribute to the specificity of leukocyte homing, with chemokines binding to specific subsets of GAGs (Witt and Lander, 1994). Although GAG binding sites are often distinct from receptor binding sites, they can overlap in some cases (Campanella et al., 2003, Severin et al., 2010, Skelton et al., 1999). The sugar chains of many GAGs are attached to a core protein to form a proteoglycan structure capable of interacting with a variety of proteins and tethering them to the cell surface (Handel et al., 2005). It has been suggested that binding to GAGs can facilitate oligomerisation and

presentation of chemokine, providing appropriate signals to migrating leukocytes to allow adherence to and extravasation through endothelial cell layers. They may also be involved in transcytosis of chemokine from the basal to apical endothelial cell surface (Hoogewerf et al., 1997, Middleton et al., 1997, Salanga and Handel, 2011, Wang et al., 2005b). The presentation of chemokine on endothelial cell surfaces promotes firm adhesion of rolling leukocytes along vasculature, allowing the leukocytes to extravasate and enter tissue sites requiring their presence. This model has been discussed in a number of reviews (Förster et al., 2008, Ley et al., 2007, Parish, 2006, Salanga and Handel, 2011, Weninger and von Andrian, 2003) and shares the general properties of naïve lymphocyte entry into LNs, shown in Figure 1.3.

1.4.2.2 Chemokines in homeostasis and inflammation

Although useful to provide an overview of when and why particular chemokines are produced, the classification of chemokines as either “homeostatic” or “inflammatory” is often rather inaccurate - in practice, many chemokines can serve in either role. In general, however, chemokines described as homeostatic are continuously produced and facilitate the development and maintenance of lymphoid tissues, as well as being involved in the continuous migration of leukocytes around resting tissues. “Inflammatory” chemokines are induced during an immune response to direct cells to the affected site in the body – their expression peaks rapidly and subsides to allow clearance of the leukocytic infiltrate from the inflamed site (Rossi and Zlotnik, 2000).

Homeostatic chemokine activity is exemplified by CXCL12, acting through its receptor CXCR4. It is constitutively produced by BM stroma, promoting B cell progenitor proliferation, and directs haematopoietic precursors to the BM during embryogenesis (Aiuti et al., 1999, Aiuti et al., 1997, D'Apuzzo et al., 1997). Mice lacking either CXCL12 or CXCR4 die perinatally, i.e. at or around birth, and exhibit marked defects in B lymphopoiesis, myelopoiesis, cardiac development and cerebellar development (Ma et al., 1998, Nagasawa et al., 1996, Tachibana et al., 1998, Zou et al., 1998). The ligand/receptor pair may also be involved in early T cell development (Hernández-López et al., 2002) and are involved in B and T cell homing to LN and Peyer’s patches (Okada et al., 2002). However, it has also been shown to be involved in neutrophil recruitment and survival in a model of lung inflammation, and is also known to be involved in metastasis of a variety of tumours (Raman et al., 2011, Yamada et al., 2011, Zlotnik, 2006). Other examples of “homeostatic” chemokines include CCL19 and CCL21, which signal through CCR7, and

CCL25, which signals through CCR9. These chemokine/receptor pairings are particularly relevant to this thesis and will be explored in depth later in this Introduction.

There are a plethora of examples of “inflammatory” chemokines, expressed during the early response to infection. The complexity and exquisite regulation of leukocyte movement through chemokine/chemokine receptor interactions is apparent in the array of chemokines upregulated during inflammation to direct the required cell to the affected tissue at the appropriate stage of the response. Expression of a variety of CXC chemokines, including CXCL1, CXCL2, CXCL5 and CXCL8, attracts neutrophils into infected tissue, with MMP cleavage involved in increasing the potency of many of these chemokines and amplifying the level of neutrophil influx (Soehnlein and Lindbom, 2010, Tester et al., 2007, Van den Steen et al., 2000). Monocytes are directed into the inflamed tissue by production of CC chemokines such as CCL2-4, CCL6-9, CCL15 and CCL20, as well as CXCL8, where they differentiate into macrophages and DCs (Berahovich et al., 2005, Soehnlein and Lindbom, 2010, Soehnlein et al., 2009). Immature DCs are also recruited to inflamed tissue by many of these chemokines (Luster, 1998, Olson and Ley, 2002). When activated, they alter their chemokine receptor profile to home to the draining lymph node, as described later in this chapter. Tissue-specific inflammatory responses are also mediated by distinct patterns of chemokine expression – for example, expression of CCR3 ligands induces recruitment of basophils into lungs during allergy-induced inflammation, and CCL2 and CCL5 expressed in the lungs are believed to induce basophil and mast cell degranulation during asthma (Lukacs and Tekkanat, 2000, Olson and Ley, 2002).

1.5 Chemokine receptors

Chemokine receptors are members of the super-family of G-protein coupled receptors, forming part of the rhodopsin family of GPCRs, the largest of five GPCR families described (Oldham and Hamm, 2008). GPCRs are membrane-associated receptors and comprise the largest family of such molecules described to date. They share a common structure of seven transmembrane domains, an extracellular amino-terminus, an intracellular carboxy-terminus, three extracellular loops and three intracellular loops. Important features of chemokine receptors, which are around 40kDa in size, include the DRY motif of the second intracellular loop, which is common to members of the rhodopsin family of GPCRs, and the various phosphorylation sites at the C-terminus. Both features are involved in coupling to G proteins for ligand-induced signalling (Murphy et al., 2000, Oldham and Hamm, 2008). Additionally, chemokine receptors, and other GPCRs, have been shown to homo- and hetero-oligomerise, with this capacity thought to influence

signalling events following ligand binding (Liu et al., 1998, Milligan, 2004, Thelen et al., 2010). Importantly, some “atypical” chemokine receptors have been described that do not appear to signal upon ligand binding, and these will be described in detail later in this Introduction.

1.5.1 Signalling through GPCRs.

Classical GPCR signalling involves transmission of a signal (such as that provided by ligand binding to receptor) through G protein heterotrimer activation. The heterotrimer consists of a complex of α , β and γ subunits. Guanosine diphosphate (GDP) bound to the $G\alpha$ subunit renders the complex inactive until the associated receptor binds its ligand. The resulting conformational change in the receptor leads to release of GDP from the $G\alpha$ subunit and formation of a stable complex between the receptor and G protein. This high affinity interaction is then destabilized by rapid binding of guanosine triphosphate (GTP), which is abundant in the cell, to the $G\alpha$ subunit. The activated $G\alpha$ -GTP subunit and $G\beta\gamma$ subunit (composed of $G\beta$ and $G\gamma$ bound together) can now interact with various downstream targets to bring about the desired changes in the cell authorized by the initial receptor-ligand binding event. The signal ends with the hydrolysis of GTP to GDP by the $G\alpha$ subunit, which contains a GTPase domain (Oldham and Hamm, 2008). The $G\alpha$ -GDP subunit reforms its complex with the $G\beta\gamma$ subunit, forming an inactive G protein complex that is now available to interact with receptors once more. These events are summarized in Figure 1.5.

It is difficult to provide a clear overview of the mechanisms involved in chemokine receptor signalling, as the pathways induced and outcomes generated are context, cell type, receptor and ligand-dependent. However, some studies have provided important insights into the specific mechanisms of chemokine receptor signalling. Members of both the CCR and CXCR families have been shown to associate with members of the Janus kinase/signal transducer and activator of transcription (JAK/STAT) family, in both transfected cells and *in vivo* (Mellado et al., 1998, Mellado et al., 2001, Rivas-Caicedo et al., 2009, Rodríguez-Frade et al., 2001, Soriano et al., 2002, Soriano et al., 2003, Stein et al., 2003, Vila-Coro et al., 1999, Wong and Fish, 1998). It is thought that ligand binding leads to activation of JAK proteins, possibly through receptor oligomerisation, which phosphorylate tyrosine (Tyr) residues in the cytoplasmic loops and C-terminal tail of the receptor. For example, JAK2 is believed to phosphorylate the Tyr residue of the DRY motif of CCR2, with phosphorylation of this residue critical for subsequent signalling in transfected cells

(Mellado et al., 1998). Similarly, CCR5 in transfected cells couples to JAK1 upon binding of CCL5 and is Tyr phosphorylated, followed by binding of STAT-5b to the receptor, with the STAT protein becoming Tyr phosphorylated and activated (Rodríguez-Frade et al., 1999, Wong and Fish, 1998, Wong et al., 2001). CXCL12 binding to CXCR4 prompts JAK1 and JAK2 activation and association with the receptor, with subsequent phosphorylation and activation of various STAT proteins that associate with the receptor (Vila-Coro et al., 1999, Zhang et al., 2001). In the case of CCR2, blocking the action of JAK2 prevents $G\alpha_i$ association with the receptor and disrupts subsequent signalling, suggesting that JAK activity is important in chemokine receptor signalling (Mellado et al., 1998).

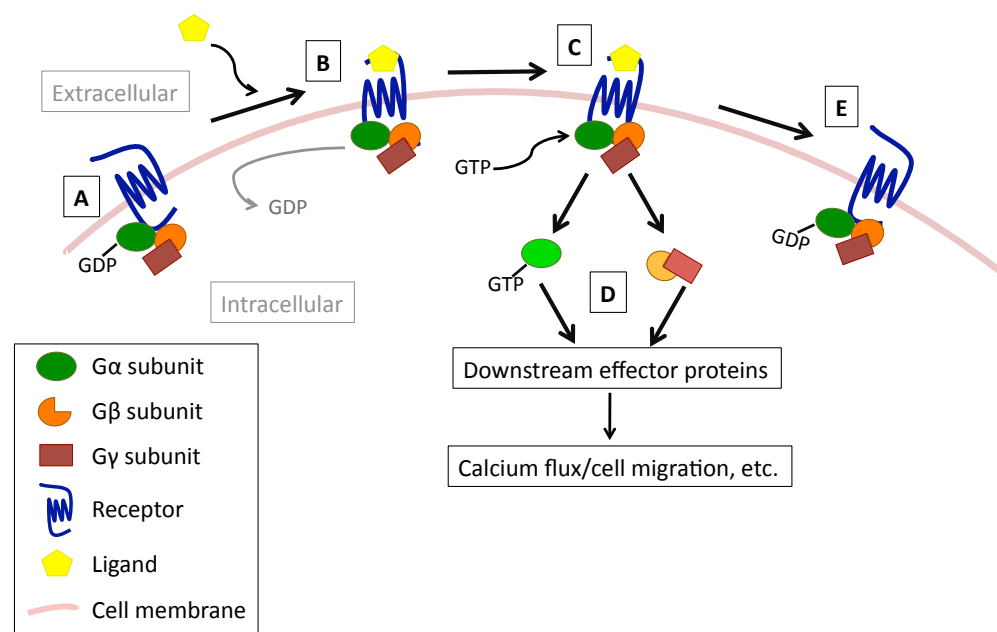


Figure 1.5: Receptor-ligand binding leads to G protein activation and downstream signaling events. (A) In the resting state, the G protein heterotrimer is associated with the membrane-spanning receptor. GDP is bound to the $G\alpha$ subunit. (B) Upon ligand binding, GDP is released from the $G\alpha$ subunit and the G protein heterotrimer forms a stable complex with the receptor. (C) This complex is rapidly disrupted when GTP binds to the $G\alpha$ subunit, leading to (D), the activation of G protein subunits $G\alpha$ -GTP and $G\beta\gamma$ and their subsequent activity on downstream effector proteins. $G\alpha$ -GTP may re-associate with the receptor in a JAK-dependent manner (not shown). (E) The $G\alpha$ subunit, which contains a GTPase domain, hydrolyses GTP to GDP and rebinds a $G\beta\gamma$ subunit, forming the inactive G protein heterotrimer that can again form a complex with a membrane-spanning receptor. Not shown – internalisation of the receptor/ligand complex and recycling of the receptor to the cell surface (believed to occur in chemokine/receptor interactions).

Of the four G protein subtypes (G_s , $G_{i/o}$, $G_{q/11}$ and $G_{12/13}$), cell migration is primarily facilitated through $G_{i/o}$ activation, although other subtypes have also been implicated, and cell type and oligomerisation state are thought to influence the subtype engaged (al-Aoukaty et al., 1996, Arai and Charo, 1996, Cotton and Claing, 2009, Rodríguez-Frade et al., 2001, Tan et al., 2006). The various α subunits of this G protein subtype are all

susceptible to pertussis toxin (Ptx), which causes an irreversible block to receptor coupling to the α subunit (Cotton and Claing, 2009, Kaslow and Burns, 1992) and thereby disrupts signalling through the receptor. This feature has provided a useful tool for chemokine biologists trying to unravel the mechanism by which chemokines and their receptors mediate immunological events. In the case of chemokine-induced cell migration, signalling through the G_i subtype is, again, not clear-cut. Migration of a CXCR4-expressing cell line in response to CXCL12 has been shown to be dependent on G_i proteins, which activate phosphatidylinositol-3-kinase (PI3K) following CXCL12 binding to CXCR4 (Curnock et al., 2003, Dutt et al., 1998). PI3K activity has a demonstrated role in chemotaxis in response to chemokines, and leads to the generation of phospholipids that accumulate at the leading edge of motile cells and are involved in activation of Rho GTPases and other downstream effectors (Curnock et al., 2003, Fischer et al., 2004, Mellado et al., 2001, Rickert et al., 2000, Sotsios et al., 1999). However, study of mice lacking either $G\alpha_{i2}$ or $G\alpha_{i3}$, which are both present in T cells, has shown that, while $G\alpha_{i2}$ is required for CXCR3-mediated T cell migration, $G\alpha_{i3}$ appears to inhibit migration, with T cells deficient in $G\alpha_{i3}$ exhibiting a marked increase in migration to CXCR3 ligands (Thompson et al., 2007). Therefore, the precise steps involved in G_i -dependent chemokine-triggered cell migration remain to be elucidated.

As mentioned earlier, chemokine receptor signalling does not occur solely through G_i proteins. Signalling through the G_s subtype leads to adenylate cyclase activation and cAMP production, while signalling through G_q leads to phospholipase C activation and the generation of inositol tri-phosphate (IP3) and diacyl glycerol (DAG) from membrane phosphatidyl inositol biphosphate (PIP2). This in turn leads to increased intracellular calcium levels through IP3 receptor binding and phosphorylation of calmodulin and other downstream effector molecules through DAG-mediated protein kinase C (PKC) activation. Both subtypes have been implicated in cell migration, albeit not through chemokine receptor signalling (Cotton and Claing, 2009). Signalling through $G_{12/13}$ leads to modulation of the actin cytoskeleton through activation of small GTP-binding proteins, and has been shown to be involved in directional migration of cells in response to CXCL12 binding to CXCR4 (Cotton and Claing, 2009, Tan et al., 2006).

1.5.2 Internalisation and desensitisation of chemokine receptors

Following activation of a GPCR through ligand binding, the receptor is typically internalised and either recycled back to the cell surface, where it can again interact with its ligand, or targeted for lysosomal degradation. The fate of the receptor following

internalisation plays a pivotal role in deciding the strength and duration of the signal received. Desensitisation can also include downregulation of receptor synthesis, leading to a drop in surface expression of the receptor (Claing et al., 2002, Grady et al., 1997). Different ligands can induce very different responses through the same receptor, as described for CCR7 later in this chapter (Bardi et al., 2001, Byers et al., 2008).

Receptor phosphorylation is an important feature of desensitization. Receptors are phosphorylated either by intracellular second messenger regulated kinases (such as protein kinase A (PKA) or PKC) or by G protein coupled receptor kinases (GRKs). The former class of kinases can act either to desensitize the activated receptor itself, i.e. “homologous” desensitization, or to desensitize another, inactive receptor, i.e. “heterologous” desensitization. GRKs, on the other hand, phosphorylate only ligand-bound receptors, which in itself is not sufficient to cause desensitization. Instead the phosphorylation event creates high affinity sites to which arrestins can bind and block future interactions with G proteins (Claing et al., 2002, Cotton and Claing, 2009, Gainetdinov et al., 2004, Hausdorff et al., 1990, Vroon et al., 2006). Of the four members of the arrestin family, the two identified β -arrestins (β -arrestin1/arrestin-2 and β -arrestin2/arrestin-3) are thought to be those most involved in this form of receptor desensitization, as well as playing a role in internalisation of receptors. They are recruited to the plasma membrane following GRK phosphorylation of ligand-bound receptors, with which they co-localise (Claing et al., 2002, Cotton and Claing, 2009, Gainetdinov et al., 2004).

The two best characterized internalisation pathways for GPCRs are via either clathrin-coated pits or caveolae, and are generally β -arrestin-dependent and independent respectively. β -arrestins interact with clathrin both directly through its heavy chain and via the clathrin adaptor protein AP-2 (Claing et al., 2002, Laporte et al., 2000, Wolfe and Trejo, 2007). Whether these interactions bring about formation of clathrin-coated pits, or occur with preformed pits is unclear. However, it is believed that the interaction with AP-2 mediates initial targeting of the receptor to clathrin-coated pits, where direct interaction between β -arrestins and clathrin may serve to stabilize the complex within the forming vesicle (Claing et al., 2002). β -arrestins also interact with various other endosomal components and the avidity of β -arrestin binding to the GPCR can influence the length of time taken for the receptor to be recycled to the cell surface (Lefkowitz and Shenoy, 2005). To complete the formation of the vesicle, dynamin is recruited. This large GTPase forms a “collar” around the neck of the budding vesicle and constricts it, followed by GTP hydrolysis, dissociation of the dynamin oligomer and complete fission of the vesicle

membranes (Pawlowski, 2010). The clathrin-coated vesicle then fuses with endosomal vesicles, leading to one of two outcomes for the ligand-bound receptor - either dissociation of the ligand from the receptor, followed by receptor dephosphorylation and recycling to the cell surface, or targeting of the receptor to the lysosomal compartment, where it is degraded. In the case of recycling to the cell surface, as mentioned above, the rate at which this occurs varies between receptors. The fate of the receptor may depend on C-terminal sequences in the receptor itself (Claing et al., 2002, Lefkowitz and Shenoy, 2005).

The best characterized clathrin-independent internalisation pathway occurs via caveolae. Caveolae are flask-shaped, lipid-rich invaginations in the plasma membrane that contain cholesterol-binding proteins called caveolins (Nichols and Lippincott-Schwartz, 2001, Parton and Simons, 2007, Pelkmans and Helenius, 2002). These oligomeric membrane proteins appear to cause formation of and/or stabilize caveolae at the cell surface (Nichols and Lippincott-Schwartz, 2001, Pelkmans et al., 2004, Thomsen et al., 2002). Caveolae also contain dynamin, the GTPase involved in budding of clathrin-coated vesicles, although some studies suggest this is a transient association. Dynamin appears to play a similar role in caveolae as in clathrin-coated vesicles, “pinching” closed the neck of the caveosome (Henley et al., 1998, Nichols and Lippincott-Schwartz, 2001, Parton and Simons, 2007, Pelkmans and Helenius, 2002). While less common as a mode of GPCR internalisation, caveolae have nevertheless been shown to be used by a number of chemokine receptors in addition to clathrin-mediated pathways, including CCR2, CCR4 and CCR5 as well as the atypical chemokine receptors, Duffy antigen receptor for chemokines, or DARC, and CCX-CKR (Borroni et al., 2010, Chaudhuri et al., 1997, Comerford et al., 2006, Pruenster et al., 2009). An important caveat of these findings, and of our knowledge of chemokine receptor internalisation and desensitization in general, is that, in the main, they rely on data from transfected cell lines and may therefore provide a restricted view of the potential complexity of chemokine receptor regulation *in vivo*.

1.5.3 Chemokine/receptor interactions

Chemokine receptors, like chemokines, can be broadly grouped as constitutive or inflammatory, based on when and where they are active. There is a high degree of promiscuity in the chemokine/receptor interactions, with most receptors capable of binding a range of chemokines and most chemokines interacting with more than one receptor (see Table 1.1). This is particularly the case for inflammatory chemokines and their receptors – for example, CCR5 binds at least 9 CC chemokines, while one of its ligands, CCL5, also binds CCR1 and CCR3 as well as the “atypical” receptors D6 and DARC, which are

discussed below (Hansell et al., 2011a). While most chemokines bind receptors within their own “class”, i.e. CC chemokines bind CCRs, CXC chemokines bind CXCRs, etc., there are a number of exceptions to this, with some chemokines and receptors capable of binding more than one class. For example, as shown in Table 1.1, CCR3, which binds multiple CC chemokines, also binds CXCL9-11 while CCL11 and CXCL9-11 are all capable of binding CXCR3. CCL26, which binds CCR1-3 and CCR5, has recently been shown to also bind CX₃CR1 (Loetscher et al., 2001, Nakayama et al., 2010, Pan et al., 2000, Xanthou et al., 2003). Thus, there is a high level of complexity in the interactions of chemokine and their receptors. While some have taken this to indicate redundancy in the system, a view supported by many *in vitro* studies, there are suggestions that *in vivo* it points towards an incredibly fine-tuned and exquisitely regulated system of directed cell migration, both in the immune system and throughout development (Devalaraja and Richmond, 1999, Johnson et al., 2005, Mantovani, 1999).

In comparison to this tangle of interactions by inflammatory chemokines and receptors, constitutive chemokine receptors bind only one or two constitutive chemokines, which in turn are relatively faithful to this pairing. For example, CCL19 and CCL21 bind to CCR7 and are its only known ligands (Cyster, 2005, Förster et al., 2008), while CCL25 has been shown to bind only one classical receptor, CCR9, which in turn binds no other ligands (Cyster, 2005). However, for all three of these ligands an “atypical” receptor has been identified called CCX-CKR, which binds each ligand without apparent subsequent intracellular signalling in transfected cells (Gosling et al., 2000, Townson and Nibbs, 2002). This receptor, and the pattern and purpose of its expression, is the focus of my thesis.

1.6 Identification and early characterisation of CCR7, CCR9 and their ligands

To enable the reader to understand the context in which CCX-CKR was discovered and is believed to function, it is necessary to describe the ligands it binds and the receptors they are known to signal through. In the mouse, CCX-CKR has three known ligands; CCL19 and CCL21, which signal through CCR7; and CCL25, which signals through CCR9. In humans, CCX-CKR also binds weakly to CXCL13, the ligand for CXCR5. However, as the work in this thesis is related to the murine receptor, I will describe in this section the discovery and expression of CCR7 and CCR9 and their ligands, followed by, in section 1.7, a description of how these receptor/ligand partners are believed to function in the

immune system. I will then present an overview of our current understanding of “atypical” chemokine receptors, the loosely related family to which CCX-CKR belongs, before describing what was known about CCX-CKR prior to this project, including its discovery and potential activity, as uncovered through *in vitro* studies.

1.6.1 CCR7 identification and expression

CCR7 was first identified in the early 1990s as an Epstein-Barr virus (EBV)-induced G protein coupled receptor, as predicted from its nucleotide sequence. It was identified following a screen of genes upregulated in cultured Burkitt’s lymphoma cells after EBV infection, and was designated EB11 until the introduction of systematic nomenclature for chemokine receptors. It was cloned shortly after its discovery, and posited to act as a chemokine receptor, as it shared gene structure and sequence features with other known chemokine receptors and the human gene was encoded in the same chromosomal region as various other CC chemokine receptors (Birkenbach et al., 1993, Schweickart et al., 1994). It remained an “orphan” receptor until the discovery of its chemokine ligands CCL19 and CCL21. The first studies investigating expression of the receptor found it to be restricted to lymphoid tissues and B- and T-lymphocyte cell lines (Birkenbach et al., 1993, Schweickart et al., 1994). Subsequent work determined that CCR7 is expressed by naïve B and T lymphocytes, with T cell entry into LN almost completely ablated in CCR7 deficient mice and B cell entry also decreased, albeit to a lesser degree (Förster et al., 1999). Studies with transgenic mice expressing a specific antigen receptor revealed that the receptor is upregulated on activated B cells and promotes their interaction with T cells through migration towards the T cell zone of lymphoid tissue (Reif et al., 2002). CCR7 expression also distinguishes central memory T (T_{CM}) cells from effector memory T (T_{EM}) cells - antibody staining revealed that T_{CM} cells express the receptor and traffic through secondary lymphoid tissues like naïve T cells until restimulated, while T_{EM} cells do not express CCR7 and home to inflamed tissues to exert their effector functions (Sallusto et al., 1999a). Regulatory T cells have been shown to express high levels of CCR7 mRNA and migrate to CCL19 and CCL21 in transwell chemotaxis assays (Szanya et al., 2002). CCR7 is also found on thymocyte subsets, depending on their stage of development (described later) (Misslitz et al., 2004), and is expressed at the mRNA level by mature DC, which exhibit calcium flux upon stimulation with CCR7 ligands, indicating surface protein expression also (Sallusto et al., 1998). It has also been shown to be responsible for migration of “semi-mature” DCs from skin to the LN, with CCR7-deficient mice lacking this population in the skin-draining LN (Ohl et al., 2004). More recent work using immunohistochemistry and Western blotting with anti-CCR7 antibody has indicated that the receptor is expressed by

astrocytes, and is upregulated during inflammation (Gomez-Nicola et al., 2010). It has also been reported to be expressed by a subset of neutrophils from both humans and mice, as shown by antibody staining and flow cytometry. In mice, this subset migrates to the lymph node in a CCR7-dependent manner following induction of inflammation, where they may influence the adaptive immune response through interaction with DCs and/or T cells (Beauvillain et al., 2011). CCR7 is also expressed by other non-immune cells, including tumour cells, which are believed to use the receptor to mediate metastasis to LN (Förster et al., 2008, Shields et al., 2007). Constitutive mRNA and protein expression of CCR7 by mesangial cells in the glomerulus of the human kidney has been demonstrated, suggesting a role in the homeostatic function of the kidney (Banas et al., 2002). Thus, CCR7 plays a central role in the development and homeostatic function of the immune system, as well as being required for efficient adaptive immune responses and potentially homeostatic functions of non-immune tissues.

1.6.2 CCL19 and CCL21 – identification, expression and interaction with CCR7

Human CCL19 and CCL21 were both identified from expressed sequence tag (EST) database mining in 1997, four years after the discovery of CCR7 (Nagira et al., 1997, Rossi et al., 1997, Yoshida et al., 1997). Rossi and colleagues found mRNA for the chemokine now known as CCL19 to be expressed in lymph node, thymus and appendix. It was expressed by activated monocytes and was designated **macrophage inflammatory protein (MIP)-3 β** (Rossi et al., 1997). Yoshida and colleagues also found it to be highly expressed in lymph node and thymus, with intermediate level expression in colon, trachea and spleen and low-level expression in a variety of tissues, including kidney, lung and small intestine. Using purified tagged CCL19, they also found that it was a ligand for CCR7, or EB11, as it bound preferentially to cells transfected with this but not other chemokine receptors. It also induced calcium flux and chemotaxis in CCR7-transfected cells. They therefore named it **EB11-ligand chemokine, or ELC** (Yoshida et al., 1997). Murine ELC/CCL19 was identified shortly after and found to act as a potent chemoattractant to CD8⁺ T cells and naïve CD4⁺ T cells, as well as being weakly attractive to memory CD4⁺ T cells and naïve B cells. At concentrations of 100ng/ml, CCL19 caused transwell migration of 60-80% of input CD8⁺ and naïve CD4⁺ T cells, compared to 20-30% of B cells and memory CD4⁺ T cells (Ngo et al., 1998). Upon stimulation with anti-IgM or LPS, B cells became more responsive to the chemokine, with an increase in migrating cells from about 20% of input to about 40%. This study also used *in situ* hybridisation, Northern blot analysis and RT-PCR to demonstrate that CCL19 was expressed by DCs in secondary lymphoid tissues,

including LN, Peyer's patches and spleen, but not in other leukocytes or in HEVs. Calcium flux assays with transfected cells showed that, as in humans, murine CCL19 was a functional ligand of CCR7 (Ngo et al., 1998). Further examination of chemokine expression by human DCs, using RT-PCR, found CCL19 was only expressed in LPS-activated DCs at late timepoints, but not by immature DCs (Sallusto et al., 1999b). Luther and colleagues found expression of the murine chemokine in splenic stroma (i.e. cells positive for gp38 expression) as well as in DCs, particularly CD8⁺ DCs. The same study used *in situ* hybridization to demonstrate that HEVs did not express CCL19, although they did express CCL21, suggesting that CCL19 was not involved in recruitment of leukocytes into LNs from the blood (Luther et al., 2000). However, a subsequent study showed that CCL19 protein was transcytosed from its site of expression in the lymph node to the lumen of HEVs and promoted recruitment of T cells into the LN. This same study found that CCL19 injected into the murine footpad drained to the LN and was presented by HEVs there, and intracutaneous injection of CCL19 into *plt/plt* (paucity of lymph node T cells) mice, which lack LN-expressed CCR7 ligands, restored migration of T cells to the draining LN (Baekkevold et al., 2001). One recent study has suggested that CCL19 is also a ligand for a newly described atypical chemokine receptor, CRAM-B, with similar affinity as for CCR7, a finding that merits further investigation (Leick et al., 2010). Current knowledge of the expression and function of CRAM will be discussed later in this chapter.

Nagira and colleagues described the mRNA of human CCL21 as encoding a protein predicted to contain not only the four definitive Cys residues of the CC chemokine family, but also a further two Cys residues in its carboxy (C)-terminus (Nagira et al., 1997). They found high levels of mRNA expression in spleen, lymph node and appendix, and demonstrated that the recombinant protein served as a strong chemoattractant to lymphocytes freshly isolated from human peripheral blood. The novel chemokine was designated secondary lymphoid tissue chemokine, or SLC (Nagira et al., 1997). Hedrick & Zlotnik, separately describing the same chemokine, found it to be highly conserved between humans and mice, and found a similar mRNA expression pattern in humans as described by Nagira et al. The mRNA expression pattern in mice was somewhat different, with high levels found in spleen and lung as well as robust expression in kidney, testis, heart and liver (Hedrick and Zlotnik, 1997). In their hands, the recombinant chemokine was chemoattractant for thymocytes and IL-2-activated T cells but not for other leukocytes, including B cells, "resting" T cells (i.e. unstimulated primary cells cultured overnight in media) and macrophages. The reason for this is unclear, as subsequent studies have found that naïve T cells in particular are highly responsive to CCL21. However, it may reflect the importance of specific post-translational modification of the protein, as the

recombinant protein used in this study was expressed in *Escherichia coli* (*E. coli*). It may alternatively point to the importance of appropriate presentation of chemokine for receptor binding or activation (see above for the role of GAGs in chemokine presentation). They named the protein 6Ckine, in reference to its unusual six Cys residues, and hypothesized that the extra two Cys residues, found in the extended C terminus of both the human and mouse protein, were involved in stabilizing the tertiary structure of the C-terminal tail (Hedrick and Zlotnik, 1997). In another separate study reported in the same year, Tanabe and colleagues described a novel murine chemokine that was highly expressed in thymus, which was designated thymus-derived chemotactic agent (TCA)-4. Northern blotting showed high levels of mRNA expression in thymus, with expression also found in spleen, kidney, heart and lung. This chemokine, now known to be murine CCL21, contained six Cys residues as described in the human chemokine and an extended, highly basic C-terminal tail (Tanabe et al., 1997). Two forms of the gene have been described in the mouse, encoding two forms of the chemokine differing by one amino acid (Vassileva et al., 1999). CCL21 mRNA expression has been reported in various secondary lymphoid tissues in humans (Willimann et al., 1998) and was found in high endothelial venules (HEVs) of lymph nodes and Peyer's patches in mice, as well as in T cell zones of murine secondary lymphoid tissue and in lymphatic endothelium in liver and small intestine (Gunn et al., 1998). Further investigation of the two murine CCL21 proteins described has shown that CCL21-ser, which has a serine residue at position 65, is expressed in lymphoid tissues, while CCL21-leu, which carries a leucine residue at this position, is found in non-lymphoid tissue including heart, stomach, colon and lung (Luther et al., 2000, Vassileva et al., 1999). This analysis was facilitated by investigation of a spontaneous mutant mouse strain named *plt/plt*, described in more detail below. CCL21 was shown to bind to and signal through CCR7, albeit with lower affinity than CCL19, leading to early proposals that both chemokines might, through CCR7, be involved in homeostatic lymphocyte recirculation (Campbell et al., 1998, Willimann et al., 1998, Yoshida et al., 1998). Campbell and colleagues also refer to the unpublished observation by A. Zlotnik of potential signalling by CCL21 through CXCR3, which is expressed on T helper (T_H)1 cells. Soto and colleagues subsequently reported the induction of calcium flux in CXCR3-transfected human embryonic kidney (HEK) cells by murine CCL21. The affinity of CCL21 for CXCR3 was lower than that of the CXCR3 ligands CXCL9 and CXCL10, which could desensitise cells to CCL21, whereas CCL21 could only partially desensitise responsiveness to these ligands (Campbell et al., 1998, Soto et al., 1998). This finding has been supported by subsequent studies suggesting CCL21 can trigger activation and chemotaxis of human and murine microglia through CXCR3 (Campbell et al., 1998, de

Jong et al., 2005, Dijkstra et al., 2004, Rappert et al., 2002). A more recent study also describes a role for CCL21 in CXCR3-mediated astrocyte activation in the mouse (van Weering et al., 2010). This may indicate an alternative means for CCL21 to exert its influence in the brain. However, other work has shown that human CCL21 does not function as a ligand for CXCR3, indicating possible species specificity of the reported interaction and leaving the possible function of such a ligand/receptor pairing unclear (Jenah et al., 1999).

Comparison of human CCL19 and CCL21 show that the two ligands only share about 32% amino acid identity, with CCL21 containing an extended C-terminal tail of approximately 32-35 residues (Tanabe et al., 1997, Yoshida et al., 1998). This unusual extension of the C-terminal tail of CCL21 is believed to promote binding to GAGs to facilitate appropriate presentation of the chemokine to cells. CCL21 binds much more strongly to GAGs than CCL19, and truncation of the C terminus of the protein resulted in failure of the chemokine to bind normally to chondroitin sulfate, a GAG shown to bind avidly to full-length CCL21. This truncation did not diminish the ability of CCL21 to signal through CCR7, as determined by calcium flux (de Paz et al., 2007, Hirose et al., 2002). An elegant recent study has shown that full-length CCL21 that was immobilized, either in sections of murine LN or in a synthetic system, activated integrin-mediated adhesion of DCs, followed by haptokinesis (i.e. random adherent migration) along the surface on which the chemokine was immobilized. Directional migration of both adhered and non-adhering cells was promoted by soluble chemokine, either CCL19 or a cleaved form of CCL21 that lacked the extended C terminus. This cleaved form of CCL21 was generated by mature DCs following interaction with full-length CCL21, but not by other leukocytes, including B and T cells. These findings provide some insight into the requirement for both an immobilized and a soluble ligand for CCR7 in the LN (Schumann et al., 2010).

The binding affinity for CCR7 is approximately similar for the two human chemokines, with CCL19 showing marginally higher affinity binding to the receptor on transfected cells (Ott et al., 2006). Binding of CCR7 by the two ligands leads to some differences in outcome. While both induce calcium flux and chemotaxis in CCR7⁺ cells, CCL19 causes rapid internalisation of the receptor and desensitizes it to further stimulation by either ligand on human peripheral blood leukocytes, transfected HEK cells and H9 cells expressing endogenous CCR7 (Bardi et al., 2001, Kohout et al., 2004). This desensitization has been attributed to receptor phosphorylation and the recruitment of β -arrestins, at least in transfected HEK cells (Kohout et al., 2004). In contrast, CCL21 does not strongly induce receptor internalisation and resensitisation of cells occurs readily (Bardi et al.,

2001). Internalisation was induced at much lower concentrations of CCL19 than CCL21, and was found to be clathrin dependent (Byers et al., 2008, Otero et al., 2006). The endocytosed receptor is recycled to the cell surface, although this occurs more rapidly after CCL21 ligation than CCL19 binding (Byers et al., 2008, Otero et al., 2006). Internalised CCL19 was shown to be directed to lysosomes for degradation (Otero et al., 2006). Murine CCL19 has also been shown to induce more receptor internalisation and desensitization of murine CCR7 than CCL21 on primary mouse leukocytes (Britschgi et al., 2008). The observed differences in ligand effect on the receptor, combined with variation in expression patterns of the two ligands, suggests that CCL19 and CCL21 may carry out distinct, non-redundant functions through CCR7 ligation. The recent work by Schumann and colleagues supports this notion, while also presenting the possibility that soluble (i.e. cleaved) CCL21 might act more like CCL19 than full-length CCL21 (Schumann et al., 2010). Additionally, CCL19 has been shown to have a role in T cell homeostasis, one that is not compensated for by CCL21. When prevented from entering LN, T cell survival is diminished. Generation of a CCL19-deficient mouse showed that, in the absence of CCL19, homeostasis of naïve T cells is disrupted. CCL19 was shown to be coexpressed with IL-7 by fibroblastic reticular cells (FRCs) of the T cell zone, and the two proteins (CCL19 and IL-7) had similar effects on T cell survival *in vitro*. However, the effect of IL-7 was more profound *in vivo*, leaving the precise role of CCL19 in T cell homeostasis unclear (Link et al., 2007).

1.6.3 Lacking CCR7 ligands – *plt/plt* mice

In 1993, Nakano et al described a spontaneous mutant mouse strain that had notably reduced lymph node cellularity (Nakano et al., 1993). Further investigation of the phenotype of these mice revealed that T cell numbers in lymph nodes were markedly reduced, especially in peripheral lymph nodes. B cell numbers were somewhat reduced in peripheral lymph nodes but were unaffected elsewhere. T cell numbers in spleen and peripheral blood were increased, while Peyer's patch T cell numbers were unchanged (Nakano et al., 1997). The ability of T cells to adhere to HEVs, known to be their point of entry into the lymph node, was not disrupted, with L-selectin and PNAd expressed and functioning as normal. The effect was determined to be due to a defect in stromal cells rather than in the lymphocytes themselves, and recruitment rather than retention of T cells was disrupted (Nakano et al., 1997). The defect was mapped to a single genomic location, later reported to be the locus carrying the genes encoding CCL19 and CCL21 (Gunn et al., 1999, Nakano et al., 1997).

Subsequent analysis of these mice led to demonstration that CCL21 mRNA was absent from lymphoid tissue of *plt/plt* mice, as well as showing decreased CCL19 expression. A defect in DC homing to LNs was also observed – the importance of CCL19, CCL21 and CCR7 in DC migration to LN is discussed in detail later in this chapter (Gunn et al., 1999). The reported absence of CCL21 from *plt/plt* mice was later found to be due to a lack of one of the two forms of CCL21 expressed in mice, specifically the CCL21-ser form found predominantly in lymphoid tissue of normal mice, while the other, predominantly non-lymphoid form was still present (Vassileva et al., 1999). Work by Luther and colleagues showed that functional CCL19 mRNA was also absent from *plt/plt* mice, with previous detectable levels of mRNA for this chemokine attributed to non-functional pseudogenes (Luther et al., 2000). For over a decade, this mouse strain has proven an invaluable tool in dissecting the role of CCR7 and its ligands in immune system development and function, and these studies are discussed below.

1.6.4 CCR9 and CCL25

Searches of murine cDNA libraries for novel chemokine sequences led to the identification of a CC chemokine that was strongly expressed in thymus, with high levels in small intestine and some expression in liver. Expression was also detected in spleen after LPS treatment. Named thymus-expressed chemokine (TECK), the human homolog was isolated soon after, with a similar expression pattern as observed in mice (Vicari et al., 1997). The study used *in situ* hybridisation, RT-PCR on purified cells and immunohistochemistry to identify thymic dendritic cells as the main source of the chemokine in the thymus, with bone-marrow derived DCs not found to express it. It was also suggested that the chemokine was likely to be involved in T cell development, given its expression pattern (Vicari et al., 1997). Two years later, a report identifying an orphan receptor GPR-9-6 as the receptor for TECK (CCL25) and designating it CCR9 was published, with both human and murine equivalents identified (Zaballos et al., 1999). Expression of CCR9 RNA was found to be strong in thymus and only weak expression was detected in spleen and lymph nodes, and both immature and mature thymocytes were found to express the receptor, further suggesting a role for CCR9/CCL25 in thymocyte development (Zaballos et al., 1999).

1.7 CCR7 and CCR9 in immune system development and function

As one might expect from the expression patterns of these receptors and their ligands, CCR7 and CCR9 are critical to a variety of processes of the immune system. In this section I will discuss their roles in thymocyte development, including the development of tolerance; the homing of lymphocytes and DCs to and within lymph nodes and spleen; and leukocyte homing to the small intestine. Where appropriate, I will also outline the roles of other key chemokines and chemotactic molecules in these processes.

1.7.1 Thymocyte development

As described earlier, haematopoietic stem cell derived precursors enter the thymus via blood vessels at the cortico-medullary junction (CMJ). These cells are CD4⁻ and CD8⁻ and are therefore termed **double-negative (DN)** cells. They also lack CD25, the α -chain of the IL2 receptor, but express high levels of CD44, a cell adhesion molecule (Nitta et al., 2008). The signals involved in the process of “seeding” the thymus are still under investigation – however, a number of molecules required for the process have been reported. CCL21 and CCL25 have both been shown to play a role in attracting thymic precursors into the thymus, with neutralizing antibodies to either chemokine shown to disrupt the process (Liu et al., 2005). In *plt/plt* mice, where CCL21-ser and CCL19 are absent, a marked defect in colonization of the thymus is made more pronounced by treatment with anti-CCL25 antibody, indicating that the three chemokines feature prominently in this process (Liu et al., 2005). Complementary studies, using single- and double-deficient mice, have shown that the classical receptors for these chemokines, namely CCR7 and CCR9, are both involved in thymic seeding. Numerous groups have indicated a role for CCR9 in the process, through investigation of the CCR9 deficient mouse, competitive adoptive transfer of WT and CCR9 deficient cells, and chemotaxis assays with purified thymocyte subpopulations (Liu et al., 2005, Schwarz et al., 2007, Scimone et al., 2006, Svensson et al., 2008, Wurbel et al., 2006). Liu and colleagues showed that both CCR7 and CCR9 are involved in seeding the foetal thymus (Liu et al., 2006), while the involvement of both receptors in recruitment of precursors to the adult thymus has also been reported, again through analysis of CCR7 and CCR9 single- and double-deficient mice (Krueger et al., 2010, Zlotoff et al., 2010).

Within the thymus, both receptors, along with CXCR4 and its ligand CXCL12, are required for proper development of maturing thymocytes, by regulating the correct

migration of maturing T cells from the cortex to the medulla (Davalos-Miszlitz et al., 2007b, Kwan and Killeen, 2004, Miszlitz et al., 2004) and for promoting exit of mature T lymphocytes from the thymus in newborn mice, a process that also involves S1P (Allende et al., 2004, Ueno et al., 2002). CCL19 and CCL21 are detectable in both the cortex, the CMJ and the medulla of the adult thymus, and CCL25 is ubiquitously expressed throughout the thymus by stromal cells of the medulla and cortex (Förster et al., 2008, Miszlitz et al., 2004).

Development of DN thymocytes is divided into four stages, termed DN1-4 (see Figure 1.6), which can be distinguished based on expression of CD25 and CD44. DN1 cells (CD25⁻ CD44^{hi}) become DN2 cells (CD25⁺ CD44^{hi}) cells, passing through a proposed intermediate stage called DN1-DN2 (CD25^{int} CD44^{hi}) (Miszlitz et al., 2004). This maturation from DN1 to DN2 occurs as the cells migrate from the CMJ to the mid-cortex, and may involve CCR7, which is expressed on approximately half of the DN1-DN2 cells compared to expression on only very low proportions of all other DN subsets. Indeed, lack of CCR7 leads to an accumulation of this cell type in the thymus and a delay in progression to DN2 (Förster et al., 2008, Miszlitz et al., 2004). Lack of CCR7 also leads to reduced numbers of DN3 (CD25^{hi} CD44^{low}) cells, presumably through disruption of maturation from earlier stages (Miszlitz et al., 2004). CCR9 does not appear to be strongly expressed prior to the DN3 stage, and is present on both DN3 and DN4 cells, with CCR9 expression by DN3 cells shown to be important for development to DN4 and subsequent stages through competitive transfer of WT and CCR9 deficient BM to reconstitute irradiated mice (Wurbel et al., 2006). These experiments also indicated that CCR9 expression is important at some earlier timepoint, since earlier subsets were also disrupted, even though they themselves did not display CCR9 expression (Wurbel et al., 2006).

From the DN4 stage, thymocytes migrate back toward the medulla, developing into double-positive (DP) cells that are CD4⁺ CD8⁺ CD69⁻. These cells are exposed to major histocompatibility (MHC) molecules associated with self peptides, which are expressed on thymic epithelial cells and thymic DCs. Depending on the strength of interaction with their TCR they are either selected for survival (weak interactions – positive selection) or deletion (strong interactions – negative selection) (Nitta et al., 2008, Smith et al., 1989). The importance of this stage in the development of central tolerance is discussed below. Positively selected DP cells then migrate to the medulla to undergo further maturation into single-positive (SP) cells, cells that are either CD4⁺ or CD8⁺ (Förster et al., 2008, Nitta et al., 2008). CCR9 is suggested to be involved in allowing cells to leave the subcapsular zone (SCZ) of the cortex and migrate back towards the medulla (Wurbel et al., 2006).

CCR7 is also expressed on a subset of DP cells, suggesting a role for this receptor in migration of these cells (Davalos-Misslitz et al., 2007b, Förster et al., 2008). SP cells mature during migration through the medulla, with immature SP cells expressing very little if any CCR7. Expression of the receptor increases as the cells mature and is required for the appropriate migration of matured thymocytes into the medulla, with fully mature $CD4^+$ and $CD8^+$ cells both expressing high levels of the receptor (Davalos-Misslitz et al., 2007b, Förster et al., 2008, Ueno et al., 2004). By contrast, CCR9 is not expressed by naïve $CD4^+$ cells but is present on naïve $CD8^+$ T cells, at least in the mouse (Wurbel et al., 2006). In humans, CCR9 expression by T cells is largely restricted to gut-homing memory $CD4^+$ and $CD8^+$ T cells (Kunkel et al., 2000, Zabel et al., 1999). The involvement of CCR7 and CCR9 in thymocyte development is outlined in Figure 1.6.

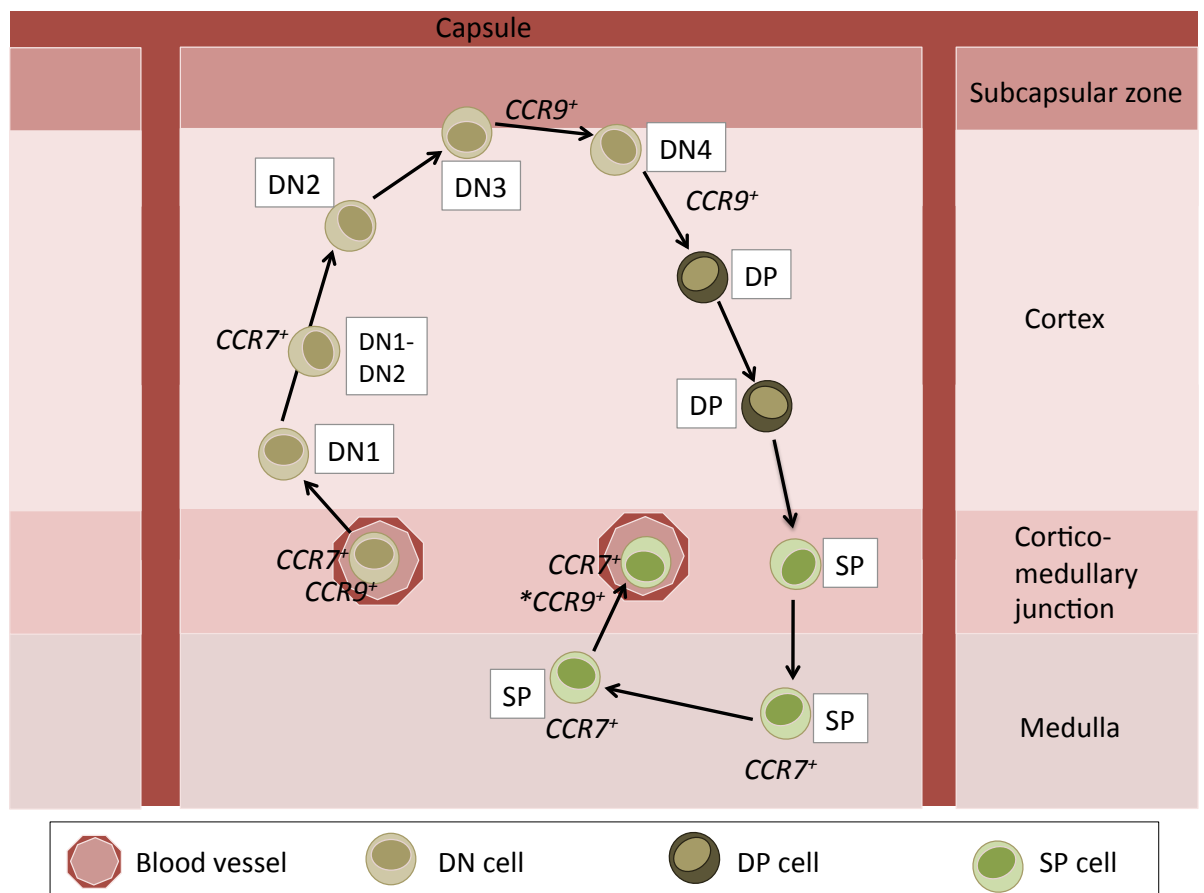


Figure 1.6: CCR7 and CCR9 in thymocyte development. Haematopoietic stem cell derived precursor cells enter the thymus via blood vessels in the cortico-medullary junction (CMJ), using CCR7 and CCR9. They migrate as double-negative (DN) cells towards the subcapsular zone, with a subpopulation of DN1-DN2 cells expressing CCR7 in the mid-cortex. DN3 cells begin to express CCR9, which is thought to facilitate the migration of the maturing thymocytes from the subcapsular zone (SCZ) through the cortex to the CMJ and medulla. Double-positive (DP) cells and immature single-positive (SP) cells interact with self-peptides and are either positively selected to mature further or deleted (negatively selected). SP cells start to upregulate CCR7 as they reach full maturity, with both $CD4^+$ and $CD8^+$ (SP) T cells expressing the receptor. CCR9 is only expressed by $CD8^+$ T cells, as denoted by *. Adapted from Förster et al., 2008.

S1P is a byproduct of sphingolipid turnover, and as such is thought to be produced by all cells during this process. It has been shown to be involved in the egress of mature thymocytes from the thymus. S1P₁, a receptor for S1P, is upregulated in mature thymocytes and egress of these cells from the thymus is disrupted in mice that specifically lack the receptor on T cells (Allende et al., 2004). In addition, Matloubian and colleagues used fetal liver chimeras and adoptive transfer of S1P₁ deficient lymphocytes to demonstrate that this receptor is required for egress of T cells from thymus and lymph nodes (Matloubian et al., 2004).

As described in this section and below, CCR7 and its ligands are crucial for appropriate directed migration of leukocytes during development, homeostasis and immune response. Unsurprisingly therefore, these molecules are central to the appropriate development of immunological tolerance, both central and peripheral. Although a detailed discussion of current knowledge of tolerance mechanisms is beyond the scope of this Introduction, I will provide a brief overview of the induction of central and peripheral tolerance before describing the importance of CCR7 and its ligands in tolerance induction.

As described above, on their journey through the cortex back to the medulla, developing DP T cells interact with complexes of self-peptide and MHC molecules presented by thymic dendritic cells and thymic epithelial cells. Those thymocytes that fail to interact or have very low affinity for the complexes die by neglect, failing to receive survival signals – approximately 90% of thymocytes die by this mechanism (Palmer, 2003). Thymocytes that are weakly reactive to self-peptide:MHC complexes are positively selected, that is, they are prompted to mature further into SP T cells. Thymocytes that are highly reactive to self-peptide:MHC complexes could lead to autoimmunity by targeting host tissues/cells and must therefore either be deleted or altered to remove this possibility. The main mechanism of this negative selection described is that of clonal deletion, where highly reactive T cells die by apoptosis. Alternatives to this mechanism include the induction of anergy, where the reactive T cell survives but cannot be stimulated to react to its cognate antigen, or receptor editing, as occurs with B cells (Hogquist et al., 2005). Some thymocytes that react too strongly to self-antigen are induced to differentiate into regulatory T (T_{reg}) cells, which are involved in suppression of autoreactivity in the periphery (Workman et al., 2009). Animals that carry a defective autoimmune regulator (*AIRE*) gene, or lack the gene entirely, develop multi-organ autoimmunity and clonal deletion is severely disrupted. *AIRE* is expressed by thymic epithelial cells in the medulla, as well as by some cells in lymph nodes and spleen and is involved in the expression of tissue-specific self-peptides that are presented to maturing thymocytes (Heino et al., 1999,

Metzger and Anderson, 2011). It has recently been suggested that AIRE is involved in the expression of CCL19 and CCL21 in the thymic medulla to induce appropriate migration and egress of developing and fully developed thymocytes (Laan et al., 2009).

While central tolerance induction is of critical importance, the ability to induce tolerance in the periphery is required to prevent excessive or aberrant reactivity to tissue-specific antigens not seen in the thymus (although AIRE is thought to be involved in the expression of some such antigens by medullary thymic epithelial cells) as well as to non-harmful antigens such as food, commensal bacteria, pollen, etc. There are a variety of mechanisms by which this peripheral tolerance can be induced and mediated. Factors such as the steady-state migration of DCs that present peripheral antigen in the absence of co-stimulatory molecules are believed to be involved (see below), as is the exclusion of naïve T cells from non-lymphoid tissues. Extravasation from the blood requires a specific combination of chemokine, integrin, adhesion molecule and other signals (see above) that are specific to lymphoid tissues, allowing “ignorance” of naïve T cells to tissue-specific antigen that might be encountered in non-lymphoid peripheral tissues. Lymph node stroma has also been implicated in the presentation of tissue specific antigen to naïve T cells in a tolerising context, leading to deletion of reactive cells (Lee et al., 2007), and various subsets of T_{reg} cells can be induced outside the thymus, through as yet poorly understood mechanisms (Vignali et al., 2008). Specialised DC subsets in the gut are believed to be important in the development of oral tolerance, whereby the host is tolerised to harmless food antigens and commensal gut flora that, as “non-self” antigens, would otherwise induce an inflammatory response. For reviews on the induction of central and peripheral tolerance, see Mowat, 2003, Mueller, 2010, Workman et al., 2009.

As described above, the development of thymocytes is defective in CCR7-deficient mice, and Misslitz and colleagues have shown that the architecture of the thymus is severely disrupted in the absence of CCR7 (Misslitz et al., 2004). Mice deficient in CCR7 develop generalised autoimmunity, with aberrant infiltration of lymphocytes into various peripheral non-lymphoid organs, including stomach, lung, liver and pancreas. Auto-reactive antibodies are also common, another hallmark of autoimmune disease (Davalos-Misslitz et al., 2007a). Also, as I will describe in section 1.7.3, CCR7 and its ligands facilitate steady-state trafficking of DCs from the periphery to LNs, promoting peripheral tolerance. Thus CCR7 and its ligands are of crucial importance to the development of both central and peripheral tolerance.

1.7.2 Lymphocyte migration to, within and from lymph nodes

As discussed in section 1.3, entry of naïve lymphocytes into lymph nodes via HEVs is a highly complex and tightly regulated process involving various adhesion molecules, integrins, selectins, chemokines and chemokine receptors (see Figure 1.3). Of the latter, CCR7 has been shown to be critically required for naïve and central memory T lymphocyte entry into lymph nodes, under both homeostatic and inflammatory conditions, as well as being involved to a lesser degree in the entry of B lymphocytes into these organs (Förster et al., 1999, Gunn et al., 1999, Okada et al., 2002). Förster and colleagues used immunofluorescent staining of tissue sections and flow cytometry to show that CCR7 deficient mice have a 2-6 fold increase in CD4⁺ T cells in peripheral blood, spleen and BM, with a concomitant decrease in these cells in LN and PP – CCR7 deficient mice had approximately 30-50% the number of CD4⁺ T cells in MLN and peripheral LN compared to WT, and approximately 75% the number of CD4⁺ T cells in PP compared to WT. The majority of the displaced T cells expressed L-selectin (CD62L), marking them as naïve T cells (Förster et al., 1999). Using adoptive transfer of WT and CCR7 deficient cells into WT and CCR7 deficient animals, Förster and colleagues further demonstrated that the defect was lymphocyte-based rather than a defect in stromal cells. The transfer of CCR7 deficient lymphocytes into WT recipients revealed that only 5-25% of CCR7 deficient T cells and 20-50% of CCR7 deficient B cells entered LN and PP compared to transferred WT lymphocytes. However, WT lymphocytes transferred into CCR7 deficient animals were able to populate these tissues as normal (Förster et al., 1999). Consistent with this, *plt/plt* mice, which lack CCL21-ser and CCL19, show marked defects in lymph node cellularity, as observed above (Gunn et al., 1999, Nakano et al., 1997, Nakano et al., 1993). Nakano and colleagues reported that the expression of and interaction between L-selectin and PNAd was intact in these mice, indicating that the involvement of CCR7 and its ligands occurred at a later stage than this initial step. CCL21, which is expressed by HEVs, was subsequently shown to trigger LFA1-dependent firm adhesion of T cells to HEVs, prompting their extravasation into LN (Nakano et al., 1997, Stein et al., 2000). Stein and colleagues also showed that CCL21 injected intracutaneously could be presented by HEVs, having entered lymphatics and drained to the LN. This process was subsequently shown to also occur for CCL19, which is not expressed by HEVs and had therefore been supposed not to be involved in the extravasation of lymphocytes into LN (Baekkevold et al., 2001, Stein et al., 2000). It should be noted that CCL19 deficient mice exhibit normal homing of naïve T cells to LN, and have normal secondary lymphoid tissue structure, indicating that CCL21 is sufficient to mediate the CCR7-dependent entry of lymphocytes into LN (Link et al., 2007). CXCR4 and its ligand CXCL12 have been shown to have a role in B cell entry

into LN, with entry of CXCR4 deficient B cells but not CXCR4⁺ B cells suppressed in *plt/plt* mice – transferred CXCR4⁺ cells entered LN and PP of *plt/plt* mice to the same extent as transferred WT cells, while CXCR4 deficient cells did not (Okada et al., 2002). Interestingly, this study also suggested that the requirement for CCR7 in T cell entry into LN was slightly reduced in C57Bl6 animals than BALB/c animals, although it was still an important element in this process.

CCR7 is also involved in the organisation of secondary lymphoid organs, which contain characteristic B cell follicles and T cell zones (see Figure 1.7), allowing controlled, efficient interactions of these lymphocytes with each other as well as with other cells, particularly DCs. In the absence of CCR7, these distinct zones are severely disrupted. Immunofluorescent imaging showed that lymphocytes from LNs of CCR7 deficient mice are distributed throughout the tissue, with some T cells aberrantly localized to the marginal sinus. FDCs do not appear to be affected. PP architecture is also abnormal in these mice, with no distinct T cell zones, but rather a small “border” of T cells found at the edge of the B cell follicle. In the spleen of the CCR7 deficient mouse, T cells are not largely confined to the PALS as they are in WT spleen, but are instead found accumulated in clusters in the red pulp and marginal sinuses. Those that are found in the PALS of CCR7 deficient spleen are mainly memory T cells, with naïve T cells mostly found outside this region. This defect in splenic organisation was demonstrated both by immunofluorescence and by adoptive transfer. Additionally, WT B cells can normally be detected within the PALS as well as in follicles of WT spleen, but adoptively transferred CCR7 deficient B cells are not in the PALS of WT mice 5 hours after transfer. They can be found at earlier timepoints, indicating a potential role for CCR7 in retention of B cells within the PALS for a time following entry into the spleen (Förster et al., 1999).

Following entry into LNs, naïve B cells become more responsive to CXCR5 ligands and as a result migrate to B cell follicles within the node (Ansel et al., 2000, Cyster, 2005). Förster and colleagues reported that CXCR5 deficient mice have severely disrupted splenic architecture with enlarged MZs and a failure of primary B cell follicles and germinal centres to form properly. These data suggest a requirement for CXCR5/CXCL13 in organisation of the B cell compartment of lymphoid tissue (Förster et al., 1996). Ansel and colleagues subsequently reported that deletion of either CXCR5 or CXCL13 led to impaired LN and PP development and disruption of B cell follicle architecture in LN and spleen, with primary follicle FDCs absent in CXCL13 deficient mice (Ansel et al., 2000).

Naïve T cells remain responsive to CCR7 ligands in the T cell zone, which promotes retention and migration of T cells and activated DCs within this area and enables their efficient interactions to initiate adaptive immune responses (Förster et al., 1999, Ohl et al., 2004). As discussed above, CCR7 deficient mice have severe defects in T cell localisation within lymphoid tissues. CCL19 and CCL21 are both expressed by FRCs in the T cell zone of LNs, with CCL21 also expressed by endothelial cells (Link et al., 2007). The interaction of DCs and T cells within the LN has been shown to involve the random migration of T cells within the T cell zone, which allows frequent interaction with DC dendrites, and the speed of T cell movement within the node is enhanced by CCR7 ligands (Miller et al., 2004, Worbs et al., 2007). Adoptive transfer of either CCR7 deficient T cells into WT animals or WT T cells into *plt/plt* mice showed that intranodal T cell motility was decreased compared to WT T cells within WT LNs. This decreased motility could be rescued by intravenous administration of CCL21. Additionally, subcutaneous injection of CCL19 into the hind paw led to aberrant accumulation of T cells within the SCS of the draining LN, corresponding to CCL19 draining to the LN via the lymph (Worbs et al., 2007). As discussed above, DCs have been shown to adhere to and randomly migrate along fibres coated with full-length CCL21, which they can then cleave to a soluble form that provides directional cues (Schumann et al., 2010). This may facilitate the efficient interaction of DCs and T cells by increasing the level of T cell motility in the immediate vicinity of the DC.

When T and B cells need to interact (e.g. for an antibody response requiring T cell help), they modify their chemokine receptor expression pattern to allow migration to the boundary between T and B cell areas (the “B/T cell boundary”) where they can interact with their cognate T cell, leading to antibody production, memory cell generation, etc (Cyster, 2005, Förster et al., 1999, Reif et al., 2002). Subsets of activated T cells, referred to as T follicular helper cells (T_{FH}), increase CXCR5 expression and migrate to B cell follicles, as demonstrated by Ansel and colleagues. They showed that antigen-specific $CD4^+$ T cells had increased CXCR5 expression (determined by flow cytometry) following immunisation that corresponded to their increased migration to B cell follicles, as shown by immunohistochemistry. These activated CXCR5-expressing T cells also exhibited reduced chemotaxis to CCR7 ligands compared to cells from non-immunised mice (Ansel et al., 1999). The importance of CCR7 in the induction of an adaptive immune response was demonstrated by Förster and colleagues, who showed that CCR7 deficient mice have impaired primary T cell responses, with both contact sensitivity and delayed type hypersensitivity (DTH) responses impaired in these mice. They also exhibit a defect in the

induction of the primary humoral response, with antigen-specific antibody production delayed in CCR7 deficient mice compared to WT (Förster et al., 1999).

Casamayor-Pallejà and colleagues reported that ligation of the BCR of human tonsillar B cells led to increased chemotaxis to CCL19 and transiently decreased chemotaxis to CXCL13, followed by a sharp increase in migration to this chemokine (Casamayor-Pallejà et al., 2002). Reif and colleagues showed that activated B cells upregulated CCR7 expression while CXCR5 expression remained constant, and this mediated migration of the B cells towards the T cell zone. This migration of activated B cells was lost in *plt/plt* mice and in CCR7 deficient B cells. CXCR5 is not required for activated B cell migration from the follicle but does influence the retention of activated B cells in the B/T cell boundary, with CXCR5 deficient cells aberrantly distributed following activation. This study also showed that CCR7 over-expression prompted B cell migration into the T cell zone, particularly along the B/T cell boundary, in the absence of activation, with localisation to the B/T cell boundary again dependent on expression of CXCR5. CXCR5 over-expression prevented the exclusion of activated B cells from the follicle (Reif et al., 2002).

Complementing this study, Okada and colleagues used two-photon microscopy to demonstrate the CCR7-dependent migration of antigen-activated B cells to the B/T cell boundary, where they interact with T cells. Interactions with non-specific T cells (i.e. T cells that do not recognise the antigen presented by the B cell) are short-lived, while antigen-specific interactions last for more than 10 minutes, sometimes continuing for up to an hour (Okada et al., 2005). Following interaction with their cognate T cell, the now fully activated B cells return to the primary B cell follicle to establish secondary B cell follicles. These comprise a “mantle” of naïve B cells and germinal centres (GCs), where activated B cells proliferate rapidly. GCs become segregated into dark and light zones, a division dependent on CXCR4 and CXCR5 expression (Allen et al., 2004). Dark zones contain proliferating centroblasts, which are B cells whose BCRs are undergoing somatic hypermutation to increase antigen-specificity. Light zones contain the progeny of these centroblasts, which are called centrocytes. This is where class switching of immunoglobulin occurs, promoting the generation of specific, antigen-appropriate antibody. These increases in antigen-specificity are facilitated by interaction with antigen-presenting FDCs (Klein and Dalla-Favera, 2008). CXCL12 is abundant in GC dark zones, and centroblasts are CXCR4⁺. In CXCR4-deficient mice, segregation of GCs does not occur, while CXCR4-deficient cells fail to enter WT dark zones. Similarly, CXCR5 deficient mice and CXCL13 deficient mice both exhibit aberrant organisation of GCs, and perturbed localisation of the GC light zone (Allen et al., 2004).

Lymphocytes are retained in the LN for a specific period (approximately 8-12 hours for T cells and 24 hours for B cells) after which, if they have not encountered their cognate antigen, they leave and recirculate throughout the body to optimise the probability of antigen encounter. The egress of lymphocytes from LN has been shown to be dependent on S1P and its receptor S1P₁. Small molecule agonists of S1P receptors (of which there are at least 5) induce sequestration of murine lymphocytes within lymph nodes by inhibiting their ability to cross the endothelial barrier between the LN paracortex and the marginal sinus (Mandala et al., 2002). T and B cells express at least two S1P receptors, S1P₁ and S1P₄. Work by Matloubian and colleagues, described above, showed a requirement for S1P₁ specifically in T cell egress from LN, and in B cell recirculation and egress from lymphoid tissue. This same study also showed that retention of antigen-activated T cells within lymph nodes is caused by downregulation of S1P₁ (Matloubian et al., 2004). Exposure to S1P, which is high in peripheral blood, leads to internalisation of S1P₁, rendering cells unresponsive to S1P and enabling their extravasation into S1P^{low} tissues, such as LN (Schwab and Cyster, 2007). Schwab and colleagues showed that lymphocyte production of S1P lyase, an S1P-degrading enzyme, controls the level of S1P within secondary lymphoid organs, maintaining an S1P^{low} environment within the organs in contrast to the high levels of S1P found in blood and lymph. When S1P lyase activity is inhibited, lymphoid tissue levels of S1P increase and lymphocyte egress from lymph nodes is blocked, with exposure to S1P leading to a decrease in surface S1P₁ expression (Schwab et al., 2005). Haematopoietic cells, particularly erythrocytes, are believed to produce the majority of S1P detected in blood, while the source of S1P in lymph is unclear but may come from lymphatic endothelial cells (Schwab and Cyster, 2007). Interestingly, S1P/S1P₁ is also involved in localisation of MZ B cells to the MZ of the spleen, in combination with CXCL13/CXCR5, indicating the critical role of this molecule and its receptor in regulating immune cell migration (Cinamon et al., 2004).

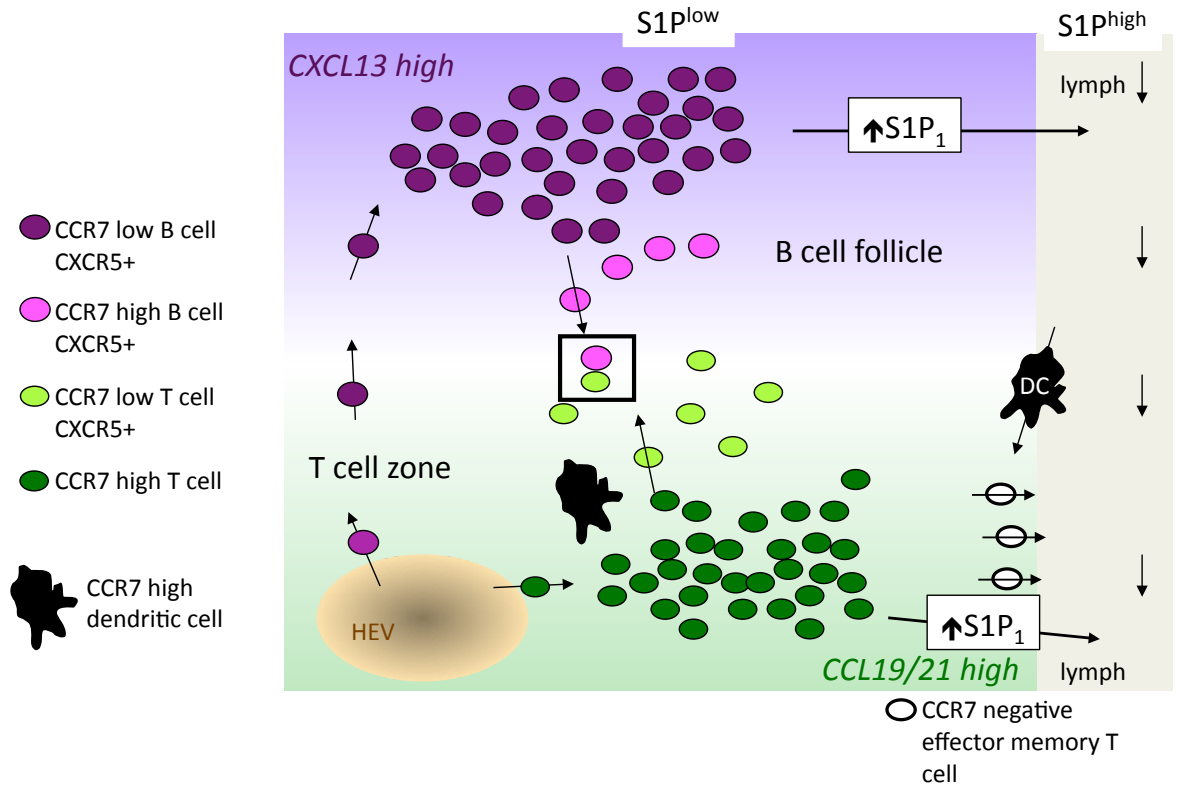


Figure 1.7: Chemokine-dependent lymph node organisation. Lymphocytes enter the lymph node in a CCR7-dependent manner. T cells remain in the CCL19/21-rich T cell zone while B cells downregulate CCR7 and migrate into the CXCL13-rich B cell follicle. S1P lyase produced by lymphocytes maintains an S1P^{low} environment in these regions, allowing retention of the lymphocytes for several hours. Lymphocytes that fail to engage their cognate antigen upregulate S1P and leave the LN via the lymph. B and T cells that become activated by antigen encounter alter their chemokine responsiveness and migrate to the B/T cell boundary (see boxed cells) to interact with their cognate lymphocyte partner and initiate adaptive immune responses (see text).

1.7.3 DC migration to lymph nodes

Under resting conditions, most DCs are resident in tissues throughout the body, acting as “sentinels” at sites such as the skin and mucosa (Banchereau and Steinman, 1998, Bell et al., 1999, Förster et al., 2008). These immature DCs are extremely efficient in internalising and processing antigen from their surroundings, enabling them to very rapidly detect any sign of infection or injury in the tissue (Banchereau and Steinman, 1998, Bell et al., 1999). A number of immature DCs also patrol the body, circulating through the bloodstream and expressing chemokine receptors such as CCR1, CCR2, CCR5 and CXCR1 as well as other molecules that allow rapid extravasation into inflamed tissues if required (Randolph et al., 1998, Sallusto et al., 1998, Sánchez-Sánchez et al., 2006, Sozzani et al., 2000, Sozzani et al., 1995).

As described above, immature or “semi-mature” DCs from peripheral tissues appear to constitutively traffic to lymphoid organs even under resting conditions and constitute a large proportion of DCs identified there. They are believed to present harmless “self” antigens and contribute to maintenance of immune tolerance by inducing anergy or death

of autoreactive T cells (Banchereau and Steinman, 1998, Lutz and Schuler, 2002, Ohl et al., 2004, Wilson et al., 2003). CCR7 is believed to be involved in this process, with the ability of Langerhans cells (LCs; a specialised subset of skin DCs) to constitutively migrate to LNs attributed to transient expression of the receptor (Ohl et al., 2004). This ability is retained in *plt/plt* mice, which lack CCL19 and CCL21-ser in lymphoid tissues but retain expression of CCL21-leu in lymphatic endothelium, suggesting that this ligand is involved in the homing process (Gunn et al., 1999). However, upon reaching the lymph nodes, the ability of DCs to correctly position themselves within T cell areas is severely impaired in these mice, and in *CCR7^{-/-}* mice, indicating a role for the receptor and its ligands in this process (Gunn et al., 1999, Ohl et al., 2004). The importance of this migration of “tolerising” DCs was made apparent in a study showing that while innocuous antigen can reach the lymph nodes of CCR7-deficient mice, tolerance to it is not established as a result of the impaired steady-state migration of DCs (Hintzen et al., 2006). Similarly, in the absence of CCR7 and steady-state DC migration oral tolerance is not established (Worbs et al., 2006), confirming a key role for the receptor and its ligands in this crucial immunological process.

During inflammation, DCs undergo rapid and extensive changes. They become activated, lose their high endocytic capacity, down-regulate inflammatory chemokine receptors and upregulate CCR7, which directs them to draining lymphatics and on to the draining lymph node. They also upregulate MHC class II molecules and various co-stimulatory molecules, which are involved in appropriately activating T cells in the lymph node (Förster et al., 2008, Martín-Fontecha et al., 2003, Sallusto et al., 1998, Sánchez-Sánchez et al., 2006, Wilson et al., 2003). The ability of mature DCs to migrate to the draining lymph node is lost in *CCR7^{-/-}* animals, and in *plt/plt* mice, those cells that do migrate through afferent lymphatics accumulate in the subcapsular sinus of the lymph node, rather than continuing to their normal destination in the T cell zone. As with steady-state migration of DCs, this suggests that CCL21-leu is involved in directing mature DCs to, but not further into, draining lymph nodes (Förster et al., 1999, Gunn et al., 1999, Ohl et al., 2004).

Additionally, in *plt/plt* mice, the number of migrating DCs is reduced, indicating that CCL21-ser and/or CCL19 produced in the lymph node may also be involved in DC migration (Gunn et al., 1999). CCL19 has also been shown to play a role in maturation of DCs *in vitro*, with exposure to the ligand also leading to increased ability to stimulate T cell proliferation (Marsland et al., 2005). In the *plt/plt* mouse, migrating activated DCs exhibit lower levels of co-stimulatory molecules than normal fully matured DCs, lending further credence to a DC maturation role for CCR7 ligands *in vivo* (Marsland et al., 2005). The ligands also caused increased endocytosis of exogenous antigen in mature DCs

(Yanagawa and Onoé, 2003). A previous study by Yanagawa and Onoé also highlighted a potential requirement for expression of both CCL21 and CCL19 in DC migration and function, as well as a potential explanation for their overlapping but not equivalent distribution. They showed that CCL19, which is highly expressed in the T cell zone by DCs themselves, induces the rapid extension of dendrites on the cells, allowing increased opportunity for interaction with T cells. Conversely, CCL21, found in lymphatics as well as within the node, blocks this activity, potentially skewing the morphology in favour of a migratory form (Yanagawa and Onoé, 2002). These data demonstrate a clear requirement for CCR7 in the normal function of DCs in tolerance induction and adaptive immunity.

1.7.4 Leukocyte homing to the small intestine

The intestinal immune system is the largest section of the immune system as a whole, and is the main site of antigen encounter in the body. It has recognised critical functions in the development of tolerance to harmless antigens, as well as being required to detect and promote immunity to harmful or invasive pathogens. Failure to successfully balance these two opposing functions leads to disease, either through infection or through overreaction to harmless antigens such as dietary protein or commensal bacteria (Mowat, 2003).

Chemokines are intimately involved in the immune function of the small intestine and CCR7 and CCR9 and their ligands play important roles in the migration of leukocytes to and within this compartment of the immune system.

A number of organised lymphoid structures can be identified in the intestine, including MLN, PP and ILFs, which resemble microscopic PP. Cryptopatches, which are small, loosely organised cellular compartments found at the base of intestinal epithelial crypts, contain LT_i cells and are thought to be precursors to the formation of ILFs (Mowat, 2003, Newberry and Lorenz, 2005). The MLN are the largest and earliest forming of all lymph nodes in the body. As described earlier, they have distinct developmental requirements from those of PPs or peripheral lymph nodes, forming in the absence of factors such as tumour necrosis factor (TNF) and its receptor (TNFR), LT $\alpha_1\beta_2$ or LT β R. The ability of lymphocytes to accumulate in the MLN depends on adhesion molecules usually involved in lymphocyte migration to peripheral (L-selectin) or mucosal ($\alpha_4\beta_7$ integrin) tissues (see Figure 1.3) (Mowat, 2003, Newberry and Lorenz, 2005). Peyer's patches are aggregates of leukocytes situated at infrequent intervals along the wall of the small intestine. They share some features of other lymphoid organs, with their organised structure of B cell follicles and T cell zones, but lack afferent lymphatics. The route of entry for antigens from the small intestine is instead through microfold (M) cells that are located in the follicle-

associated epithelium (FAE), situated above the lymphoid area of the Peyer's patch. Antigen is passed from the M cells to DCs residing in the subepithelial dome (SED), which lies between the FAE and the lymphoid areas. The DCs can then either interact with T and B cells in the Peyer's patch or migrate to the MLN via lymphatic vessels, using CCR7 and its ligands (Jang et al., 2006, Mowat, 2003). These DCs, as well as DCs that migrate to the MLN from the lamina propria, are capable of constitutive homing to the MLN using CCR7, a process believed to be important in induction of tolerance to harmless antigens such as food and commensals. Lamina propria-derived DCs, which express CCR7 and migrate in response to CCL21, are markedly reduced in the MLN of *plt/plt* mice and CCR7 deficient mice (Jang et al., 2006). T cells that are activated by gut-derived DCs in PP or MLN are primed to home to the small intestine again by maintenance of CCR9 and induction of $\alpha_4\beta_7$ -integrin expression. CCR9⁺ cells migrate in response to CCL25, which is constitutively expressed by epithelial cells in the small intestine (Kunkel et al., 2000). Using T cells expressing an ovalbumin (OVA)-specific TCR detectable by antibody staining, Campbell and Butcher reported that, following intraperitoneal challenge with OVA plus lipopolysaccharide (LPS) as an adjuvant, activated CD4⁺ T cells isolated from peripheral LNs had increased P-selectin ligand expression, while those isolated from MLNs had increased $\alpha_4\beta_7$ integrin expression. They also showed that the activated T cells isolated from MLN were much more responsive to CCL25 than those isolated from peripheral LN, indicating higher CCR9 expression in T cells activated in the MLN (Campbell and Butcher, 2002). Subsequently, Mora and colleagues isolated DC subsets from spleen, peripheral LN and PP and showed that CD8⁺ T cells stimulated by PP DCs displayed similar levels of a variety of activation markers but expressed higher levels of $\alpha_4\beta_7$ integrin than CD8⁺ T cells stimulated by DCs from the other tissues. They further showed that, although all stimulated cells showed a lower propensity to migrate in response to CCL25 compared to naïve CD8⁺ T cells, those activated by PP DCs had a significantly higher chemotactic index to the chemokine than those stimulated by spleen or peripheral LN DCs (Mora et al., 2003). Corresponding to this, competitive transfer of naïve CD8⁺ T cells with CD8⁺ T cells activated by either PP or peripheral LN DCs showed that PP DC-stimulated cells preferentially homed to PP while LN DC-stimulated cells homed to the PLN, although naïve T cells trafficked more readily to LN and PP than activated T cells of either type. When PP DC-stimulated CD8⁺ T cells and LN DC-stimulated CD8⁺ T cells were competitively transferred together, those stimulated by PP DCs showed enhanced ability to home to small intestine (but not colon), as well as to PP and MLN, although this difference was more modest than the contrast in small intestine homing. The ability to home specifically to the gut was shown to correlate with $\alpha_4\beta_7$

expression and responsiveness to CCL25 (Mora et al., 2003). This finding concurred with a previous report from Svensson and colleagues, who used OVA-specific CD8⁺ T cells to show that activated CD8⁺ T cells in the MLN, but not PLN, expressed CCR9 following challenge with OVA+LPS. This study also demonstrated the importance of intestinal CCL25 expression in directing activated T cells to the small intestine. They demonstrated that the increase in number of specifically activated T cells in the lamina propria of the small intestine seen during normal response to challenge was dramatically reduced when neutralising anti-CCL25 antibody was administered subsequent to intraperitoneal challenge with OVA+LPS (Svensson et al., 2002). Surprisingly, CCR9 deficient mice have normal numbers of T cells in the lamina propria, although Pabst and colleagues showed that CCR9 deficiency leads to a defect in plasma cell homing to the lamina propria (Pabst et al., 2004). However, when transferred in competition with WT cells, activated CD4⁺ T cells from CCR9 deficient mice exhibited a defect in lamina propria homing, with residual homing suggested to be due to increased CCR5 expression by the CCR9 deficient cells (Stenstad et al., 2006). The ability of IgA-producing plasma cells to home to the gut using CCR9, as demonstrated by Pabst and colleagues, is required for appropriate induction of specific antibody responses to oral antigens, with CCR9 deficient mice lacking OVA-specific antibody following challenge with OVA plus cholera toxin (CT). Interestingly, IgA⁺ plasma cells do not express CCR9 within the lamina propria suggesting that, once they have reached their destination, other factors are involved in keeping them there (Pabst et al., 2004).

The induction of gut-homing markers (i.e. CCR9 and $\alpha_4\beta_7$ integrin) on lymphocytes depends upon retinoic acid (RA), which is produced by gut DCs, as well as by lamina propria macrophages and intestinal epithelial cells (Mora and von Andrian, 2009). It has long been known that vitamin A deficiency contributes to impaired localisation of adoptively transferred radiolabelled MLN-derived lymphocytes to the gut in rats (McDermott et al., 1982). In 2004, Iwata and colleagues neatly demonstrated that RA, a metabolite of vitamin A, could induce a gut-homing phenotype in primary T cells that had been stimulated *in vitro* in the absence of other cell types. Addition of RA to the cultures led to upregulation of $\alpha_4\beta_7$ integrin and increased expression of CCR9, along with improved migratory capacity to CCL25 and decreased expression of molecules involved in homing to other secondary lymphoid organs. Competitive adoptive transfer of RA-treated and untreated activated T cells showed an increased propensity for treated cells to migrate to MLN, PP and lamina propria, with reduced ability to home to peripheral LN. The group further demonstrated that DCs from PP and MLN strongly expressed retinal

dehydrogenase (RALDH), an enzyme involved in RA synthesis, whereas only weak expression of RALDH was detected in DCs from peripheral LN. Inhibition of RALDH activity led to decreased ability of MLN- and PP-derived DCs to imprint a gut-homing phenotype on T cells (Iwata et al., 2004). Following this report, Mora and colleagues showed a similar requirement for RA in the homing of IgA-secreting plasma cells to the small intestine. PP-derived DCs or exogenous addition of RA to media were able to induce $\alpha_4\beta_7$ integrin expression and maintain CCR9 expression on activated B cells *in vitro* while peripheral LN-derived DCs or RA-free media could not. This study also showed that vitamin A-deficient mice lacked intestinal IgA-secreting cells, and that, while RA was required for homing of these cells to the gut, it was also involved in the induction of IgA secretion, in synergy with IL-5 and/or IL-6 (Mora et al., 2006). These studies show that RA, which I earlier described as an intrinsic element of lymphoid tissue organogenesis, has an ongoing role in the development and maintenance of appropriate immune responses in the gut through regulation of $\alpha_4\beta_7$ integrin and CCR9 expression on gut-homing lymphocytes. Interestingly, CCR9 is also involved in the homing of plasmacytoid DCs (pDCs) to the gut, under both steady state and inflamed conditions (Wendland et al., 2007). These specialised DCs are believed to be involved in tolerance induction (Matta et al., 2010), as well as anti-viral activity through type I interferon (IFN) production (Marshall et al., 2006). Toll-like receptor (TLR)7, which is expressed by pDCs, is involved in recognition of viruses (McKenna et al., 2005). CCR9 deficient animals lack pDC in the lamina propria and, unlike WT animals, are unable to efficiently mobilise lamina propria DC to MLN in response to orally administered R848, an agonist of TLR7/8. Adoptive transfer of WT pDCs into CCR9 deficient animals prior to challenge with oral R848 rescued this defect (Wendland et al., 2007).

Taken together, these reports demonstrate that CCR7 and CCR9 and their ligands are crucial in both the induction of gut-specific immune responses and the development and maintenance of tolerance to oral antigens. At the start of my project, another student in the lab had recently embarked on an investigation of the ability of CXCR3 to modulate intestinal immune responses and induction of oral tolerance. Her findings will be discussed in chapter 7.

1.8 Atypical chemokine receptors

Within the chemokine receptor biology field, a small subsection stands apart. The area of atypical chemokine receptor research is one that has grown rapidly in the last decade or so, with at least five identified atypical chemokine receptors now under investigation. These

receptors are characterised by an inability to induce signalling upon ligand binding through pathways used by other “classical” chemokine receptors when exogenously expressed *in vitro*. This apparent lack of signalling is associated with an inability to mediate chemotaxis in response to environmental chemokine. Of the atypical receptor family, the best known and best characterised are the Duffy antigen receptor for chemokines (DARC) and D6, both of which bind inflammatory chemokines and are proposed to act as “decoy”, transport or scavenging receptors. Of particular interest for this thesis is the atypical receptor CCX-CKR, which binds only three constitutive chemokines in mouse, as mentioned above. Finally, more recent work has identified some novel receptors, namely CXCR7, which binds CXCL11 and CXCL12, and CCRL2, or CRAM, which is thought to bind CCL19 and a chemo-attractant called chemerin. In this section I will provide an overview of our current understanding of the role of DARC and D6 in the immune system, followed by a brief description of the newest members of this small family, namely CXCR7 and CCRL2. Lastly, I will detail what is known about the receptor that is the focus of this work, CCX-CKR, presenting work leading up to this project.

1.8.1 DARC

First identified in 1950, the Duffy blood group antigen was later shown to be an erythrocyte receptor for the malaria parasite *Plasmodium vivax*, with Duffy-negative individuals resistant to infection (Cutbush et al., 1950, Miller et al., 1975). It was later shown to act as a chemokine binding protein for both CC and CXC chemokines on erythrocytes, including CXCL1, CXCL8, CCL2 and CCL5. Horuk and colleagues have demonstrated that preincubation of Duffy-positive erythrocytes with CXCL1 or CXCL8 could block almost all Duffy-dependent infection by *P. knowlesi*, a simian malarial parasite that can use the human receptor for entry (Darbonne et al., 1991, Horuk et al., 1993, Neote et al., 1993). The demonstrated ability of the receptor to bind chemokines led to its being designated the **Duffy antigen/receptor for chemokines**, or DARC. It has been suggested that the receptor acts as a “sink” or reservoir for plasma chemokines, and in a recent review my colleagues and I described a proposed mechanism by which erythrocyte-expressed DARC could buffer chemokine levels during and after inflammation (see Figure 1.1) (Darbonne et al., 1991, Dawson et al., 2000, Hansell et al., 2011a). This is suggested as a means of regulating leukocyte responsiveness to chemokines, preventing inappropriate extravasation of leukocytes into tissues (Hansell et al., 2011a).

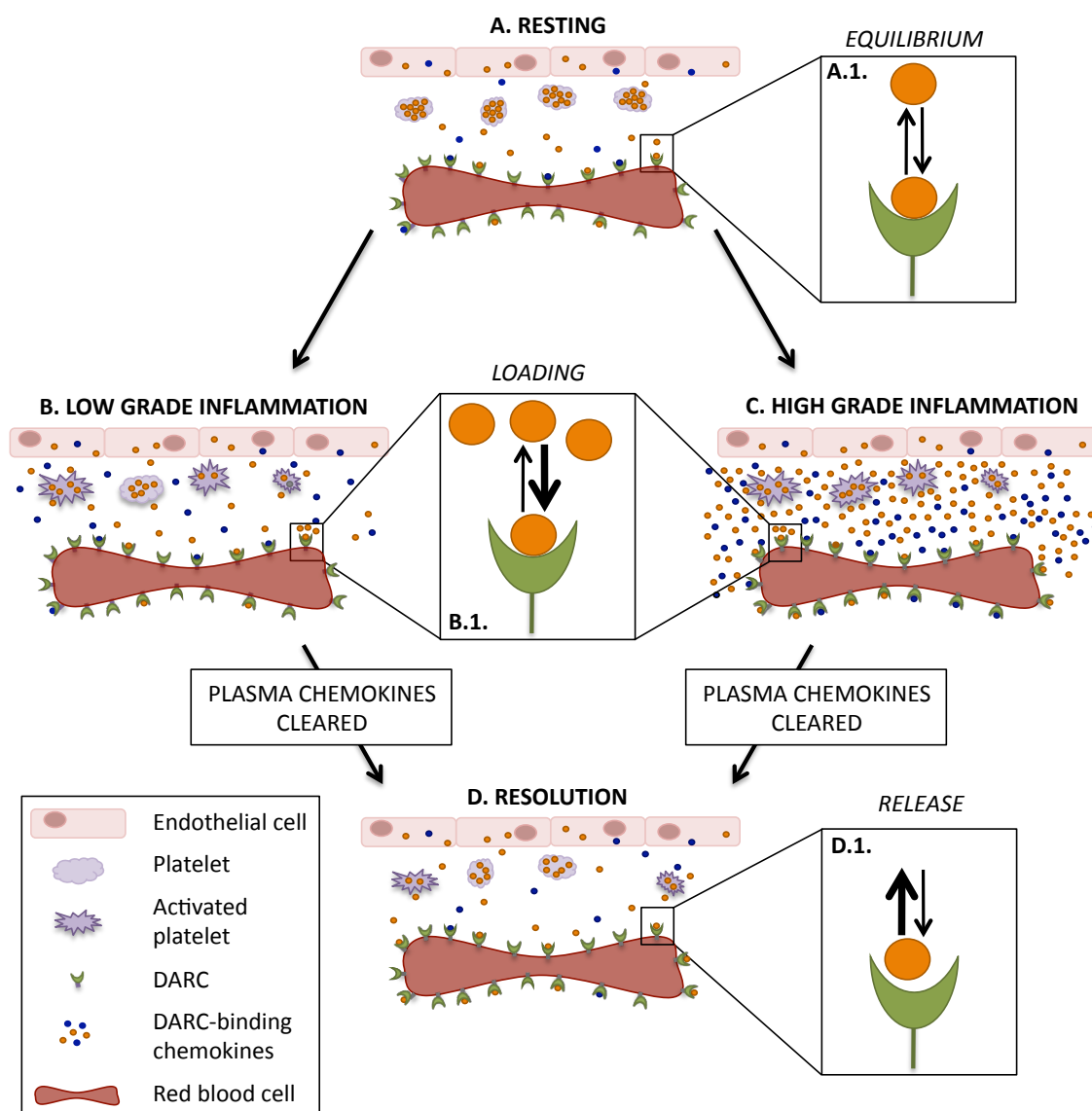


Figure 1.8: Proposed activity of erythrocyte DARC as a buffering system for blood-borne chemokine. (A) During homeostasis, a proportion of erythrocyte-expressed DARC will be occupied by constitutively expressed chemokine such as CXCL5 and CCL2. Under these circumstances, these chemokines will be in dynamic equilibrium with free chemokine (A1), the levels of which will be maintained by release of DARC-bound chemokine. The plasma chemokine can then be subjected to posttranslational modification and removed by DARC-independent mechanisms. Platelets contain high levels of CXCL5 that is released upon activation. (B) Induction of low-level inflammation will lead to a transient rise in plasma chemokine levels through release of DARC ligands from platelets, endothelial cells, etc., disrupting the homeostatic equilibrium and leading to “loading” of chemokine onto DARC molecules (B1). This will prevent sharp rises in plasma chemokine levels and limit the induced inflammation. (C) Induction of high-grade inflammation will lead to substantial release of chemokine, overwhelming the “sink” provided by DARC. (D) Clearance of plasma chemokines during resolution of inflammation will lead to a return to equilibrium, with release of chemokine from erythrocyte DARC (D1) blunting the rate of chemokine clearance from the blood. Figure and text adapted from Hansell et al., 2011a.

Evidence for activity of DARC as a chemokine “sink” comes from studies with both humans and mice. Mayr and colleagues conducted a study comparing plasma and erythrocyte-associated chemokine levels between humans who express DARC normally (“Duffy positive”) and those lacking erythrocytic DARC (“Duffy-null”). Untreated Duffy-null patients exhibited altered plasma chemokine levels and reduced erythrocyte-associated

CXCL1 and CCL2. Treatment of both patient groups with intravenous LPS led to a sharp increase in erythrocyte-associated chemokine, including CXCL1, CXCL8 and CCL2, in Duffy-positive but not Duffy-null patients (Mayr et al., 2008). Complementing this, mice lacking DARC have been shown to have lower resting levels of plasma CCL2 and CCL11, while intravenously administered CCL11 and CXCL1 was cleared more rapidly from DARC deficient mice than WT (Fukuma et al., 2003).

The receptor is also expressed at a number of sites other than erythrocytes, and individuals whose erythrocytes are Duffy negative tend to retain expression of DARC at these disparate sites. Other sites of expression include blood vessel endothelial cells of postcapillary venules, high endothelial venules of lymph nodes and tonsils, lymphatic endothelial cells of skin lymphatic pre-collectors, inflamed synovial endothelium, some epithelial cells in lung and kidney, and Purkinje neurons (Chaudhuri et al., 1997, Girard et al., 1999, Hadley et al., 1994, Hansell et al., 2011a, Kashiwazaki et al., 2003, Lee et al., 2003, Middleton et al., 1997, Patterson et al., 2002). It has been detected in caveolae of endothelial and epithelial cells, and has been postulated to act as a chemokine transporter, with caveolae vesicles commonly associated with transcytosis of proteins (Chaudhuri et al., 1997, Pelkmans and Helenius, 2002, Rot, 2005). By tracking the path taken by radiolabelled chemokines across rabbit and human skin, Middleton and colleagues showed that chemokines were rapidly transcytosed via caveolin-containing vesicles to the lumen of the endothelium following intravenous injection (Middleton et al., 1997). While the GAG heparan sulfate was postulated to play a role in this transcytosis, the “fingerprint” of chemokine binding to endothelial cells suggested a specific role for DARC in the process. Pruenster and colleagues showed that DARC co-localised with injected chemokines in human skin, while Madin-Darbin canine kidney (MDCK) cells transfected with DARC showed increased propensity to transcytose chemokine from the basolateral to apical surface compared to mock-transfected cells (Pruenster et al., 2009). The same study also showed that transgenic mice overexpressing DARC on blood vessel endothelium exhibited increased neutrophil extravasation in response to CXCL1 compared to WT mice (Pruenster et al., 2009).

Duffy-null humans are reported to display reduced resting numbers of neutrophils and monocytes compared to their Duffy-positive counterparts (Mayr et al., 2008). This defect is not observed in DARC deficient mice. Zarbock and colleagues reported a slight but significant decrease in total leukocyte count, but also slightly elevated neutrophil numbers in resting DARC deficient mice compared to WT (Zarbock et al., 2010). Another study

found no difference in peripheral blood leukocyte numbers between DARC deficient and WT mice (Luo et al., 2000).

The ability of DARC to bind a number of chemokines known for their angiogenic properties has been highlighted during investigation of the effect of DARC expression on tumour development. Shen and colleagues reported that in a murine model of prostate cancer, tumours from DARC deficient mice had increased levels of angiogenic chemokines such as CXCL1 and CXCL8, as well as increased intratumoral vasculature and improved growth compared to those from WT (Shen et al., 2006). Additionally, Addison and colleagues showed that a human lung cancer cell line transfected with DARC produced less angiogenic chemokine in culture compared to untransfected cells, and, *in vivo*, transfected cells developed into larger but more necrotic tumours that were poorly metastatic and had reduced vasculature compared to untransfected cells (Addison et al., 2004).

DARC has also been implicated in the neutrophil response to infection and injury, with a number of models reporting reduced neutrophil infiltrate into affected tissues of DARC deficient mice following challenge (Dawson et al., 2000, Luo et al., 2000, Zarbock et al., 2007). Using a model of acute kidney failure, Zarbock and colleagues suggested that a defect in endothelial cell presentation of chemokine in DARC deficient mice was the cause of reduced neutrophil recruitment following challenge (Zarbock et al., 2007). The same group also reported that transfer of DARC deficient neutrophils into WT mice was sufficient to confer protection from acid-induced lung injury, a model in which DARC deficient mice were protected and neutrophil recruitment into injured lungs did not occur in the absence of the receptor (Zarbock et al., 2010). These data suggest that DARC can influence disease progression both through regulation of local chemokine levels and by influencing neutrophil function, a theory supported by the neutrophil defect observed in Duffy-null humans.

1.8.2 D6

D6 was first cloned in 1997. Nibbs and colleagues used radioligand binding and competition with unlabelled chemokines to identify it as a highly promiscuous receptor for CC chemokines (Nibbs et al., 1997a, Nibbs et al., 1997b). Generation of anti-human D6 antibody and *in situ* hybridisation has been used to show that D6 is expressed in lymphatic endothelium of the gut, skin and lungs, although it is absent from lymphatics of other organs (Nibbs et al., 2001). It is also found in human trophoblasts, hepatocytes, mast cells

and macrophages (Hansell et al., 2011a, Madigan et al., 2010, Nibbs et al., 2001). Using a chemokine internalisation assay, D6 receptor activity has recently been shown to be detectable on murine innate-like B cells, including splenic MZ B cells and B1 cells from various tissues (Hansell et al., 2011b), while mRNA for the receptor is detectable in a number of non-lymphoid tissues (Hansell et al., 2011a, Madigan et al., 2010, Nibbs et al., 2001).

The human D6 receptor has been shown to bind CCL2-5, CCL7-8, CCL11, CCL13-14, CCL17-18, CCL22, CCL24, CCL26 and CCL3L1, does not bind CCL1, CCL15, CCL19-20 and CCL23, and has not been tested for affinity to other CC chemokines (R. Kinstrie, pers. comm., Hansell et al., 2011a). It does not bind CXC chemokines (R. Kinstrie, pers. comm.) and has not been shown to bind chemokines of any other class, although not all have been tested. The binding profile of murine D6 is less well characterised, although published work has shown that CCL2-5, CCL11-12, CCL17 and CCL22 are ligands for the murine receptor (Hansell et al., 2011b, Nibbs et al., 1997a). This profile distinguishes D6 as a receptor for mainly pro-inflammatory chemokines. It lacks the capacity to signal conventionally, with exogenously expressed D6 binding ligands without induction of calcium flux or chemotaxis *in vitro* (Fra et al., 2003). Ligand binding by endogenously expressed D6 similarly fails to induce classical signalling responses on primary B cells (Hansell et al., 2011b). This may be due to an altered DRYLAIV motif common to classical chemokine receptors – in D6, the sequence is altered to DKYLEIV (Nibbs et al., 1997b). Mutation of the glutamic acid (Glu – E) to alanine (Ala – A) introduces weak calcium flux potential through D6, and mutation of DRYLA in CCR5 to DYKLE blocks signalling through this receptor (R. Nibbs, unpublished data). The DRYLAIV sequence, found in the second intracellular loop of normal receptors, is involved in coupling to G-proteins (see above). In transfected HEK293 cells, the vast majority of the receptor is detected inside the cell, with less than 5% of the expressed protein found on the cell surface, as demonstrated by immunofluorescent staining of D6 transfectants with anti-D6 antibody and imaging of D6-GFP transfectants. In these cells, the intracellular localisation of D6 is due to the constitutive cycling of the receptor to and from the cell surface, which is independent of ligand binding (Weber et al., 2004). Internalisation of D6 is facilitated through clathrin-coated pits, although the exact mechanics of this activity are still under investigation. Early reports indicated a requirement for β -arrestins in the internalisation process, but this finding has been contradicted by subsequent work from our group showing that β -arrestin involvement is dispensable for constitutive internalisation of D6 (Galliera et al., 2004, McCulloch et al., 2008, Weber et al., 2004). Knock-down of

endogenous D6 expression in BeWo cells, a trophoblast-derived choriocarcinoma cell line, disrupts *in vitro* chemokine depletion by this cell line (Madigan et al., 2010). Thus, D6 is able to rapidly and efficiently internalise ligands *in vitro* without the requirement for signalling found with most conventional chemokine receptors. Internalised chemokines are subsequently targeted for degradation. This property, along with effects on murine chemokine levels *in vivo* (see below), has led to the hypothesis that the function of D6 is to act as a decoy receptor to modulate chemokine levels and inflammatory responses *in vivo* (Bonecchi et al., 2004, Fra et al., 2003, Hansell et al., 2011a, Weber et al., 2004), although other potential functions have not been ruled out. An inability to mediate efficient transport of radiolabelled CCL2 across cultured murine lymphatic endothelial cells and failure to transport CCL3L1 across confluent BeWo cells indicated that D6 is unlikely to act as a mechanism for chemokine transcytosis, as has been suggested for DARC (Fra et al., 2003, Martinez de la Torre et al., 2007). However, recent evidence from our lab has hinted at a role for D6 in indirect modulation of responses to chemokines other than those directly bound by D6. B1 B cell migration to CXCL13, the ligand for CXCR5, is enhanced in the absence of D6, although the mechanism of this dysregulation is unclear (Hansell et al., 2011b).

Analysis of D6 deficient mice has provided some evidence to support its hypothesised role as a scavenger or decoy. Jamieson and colleagues used a model of cutaneous skin inflammation to examine the proposed role of D6 in resolution of inflammation through chemokine scavenging. This model uses repeated topical application of TPA, a phorbol ester irritant, to induce inflammation in the skin, leading to rapid infiltration of leukocytes into the skin and increased DC migration to the draining LN. Local TNF α production induces the production of inflammatory chemokines that drives leukocyte infiltration, which in WT mice resolves approximately 4-6 days after ceasing application of TPA. The study showed that the absence of D6 leads to prolonged and exaggerated responses, with higher levels of inflammatory CC chemokines detected in the skin of D6 deficient mice (Jamieson et al., 2005). Inflammation of D6 deficient skin is more severe and much longer lasting with a psoriatic pathology, suggesting a pivotal role for D6 in resolution of inflammation (Jamieson et al., 2005). Aberrant inflammatory responses were observed in another model of skin inflammation induced by subcutaneous injection of complete Freund's adjuvant (CFA). In this study, D6 deficient animals were much more prone to development of cutaneous lesions in response to CFA injection, with almost 65% of D6 deficient animals developing moderate to severe lesions compared to less than 10% of WT mice. This model also showed an increase in cellularity and inflammatory chemokine level

in the draining lymph node of D6 deficient animals compared to WT (Martinez de la Torre et al., 2005). Previous work has shown that CCL2 produced in inflamed skin of WT mice, or injected intracutaneously into CCL2 deficient mice, drains to the LN via lymphatics and is presented on HEVs where it mediates directed migration of inflammatory monocytes into the LN (Palframan et al., 2001). The observations of Martinez de la Torre and colleagues suggest that, by limiting the level of chemokine at the site of induced inflammation, D6 could influence the level of chemokine draining to the LN, thus regulating the influx of leukocytes to this tissue and modulating the adaptive immune response. If, as is the case in humans, murine D6 is expressed on lymphatic endothelial cells, there may also be a direct role for D6 in limiting the level of chemokine that makes it through lymphatic vessels to the LN.

The investigation of the role of D6 in regulating skin inflammatory responses has been expanded to analysis of tumour induction in D6 deficient mice. D6 has been shown to affect the formation of papillomas in a TPA/DMBA model of tumourigenesis. In this model, DMBA, a mutagen, is applied topically to shaved dorsal skin, followed by repeated application of TPA several times a week over a number of weeks. Our lab showed that deletion of D6 led to the formation of papillomas in a formerly resistant strain of mice (C57Bl6/129 mice), while in a susceptible strain (FVB mice), lack of D6 led to increased tumour burden (Nibbs et al., 2007). The report also examined oral squamous cell carcinomas (SCCs) from humans, which develop in a similar way to the papillomas of the mouse model described above. SCCs tend to develop after repeated exposure to mutagenic and inflammatory factors, such as those found in tobacco smoke. D6 expression was found to be associated with SCCs, with increased lymphatic endothelial cell expression of the receptor around and contacting the tumours. This was taken as an indication of a role for D6 in regulating the inflammatory chemokine environment during development of these tumours, possibly in an attempt to limit tumour growth (Nibbs et al., 2007).

Complementing the knock-out data described above, Nibbs and colleagues also showed that transgenic overexpression of the receptor in keratinocytes led to reduced inflammation and increased resistance to tumour formation in susceptible strains. Transgenic murine D6, under the control of the keratinocyte-specific promoter K14, was expressed specifically in the keratinocyte layer of the epidermis of transgenic mice, and cultured keratinocytes expressing D6 successfully and efficiently depleted biotinylated CCL3 from culture media while WT keratinocytes did not. Phorbol-ester induced cutaneous inflammation was resolved more rapidly in the transgenic mice, and papilloma formation following DMBA/TPA treatment was reduced compared to WT. These phenotypes were linked to increased or decreased inflammatory chemokine levels in the absence or overexpression of

the receptor respectively, indicating an important role for chemokine production in tumour formation (Nibbs et al., 2007).

D6 has also been implicated in the progression of a variety of other inflammatory disease models, including allergic lung inflammation, *Mycobacterium tuberculosis* infection and acute liver damage. Increased inflammatory infiltrate and elevated inflammatory chemokine levels were associated with more severe disease in D6 deficient mice in each case (Berres et al., 2009, Di Liberto et al., 2008, Whitehead et al., 2007). Conflicting reports as to the involvement of D6 in the development of dextran sodium sulphate (DSS)-induced colitis have left the requirement for the receptor in this disease model unclear. Vetrano and colleagues reporting increased leukocyte infiltrate and more severe disease in D6 deficient mice compared to WT, while Bordon and colleagues demonstrated reduced disease severity in D6 deficient mice, which was linked to increased IL-17A levels due to elevated numbers of IL-17A-secreting $\gamma\delta$ T cells in D6 deficient inflamed colons compared to WT (Bordon et al., 2009, Vetrano et al., 2010).

Taken together, the data presented above provide some support for the current favoured model of D6 as a scavenging chemokine receptor that regulates inflammatory responses and mediates resolution of inflammation. However, as outlined in our recent review, there are some unresolved issues to be clarified before this paradigm can be fully accepted (Hansell et al., 2011a). Interpretation of murine *in vivo* data in the context of human expression studies ignores the lack of robust information available on the expression pattern of D6 in the mouse. Work from our lab has demonstrated functional D6 expression (i.e. D6-mediated chemokine internalisation) by innate-like B cells, and has provided indications that D6 may influence chemokine signalling through other receptors (Hansell et al., 2011b). However, although it has been assumed that D6 will be expressed on lymphatic endothelial cells in the mouse, as it is in humans, this has yet to be conclusively proven. Additionally, increased chemokine protein levels in the absence of D6 have been taken as indication of a distinct scavenging role for this receptor. However, Cardona and colleagues have reported that deletion of conventional chemokine receptors, such as CCR2, CXCR2 and CX₃CR1, leads to increased circulating levels of their chemokine ligands even in resting unchallenged mice, suggesting that in fact, these receptors can themselves control levels of chemokine *in vivo* (Cardona et al., 2008). The designation of D6 as a “non-signalling” receptor has been largely based on limited *in vitro* analysis of transfected cells and as such may not reflect the true extent of *in vivo* complexity. Therefore, much work remains to be carried out before a complete understanding of D6 function is gained.

1.8.3 CXCR7

During a study aimed at characterising the role of CXCR4 in development, comparison of CXCR4 deficient and WT fetal liver cells showed that, unexpectedly, CXCL12 bound with equal affinity to both. Similarly, some tumour cell lines that did not exhibit CXCR4 expression when analysed with anti-CXCR4 antibody were shown to bind CXCL12 without induction of calcium flux or migration. These data suggested the existence of another receptor for the chemokine, which had previously been thought to bind exclusively to CXCR4. Burns and colleagues identified CXCR7 as a high affinity receptor for CXCL12, the ligand for CXCR4. Binding of CXCL12 to CXCR7 but not to CXCR4 was inhibited by addition of CXCL11, a ligand for CXCR3, but not by CXCL9 or CXCL10 (other ligands for CXCR3). Additionally, ligand binding by CXCR7 did not lead to calcium mobilisation or cell migration. Thus, CXCR7 was identified as an atypical receptor for CXCL11 and CXCL12 (Burns et al., 2006). Expression of CXCR7 mRNA was quite widespread, with Northern blot analysis revealing expression in various tissues including heart, brain, lung, spleen, testes and ovary. However functional protein expression, as determined by radioligand binding and antibody staining, was reported to be limited. Surface protein expression of the receptor was detected on various tumour cell lines, activated endothelial cells and fetal liver cells (Burns et al., 2006). Sierro and colleagues reported mRNA expression of CXCR7 on human and mouse leukocyte subsets, including T cell subsets, NK cells, human memory B cells and murine MZ B cells. They generated CXCR7 deficient mice, of which most died at birth due to heart defects. Conditional deletion of endothelial CXCR7 mimicked complete knockout of the receptor, highlighting this expression site as important in heart development. Interestingly, although CXCR7 did not mediate calcium flux or cell migration in transfected cells upon ligand binding, Sierro and colleagues reported increased signalling upon CXCL12 binding when CXCR7 was co-expressed in HEK cells with CXCR4, compared to CXCR4 expression alone. This intriguing aspect of the biology of these two receptors was attributed to their heterodimerisation, as detected by fluorescence resonance energy transfer (FRET), and may provide a mechanism by which CXCR7 could modulate CXCR4 activity *in vivo*. Although preliminary, this finding provides support for the theory (discussed above) that receptor dimerisation may be an important aspect of chemokine biology (Sierro et al., 2007). However, in spite of the reported mRNA expression of CXCR7 on leukocytes, Berahovich and colleagues recently reported that CXCR7 protein was not detectable on peripheral blood leukocytes from adult human or mouse using anti-CXCR7 antibodies in flow cytometry and immunohistochemistry and competition with unlabelled CXCL11, CXCL12 and small molecule CXCR7 antagonists for radiolabelled CXCL12 binding

(Berahovich et al., 2010). In addition to the reported heart defects, CXCR7 has recently been suggested to have an important role in primordial germ cell (PGC) migration during zebrafish development, possibly indicating a general role for the receptor in mediating appropriate positioning of cells during embryonic development. The influence of CXCR7 on PGC migration is not a cell autonomous effect, as PGCs themselves do not appear to express the receptor. Rather, it is expression of the receptor by somatic cells, and its role in sequestering CXCL12 along the route of PGC migration during development that is thought to be important for appropriate embryonic development (Boldajipour et al., 2008).

In vitro, the receptor has been shown to efficiently internalise CXCL11 and CXCL12 without saturation in mammalian cells, and constitutively cycles to and from the surface of both mammalian and zebrafish cells regardless of ligand binding. It also lacks the canonical DRYLAIV motif associated with chemokine receptor signalling, and ligand binding does not induce conventional signalling responses, such as calcium flux. However, Zabel and colleagues have reported association with β -arrestins upon ligand binding, followed by internalisation, at least in transfected Chinese hamster ovary (CHO) cells (Naumann et al., 2010, Zabel et al., 2009). A recent publication by Rajagopal and colleagues suggested that CXCR7 could in fact induce intracellular signalling through β -arrestins, independent of G protein activation. They reported that incubation with CXCL11 or CXCL12 led to β -arrestin-mediated mitogen activated protein (MAP) kinase activation (as assessed by induction of extracellular-signal regulated kinase (ERK) phosphorylation) in HEK cells transiently transfected with CXCR7. This was complemented by the finding that both ligands induce rapid recruitment of β -arrestin to the plasma membrane upon binding. However, CXCL12-induced recruitment of β -arrestin was followed by localisation to cytoplasmic vesicles, while CXCL11 binding led to recruitment of β -arrestins that remained localised to the plasma membrane at later timepoints. This suggests that CXCR7 may respond differently to its two ligands (Rajagopal et al., 2010). Interestingly, ERK phosphorylation was not detected upon ligand exposure in rat vascular smooth muscle cells, which endogenously express CXCR7. However, these cells did migrate in response to CXCL11, and this migration was inhibited by addition of CXCR7 small molecule antagonists. It also relied on β -arrestins, as knock-down of β -arrestin2 by small interfering RNA (siRNA) inhibited migration, but treatment with pertussis toxin had no such inhibitory effect, eliminating the possibility that G_i signalling was required (Rajagopal et al., 2010).

These recent findings provide an intriguing avenue for investigation of other “atypical” receptors, and it will be interesting to see how the story of CXCR7 develops, especially in terms of its capacity to signal and directly modulate signalling through other receptors. As suggested for D6 above, the suggestion that atypical chemokine receptors can induce intracellular signals independent of G protein coupling is a field worthy of much more detailed examination.

1.8.4 CCRL2

One of the most recent additions to the atypical chemokine receptor family is CCRL2, also known as CRAM. CCRL2 is reported to act as a receptor for CCL19 and CCL5, as well as the non-chemokine chemoattractant chemerin, which also binds the chemokine-like receptor (CMKLR)-1, alternatively known as ChemR23. ChemR23 is expressed by human pDCs and may be involved in their migration into inflamed tissue (Vermi et al., 2005, Zabel et al., 2005). Human CCRL2 mRNA is detectable in activated astrocytes, microglia and macrophages, as well as being constitutively expressed by bronchial epithelium. The human protein is detectable on a variety of human leukocytes, including T cells, mast cells, neutrophils, monocytes, macrophages and DCs (Zabel et al., 2008). It has also been reported on human B cells (Hartmann et al., 2008). CCRL2 ligand binding has been reported to occur without internalisation or signalling in a conventional manner. In a study by Hartmann and colleagues, CCL5-induced ERK phosphorylation was attributed to CCRL2 expression on Nalm6 cells (a cultured human pre-B cell line) in the absence of expression of conventional CCL5 receptors. However, exposure to CCL5 did not induce calcium flux or cell migration (Hartmann et al., 2008). Zabel and colleagues identified chemerin as a ligand for CCRL2 initially through chance observation of the ability of chemerin to inhibit labelling of mast cells with anti-CCRL2 antibody. They confirmed the interaction of chemerin and CCRL2 by conducting radioligand binding assays with radiolabelled chemerin, which bound to CCRL2-transfected cells but not untransfected cells. The affinity was found to be slightly higher than that of chemerin for ChemR23 (Zabel et al., 2008). Exposure of murine peritoneal mast cells, which naturally express CCRL2, or CCRL2-transfected cell lines to chemerin did not induce calcium flux or cell migration. Additionally, chemerin was not internalised by CCRL2 but was bound on the cell-surface, prompting speculation that CCRL2 acts to concentrate and present chemerin to cells expressing ChemR23 (Zabel et al., 2008). One recent study has suggested that CCL19 may also be a ligand for CCRL2, with radiolabelled CCL19 able to bind to CCRL2-transfected cells. Interestingly, the level of binding increased with addition of CCL5, supporting the suggestion that CCL5 induces upregulation of CCRL2 surface

expression. Internalisation of radiolabelled CCL19 by CCRL2-transfected CHO cells was demonstrated by comparison of cells incubated at either 4°C or 37°C (to allow internalisation) followed by acid-wash or PBS wash. Transfectants incubated at 37°C had significantly increased levels of cell-associated radioactivity compared to either untransfected cells or those incubated at 4°C (Leick et al., 2010).

While these early studies have provided some interesting indications of CCRL2 function, at least *in vitro*, study of this receptor is in its infancy and much work remains to be carried out before a fuller understanding of its role is reached.

1.8.5 Identification and preliminary characterisation of CCX-CKR

A novel human chemokine receptor was identified in 2000 (Gosling et al., 2000, Khoja et al., 2000, Schweickart et al., 2001, Schweickart et al., 2000), from analysis of EST databases. The receptor was a 350 amino acid protein named CCX-CKR, for **ChemoCentryx Chemokine Receptor** (in reference to the company that was among the first to clone it – it is also referred to in the literature as CCR11 and CCRL1). It is highly homologous to a bovine gustatory receptor, PPR1, which was used in one study as an entry point to mining of EST databases in search of human chemokine receptors (Gosling et al., 2000). CCX-CKR also displays a high level of sequence homology at the amino acid level with other CC chemokine receptors, notably CCR7 and CCR9 (Khoja et al., 2000, Townson and Nibbs, 2002). Khoja and colleagues failed to determine the ligand binding profile for CCX-CKR, despite assaying a variety of ligands, including CCL3, CCL16, CCL18-20, CXCL3, CXCL8-10 and CXCL12. However, their approach relied on detecting the induction of calcium signalling following ligand binding, a property lacking in atypical chemokine receptors (Khoja et al., 2000). Gosling and colleagues successfully identified the major ligands for the receptor using a novel approach where cells were transfected with CCX-CKR and then passed over glass slides carrying immobilized chemokine presented on stalk-like structures (referred to as “stalkokines”). This identified human and murine CCL19, CCL21 and CCL25 as high affinity ligands for CCX-CKR, with a half-maximal inhibitory concentration (IC_{50}) <15nM, based on displacement of radiolabelled CCL19 binding. Human CXCL13 and a virally-encoded chemokine, vMIP-II, demonstrated lower, but detectable binding (IC_{50} <150nM). A panel of more than 80 purified chemokines, both human and murine, were assessed with minimal or no binding affinity detected for any other ligands (Gosling et al., 2000).

In 2002, Townson and Nibbs successfully identified murine CCX-CKR and showed that radiolabelled human CCL19 bound to CCX-CKR transfected HEK cells but not untransfected cells. Using displacement of radiolabelled CCL19 binding as a measure of affinity, they demonstrated that murine CCX-CKR shared the same high affinity ligands as its human counterpart, i.e. mCCL19, mCCL21 and mCCL25. Affinity for mCCL19 was highest ($IC_{50} \sim 3nM$), with slightly lower affinity for mCCL21 and mCCL25 ($IC_{50} \sim 10nM$). Unlike the human receptor, murine CXCL13 binding was not found to occur for the murine receptor. As with human CCX-CKR, ligand binding by murine CCX-CKR did not lead to subsequent intracellular signalling as measured by calcium flux, nor was any CCX-CKR-dependent MAP kinase phosphorylation observed (Townson and Nibbs, 2002). This ligand binding profile, as well as the reported failure to induce calcium flux in response to ligand binding was confirmed by Heinzl and colleagues in 2007 (Heinzl et al., 2007).

The expression profile of CCX-CKR has been examined at the mRNA level for both the human and the murine receptor. The expression pattern of human CCX-CKR mRNA was determined by RT-PCR analysis of RNA from various tissues and by human cDNA analysis (Gosling et al., 2000). Expression was found in monocyte-derived immature DCs, T cells, spleen and lymph node. It was also detected in a variety of non-lymphoid tissues including heart, kidney, placenta, trachea and brain. However, it should be noted that controls for genomic contamination, such as assessment of samples lacking reverse transcriptase, were not reported to be included (Gosling et al., 2000). Townson and Nibbs used Northern blotting and RT-PCR to analyse expression of the murine receptor. They reported expression in a variety of murine tissues, both lymphoid and non-lymphoid, including heart, lung, testis, spleen and skeletal muscle. Lymph nodes, Peyer's patches and peripheral blood showed only low levels of CCX-CKR mRNA expression. Northern blot analysis of human CCX-CKR mRNA expression was also conducted and expression was detected in heart, lung, small intestine, brain, colon and skeletal muscle, but not in leukocytes, contrary to previous reports (Gosling et al., 2000, Townson and Nibbs, 2002). Southern blotting of human genomic DNA revealed the existence of two forms of the human gene that differ in sequence by three nucleotides, found at positions 85, 152 and 669 (Townson and Nibbs, 2002).

Another, more recent study, addressed the question of where the protein was expressed. Heinzl and colleagues generated CCX-CKR1-EGFP knock-in mice and looked for EGFP expression in heterozygous animals (which were phenotypically indistinguishable from wild-type). They found that CCX-CKR-driven EGFP expression was not detectable by flow cytometry on haematopoietic cells from a variety of sources. However, using confocal

microscopy, they did detect expression by non-haematopoietic cells in various tissues, including thymus, lymph node, epidermis and intestine. Contrary to the reported pattern of mRNA expression, they did not detect EGFP in heart, kidney, spleen or brain, nor did they find it in liver (Heinzel et al., 2007). However, this study failed to confirm the expression profile of the knocked-in gene as being a true reflection of CCX-CKR expression. Moreover, a LacZ reporter knock-in generated at Deltagen Inc. showed a different expression profile, with expression detected in keratinocytes, hair follicles and heart pericardium, but not in any lymphoid tissues examined, including lymph node and thymus (expression data available through the Mouse Genome Informatics website, at <http://www.informatics.jax.org/> - search “Ccr11” – choose Ccr11^{tm1Dgen} – choose Expression – assay results). These conflicting data leave the true cellular source of murine CCX-CKR expression unclear.

The discovery of this receptor, with its atypical attributes, prompted speculation that it may play a role in limiting or otherwise regulating constitutive chemokine levels. Comparing CCX-CKR transfected HEK293 cells with cells transfected with CCR7, our group have shown, *in vitro*, that cells expressing exogenous transfected CCX-CKR can uptake CCL19 rapidly, retaining and eventually degrading the chemokine. This study also showed that the ability of CCX-CKR to sequester the chemokine was increased when exposed to chemokine (Comerford et al., 2006), in contrast to CCL19-induced desensitization of CCR7. These *in vitro* data have suggested that CCX-CKR may play a regulatory role, preventing prolonged/over-stimulation of lymphocytes by “mopping up” excess chemokines. It may also regulate the migration of various leukocyte subsets that are known to be dependent on CCR7 and CCR9 ligands by controlling the bioavailability of the ligands. Heinzel and colleagues reported that deletion of CCX-CKR leads to perturbation of dendritic cell migration to skin-draining lymph nodes under resting conditions, with a reduced number of MHCII^{high} CD11c⁺ DCs found in CCX-CKR deficient LNs compared to WT. They also found that, while thymocyte maturation and migration appears normal in CCX-CKR-deficient mice, transgenic over-expression of CCX-CKR in thymic epithelial cells (where they had previously detected CCX-CKR-dependent EGFP expression) led to a defect in thymic precursor homing to the thymic anlage at embryonic day 12.5 (Heinzel et al., 2007). If CCX-CKR is acting as a scavenger, as is suggested by the *in vitro* data presented above, this defect could be due to aberrant clearance of CCX-CKR ligands from the thymus, disrupting thymocyte precursor homing to this tissue (see above for the importance of CCR7, CCR9 and their ligands in thymic development and function). Heinzel and colleagues did not find any difference in CCL25 protein localisation in the thymus of transgenic mice overexpressing CCX-CKR compared to WT. However,

attempts to quantify levels of bioavailable CCL25 in either mouse were unsuccessful (Heinzel et al., 2007).

While current evidence favours the “scavenging” hypothesis, there are other possible roles that this receptor could play. One potential function involves activity as a transporter of chemokines, rather like the functions proposed for DARC, for example transcytosing them from the site of production in lymph nodes across high endothelial cells (HECs) to be displayed to passing peripheral lymphocytes. This would fit with current knowledge of how one CCR7 ligand, CCL19, is presented to T cells on the luminal surface of HEVs, facilitating T cell recruitment into lymph nodes (Baekkevold et al., 2001). Also, CCX-CKR uses caveolins to mediate chemokine internalisation, rather than the β -arrestin dependent clathrin-coated pits used by classical chemokine receptors (Comerford et al., 2007). Caveolins are often associated with transcytosis (Pelkmans and Helenius, 2002), lending further credence to this hypothesis. However, demonstration of this capacity, either *in vitro* or *in vivo*, remains to be reported.

As described above, when my project began, information about the expression pattern or possible function of CCX-CKR *in vivo* was extremely limited. Previous studies had provided indications of which tissues expressed the receptor at the mRNA level but had not provided quantification of this expression. Conflicting reports examining protein expression of the receptor have left the site of CCX-CKR protein expression unclear. *In vitro* studies had suggested a potential for scavenging by the receptor, and a previous student had generated CCX-CKR deficient mice to examine the effect of deletion of this receptor and to provide a tool for accurate identification of cells expressing CCX-CKR. Another student in the lab had begun analysing the intestinal compartment of the CCX-CKR deficient mouse, so I began my project with the broad aim of identifying cells expressing CCX-CKR and uncovering a role for CCX-CKR in secondary lymphoid tissues and other peripheral tissues. As there were no commercially available antibodies to CCX-CKR, a novel approach needed to be adopted to circumvent this difficulty, and I developed and optimised a protocol to facilitate this aim. These experiments are detailed in chapter 3. In light of *in vitro* data suggesting a scavenging function for the receptor, I also wished to investigate the potential for CCX-CKR to regulate chemokine levels *in vivo*. Chapter 4 reports my findings in this regard. Given the potential for CCX-CKR to affect chemokine levels, as well as the reported defect in DC homing to LN under resting conditions, a detailed analysis of any defects in lymphoid tissue cellularity attributable to CCX-CKR deletion was also desirable, and experiments addressing this question are detailed in chapter 5. I also wanted to examine the potential for CCX-CKR to affect inflammatory

responses. There was limited information available on the role of CCX-CKR in the immune response at the start of my PhD, with only preliminary analysis of the CCX-CKR deficient mouse carried out prior to my project. Therefore, I carried out an analysis of CCX-CKR involvement in induced short-term cutaneous inflammation as well as in a model of tumorigenesis involving chronic inflammation, described in chapter 6. The interpretation and discussion of the data from these experiments, as well as further information that emerged throughout the course of my investigations, are discussed in chapter 7.

2 Materials and Methods

2.1 Animals

CCX-CKR deficient mice were generated by I. Comerford and R. Nibbs (Comerford et al., 2010) and backcrossed for 11 generations onto a C57Bl/6 genetic background (CD45.1⁻ CD45.2⁺ H-2^b). These animals were bred and maintained under specific pathogen free conditions in the Central Research Facility, University of Glasgow. Wild-type (WT) C57Bl/6 mice, originally littermates of the CCX-CKR deficient mice, were bred and maintained under the same conditions in this facility. CCX-CKR deficient and WT mice on an FVB background were generated from the original CCX-CKR deficient C57Bl/6 mice detailed above by backcrossing with WT FVB for 6 generations. After genotyping tail tip biopsies by PCR, separate WT and CCX-CKR deficient colonies were established and bred and maintained under the same conditions as the C57Bl/6 in the Central Research Facility. All procedures were carried out in accordance with United Kingdom Home Office regulations under the auspices of appropriate Project and Personal Licences.

2.2 Genotyping

Animals were periodically genotyped by polymerase chain reaction (PCR) to ensure the deletion or presence of the CCX-CKR gene in CCX-CKR deficient (KO) or WT mice respectively. Primers used for genotyping were synthesised by VH Bio, Gateshead, UK. Sequences are listed in Table 2.1. The primers were designed to allow identification of WT, KO and heterozygous (het) animals – 11com5 binds to both WT and KO alleles while the others bind either WT (11wt5) or KO (3IRES), as shown in Table 2.1. The primers were stored at a stock concentration of 100µM in water at -20°C.

Primer	Sequence	Specificity
11wt5	AAT CGC CAC AAC TAC GGA GTT C	WT
11com5	TGC TGG TGA GCT CTG GGT TC	WT and KO
3IRES	CCC TAG ATG CAT GCT CGA CG	KO

Table 2.1: Primers used for genotyping. Primers were synthesised by VH Bio and used as described in the text.

These primers were used to make a “primer mix”, with each stock primer present in the following amounts:

11wt5	10µl
11com5	10µl
3IRES	2.5µl

Nuclease-free water (Applied Biosystems, Warrington, UK) was added to a total volume of 100µl.

Animal tailtips were incubated in 100µl lysis buffer containing 100mM Tris-HCl (pH 8.5; Sigma, Poole, Dorset, UK), 5mM ethylenediaminetetraacetic acid (EDTA; Sigma), 0.2% sodium dodecyl sulphate (SDS; Sigma) and 200mM sodium chloride (NaCl; Sigma), at 55°C overnight. Lysed samples were incubated at 96°C for 5 minutes and then diluted in 400µl water. Cell debris was removed by centrifugation at 15000 x g for 5 minutes and the supernatant used as template in a standard PCR reaction. ABgene 1.1X Prealiquoted Reddymix™ PCR master mix 50µl reaction tubes (Applied Biosystems, Warrington, UK), containing 45µl of PCR master mix, were used to carry out the PCR reaction. For each sample, 2.5µl of template DNA plus 2.5µl of primer mix was added to a Reddymix™ tube. The PCR reaction was carried out in a PTC-200 Peltier Thermal Cycler (MJ Research, Massachusetts, USA) using the following conditions:

<u>94°C</u>	<u>5 min</u>	
94°C	15 sec	 x 35
60°C	30 sec	
<u>72°C</u>	<u>45 sec</u>	
72°C	10 min	
4°C	∞	

PCR products were electrophoresed on a 2% agarose gel containing SYBR® Safe (Invitrogen, Paisley, UK), as per manufacturer's instructions, at 100V and visualised using a transilluminator. Product size was determined by comparison with HyperLadder™ I (Bioline, London, UK), with WT samples yielding a product of 610 base pairs (bp) and CCX-CKR^{-/-} samples yielding a product of 420 bp. Heterozygotes will have both bands present. Figure 2.1 shows an example of a genotyping gel.

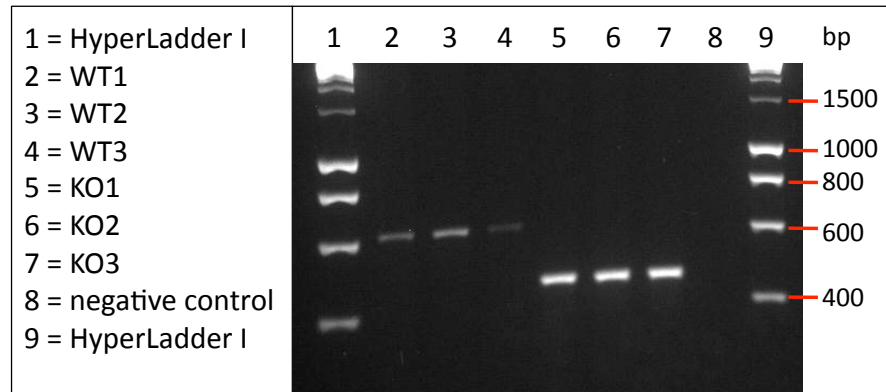


Figure 2.1: Genotyping wild-type and CCX-CKR deficient mice. Tail-tips from wild-type (WT) and CCX-CKR deficient (KO) samples were lysed and used to generate template genomic DNA. Template DNA was used in a standard PCR reaction using primers 11wt5, 11com5 and 3IRES (see main text), with water used as a negative control. The products of this reaction were electrophoresed on a 2% agarose gel containing SYBR®Safe and visualised using a transilluminator. WT products are 610 bp in size, KO products are 420 bp in size. HyperLadder™ I was used to determine product size, size of bands in ladder are indicated.

2.3 Isolation of cells from primary tissue

Age-matched males aged between 6 and 10 weeks were used for all experiments. Animals were sacrificed by cervical dislocation or CO₂ inhalation either under resting conditions or subsequent to procedures described later in this section. Tissues were immediately dissected and either placed in Roswell Park Memorial Institute (RPMI)-1640 medium (Sigma) supplemented with 10% heat-inactivated foetal calf serum (Invitrogen), 10 U/ml penicillin/streptomycin (Invitrogen) and 0.2 mM L-glutamine (Sigma) (referred to hereafter as “complete RPMI”), or *RNAlater*[™] RNA Stabilisation Reagent (*RNAlater*[™]; Qiagen, West Sussex, UK), or snap-frozen in liquid nitrogen. Peritoneal cavity lavage was harvested for flow cytometry and QPCR by injecting 2 x 5ml cold Dulbecco’s phosphate buffered saline (DPBS) containing 2mM EDTA into the cavity and retrieving the lavage using 5ml syringes with 18-gauge needles. Total lavage for each individual (approximately 10ml, pooled) was stored on ice in 10ml complete RPMI until processed. Whole blood was collected into tubes with or without heparin (Sigma). For tubes with heparin, 200-300µl of heparin was added to each tube, tubes were flicked to coat sides with heparin and excess heparin was decanted. Whole blood was harvested from the inferior vena cava using heparinised needles and syringes where appropriate to prevent clotting.

Single cell suspensions were prepared from peripheral lymph nodes, spleen, whole blood and peritoneal cavity. Lymph node and spleen samples were minced and incubated at 37°C with collagenase D (Roche, Hertfordshire, UK; 1 mg/ml) in Hanks Balanced Salt Solution (HBSS) medium (Invitrogen), for 45 minutes with shaking on either a Thermomixer comfort (Eppendorf, Cambridge, UK) or an Innova® 44 Incubator Shaker (New

Brunswick Scientific, Cambridge, UK), except where indicated. Collagenase-treated samples and untreated secondary lymphoid organs were mashed through 50µm nitex (Cadisch, London, UK) or cell strainers (BD, Oxford, UK) in complete RPMI. Red blood cells in spleen and peritoneal cavity lavage samples were lysed using red blood cell lysing buffer (Sigma), according to manufacturer's instructions. Whole blood was incubated at a 1:11 dilution in ammonium chloride solution (StemCell Technologies, Grenoble, France) to lyse red blood cells. Single cell suspensions from each tissue were washed twice in complete RPMI by centrifugation at 350 x g for 5 minutes at 4°C, resuspended in complete RPMI and counted using a haemocytometer with an inverted microscope. Viability was determined based on brightness and morphology.

2.4 Antibodies and chemokines

Antibodies labelled with fluorescein isothiocyanate (FITC), phycoerythrin (PE), peridinin-chlorophyll-protein (PerCP) or PE conjugated to cyanine 5.5 (PE-Cy5.5), as well as biotinylated CCL19 (BioCCL19 – Almac, Craigavon, UK) and streptavidin labelled with either PE (StrPE) or allophycocyanin (StrAPC), both from Invitrogen, were used for FACS and/or immunofluorescent staining. ViaProbe (BD) was used where described to determine viability. All antibodies were stored in original vials at 4°C and used at final concentrations between 1-5µg/ml. All fluorescent antibodies used are listed in Table 2.2.

Antigen	Clone name	Supplier	Isotype control
CD45	30-F11	BD	Rat IgG2b
CD5	53-7.3	BD	Rat IgG2a
CD19	1D3	BD	Rat IgG2a
CD3	145-2C11	BD	Hamster IgG1
CD21/CD35	7G6	BD	Rat IgG2a
CD23	B3B4	BD	Rat IgG2a
F4/80	BM8	Caltag*	Rat IgG2a
CD11b	M1/70	BD	Rat IgG2b
CD11c	N418	eBioscience**	Armenian Hamster IgG
IgM	Polyclonal	Invitrogen	none

Table 2.2: List of fluorescently labelled antibodies used in the experiments described in this thesis. *Caltag, Buckingham, UK; ** eBioscience, Hatfield, UK.

BioCCL19/StrAPC tetramers were formed by mixing 6µg BioCCL19 with 100µg StrAPC per ml in PBS (except where stated) and then incubating the mixture in darkness for 45

minutes at room temperature. Controls lacking BioCCL19 were made with the corresponding concentration of StrAPC in PBS and incubated in the same way. Recombinant chemokines were used in competition assays. Unlabelled murine MIP-3 β (CCL19) and unlabelled murine Exodus-2 (CCL21) were from PeproTech EC, London, UK. Unlabelled purified PM2 - a non-aggregating mCCL3 derivative with the same bioactivity as wild-type (Graham et al., 1994) - was provided by R. Nibbs. These chemokines were resuspended to a stock concentration of 0.1mg/ml in endotoxin-free water (Invitrogen) and stored at -20°C.

2.5 Internalisation and binding assays

Equal numbers of cells (ranging from 0.5-2 x 10⁶/sample, depending on experiment) were harvested by centrifugation at 4°C at 400 x g and resuspended in 50 μ l binding buffer (complete RPMI plus 20mM 4-(2-hydroxyethyl)-1-piperazineethanesulfonic acid (HEPES; Invitrogen), pH 7.4), with or without fluorescently labelled CCL19 tetramers or StrAPC alone, prepared as described above. Fluorescent tetramers or StrAPC in PBS were added to samples to a final concentration of 0.6ng/ μ l BioCCL19 and 10ng/ μ l StrAPC, except where stated. Samples were then incubated at 37°C (internalisation) or 4°C (binding) for 1 hour in darkness, with occasional agitation to keep cells in suspension. Cells were then stained at 4°C with antibodies for leukocyte markers, described below.

2.6 Competition assays

Competition assays were carried out as for the internalisation/binding assays except with the addition of a ten-fold molar excess of unlabelled chemokine (i.e. 300ng/sample) directly prior to addition of fluorescently labelled CCL19 tetramers (30ng/sample). After incubation at 4°C or 37°C as above, cells were then stained with fluorescent antibodies for leukocyte markers.

2.7 Antibody staining

Freshly isolated cells or cells from internalisation/binding/competition assays were harvested by centrifugation for 5 minutes at 4°C at 400 x g and resuspended in chilled Fc block™ (BD) for 15 minutes on ice. They were then incubated with fluorescently-labelled antibodies or isotype controls in fluorescence-activated cell sorting (FACS) buffer (phosphate buffered saline (PBS) plus 1% heat inactivated foetal calf serum, 0.02% sodium azide (Sigma), 5mM EDTA) on ice for 15 minutes. Samples were washed twice with 1ml chilled FACS buffer, with cells pelleted by centrifugation at 400 x g at 4°C and

resuspended in a final volume of 200µl of either FACS buffer or 2% paraformaldehyde (PFA – fixative; Sigma). Stock PFA was prepared from powdered PFA to a concentration of 4% w/v in PBS, with stirring on a hotplate until dissolved.

2.8 Flow cytometry

Stained cells with and without fixative were analysed using a FACSCalibur flow cytometer (BD) and CELLQuest software (BD). Acquisition parameters were established using unstained and single-stained cells, i.e. cells with no or only one fluorescent antibody stain included. Data were analysed subsequent to acquisition using FlowJo software from Treestar Inc. (Ashland, OR, USA), using unstained and single-stained samples to set gates.

2.9 Cell sorting using the FACS Aria

Cells ($1-2 \times 10^7$ /ml) were isolated and stained with fluorescently-labelled antibodies (see section 2.6), using MACS Buffer (DPBS without calcium or magnesium (Invitrogen), supplemented with 1% bovine serum albumin (Sigma) and 2mM EDTA (Invitrogen)), in place of FACS Buffer. Cells were then passed through a 40 µm cell strainer (BD) and sorted using the BD FACS Aria™ cell sorter (BD). Parameters were established using unstained and single-stained samples, as for FACS. Set-up, calibration and sorting were carried out by, and/or under the supervision of, A. Gilmour (University of Glasgow). Cells were sorted into RPMI-1640 medium supplemented with 20% heat-inactivated FCS, 10 U/ml penicillin/streptomycin and 0.2 mM L-glutamine. Sorted populations were then pooled according to subtype and retrieved by centrifugation at 450 x g, washed with complete RPMI, and resuspended in 1ml of complete RPMI. Cells were pelleted, supernatant removed and cell pellets stored at -80°C for subsequent RNA isolation, as described in section 2.11 below.

2.10 Isolation of RNA from whole tissues

Individual tissues were dissected from mice and stored in RNAlater™ (Qiagen) for 24 hours, then removed and stored at -80°C. Frozen tissues were ground up in liquid nitrogen using a pestle and mortar. Ground up tissue was transferred while frozen to a 15ml Falcon tube, 1 ml of TRIzol™ (Invitrogen) was added and RNA was extracted according to TRIzol™ manufacturer's instructions. Briefly, ground up tissue was incubated in TRIzol™ at room temperature for 5 minutes then transferred to RNase-free microfuge tubes (Applied Biosystems), and 0.2 ml chloroform (Sigma) was added. Samples were shaken vigorously, incubated at room temperature for 2-3 minutes and spun down at 12000 x g for 15 minutes

at 4°C. The aqueous phase was transferred to a fresh RNase-free tube, and 0.5 ml isopropanol was added to precipitate nucleic acid. Samples were inverted gently to mix, incubated at room temperature for 10 minutes and then spun down at 12000 x g for 10 minutes at 4°C. Supernatant was removed and the RNA pellet was washed with 1 ml of 75% ethanol before being dissolved in 100µl of nuclease-free water (Applied Biosystems). This sample was then cleaned using the “RNA Clean-up” protocol in the Qiagen RNeasy® Mini Kit, including an on-column DNase digestion step using the Qiagen RNase-Free DNase Set. The RNA concentration of each sample was determined using a ThermoFisher Nanodrop 1000™ spectrophotometer. Each sample was stored at -80°C prior to further DNase treatment (see section 2.12).

2.11 Isolation of RNA from single cell suspensions

Cells were isolated from tissues and either whole tissue mixed isolates or sorted populations were resuspended in 1ml complete RPMI. Samples were spun down at 450 x g, supernatant was removed completely and each sample was resuspended in 100-350 µl RLT Buffer for storage at -80°C. RNA was then isolated following the Qiagen RNeasy® Mini Kit instruction manual. This included the optional on-column DNase digestion step using the Qiagen RNase-Free DNase Set. The RNA concentration of each sample was determined using a ThermoFisher Nanodrop 1000™ spectrophotometer. Each sample was stored at -80°C prior to further DNase treatment (see section 2.12).

2.12 DNase treatment of RNA

RNA was treated with Promega RQ1 RNase-free DNase (Promega, Hampshire, UK) according to manufacturer’s instructions. Briefly, at least 1 unit of DNase/µg of RNA was added to up to 4.5µg of RNA in nuclease-free water plus 1µl of 10x Reaction Buffer, made up to a final volume of 10µl with nuclease-free water in nuclease-free 0.2ml tubes. This reaction was incubated at 37°C for 30 minutes, at which time 1µl of RQ1 DNase Stop Solution was added. The reaction was then incubated at 65°C for 10 minutes to inactivate the DNase. The RNA concentration of each sample was determined using a ThermoFisher Nanodrop 1000™ spectrophotometer.

2.13 Synthesis of cDNA from RNA

Complementary DNA (cDNA) was reverse-transcribed from RNA using AffinityScript™ Multiple Temperature cDNA Synthesis Kits (Agilent, Edinburgh, UK), according to manufacturer’s instructions. Briefly, equal µg amounts (300ng-1µg, depending on

experiment) of starting RNA for each sample were made up to 14.7 μl with nuclease-free water and 1 μl of oligo(dT) primer (0.5 $\mu\text{g}/\mu\text{l}$) was added. Samples were then incubated at 65°C for 5 minutes to remove any secondary structures in the RNA and then at 21°C for 10 minutes to allow primers to anneal to the RNA. To each sample, a 4.3 μl mix of the following components (final concentrations) was added: 1X AffinityScript RT Buffer, 2mM dNTP mix (0.5mM of each dNTP), 20U RNase Block Ribonuclease Inhibitor, and 1 μl AffinityScript Multiple Temperature reverse transcriptase (RT; 1 μl nuclease-free water was added in place of RT to -RT controls). Samples were incubated at 42°C for 5 minutes to initiate the reaction, 55°C for 1 hour to extend the products and then 70°C for 15 minutes to terminate the reaction. Reactions were then stored at either 4°C or -20°C until they were used for QPCR.

2.14 Measuring relative mRNA expression by quantitative polymerase chain reaction (QPCR)

Synthesised cDNA was used to determine the expression of various chemokines and receptors at the level of mRNA. Briefly, equal amounts of cDNA were added to a 96-well or 384-well MicroAmp® Fast Optical Reaction Plate (Applied Biosystems) in triplicate per biological sample with: 1X TaqMan® Universal PCR Master Mix, No AmpErase® UNG (Applied Biosystems), 1X appropriate probe (either target-specific inventoried assays or endogenous control assays, as defined in the text – see Table 2.3; Applied Biosystems), and nuclease-free water.

Target gene	Assay ID
Ccr11 (CCX-CKR) *	Mm02620636_s1
Ccr7 *	Mm01301785_m1
Ccr9 *	Mm02620030_s1
Ccl19 *	Mm00839967_g1
Ccl25 *	Mm00436443_m1
Gapdh **	4352932E

Table 2.3: Taqman® probes used for QPCR assays. All assays from Applied Biosystems. Assay type indicated as follows: * = Taqman® Gene Expression Assay, Inventoried; ** = Mouse GAPD (GAPDH) Endogenous Control. All assays contain sequence-specific unlabeled primers plus a Taqman® probe labeled with a fluorescent FAM™ dye and minor groove binder (MGB) on the 5' end and a non-fluorescent quencher (NFQ) on the 3' end.

Plates were loaded into a 7900HT Fast Real-Time PCR System machine (Applied Biosystems) and incubated at 95°C for 10 minutes followed by 40 cycles of incubation at

95°C for 15 seconds, then 60°C for 1 minute. Data produced was analysed using RQ Manager software (Applied Biosystems) to give relative quantity (RQ) values for each sample, relative to selected calibrator samples given an RQ value of 1. Samples with poor technical replicate values or Ct values higher than 38 were excluded from analysis.

2.15 Preparing samples for chemokine measurement

Tissues to be analysed were immersed in homogenisation solution (T-PER Tissue Protein Extraction Reagent (Thermo Scientific) with cOmplete, Mini, EDTA-free Protease Inhibitor Cocktail Tablets (Roche) dissolved in water and added at the appropriate concentration (see manufacturers' instructions)). The tissues were homogenised in this solution using an IKA® T8 basic ULTRA TURRAX® homogenizer with S8N-5G dispersing tool (VWR, Leicestershire, UK). Tissue debris was removed by centrifugation at 10000 x g for 5 minutes and supernatants retrieved for analysis. Whole blood was retrieved from the posterior vena cava and allowed to clot at room temperature for 30 minutes. Serum was separated from blood by centrifugation at 13000 x g for 20 minutes. Peritoneal cavity lavage was carried out with 2ml saline. Cells were pelleted by centrifugation at 400 x g and supernatants retrieved for analysis. All processed samples were stored at -20°C until they were analysed. Where required, tissue supernatants were diluted prior to analysis in homogenization solution. The total protein content of these preparations was determined using a Bicinchoninic acid (BCA) assay kit (Pierce, Loughborough, UK) according to the manufacturer's guidelines and using serial dilutions of BSA (Pierce) as standards.

2.16 Measuring chemokine concentrations by Enzyme-linked Immunosorbent Assays (ELISAs)

CCL19 and CCL21 protein levels were measured using specific DuoSet ELISA development kits (R&D Systems, Abingdon, UK). Immulon-4 ELISA plates (Corning, Amsterdam, the Netherlands) were coated overnight at room temperature with 100µl per well of specific capture antibodies at 2µg/ml (CCL19) or 4µg/ml (CCL21) in PBS. Plates were washed at least 3 times with PBS + 0.05% Tween and then blocked with 300µl of Reagent Diluent (1% BSA in PBS; R&D Systems) for 1 hour at room temperature. Meanwhile, standards (included in kits) were prepared as per manufacturer's instructions. Plates were washed as before and 100 µl sample or standards were added in duplicate and the plates incubated for 2 hours at room temperature. Plates were washed as before and 100µl of specific detection antibodies added at 100ng/ml (CCL19) or 50ng/ml (CCL21) in

Reagent Diluent. This was incubated for a further 2 hours at room temperature. Plates were washed as before and 100µl of Streptavidin-HRP (included in kits) diluted in Reagent Diluent as per manufacturer's instructions was added to each well. Plates were incubated at room temperature for 20 minutes in the dark. Plates were washed as before and 100µl of Substrate Solution (R & D Systems) was added to each well and incubated at room temperature for 20 minutes in the dark. 50 µl of Stop Solution (R & D Systems) was added to each well and the optical density read on a Sunrise™ microplate absorbance reader (Tecan, Reading, UK) using Magellan™ software (Tecan). Sample chemokine concentrations were calculated from the standard curve obtained, using Magellan™ software. Sample concentrations falling outside the standard curve were deemed invalid, with these samples re-analysed in a separate ELISA following dilution in homogenization solution.

2.17 Embedding tissues for sectioning

Dissected tissues were either fixed into formalin at room temperature for paraffin embedding or placed into Shandon Cryomatrix™ (ThermoFisher) and snap frozen in liquid nitrogen for frozen sections. Frozen spleen sections were cut to a thickness of 7µm onto PolyFrost® microscope slides (ThermoFisher) by C. Nixon at the Beatson Institute for Cancer Research, Glasgow and stored at -80°C. Formalin-fixed tissues were processed using a Shandon Citadel 1000 tissue processor (ThermoFisher) and embedded in paraffin wax using a Shandon Histocentre 3 (ThermoFisher) for subsequent sectioning using a Shandon Finesse 325 (ThermoFisher). Sections were cut at 6-10 µm thickness and floated on distilled water at 40°C in a Tissue Floatation Bath (ThermoFisher) to stretch and remove any wrinkles/folds from the section. Sections were then adhered to Polysine® microscope slides (VWR) and dried on a Hotplate (ThermoFisher) at 60°C for at least an hour.

2.18 Haemotoxylin and eosin staining

Paraffin-embedded sections were incubated at 60°C on a Hotplate (ThermoFisher) for at least 35 minutes to soften the paraffin wax. They were then incubated in xylene (ThermoFisher) for 3 minutes to remove the wax, followed by repeated short immersions in 100% ethanol, repeated short immersions in 70% ethanol and immersion in running tap water for 1 minute. Frozen sections were brought to room temperature from -80°C and then fixed in ice-cold acetone for 20 minutes, air-dried and immersed in running tap water for 1 minute. All slides were then stained as follows: immersion in haemotoxylin (Sigma)

for 2 minutes; immersion in running tap water until water runs clear; repeated short immersions in 1% acid/alcohol (ThermoFisher); rinse in running tap water; immersion in Scotts Tap Water Substitute (CellPath, Powys, UK) for 30 seconds; rinse in running tap water; immersion in eosin (Sigma) for 2 minutes; rinse in running tap water; immersion in 70% ethanol for 30 seconds; immersion in 90% ethanol for 1 minute; immersion in 100% ethanol for 3 minutes x 2; immersion in xylene for 3 minutes x 2. Slides were then allowed to air-dry before glass coverslips were mounted onto the sections using DPX mountant (VWR). Sections were visualized using an Axiostar plus microscope (Zeiss, Hertfordshire, UK) and analysed using Axiovision software (Zeiss).

2.19 Immunofluorescent staining of frozen sections

Frozen sections of mouse tissue that had been stored wrapped in foil at -80°C were brought to room temperature by incubating them at room temperature still wrapped in foil for 20 minutes, followed by unwrapping and incubating at room temperature for a further 10 minutes. Sections were then fixed in ice-cold acetone for 20 minutes in an ice-cold staining jar and air-dried at room temperature. Sections were delineated on each slide using an ImmEdge™ Hydrophobic Barrier Pen (Vector Laboratories, Peterborough, UK). Sections were then washed three times with 0.5% BSA in PBS for 5 minutes each, followed by incubation in permeabilisation solution (0.2% saponin (Sigma); 0.03M sucrose (Fisher Scientific, UK); and 1% BSA (Sigma) in PBS) for 5 minutes. Sections were then washed once with 0.5% BSA in PBS for 5 minutes, followed by blocking with 5% normal goat serum in PBS for 15 minutes to prevent non-specific labeling by antibody. Sections were then washed once with 0.5% BSA in PBS for 5 minutes, followed by incubation with appropriate antibodies or isotypes in PBS for one hour at room temperature in darkness. Sections were then washed three times with 0.5% BSA in PBS for 5 minutes each, then once with PBS alone. Coverslips were mounted onto the sections using Vectashield® Hard-Set™ Mounting Medium with DAPI (Vector Laboratories), which was allowed to harden overnight at 4°C before analysis using a Zeiss LSM 510 Confocal microscope and Carl Zeiss AIM software (Zeiss).

2.20 Induction of skin inflammation

Mice were shaved dorsally 24 hours prior to painting dorsally with $150\mu\text{L}$ of $50\mu\text{M}$ 12-O-tetradecanoylphorbol-13-acetate (TPA; Invitrogen) in acetone. TPA painting was carried out on 3 consecutive days. Animals were sacrificed 3 and 6 days later and tissues harvested for subsequent analysis by FACS, immunohistochemistry and QPCR.

2.21 Tumorigenesis

This protocol was established in the lab by Dr Mairi Clarke and carried out in collaboration with her. Mice were shaved dorsally 24 hours prior to painting dorsally with 25µg 7,12-dimethylbenz(a) anthracene (DMBA; Sigma) in 200µL acetone. Seven days post-DMBA paint, mice were painted dorsally with 150µL of 50µM TPA in acetone. TPA procedure was repeated twice weekly for 26 weeks or until an animal reached the end point of the experiment. Tumour burden was scored weekly. Tissues were retrieved and stored at -80°C for subsequent analysis by QPCR.

2.22 Statistical analysis

Data were analysed using GraphPad Prism software (San Diego, CA) applying appropriate statistical tests as described in figure legends. Normality was tested where appropriate using a D'Agostino and Pearson omnibus normality test. Probability values of $p < 0.05$ were considered statistically significant.

3 Expression and activity of CCX-CKR in resting mice

3.1 Quantifying expression of CCX-CKR mRNA in whole tissue

The aim of this project was to identify cells expressing CCX-CKR *in vivo*; to investigate its activity and function on these cells; and to examine whether CCX-CKR plays any role in regulating immune and inflammatory responses. Prior to this study, only limited analyses of sites of expression of CCX-CKR had been carried out (Gosling et al., 2000, Heinzl et al., 2007, Townson and Nibbs, 2002), with no information available on the relative expression of CCX-CKR in various tissues or on the specific cells responsible for expression in these tissues. It was decided that a quantitative polymerase chain reaction (QPCR) assay approach would be the best way to acquire this information. Taqman® Gene Expression Assays, from Applied Biosystems, provide an efficient and highly specific method for measuring relative quantities of expression of specific mRNA species in tissues and cells.

The assay chosen for this study was designed to amplify a small region of 146 base pairs (bp) within exon 3 of the *Ccr11* gene (Figure 3.1A). This exon contains the open reading frame (ORF) that encodes CCX-CKR. Choosing this type of assay eliminates the possibility that expression of some but not all splice variants may be detected, a problem that can occur when primers span an exon-exon junction. This is a possibility for CCX-CKR, the gene for which contains multiple exons in both human and mouse (Townson and Nibbs, 2002). Expression analysis from collaborators using intron-spanning primers suggested the main site of expression of CCX-CKR mRNA was in the thymus, with expression at other sites very low in comparison (R. Nibbs, pers. comm.), a result contradicted by published RT-PCR expression data that shows robust expression in a variety of tissues, both lymphoid and non-lymphoid (Townson and Nibbs, 2002). By choosing an assay that is not intron-spanning, it should be possible to detect all relevant mRNA species with the capacity of generating functional protein. It does, however, introduce the risk of false positive results due to genomic contamination of the sample, as the assay will not be able to distinguish between genomic DNA and complementary DNA (cDNA). This possibility was minimised by DNase treatment of each RNA sample. To verify that there was no genomic DNA contamination in the samples, “-RT” controls were used, in which the reverse transcriptase (RT) was left out of the cDNA synthesis mix. The region amplified by the assay is also outwith any exons of the *Acad11* gene, which runs

antisense to the *Ccr11* gene (Townson and Nibbs, 2002), eliminating the possibility of the assay detecting mRNA from this gene and producing false positive results. All data shown have been generated from experiments in which no specific CCX-CKR amplification was detected in -RT controls.

It was important to verify that the assay was capable of detecting CCX-CKR mRNA expression in wild-type (WT) but not CCX-CKR deficient tissue before using it as a means to quantify expression levels of this product in various WT tissues. Thymus samples were used to test this, as the thymus has been identified as a site of CCX-CKR expression (Heinzel et al., 2007, Townson and Nibbs, 2002). As well as an endogenous control assay for GAPDH expression, an assay specific for CCR7 was included to demonstrate that chemokine receptor mRNA was detectable in both WT and CCX-CKR deficient samples by this method. As shown in Figure 3.1B, CCX-CKR expression was only robustly detected in the WT sample. The low level amplification seen in the CCX-CKR deficient sample was comparable to that seen in no template controls. CCR7 was detectable in both the WT and CCX-CKR deficient samples, as expected. A standard PCR was also run on cDNA from WT spleen and LN samples, using the *Ccr11* assay as the primer mix. This showed that the amplified fragment corresponded to the expected amplicon size of 146 bp (Figure 3.1C). Thus the assay amplifies the correct DNA fragment and provides reliable detection of CCX-CKR.

To directly compare multiple tissues, I established and optimised a QPCR assay using 384-well plates. This is now routinely used in the lab for this type of analysis when sample numbers exceed the capacity of commonly used 96 well plates. Using the inventoried assay for *Ccr11* (CCX-CKR) it was possible to detect mRNA for CCX-CKR in all lymphoid tissue tested, as well as in some non-lymphoid tissues (Figure 3.2). Skin and small intestine showed similar levels of expression of CCX-CKR, compared to lymphoid tissue, while liver and peritoneal wall displayed minimal levels of expression ($p < 0.001$ compared to thymus; Figure 3.2). Peritoneal wall was included to accompany subsequent planned experiments analysing peritoneal cavity lavage cells. These data, combined with unpublished RT-PCR data that suggested B cells expressed CCX-CKR (R. Nibbs, pers. comm.), and the distribution of expression seen by Heinzel and colleagues, led us to investigate whether CCX-CKR was expressed by, and active on, leukocytes. Although this assay does not provide absolute quantification of mRNA expression and comparison between genes is therefore not quantitatively valid using this assay, Taqman assays are designed to provide equivalent amplification efficiencies. Therefore, it is interesting to

note that CCX-CKR amplification yielded higher Ct values in most tissues than CCR7, suggesting a lower expression level of CCX-CKR compared to CCR7.

3.2 Towards the identification of cells expressing functional CCX-CKR

3.2.1 Optimisation of an assay for detecting CCL19 receptor “activity”

Antibodies against chemokine receptors have proven to be unreliable at detecting native receptor expression. They are difficult to generate, particularly against murine receptors, since the mouse is the usual animal of choice for inoculation to produce effective monoclonal antibodies. Also, many receptor antibodies are generated against peptides rather than the receptor in its native conformation. While useful in assays where the protein is denatured, such as in Western immunoblotting, this type of antibody is usually of limited use in detecting the protein in its native, folded conformation, as the epitope recognised by the antibody may be partly or completely unavailable. At the time of these experiments, there was no commercially available antibody to CCX-CKR, and those that have subsequently been generated fail to detect exogenous mouse CCX-CKR on transfected cells (R. Nibbs, pers. comm.). Moreover, a widely used commercial antibody against CCR7 only detected high levels of expression of this receptor (data not shown). The absence of suitable antibodies, combined with evidence that another atypical receptor, D6, is present mainly internally rather than at the cell surface (Madigan et al., 2010, Weber et al., 2004), suggested that detection of surface-expressed CCX-CKR might be difficult. However, CCX-CKR and D6 internalise using different pathways and thus may not share this property (see Introduction). Efforts to minimise problems of detectability required the development of a highly sensitive assay that would allow distinction between not only CCX-CKR activity and CCR7 activity, but also between cells with no CCX-CKR expression and cells with only low CCX-CKR activity. Therefore a novel approach was adopted whereby cells under investigation were incubated at 37°C with fluorescently-labelled CCL19 tetramers and subsequently analysed by flow cytometry. The methodology is outlined in Figure 3.3. In theory, this method should allow the detection of receptors that are “active”, i.e. capable of internalising ligand. We reasoned that if CCX-CKR acts as a chemokine scavenger, as has been proposed from *in vitro* studies (Comerford et al., 2006), it should be particularly sensitive to detection by this approach. By comparison of WT cells with cells from CCX-CKR-deficient mice, it should be possible to distinguish CCX-CKR-mediated internalisation of the fluorescent CCL19 tetramers from that mediated by

other receptors (e.g. CCR7). This approach is broadly similar to one used successfully in the lab to detect D6 activity on primary murine leukocytes (Hansell et al., 2011b). We also included unlabelled chemokines as competitors to aid confirmation of the likely receptor(s) responsible for internalisation, as described below. Additionally, we predicted that, using this approach, we might be able to improve the detectability of CCR7 beyond that achievable with existing anti-mouse CCR7 antibodies. Moreover, human chemokines often bind chemokine receptors from other species, so the assay may be readily applicable to the analysis of CCL19 receptors in species other than mice where anti-chemokine receptors are even less commonly available. In this regard, it is interesting to note that ongoing work in our lab has shown that fluorescent human CCL2 and human CXCL8 provide sensitive detection of chemokine receptors on rat leukocytes, and these reagents are now being applied to other species, including birds. The fluorescent chemokine assay is arguably less suited to detection of “inactive” receptors, i.e. receptors that may bind but not internalise chemokine. A modified version of the assay, where cells are incubated with chemokine at 4°C, allows binding of fluorescently labelled chemokine to surface-expressed receptors – however, the fluorescence associated with this is much weaker than that seen after incubation at 37°C. Internalisation allows for accumulation of fluorescence within the cell, vastly increasing the potential level of fluorescence associated with the presence of the receptor. Due to the nature of the assay, the term “receptor activity” is used throughout this thesis when referring to cells capable of mediating chemokine internalisation.

As mentioned above, the protocol was modified from an assay developed in the lab for detection of D6 on primary cells, using directly conjugated fluorescently-labelled chemokine (CCL2 or CCL22). Like CCX-CKR, D6 expression by primary mouse cells is not detectable by any other means to date. Our protocol also drew on related assays used in the lab to detect CCX-CKR activity on transfected cells, using biotinylated or radiolabelled chemokine (Comerford et al., 2006, Hansell et al., 2011b). The assay was optimised for detection of CCL19 receptors, using fluorescent CCL19 tetramers prepared as described in detail in Materials and Methods (chapter 2) and outlined in Figure 3.3.

Successful detection of chemokine receptors using this method requires use of sufficient fluorescent chemokine over a long enough period to allow detectability over background levels of fluorescence. Therefore, before initiating the study, titration and timecourse assays were carried out to determine the optimal conditions of the assay. WT splenocytes were chosen to test the assay for a number of reasons. Firstly, the spleen contains a large number of easily isolated cells, allowing minimal animal usage for an experiment requiring a large number of samples. Secondly, WT spleen has readily detectable expression of

CCX-CKR mRNA, as determined by QPCR (see Figure 3.2). Finally, the spleen also contains a large number of lymphocytes, including T cells, which express CCR7. This provides an internal control to show that the assay is technically successful and the fluorescent chemokine tetramers are being internalised.

Live cells were gated based on size and granularity characteristics (forward scatter (FSC) and side scatter (SSC)). As shown in Figure 3.4, the level of fluorescence detectable was directly related to the initial concentration of fluorescent chemokine to which the cells were exposed. Even relatively low concentrations were enough to allow detectable internalisation, with the shift in fluorescence increasing with increasing concentrations of fluorescent chemokine (Figure 3.4b, left panel). However, this increase in fluorescence did not appear to increase markedly over time (Figure 3.4b, right panel), suggesting that, for splenocytes, the majority of internalisation occurred in the first 5-15 minutes of exposure to ligand.

These experiments suggested that the majority of chemokine internalisation activity might be down-regulated very early. Alternatively, there may be a threshold of intracellular chemokine concentration beyond which the chemokine gets degraded, meaning the chemokine could continue to be internalised without a corresponding increase in fluorescence. However, down-regulation of chemokine internalisation makes sense in light of *in vitro* data that shows down-regulation of CCR7-dependent ligand internalisation through exposure to CCL19 (Britschgi et al., 2008, Comerford et al., 2006). Data from Comerford et al. showed that, at least *in vitro*, CCX-CKR does not display this sensitivity to ligand exposure. CCX-CKR transfected cells were capable of continuous internalisation of chemokine from media, and in fact internalisation through CCX-CKR appeared upregulated upon exposure to CCL19 (Comerford et al., 2006). Therefore, the majority of fluorescence detected, which plateaus over time, is likely due to CCR7-mediated internalisation. However, one might expect that exposing cells to fluorescent chemokine for longer than 15 minutes, i.e. beyond the timeframe of CCR7 desensitisation, might enhance the detectability of CCX-CKR-dependent ligand internalisation when comparing WT and KO tissues. Thus, in all subsequent internalisation assays, $1-2 \times 10^6$ cells (depending on the experiment) were exposed to 30 ng biotinylated CCL19 plus 500 ng streptavidin-APC for 30 minutes at 37°C, except where stated.

To allow use of this method to detect CCL19 receptors, it was necessary to ensure that the fluorescent CCL19 tetramers were not being internalised non-specifically by cells. To do this, binding and internalisation assays were carried out on splenocytes in the presence or

absence of a ten- or twenty-fold molar excess of various chemokines to confirm the specificity of the interaction of the fluorescent CCL19 tetramers with receptor (Figure 3.5). Non-specific internalisation, for example through pinocytosis, would not be expected to be inhibited by excess unlabelled chemokine, while CCR7/CCX-CKR-mediated internalisation should be blocked, at least to some extent, by CCL19 or CCL21, but not by other chemokines that are not ligands for these receptors.

Binding of the fluorescent chemokine to lymphocytes at 4°C gave small increases in cell-associated fluorescence above controls and this was slightly, but significantly reduced in the presence of both unlabelled CCL19 and unlabelled CCL21 (Figure 3.5). PM2, a non-aggregating form of mouse CCL3 (Graham et al., 1994), was included as a negative control, as it does not bind to CCL19 receptors and should not compete for binding or internalisation of CCL19. As expected, PM2 did not reduce the binding of fluorescent CCL19 to splenocytes (Figure 3.5). When cells were allowed to internalise the chemokine at 37°C, there was a large increase in cell-associated fluorescence compared to experiments carried out at 4°C. PM2 did not impair internalisation of the fluorescent CCL19 tetramers, as expected. However, uptake of the fluorescent CCL19 tetramers was almost completely abolished in the presence of excess unlabelled CCL19 and was also significantly reduced in the presence of CCL21, although the effect seen in the presence of CCL21 was significantly less pronounced. CCL21 was included in both 10-fold and 20-fold excess to investigate whether this loss of competition might be due to lack of availability of the chemokine. CCL21 is known to be relatively “sticky” in comparison to other chemokines, due to an extended C-terminal tail (see Introduction), and this property may cause it to adhere to the plates used to carry out the assay. However, there was no significant reduction in binding or internalisation of fluorescent CCL19 in the presence of a 20-fold excess of unlabelled CCL21 compared to 10-fold excess.

Collectively, these data suggest that some binding, and the majority of internalisation, of fluorescently labelled CCL19 tetramers by splenocytes occurred specifically through CCL19 receptors.

3.2.2 Investigating CCX-CKR expression in the spleen

Having optimised the internalisation assay for detection of CCL19 receptors, the next experiments aimed to identify CCX-CKR expressing cells. The first tissue interrogated was the spleen. QPCR data presented previously shows easily detectable levels of CCX-CKR mRNA expression in whole spleen. Additionally, the spleen is easily disrupted and yields

large numbers of cells, providing ample material for analysis by flow cytometry. Due to conflicting evidence with regard to which cells might be the main source of active CCX-CKR (Gosling et al., 2000, Heinzl et al., 2007, Townson and Nibbs, 2002), a number of lineages were investigated. The nature of the assay allowed for investigation into potential effects of CCX-CKR on CCR7 activity as well, and observations in relation to this are also discussed here.

3.2.2.1 Expression of CCL19 receptors on T and B cells in the spleen

The first major cell types investigated were T cells, defined as CD3⁺ (or CD5⁺ CD19⁻ in some experiments) and B cells, defined as CD19⁺ (or B220⁺ in some experiments). These lymphocyte populations make up the vast majority of CD45⁺ cells in the spleen. Both cell types, but particularly T cells, require CCR7 for normal trafficking to and within lymphoid organs and for interactions during an immune response (see Introduction; Förster et al, 2008). Additionally, previous work in the lab, using RT-PCR from sorted cell samples, had indicated possible expression of CCX-CKR mRNA by B cells (R. Nibbs, pers. comm.). Therefore it was hypothesised that lymphocytes might be candidates for expression of CCX-CKR, which could act to allow cell autonomous regulation of responsiveness to CCR7 (and CCR9) ligands. This type of function has recently been suggested for another atypical receptor, D6, which is expressed by innate-like B cells and suppresses the migration of these cells (Hansell et al., 2011b).

The internalisation assay described previously in this chapter was used to investigate whether T and/or B cells showed any CCX-CKR activity. As shown in Figure 3.6, by comparing internalisation by WT and CCX-CKR deficient cells, it was clear that neither population displayed any detectable CCX-CKR activity, although both exhibited CCL19-dependent internalisation, presumably due to CCR7 activity. Data from competition experiments described above are consistent with this. The level of internalisation was the same between WT and KO samples, suggesting that CCR7-mediated internalisation was unaffected by the absence of CCX-CKR on these cells. Supporting this theory, T cells displayed a significantly higher level of fluorescence compared to B cells (Figure 3.6), indicative of their higher level of CCR7 expression. T cells use CCR7 and its ligands to correctly position themselves within lymphoid organs, while B cells are less reliant on these chemokines and their receptor (Förster et al., 1999).

Pre- and co-incubation with fluorescent chemokine was carried out on these subsets to determine whether CCX-CKR activity might be triggered by either stimulus, as well as to

verify the specificity of the internalisation (Figure 3.7). As discussed in the Introduction, our group has previously shown that, *in vitro*, CCX-CKR-mediated internalisation of CCL19 is increased upon exposure to the ligand, while CCR7-mediated internalisation is downregulated (Comerford et al., 2006). Additionally, work from our lab investigating D6 and other receptors for pro-inflammatory chemokines has shown that pre-incubation with various chemokines can augment fluorescent chemokine internalisation in both cultured and primary cells (M. Clarke, C. Hansell, R. Nibbs, pers. comm.). Therefore, it was hypothesised that pre-incubation with CCL19 might allow detection of internalisation through CCX-CKR while also reducing background fluorescence caused by CCR7-mediated internalisation. Both treatments led to an almost complete abolition of internalisation, particularly in T cells (Figure 3.7B and C), consistent with downregulation of CCR7 activity. Neither cell type displayed any detectable CCX-CKR-dependent CCL19 internalisation.

Innate-like B cells in the spleen include MZ B cells and B1 cells. These cells are rare in comparison to the relative abundance of classical follicular B cells found in most lymphoid tissues and in circulation. As described in the Introduction, they are believed to be involved in bridging the gap in immune defence between the innate and adaptive responses (Allman and Pillai, 2008). Recent work from our lab has shown that another atypical chemokine receptor, D6, is present on these cells, but not on classical follicular B cells (Hansell et al., 2011b). Given the demonstrated expression of D6 and CXCR7 by these cells (Hansell et al., 2011b, Sierro et al., 2007), and the sensitivity of these cells to CCR7 deletion in other anatomical locations (Höpken et al., 2004), it was hypothesised that they might also express CCX-CKR to regulate migration in response to homeostatic ligands. However, when these cells were analysed using the internalisation assay, no CCX-CKR-dependent internalisation was detected (Figure 3.8). There were some differences in the level of CCL19 internalisation between the different cell types, i.e. MZ B cells (defined as CD19⁺ CD21⁺ CD23^{-/low}) and B1 B cells (CD19⁺ CD5⁺ CD23⁻). These are likely due to varying levels of CCR7 activity.

Taking these data together with the data for overall T and B cell populations in the spleen, it was concluded that CCX-CKR expression in the spleen is unlikely to be due to lymphocyte expression of this receptor. Therefore, other leukocyte subsets were investigated to try to define CCX-CKR-expressing populations in the spleen.

3.2.2.2 CCL19 tetramer internalisation by myeloid cells in the spleen

The spleen contains a variety of myeloid cell subsets, including DCs, macrophages and neutrophils. Cells of the myeloid lineage are involved in both the innate and the adaptive arms of the immune response, with roles ranging from pathogen recognition and presentation of antigen to ingestion of whole organisms or cytotoxic activity against invading and/or diseased cells (Murphy et al., 2010). They are highly responsive to, and producers of, chemokines that allow localised orchestration of an effective and efficient immune response. As such, it was hypothesised that they might use an atypical chemokine receptor such as CCX-CKR to control their own immediate microenvironment, or to direct the migration and activation of other cells, through modulation of the chemokine environment within the tissue or in circulation.

These cells were identified on the basis of their expression of various standard myeloid markers, including F4/80, CD11b and CD11c. While these markers are typically used to define distinct lineages (e.g. CD11c is used to define DCs, F4/80 is used to define macrophages), there is a high level of overlap in these markers (e.g. CD11b⁺ CD11c⁺ DCs), and variation in level of expression of each marker, as well as some debate among researchers about appropriate definitions for myeloid subsets. Therefore, in this section, cells are described by their marker expression profile to avoid inaccurate definitions (for gating, see Figure 3.9). Cells negative for all three markers are not included in this analysis as the vast majority of these are T and B cells, which have been analysed previously. These cells demonstrated expected internalisation profiles for lymphocytes (data not shown), indicating that the assay was technically successful and results were reproducible.

Using the internalisation assay, no CCX-CKR dependent internalisation was detected by any of the cell types analysed (Figure 3.10). There was some clear inter-subset variation in the level of chemokine internalisation, possibly attributable to variation in CCR7 activity between different cell types.

To investigate the possibility that these cells might upregulate CCX-CKR in the presence of high levels of CCL19, pre- and co-incubation experiments were also carried out as before. This should also, as before, disrupt CCR7-mediated internalisation, allowing easier detection of CCX-CKR activity, as well as providing information on the specificity of the CCL19 internalisation seen in the previous experiment (Figure 3.10). No CCX-CKR dependent internalisation was identified as a result (Figure 3.11). The level of knockdown of internalisation varied between cell types for both pre- and co-incubation, consistent with

the non-specific internalisation capacity of phagocytic cells such as macrophages. Internalisation of particles through pinocytosis can take place independent of receptor stimulation (Pratten and Lloyd, 1986, Rogers and Basu, 2005). This raises questions as to the level of requirement for CCR7 in this internalisation of fluorescent CCL19 tetramers on these cells. However, in the absence of biotinylated CCL19 (i.e. in StrAPC alone controls), fluorescence was decreased, suggesting a significant degree of specific internalisation, that is, the internalisation was chemokine dependent. These cells may therefore use a mechanism for clearance/internalisation of CCL19 that is both CCR7- and CCX-CKR-independent. Interestingly, CD11b^{low} F4/80⁻ (population C) cells from CCX-CKR deficient spleen exhibited a small but statistically significant increase in internalisation of fluorescent CCL19 tetramers compared to WT (Figure 3.11, bottom left panel). Additionally, for some CCX-CKR deficient populations, specifically the CD11b^{high} F4/80^{low} (population B) and CD11b^{low} F4/80⁻ (population C) populations, there is a difference in the level of knock-down of internalisation observed between pre- and co-incubation conditions (Figure 3.11). This is not seen in the corresponding WT samples. Similarly, internalisation of fluorescent CCL19 tetramers by CCX-CKR deficient CD11b^{low/med} F4/80^{med} (population D) cells is not significantly decreased by co-incubation with unlabelled CCL19, but pre-incubation with the chemokine does cause a drop in internalisation, whereas both treatments cause a decrease in internalisation in the WT population (Figure 3.11). The differences are slight, and may simply be a product of variation between samples. However, it is tempting to speculate that in the absence of CCX-CKR, CCR7 activity and/or interaction with its ligand is in some way altered on these cells.

3.2.2.3 CCL19 tetramer internalisation by CD45⁻ cells in the spleen

Having demonstrated that CCX-CKR was not detectable on leukocyte subsets using the internalisation assay, focus turned to CD45⁻ cells, which are mainly stromal cells. Stromal cells are the structural component of the tissue and are known to produce a variety of factors that influence cell viability and growth as well as acting as a network upon which leukocytes can migrate. They can produce chemokines to influence the migration of leukocytes, both during the initial development of lymphoid organs and during normal immune system function in the adult (Bajénoff et al., 2006, Cyster, 2000, Cyster et al., 2000, van de Pavert and Mebius, 2010). It was theorised that stromal cells might use CCX-CKR either as a transport or presentation mechanism, as has been suggested for DARC (Chaudhuri et al., 1997, Hansell et al., 2011a, Rot, 2005). Alternatively, CCX-CKR

on these cells could act as a scavenger to buffer chemokine levels and allow maintenance of an appropriate microenvironment within the tissue.

As shown in Figure 3.12, CD45⁻ cells do not detectably internalise fluorescent CCL19. CD45⁺ cells (leukocytes) internalisation was normal (indicated by dashed line on graph, Figure 3.12C), acting as an internal positive control to demonstrate the technical success of the assay. This was reproducible in repeated experiments (not shown). To determine the specificity of internalisation by WT and CCX-CKR deficient cells, cells were co-incubated with a 10-fold excess of unlabelled CCL19 (Figure 3.12). Pre-incubation with a 10-fold excess of CCL19 was also carried out (Figure 3.12), to determine whether the same desensitisation phenomenon seen *in vitro* could be detected *ex vivo* in stromal cells (Comerford et al., 2006). However, there is no increase in fluorescence observed in CD45⁻ cells following either treatment.

3.2.3 Searching for CCX-CKR expressing cells in inguinal lymph nodes

Having demonstrated that leukocytes in the spleen did not use CCX-CKR to internalise fluorescent CCL19 tetramers, attention focussed on peripheral lymph nodes, specifically the inguinal lymph nodes (ILNs). Migration to and within these tissues is tightly regulated and relies heavily on CCR7 and its ligands (Förster et al., 2008), as described in the Introduction. T cells, B cells and DCs all rely on CCR7 and its ligands to allow them to patrol the body and efficiently and precisely respond to and resolve infections or other injuries (Förster et al., 2008). In both CCR7-deficient mice and in *plt/plt* mice, which lack CCL19 and lymphoid tissue CCL21 (but not peripheral/lymphatic CCL21), T and B cell populations are substantially disrupted (Förster et al., 2008). This is particularly true for T cells, which rely heavily on these ligands to direct them around the body and into and around lymphoid tissue (Nakano et al., 1997). Significantly, CCR7 is more important in leukocyte entry into lymph nodes than the spleen (Förster et al., 1999). It was therefore hypothesised that cells entering, residing within or exiting lymph nodes might use CCX-CKR to finely regulate the response to CCL19 and CCL21. This might occur through expression on leukocytes, either to modulate their own response to chemokine or to influence the fate of cells in the vicinity. The receptor might also be used by stromal cells, either as a mechanism for presentation of chemokine or as a sink to create haptotactic or chemotactic gradients within the tissue to direct leukocytes to the appropriate location. A study by Heinzl and colleagues reported that CCX-CKR expression was found in lymph nodes but not in spleen, using a CCX-CKR-EGFP knock-in reporter mouse. The reporter was not detected in haematopoietic cells by FACS, although this method may not be

sensitive enough to detect low levels of receptor expression. Confocal imaging showed cells positive for CCX-CKR-EGFP expression in the subcapsular region of the lymph node (Heinzel et al., 2007). These cells were reported as stromal cells, although there are a number of cell types, both haematopoietic and stromal, that can be found in this region, including macrophages and lymphocytes (Heinzel et al., 2007, Phan et al., 2009). Analysis of leukocyte subsets and stromal cells was carried out using the fluorescent CCL19 tetramer internalisation assay.

3.2.3.1 CCL19 tetramer internalisation by cells in the inguinal lymph nodes

The internalisation assay revealed no CCX-CKR dependent internalisation, although it did show that, as in the spleen, the level of internalisation by B cells is much lower than that of T cells (Figure 3.13), reflecting their different levels of reliance on CCR7 and its ligands. Notably, the extent to which the two cell types differ is more dramatic in the ILN than in the spleen (Figure 3.6). This reflects the greater dependence of T cells on CCR7 for entering the LN compared to the spleen, and supports the notion that the majority of internalisation detected is CCR7-dependent. It also revealed a small but statistically significant increase in fluorescence in CCX-CKR deficient B cells, as compared to WT (Figure 3.13).

Taking into account these data, as well as the extensive characterisation carried out for splenic lymphocytes, it was considered unlikely that pre- or co-incubation experiments would reveal CCX-CKR expression on these leukocytes.

As in the spleen, various myeloid cells were investigated in the ILN, and were identified based on staining for expression of CD11b, F4/80 and CD11c (Figure 3.14). Most populations did not show any CCX-CKR dependent CCL19 internalisation (Figure 3.14B and C). However, CD11b^{high} F4/80⁻ CD11c⁺ (A+) cells and CD11b^{int/high} F4/80^{low} CD11c⁺ (B+) cells from CCX-CKR deficient animals showed small but significant reductions in internalisation of fluorescent CCL19 tetramers compared to WT (Figure 3.14C), potentially identifying them as a source of CCX-CKR expression in the ILN. This possibility will be discussed in chapter 7.

CD45⁻ cells make up less than 1% of total live cells retrieved from ILNs, making analysis difficult and somewhat variable. However, as in the spleen, CD45⁻ cells in the ILN showed no internalisation of fluorescent CCL19 tetramers (Figure 3.15), while CD45⁺ cells in the same experiment readily internalised the chemokine (see graph, Figure 3.15). Competition

and pre-incubation with unlabelled CCL19 did not reveal any CCX-CKR-dependent internalisation of fluorescent CCL19 tetramers (not shown).

3.2.4 Investigating CCL19 tetramer internalisation by leukocytes in other compartments – analysis of whole blood and peritoneal lavage

Leukocyte movement through other compartments is influenced by CCR7 and its ligands, including extravasation of leukocytes from the blood and entry and exit of leukocytes to and from the peritoneal cavity (Förster et al., 2008, Höpken et al., 2004, Höpken et al., 2010). Additionally, peritoneal B1 cells have been shown to express D6, which appears to moderate responses to chemokines on these cells (Hansell et al., 2011b). Therefore, leukocytes from peripheral blood and peritoneal lavage from both WT and CCX-CKR deficient animals were analysed to determine whether CCX-CKR might be expressed there to modulate responses to its ligands.

Lymphocytes were focussed on as the main leukocyte population in the blood. T and B cells, identified based on expression of CD5 or CD19 respectively, were shown to lack CCX-CKR-dependent internalisation of fluorescent chemokine (see Figure 3.16). As in spleen and ILN, peripheral blood T cells display significantly more internalisation of fluorescent CCL19 tetramers than B cells (Figure 3.16).

Peritoneal lavages were carried out and the retrieved leukocytes were analysed for CCX-CKR-dependent CCL19 internalisation. Cells were identified using size and granularity characteristics, as well as lineage markers. Populations identified included T cells ($CD5^+ CD11b^- CD19^-$) and B cells ($CD11b^{low/neg} CD19^+$), as shown in Figure 3.17. B cells were separated into B1a, B1b and B1c cells as well as “classical” B2 cells, based on CD5 and CD11b expression, as shown in Figure 3.17 (Hansell et al., 2011b). The peritoneal cavity also contains a substantial macrophage population that makes up the majority of the large $FSC^{low} SSC^{med-high}$ population observed Figure 3.17. These cells were fractionated based on expression of CD11b. Conjugates ($CD11b^+ CD19^+$ cells and $CD19^+ CD5^{high}$ cells) were excluded from the analysis, as were $CD11b^{high} CD19^-$ cells in the “lymphocyte” gate, which were likely macrophages. None of the analysed populations showed any CCX-CKR dependent CCL19 internalisation (Figure 3.18). On the contrary, T cells from CCX-CKR deficient peritoneal cavity lavage showed a significant increase in internalisation. The histogram shown in Figure 3.18 shows a loss of a $CCL19^{low}$ population of T cells from the CCX-CKR deficient peritoneal cavity. Notably, in contrast to spleen, ILN and peripheral blood, WT peritoneal cavity T and B cells displayed the same overall level of

internalisation of fluorescent CCL19 tetramers. Thus it would appear that CCR7 levels are similar between T and B cells in the spleen.

3.3 Attempts to identify cells expressing CCX-CKR mRNA in the spleen by cell fractionation

Having extensively characterised the internalisation profile of leukocytes as well as CD45⁻ cells in a variety of lymphoid tissues, in circulation and in the peritoneal cavity, a small proportion of myeloid cells in the LN displayed CCX-CKR-dependent internalisation of fluorescent CCL19 tetramers. No other cells, from LN, spleen, PerC or blood demonstrated likely CCX-CKR expression, although many other cells readily internalised the chemokine, most likely through CCR7. This did not correspond to the QPCR data that showed easily detectable and comparable expression of CCX-CKR mRNA in various tissues, including those tested in the internalisation assays. Therefore, a more molecular approach was decided upon, whereby cells were isolated from tissues, sorted by FACS and analysed by QPCR for expression of CCX-CKR mRNA.

Single cell suspensions were prepared as for internalisation assays. They were then stained with antibodies against various lineage markers and sorted using a BD FACSAria (Figure 3.19). The initial group of antibodies was chosen to allow isolation of CD45⁻ cells (e.g. stromal cells), T cells (CD45⁺ CD3⁺ cells), B cells (CD45⁺ CD19⁺ cells) and other, mainly myeloid cells (CD45⁺ CD3⁻ CD19⁻ cells). These cells were then washed and pelleted. RNA was extracted using an RNeasy Mini kit (see Materials and Methods).

Extracting RNA from purified CD45⁻ cells proved difficult, and not enough good quality RNA was retrieved to allow subsequent QPCR analysis. This may be because the isolation and sorting procedure causes a high level of death in these cells. When cells were counted after sorting, less than 10% of cells were found to be alive based on Trypan Blue exclusion (data not shown). This contrasted with each CD45⁺ population isolated, where at least 50% of cells were viable after sorting (data not shown). This issue, in combination with low yields of CD45⁻ cells (less than 3% of total; Figure 3.19) meant these cells were not analysed by QPCR.

Early attempts to isolate RNA from the healthier CD45⁺ populations were unsuccessful. However, some optimisation of the protocol led to successful isolation of enough RNA to analyse RNA from 1-2 samples per cell type, allowing a pilot study of CCX-CKR expression in these cells (Figure 3.20). Whole spleen, which had already been shown to

contain readily detectable CCX-CKR mRNA expression (Figure 3.2), was used as a positive control. Comparing this to the isolates of CD45⁺ populations, CD19⁻ CD3⁻ cells were negative, expression in T cells was at the limit of detectability and expression in B cells was very low. This level of expression was approximately 40-fold lower than that seen in whole spleen, suggesting that CD45⁺ cells are not responsible for the majority of expression seen in this tissue.

Bearing in mind the difficulty in purifying viable CD45⁻ cells, it was decided that an analysis of the isolation procedure be carried out to ensure that CCX-CKR mRNA expression was still detected in disrupted spleen. Samples were taken at various stages of the isolation procedure (see Table 3.1) to try to identify at which point, if any, expression was lost. This was to allow modification, if possible, of the purification procedure to allow optimal detection of CCX-CKR expression. As seen in Figure 3.21, expression drops dramatically once the tissue is disrupted, in both the filtered fraction, which is mainly leukocytes, and in the fraction that does not pass through the filter. Expression is undetectable in the majority of other fractions. Expression analysis of CCR7 was included as a control, demonstrating that whatever effect of disruption is causing the decrease in detectable CCX-CKR mRNA expression does not similarly affect this related receptor. On the contrary, expression of this receptor increased with progression through the isolation procedure. This may be due to an increased proportion of leukocytes in later samples, or increased activation of leukocytes in these samples. However, this would need to be repeated for verification.

These data, while based on individual samples and requiring repetition to be verified, provide a possible explanation for the difficulties experienced in detecting CCX-CKR in sorted cells. It may also provide an explanation for the lack of CCX-CKR activity detected in internalisation assays, since the time between initial disruption of each tissue and its incubation with fluorescent chemokine is at least 4-5 hours in most cases. Depending on how CCX-CKR is regulated at the protein level, this might provide a long enough window for down-regulation of the receptor through disruption of mRNA expression. However, it should also be noted that peritoneal cavity lavage cells, which are largely leukocytic and easily and rapidly isolated, do not express any detectable CCX-CKR mRNA in this assay (data not shown), suggesting that, at least at this site, leukocytes do not express this receptor.

3.4 Summary

1. CCX-CKR mRNA is expressed in spleen, inguinal and mesenteric lymph nodes, thymus, Peyer's patches, small intestine and skin, but not liver or peritoneal wall.
2. Binding and internalisation of fluorescent CCL19 tetramers by splenocytes is readily detectable by FACS and is competable by excess unlabelled CCR7 ligands, CCL19 and CCL21, but not by excess unlabelled CCL3.
3. Primary splenocytes do not exhibit CCX-CKR-dependent internalisation of fluorescent CCL19 tetramers.
4. Primary splenic T cells internalise almost twice as much fluorescent CCL19 tetramer as primary splenic B cells. Internalisation by both cell types is disrupted by pre- or co-incubation with excess unlabelled CCL19.
5. Primary splenic B1 B cells internalise significantly more fluorescent CCL19 tetramer than primary splenic MZ B cells.
6. Primary splenic myeloid cells internalise fluorescent CCL19 tetramers to varying degrees and with varied specificity. CD11b^{low} F4/80⁻ cells from CCX-CKR deficient spleens internalise more of the tetramers than those from WT spleens, and in both cases internalisation is disrupted by pre- and co-incubation with excess unlabelled CCL19.
7. Preincubation of CD11b^{high} F4/80^{low} and CD11b^{low} F4/80⁻ cells from CCX-CKR deficient spleens with excess unlabelled CCL19 leads to decreased internalisation of fluorescent CCL19 tetramers compared with co-incubation of the same cell subsets with excess unlabelled CCL19. This is not seen with the same subsets from WT spleens.
8. CD45⁻ cells from spleen and ILN do not internalise fluorescent CCL19 tetramers.
9. CD11b^{high} F4/80⁻ CD11c⁺ cells and CD11b^{int/high} F4/80^{low} CD11c⁺ cells from CCX-CKR deficient ILNs display decreased internalisation of fluorescent CCL19 tetramers compared to the same cells from WT ILNs. This reduction is not consistently observed in any other cell type in the CCX-CKR deficient ILN.

10. Primary ILN T cells exhibit approximately four times as much fluorescence following incubation with fluorescent CCL19 tetramers as primary ILN B cells. B cells from CCX-CKR deficient ILNs internalise slightly more fluorescent CCL19 tetramers than those from WT ILNs.

11. Primary T cells from peripheral blood exhibit approximately twice as much fluorescence following incubation with fluorescent CCL19 tetramers as primary B cells from peripheral blood. Neither cell type exhibits CCX-CKR-dependent internalisation of the tetramer.

12. Primary peritoneal cavity T cells from WT animals internalise the same amount of fluorescent CCL19 tetramer as primary WT B cells from the peritoneal cavity. Overall, peritoneal cavity T cells from CCX-CKR deficient animals internalise more fluorescent CCL19 tetramer than those from WT animals, possibly due to loss of a CCL19^{low} population of T cells from the CCX-CKR deficient peritoneal cavity. Peritoneal B cells from CCX-CKR deficient animals internalise the same level of fluorescent CCL19 tetramer as those from WT.

13. Splenic expression of CCX-CKR mRNA decreases upon disruption of the spleen.

These findings suggest subtle effects of CCX-CKR deletion on CCR7 activity (i.e. CCR7-dependent internalisation of fluorescent CCL19 tetramers) and suggest ILN CD11b^{high} F4/80⁻ CD11c⁺ cells and CD11b^{int/high} F4/80^{low} CD11c⁺ cells as possible sites of CCX-CKR expression.

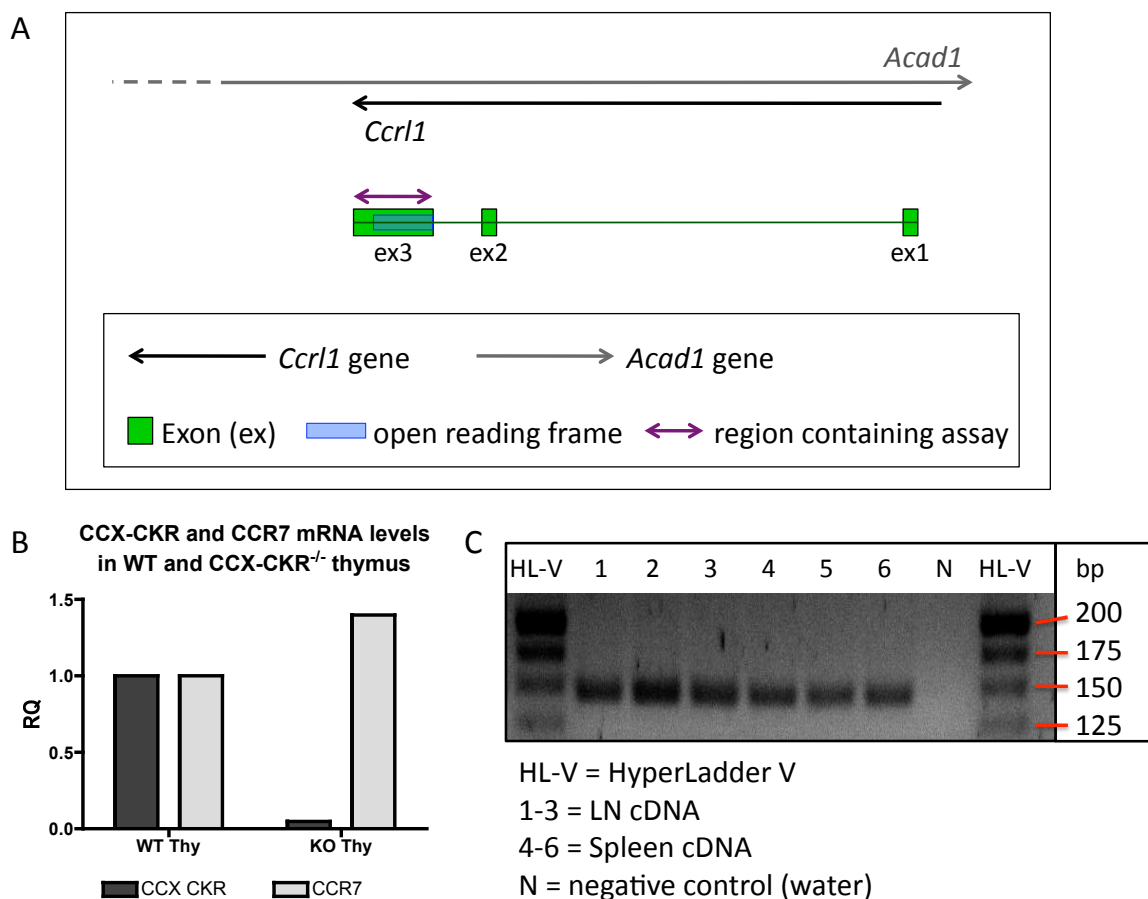


Figure 3.1: Detection of CCX-CKR mRNA expression using a Taqman® Gene Expression Assay. (A) Alignment map showing the region containing the primers used in the Taqman® Gene Expression Assay for *Ccr11* (CCX-CKR) from Applied Biosystems (specific primer sequences are not provided by the company). The *Ccr11* gene is shown anti-sense to the *Acad1* gene. *Ccr11* exons (ex) are shown as green boxes. The open reading frame (ORF) is indicated by a blue box. Purple arrows indicate the region that contains the target sequence amplified by the assay. Adapted from Applied Biosystems website. (B) RNA was isolated from whole thymus (Thy) from one wild-type (WT) and one CCX-CKR deficient (KO) mouse. Levels of CCX-CKR mRNA were determined by QPCR using the Gene Expression Assay described above. A Gene Expression Assay for CCR7 was also used, to verify the presence of other intact mRNA in the KO sample. GAPDH was used as an endogenous control to calculate relative quantities (RQ) of mRNA. For both CCX-CKR and CCR7, the WT sample was given an RQ value of 1. (C) The size of the amplicon (146 bp) produced using the CCX-CKR assay was verified by using cDNA from spleen and lymph node (LN) samples as templates and the assay as the primer mix in a standard PCR.

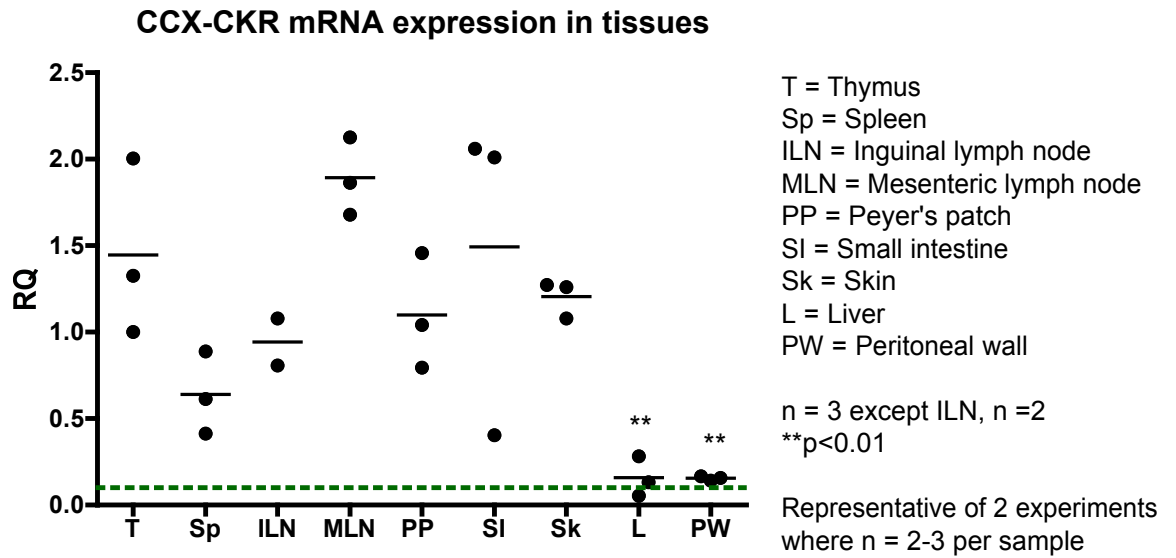


Figure 3.2: Detection of CCX-CKR mRNA expression in whole tissue. RNA was isolated from tissues from resting WT animals. Equal amounts of RNA per sample were used to synthesise cDNA, which formed the template for a QPCR reaction using a Taqman Gene Expression Assay for *Ccr1*, with GAPDH expression used as an endogenous control. One of the thymus samples was given an RQ value of 1, with CCX-CKR expression in all other tissues expressed relative to this. Green dashed line indicates approximate RQ value of KO thymus sample (data from **Figure 3.1B**). The data shown represent one of two experiments showing the same pattern of expression. n = 3 except for ILN samples, n = 2. Data were analysed by 1-way ANOVA with Bonferroni post-test, comparing all samples to Thymus, **p<0.01.

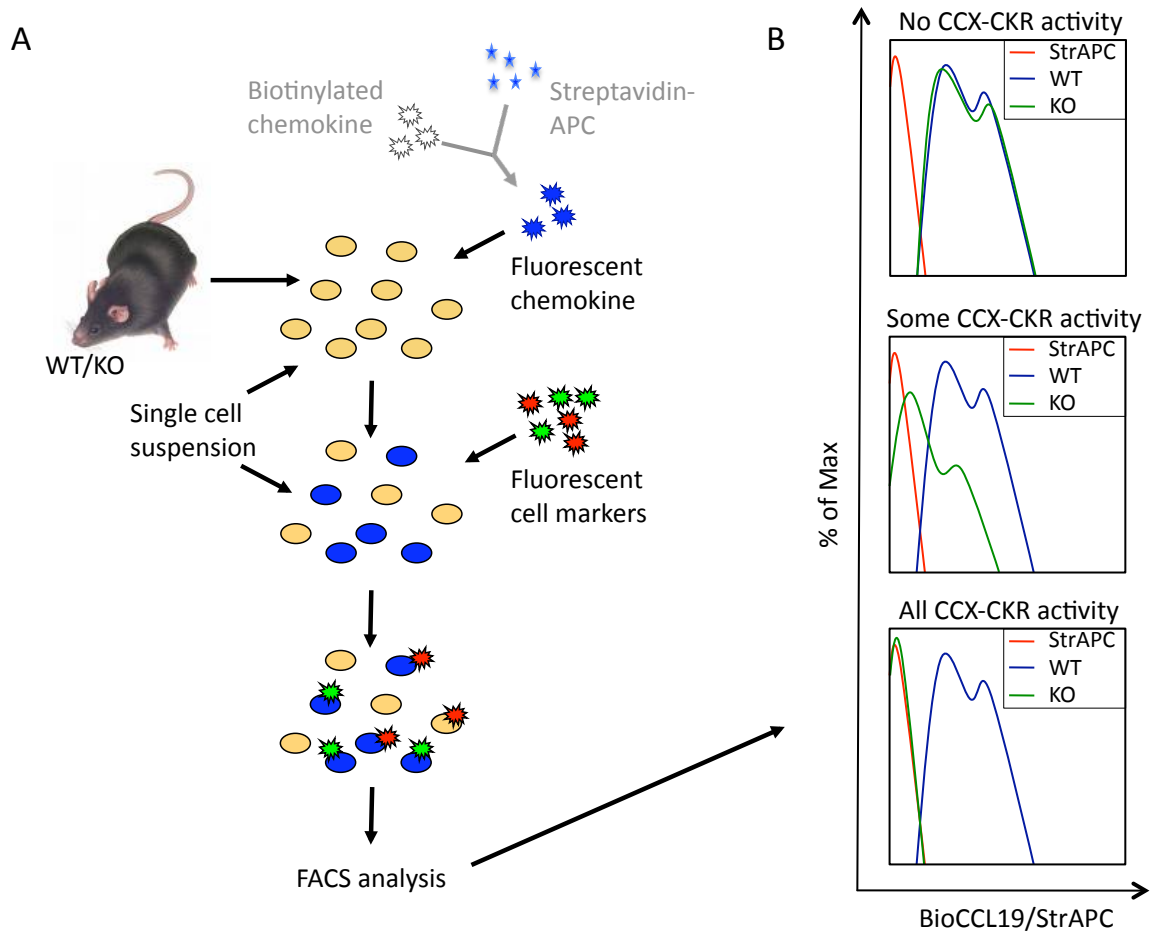
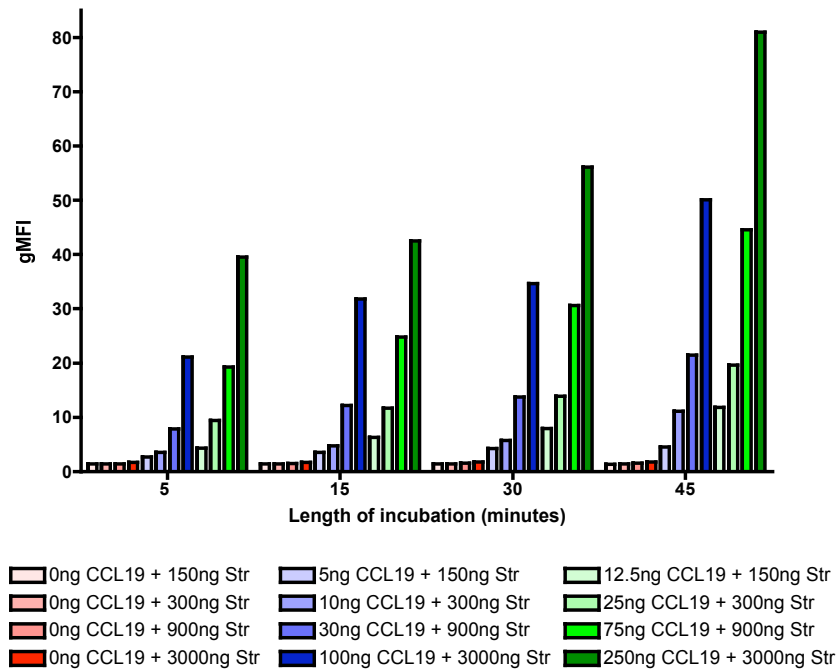


Figure 3.3: Designing an assay to detect CCL19 receptors using fluorescent CCL19 tetramers. (A) Tetrameric fluorescent CCL19 is formed by incubating biotinylated CCL19 with fluorescently-labelled streptavidin at room temperature in darkness. The labelled chemokine tetramers are then incubated with a single cell suspension from the tissue of choice at either 4°C (binding/surface staining) or 37°C (internalisation/activity). Samples are subsequently stained with fluorescently labelled antibodies to cell surface markers and analysed using flow cytometry. In theory, comparison of cells from wild-type (WT) and CCX-CKR deficient (KO) animals enables identification of the receptor responsible for internalisation of the chemokine. (B) Example histograms show expected possible profiles in the case of some, all or none of the CCL19 internalisation being CCX-CKR dependent. All experiments used allophycocyanin (APC)-labelled streptavidin (StrAPC) except where otherwise specified. StrAPC alone was used as a control for background fluorescence caused by chemokine-independent internalisation or binding of the labelled streptavidin.

A

**Internalisation of fluorescently labelled CCL19
at varying concentrations over time**



B

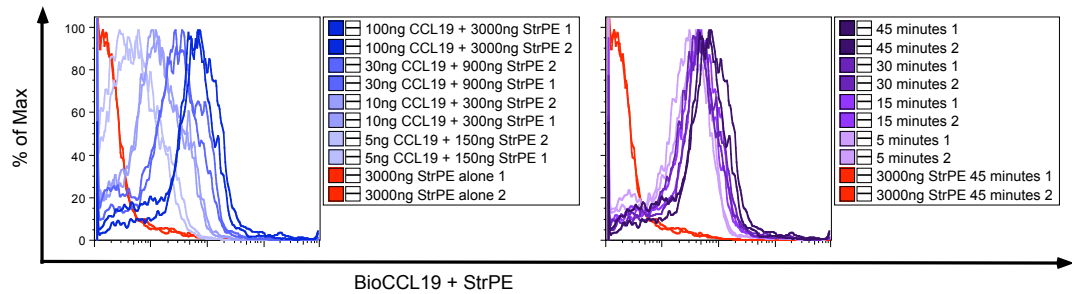


Figure 3.4: Optimisation of internalisation assay conditions. (A) Total splenocytes were exposed to a range of biotinylated CCL19/streptavidin-PE mixes, where the concentration of both biotinylated chemokine (CCL19) and PE-labelled streptavidin (Str) was varied. They were incubated with the fluorescent chemokine for between 5 and 45 minutes before being analysed by flow cytometry. Live cells were gated based on size and granularity characteristics. Bars show mean fluorescence of duplicate samples, gMFI = geometric mean fluorescence intensity. (B) Representative histograms showing cells exposed to increasing levels of fluorescent chemokine for 45 minutes (left panel) or to 100 ng CCL19 plus 3000 ng PE-labelled streptavidin (StrPE) for increasing lengths of time (right panel). Similar results were obtained using APC-labelled streptavidin.

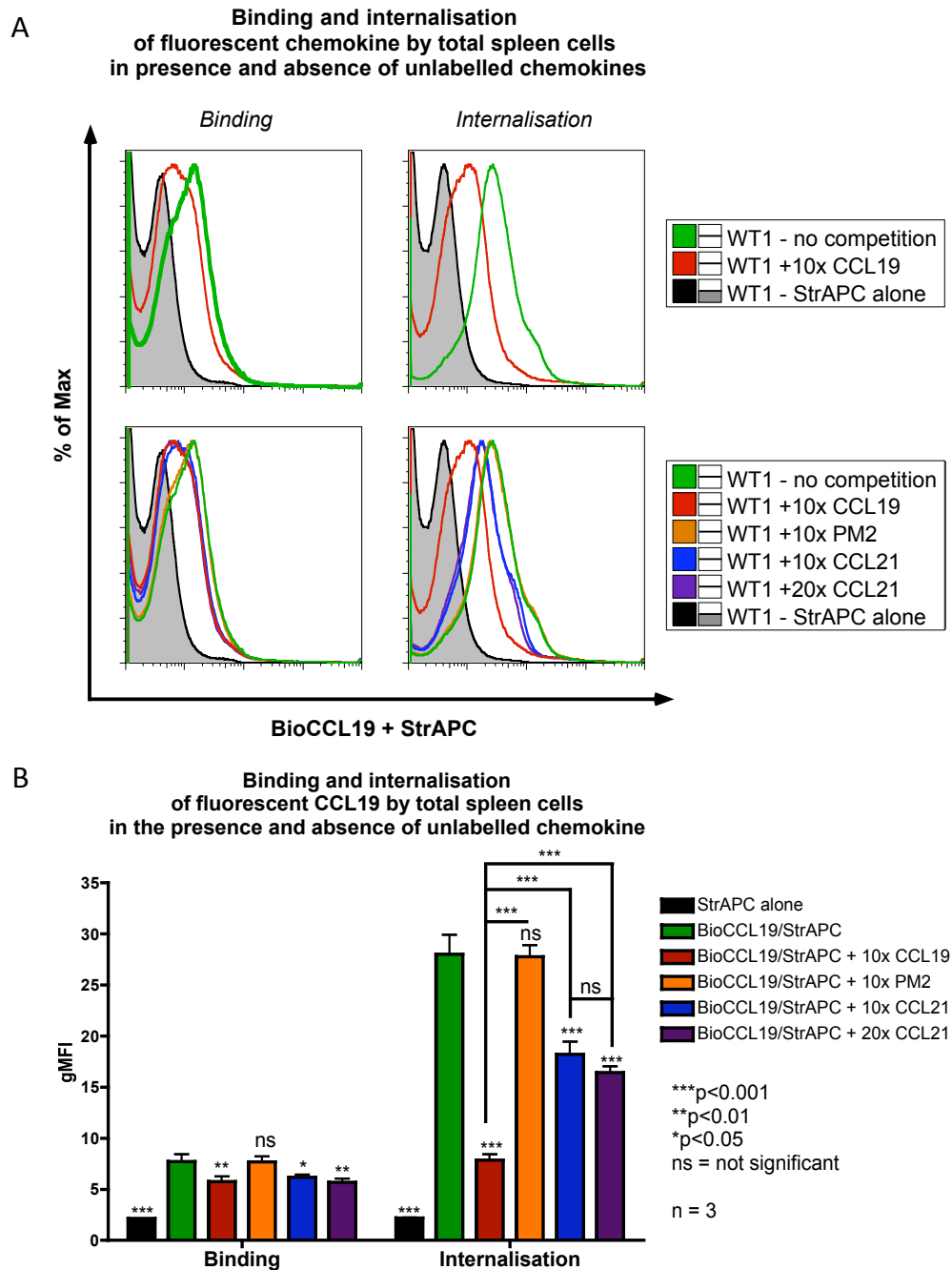


Figure 3.5: Binding and internalisation of fluorescent CCL19 tetramers is significantly reduced in the presence of CCR7 ligands. (A) Cells isolated from WT spleens were incubated with fluorescent CCL19 tetramers (BioCCL19/StrAPC) for 30 minutes at either 4°C (binding; left panels) or 37°C (internalisation; right panels), in the presence or absence of a 10-20 fold excess of unlabelled chemokine. Figure shows representative histograms of binding or internalisation in the presence or absence of indicated unlabelled chemokines. (B) Quantitative representation of data from (A). Data are mean of three biological replicates. Data were analysed using 1-way ANOVA with Bonferroni post-test. Stars directly above columns indicate differences relative to uncompleted samples (i.e. “BioCCL19/StrAPC”), stars with black lines indicate differences between indicated samples. *** = $p < 0.001$, ** $p < 0.01$, * = $p < 0.05$, ns = not significant. gMFI = geometric mean fluorescence intensity.

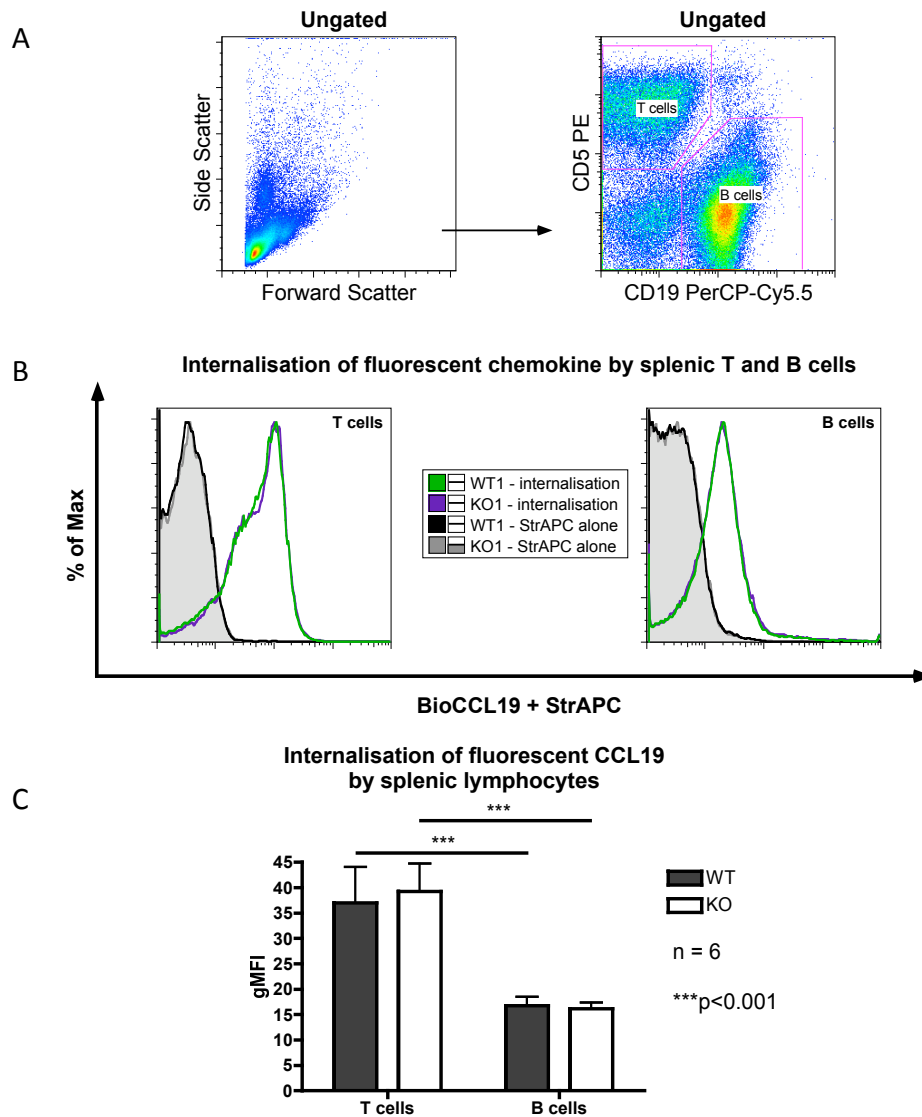


Figure 3.6: T and B cells in the spleen do not exhibit CCX-CKR-dependent internalisation of fluorescent CCL19 tetramers. (A) Gating strategy – dead cells were excluded at the acquisition stage based on size and granularity. Cells are defined as T cells or B cells based on antibody staining for CD5 and CD19 respectively. (B) Representative histograms - wild-type (WT) and CCX-CKR deficient (KO) cells were incubated with fluorescent CCL19 tetramers (BioCCL19 + StrAPC; WT = green line, KO = purple line) or StrAPC alone (WT = black line, KO = grey fill) for 30 minutes, stained with fluorescent antibodies for lineage markers and then analysed for internalisation by FACS. (C) Quantitative representation of pooled data from two experiments. Data are mean of values for six biological replicates, n=3 per experiment. Data were analysed by 2-way ANOVA with Bonferroni post-test, ***p<0.001. Error bars represent standard deviation from the mean. gMFI = geometric mean fluorescence intensity.

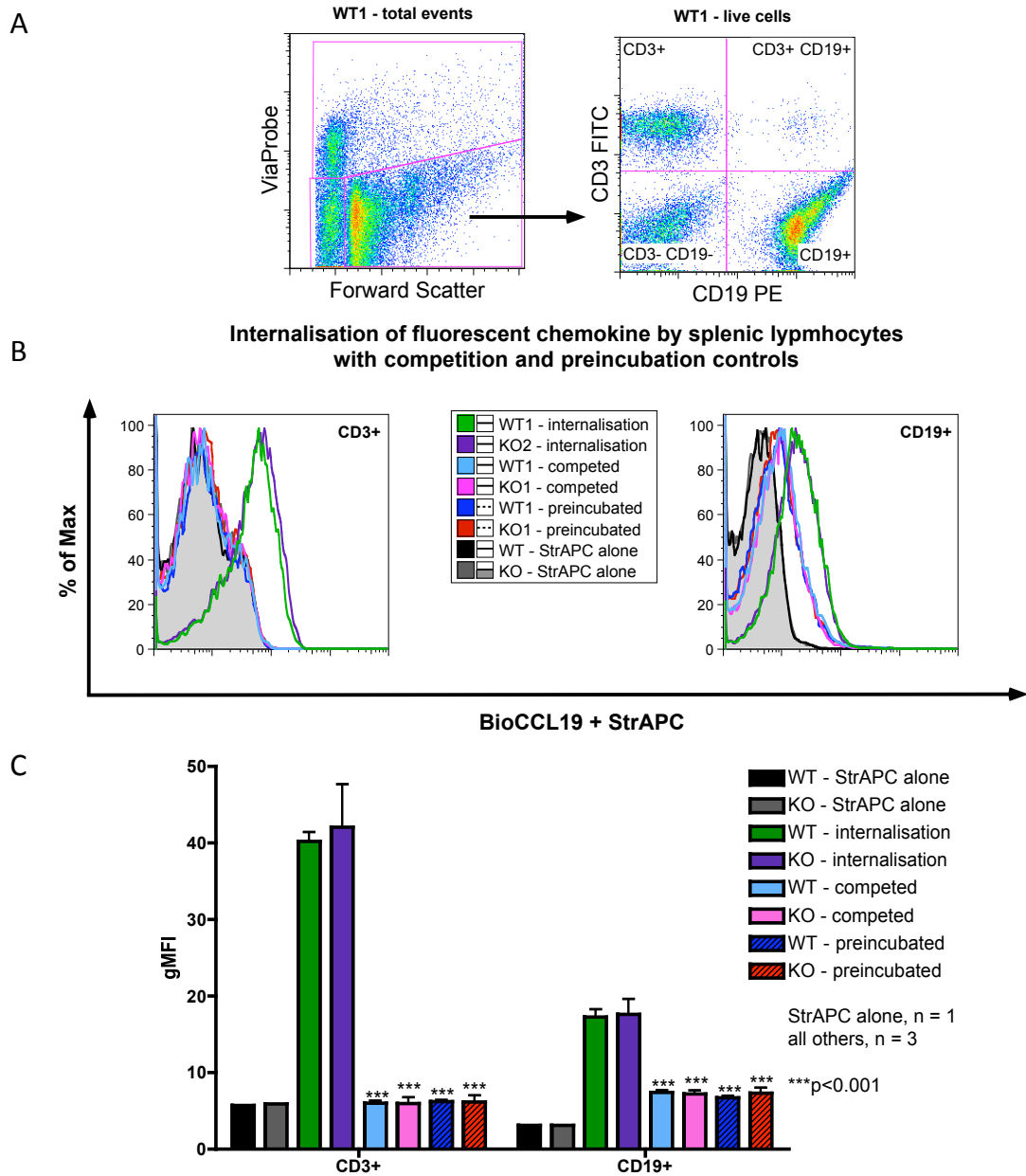


Figure 3.7: Pre-incubation or co-incubation with unlabelled CCL19 does not lead to detectable CXCR-dependent internalisation of fluorescent CCL19 tetramers in splenic T and B cells. (A) The internalisation of fluorescent CCL19 tetramers by WT and KO cells with or without co-incubation with a 10-fold excess of unlabelled CCL19. (B) The internalisation of fluorescent CCL19 tetramers by WT and KO cells with or without pre-incubation with a 10-fold excess of unlabelled CCL19. In representative histograms in (A) and (B), dark green (WT) and dark purple (KO) lines show internalisation in the absence of unlabelled CCL19 (“internalisation”). Black (WT) and grey (KO) lines show internalisation of StrAPC alone. In (A), light blue (WT) and pink (KO) lines show internalisation in the presence of excess unlabelled CCL19 (“competed”). In (B), dark blue (WT) and red (KO) lines show internalisation following pre-incubation with unlabelled CCL19 (“preincubated”). (C) Quantitative representation of data from (A) and (B). For each condition, n=3 except for StrAPC alone controls, n=1. gMFI = geometric mean fluorescence intensity. Data were analysed by 2-way ANOVA with Bonferroni post-test, ***p<0.001. Stars indicate comparison to Internalisation samples (WT samples compared to “WT – internalisation”, KO samples compared to “KO – internalisation”). No differences were observed between WT and KO samples for each condition.

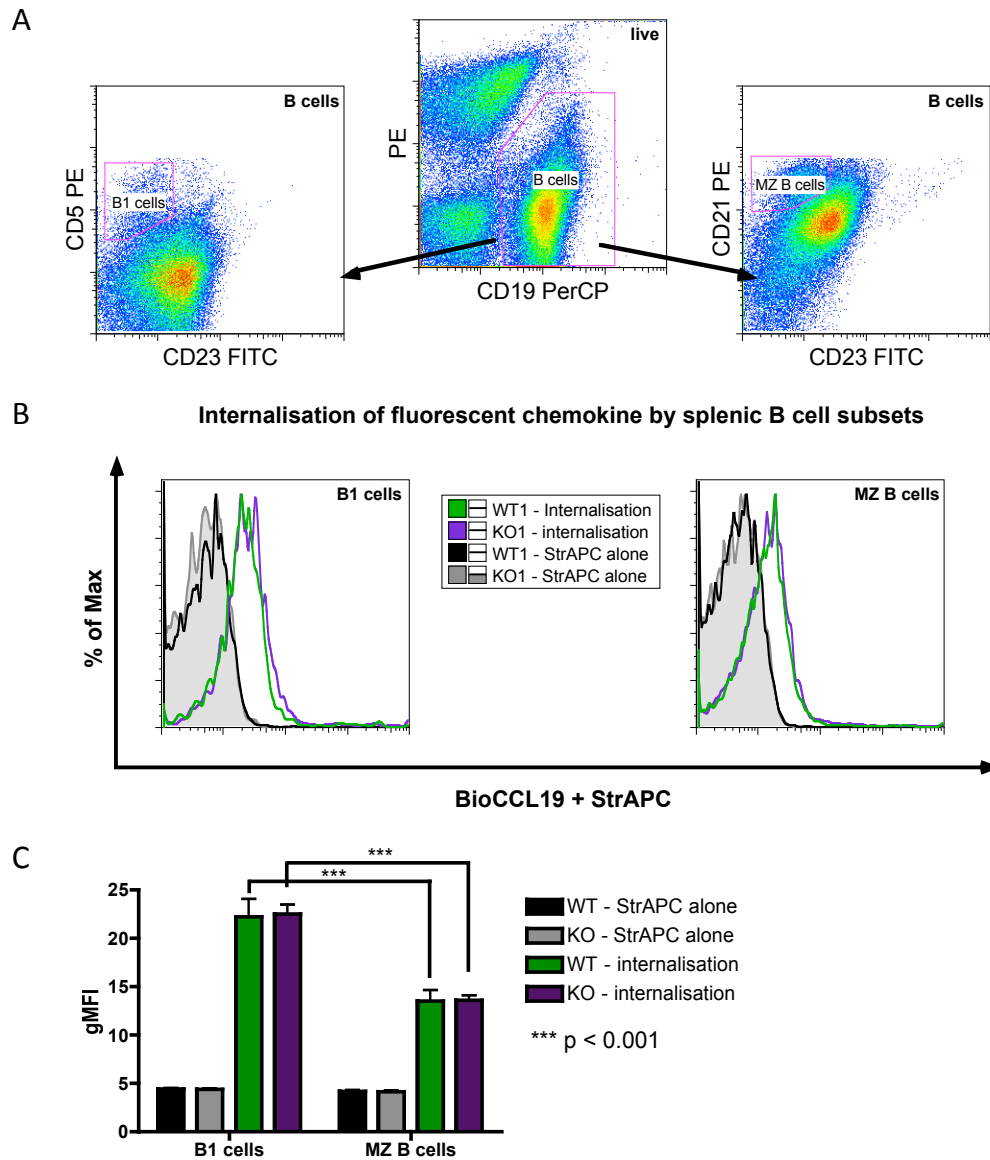
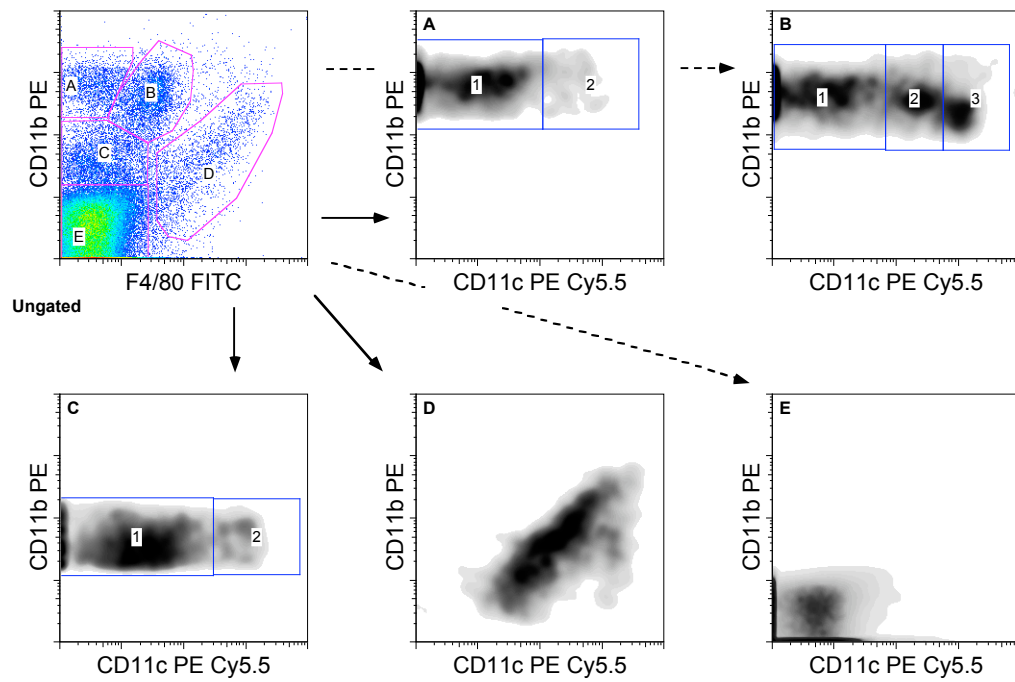


Figure 3.8: B1 cells and marginal zone B cells in the spleen do not exhibit CCX-CKR-dependent internalisation of CCL19. (A) Gating strategy – dead cells were excluded at the acquisition stage based on size and granularity. Cells are defined as B cells based on CD19 positivity. “PE” stain in representative gating plot is anti-CD5 PE staining, “B cells” gate was the same for plots with anti-CD21 PE and anti-CD19 PerCP (MZ B cell staining). B1 cells or marginal zone (MZ) B cells were defined based on staining for CD5 and CD23 (B1 cells; CD5⁺ CD23⁺) or CD21 and CD23 (MZ B cells; CD21⁺ CD23⁺). (B) Representative histograms - wild-type (WT) and CCX-CKR deficient (KO) cells were incubated with fluorescent CCL19 (BioCCL19 + StrAPC; WT = green line, KO = purple line) or StrAPC alone (WT = black line, KO = grey fill) for 30 minutes, stained with fluorescent antibodies for lineage markers and then analysed for internalisation by FACS. (C) Quantitative representation of data from (B). Data are mean of values for three biological replicates. Error bars represent standard deviation from the mean. Data were analysed by 2-way ANOVA with Bonferroni post-test, *** $p < 0.001$. gMFI = geometric mean fluorescence intensity.



Cell type	Marker profile	Cell type	Marker profile
A/1	CD11b high, F4/80 neg, CD11c neg/low	C/1	CD11b low, F4/80 neg, CD11c low
A/2	CD11b high, F4/80 neg, CD11c med/high	C/2	CD11b low, F4/80 neg, CD11c high
B/1	CD11b high, F4/80 low, CD11c neg/low	D	CD11b low/med, F4/80+, CD11c+
B/2	CD11b high, F4/80 low, CD11c med	E	CD11b-, F4/80-, CD11c-
B/3	CD11b high, F4/80 low, CD11c high		

Figure 3.9: Gating strategy to identify myeloid cells in the spleen. Splenocytes were incubated with or without fluorescent chemokine tetramers at 37°C and then stained with antibodies recognising CD11b, F4/80 and CD11c. Live cells, identified based on forward and side scatter properties (and ViaProbe staining, where applicable), were then defined based on expression of these surface molecules as described above. Where experiments did not include antibodies recognising CD11c (see text and figure legends), cells were identified as in the first panel (populations A-E).

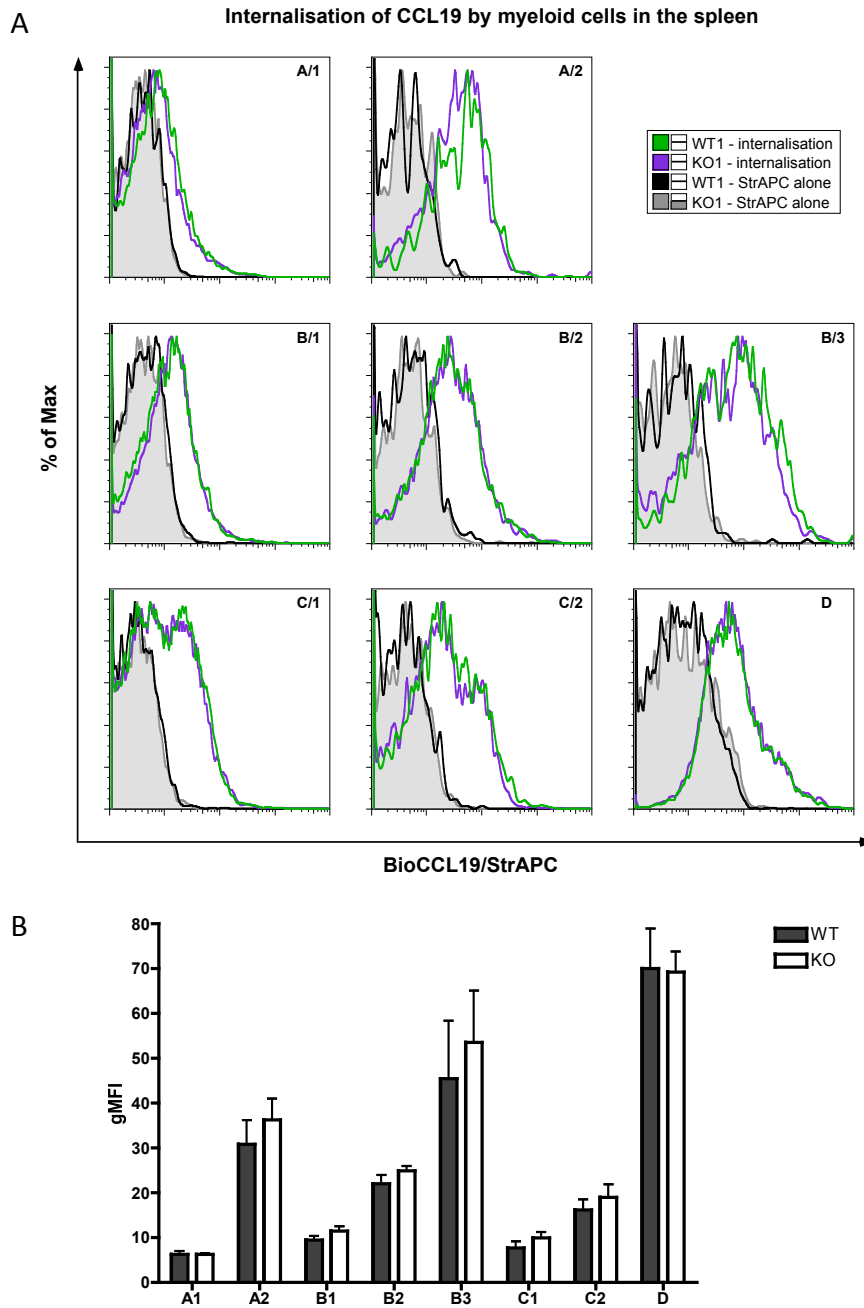


Figure 3.10: Myeloid cells in the spleen do not exhibit CCX-CKR-dependent CCL19 internalisation. Cell subsets (A/1-D) were gated as shown in **Figure 3.9**, with live cells identified by forward and side scatter characteristics. (A) Representative histograms - wild-type (WT) and CCX-CKR deficient (KO) cells were incubated with fluorescent CCL19 (BioCCL19 + StrAPC; WT = green line, KO = purple line) or StrAPC alone (WT = black line, KO = grey fill) for 30 minutes, stained with fluorescent antibodies for lineage markers and then analysed for internalisation by FACS. (B) Quantitative representation including data from (A). Data are mean of values for triplicate samples. Error bars represent standard deviation from the mean. gMFI = geometric mean fluorescence intensity.

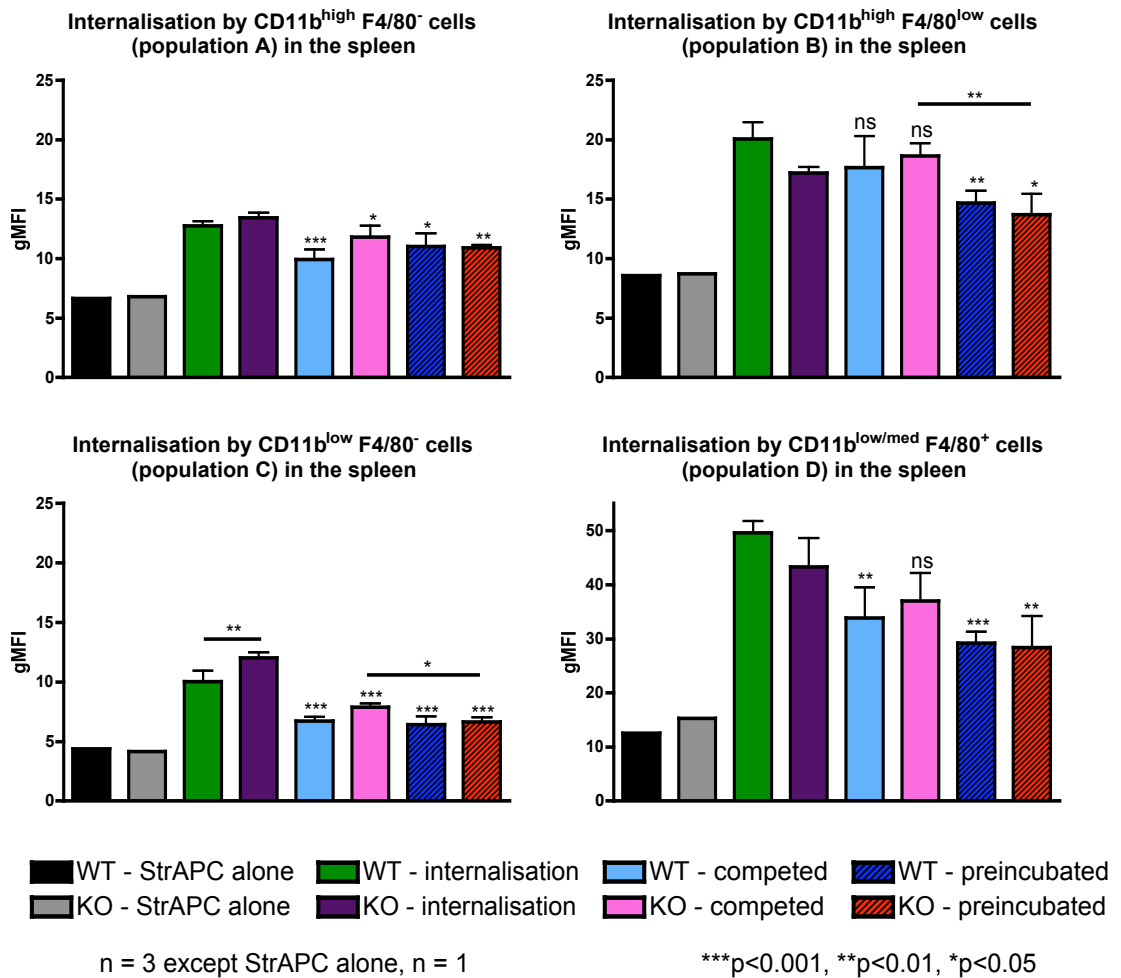


Figure 3.11: Pre-incubation or co-incubation with unlabelled CCL19 does not lead to detectable CCX-CKR-dependent internalisation of fluorescent CCL19 in splenic myeloid cells. Cells were incubated with fluorescent CCL19 as described in Materials and Methods, followed by antibody staining for lineage markers associated with myeloid cells. Cells were gated based on CD11b and F4/80 staining – see **Figure 3.9**. For each condition, n=3 except for StrAPC alone controls, n=1. gMFI = geometric mean fluorescence intensity. Data were analysed by 2-way ANOVA with Bonferroni post-test, ***p<0.001, **p<0.01, *p<0.05, ns = not significant. Error bars represent standard deviation from the mean. Stars directly above bars indicate comparison to Internalisation samples (WT samples compared to WT internalisation, KO samples compared to KO internalisation), stars with black lines indicate differences between indicated samples.

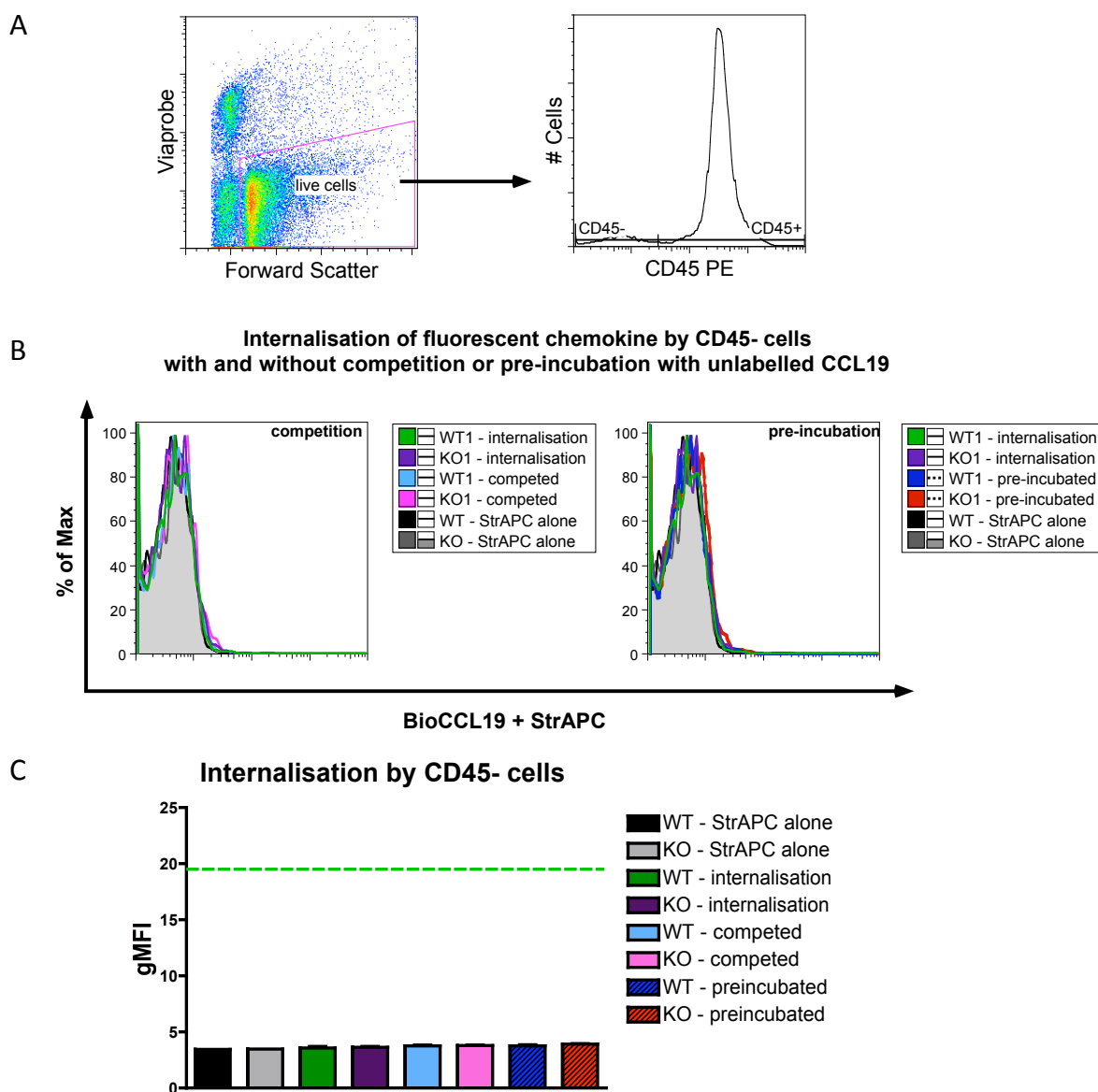


Figure 3.12: CD45⁺ and CD45⁻ cells in the spleen do not exhibit CCX-CKR-dependent internalisation of CCL19 with or without pre- or co-incubation with excess unlabelled CCL19. (A) Gating strategy – live cells are defined based on size and ViaProbe negativity. Live cells are defined as CD45⁺ and CD45⁻ based on antibody staining for CD45. (B) The internalisation of fluorescent CCL19 by WT and KO cells with or without co-incubation (left panel) or pre-incubation (right panel) with a 10-fold excess of unlabelled CCL19. In representative histograms, dark green (WT) and dark purple (KO) lines show internalisation in the absence of unlabelled CCL19 (“internalisation”). Black (WT) and grey (KO) lines show internalisation of StrAPC alone. Pale blue (WT) and pink (KO) lines show internalisation in the presence of excess unlabelled CCL19 (“competed”). Dark blue (WT) and red (KO) lines show internalisation following pre-incubation with unlabelled CCL19 (“preincubated”). (C) Quantitative representation of data from (B). For each condition, n=3 except for StrAPC alone controls, n=1. gMFI = geometric mean fluorescence intensity. Dashed green line indicates average gMFI of CD45⁺ cells in the same experiment (n = 3).

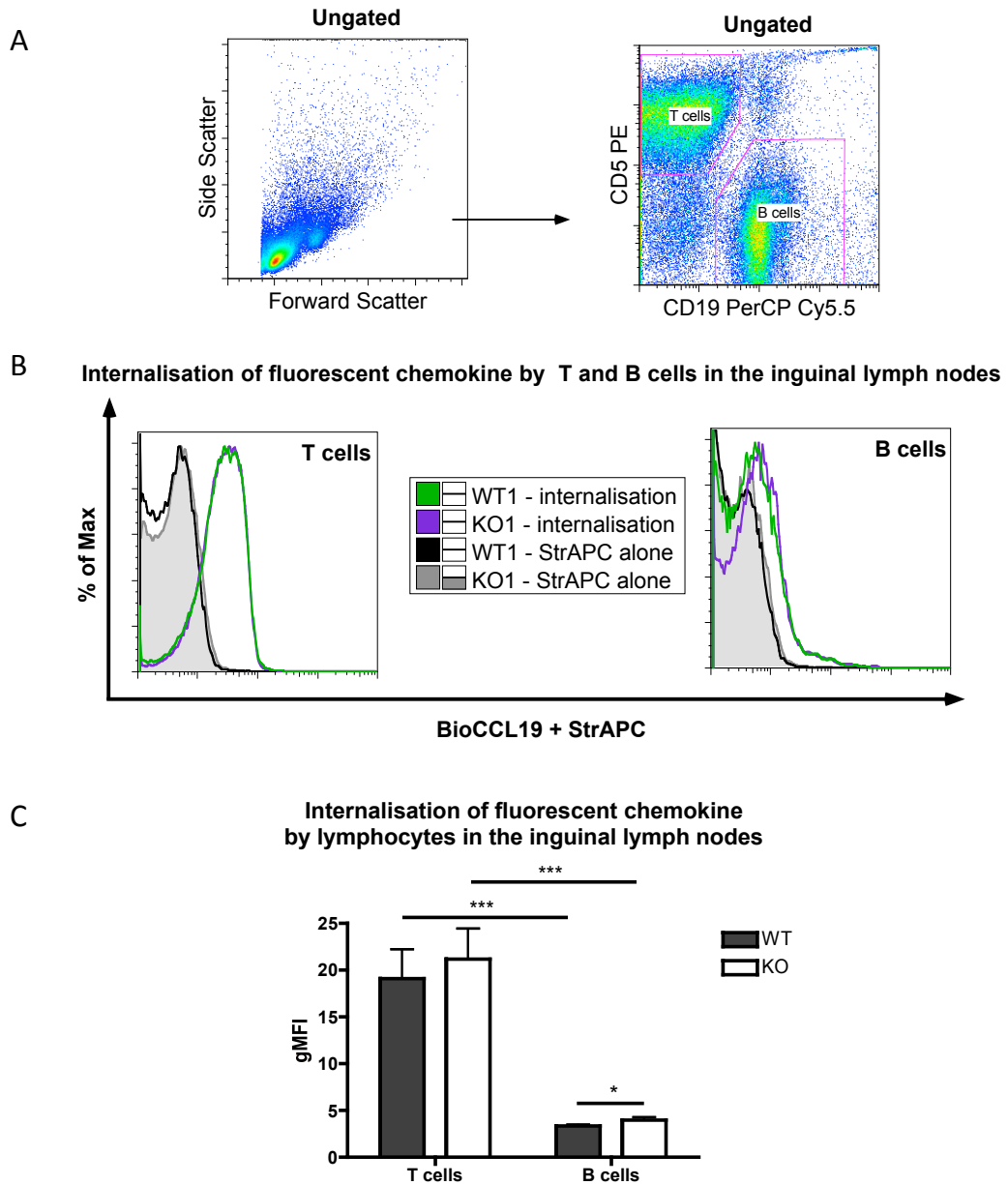


Figure 3.13: T and B cells in the inguinal lymph nodes do not exhibit CCX-CKR-dependent internalisation of CCL19. (A) Gating strategy – dead cells were excluded at the acquisition stage based on size and granularity. Cells are defined as T cells or B cells based on antibody staining for CD5 and CD19 respectively. (B) Representative histograms - wild-type (WT) and CCX-CKR deficient (KO) cells were incubated with fluorescent CCL19 (BioCCL19 + StrAPC; WT = green line, KO = purple line) or StrAPC alone (WT = black line, KO = grey fill) for 30 minutes, stained with fluorescent antibodies for lineage markers and then analysed for internalisation by FACS. (C) Quantitative representation of data from (B), $n=3$ per sample. Error bars represent standard deviation from the mean. gMFI = geometric mean fluorescence intensity. Data were analysed by 2-way ANOVA with Bonferroni post-test, $***p<0.001$, $*p<0.05$.

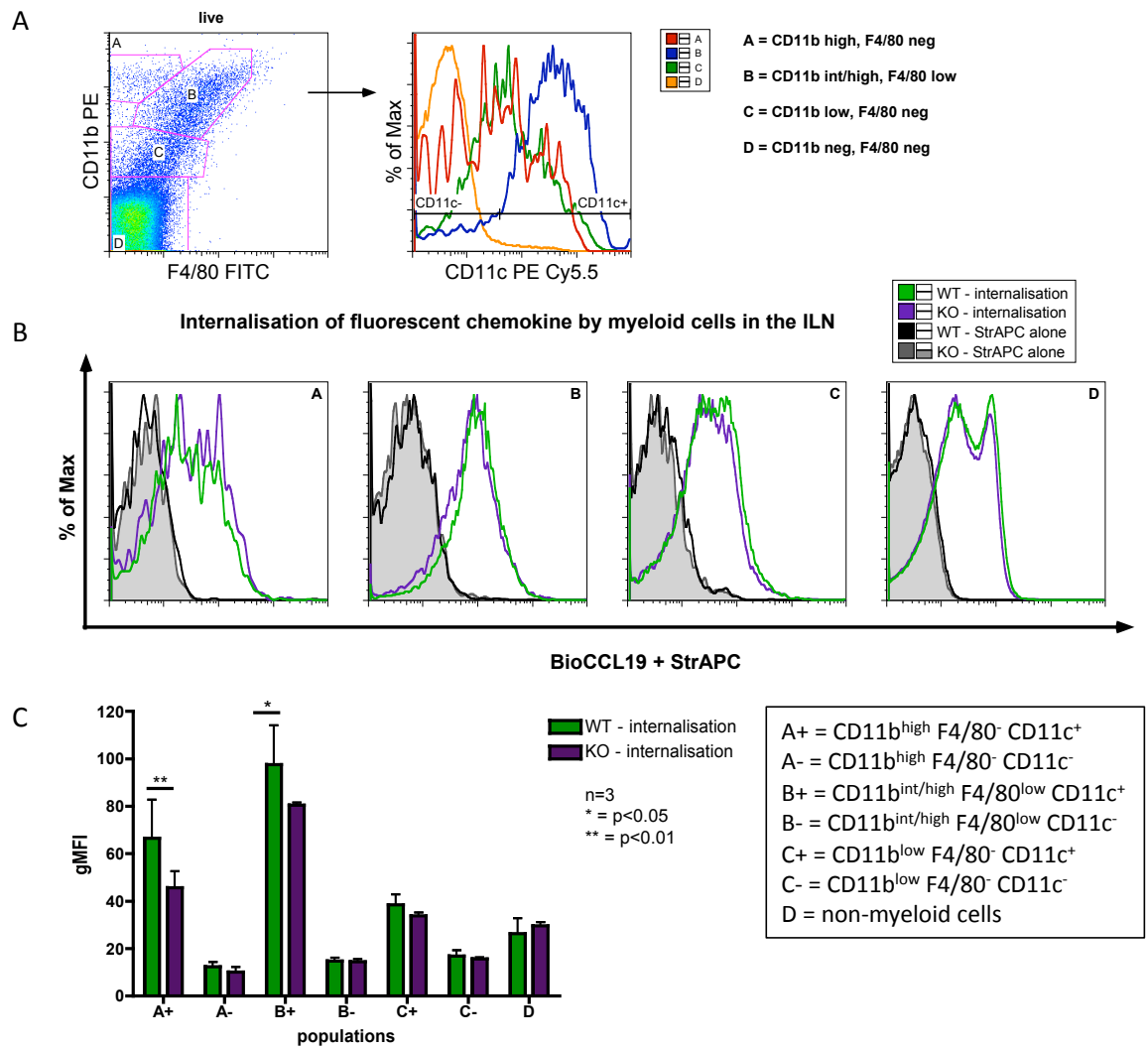


Figure 3.14: Myeloid cells within the inguinal lymph node exhibit some CCX-CKR dependent internalisation of CCL19. (A) Gating strategy. Live cells were defined based on size and granularity at the acquisition stage. Cells were further defined based on their CD11b, CD11c and F4/80 staining as shown. (B) Representative histograms for populations defined based on CD11b and F4/80 - wild-type (WT) and CCX-CKR deficient (KO) cells were incubated with fluorescent CCL19 (BioCCL19 + StrAPC; WT = green line, KO = purple line) or StrAPC alone (WT = black line, KO = grey fill) for 30 minutes, stained with fluorescent antibodies for lineage markers and then analysed for internalisation by FACS. (C) Quantitative representation of data from (B), with further division of cells based on CD11c staining (as in (A), right panel). Error bars represent standard deviation from the mean, n=3 per sample. gMFI = geometric mean fluorescence intensity. Data were analysed by 2-way ANOVA and Bonferroni post-test, ** = p<0.01, * = p<0.05.

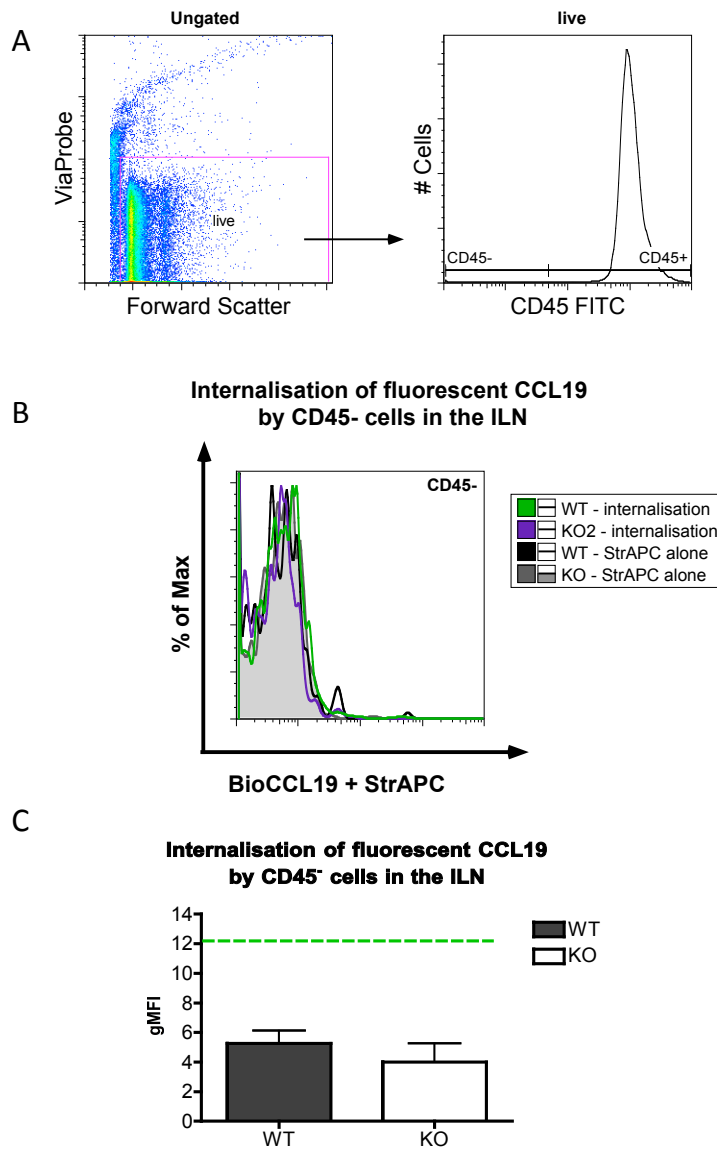


Figure 3.15: CD45⁻ cells in the inguinal lymph node do not exhibit CCX-CKR-dependent internalisation of CCL19. (A) Gating strategy – live cells are defined based on size and ViaProbe negativity. Live cells are defined as non-leukocytes/stromal cells (CD45⁻) based on antibody staining for the common leukocyte antigen CD45. (B) Representative histogram - wild-type (WT) and CCX-CKR deficient (KO) cells were incubated with fluorescent CCL19 (BioCCL19 + StrAPC; WT = green line, KO = purple line) or StrAPC alone (WT = black line, KO = grey fill) for 30 minutes, stained with fluorescent antibodies for lineage markers and then analysed for internalisation by flow cytometry. (C) Quantitative representation of data from (B). WT internalisation samples, n=4; KO internalisation samples, n=3. Error bars represent standard deviation from the mean. Data were analysed by unpaired t-test. gMFI = geometric mean fluorescence intensity. Dashed green line indicates mean gMFI of WT CD45⁺ cells from the same experiment.

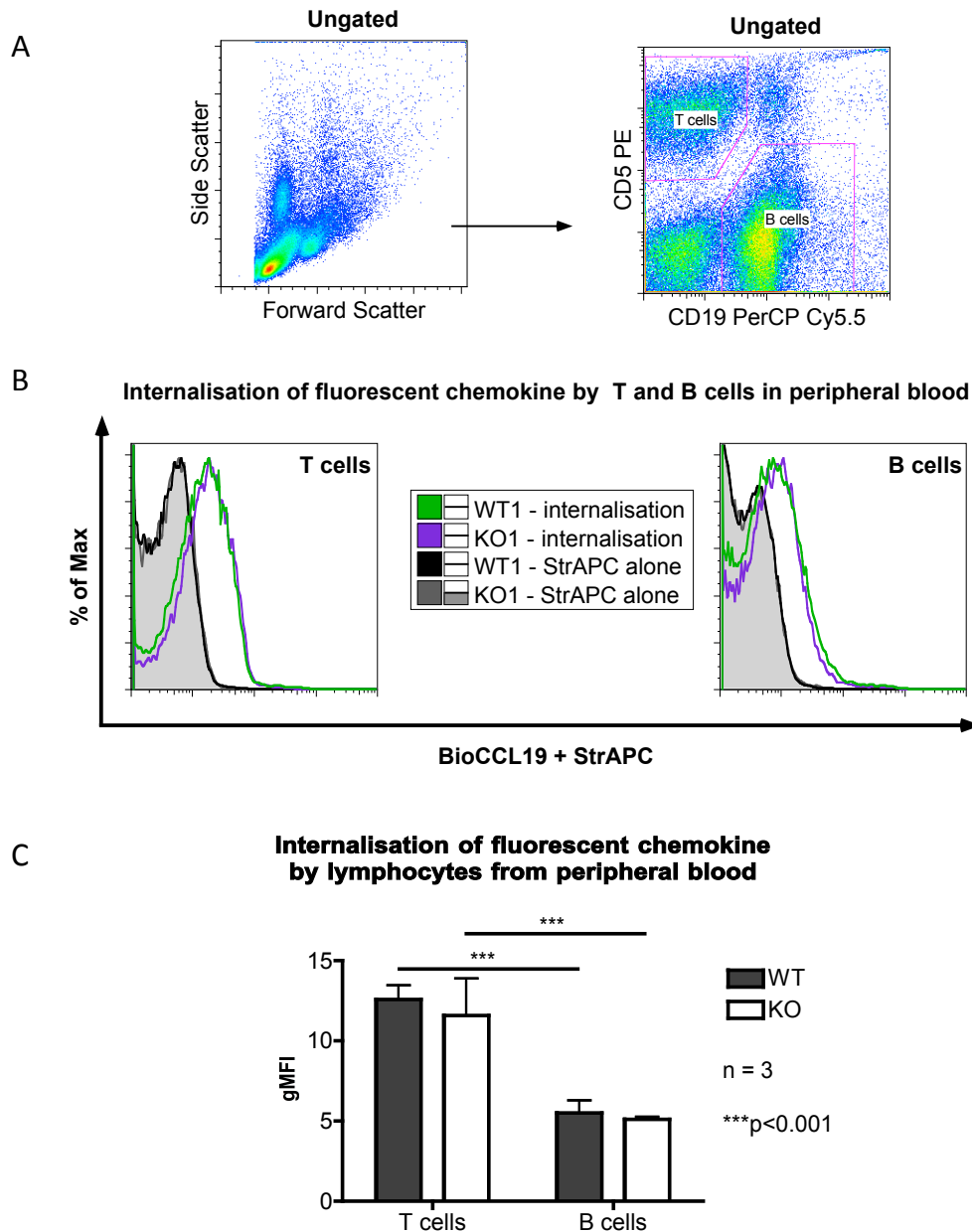


Figure 3.16: T and B cells in the blood do not exhibit CCX-CKR-dependent internalisation of CCL19. (A) Gating strategy – dead cells were excluded at the acquisition stage based on size and granularity. Cells are defined as T cells or B cells based on antibody staining for CD5 and CD19 respectively. (B) Representative histograms - wild-type (WT) and CCX-CKR deficient (KO) cells were incubated with fluorescent CCL19 (BioCCL19 + StrAPC; WT = green line, KO = purple line) or StrAPC alone (WT = black line, KO = grey fill) for 30 minutes, stained with fluorescent antibodies for lineage markers and then analysed for internalisation by FACS. (C) Quantitative representation of data from (B), n=3 per group. Data were analysed by 2-way ANOVA with Bonferroni post-test, ***p<0.001. Error bars represent standard deviation from the mean. gMFI = geometric mean fluorescence intensity.

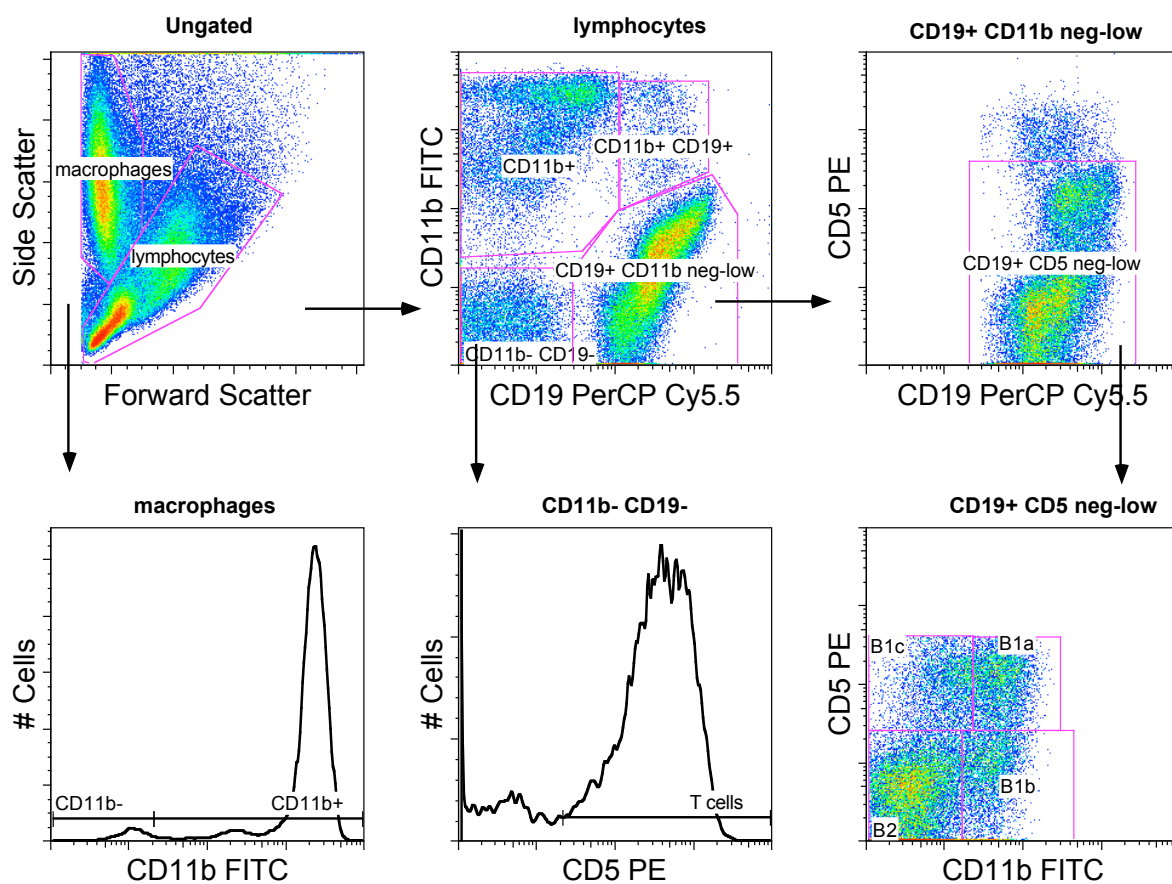


Figure 3.17: Gating of peritoneal cavity lavage cells. Cells were defined as macrophages or lymphocytes based on size and granularity (top left panel). Macrophages were then defined as either CD11b⁺ or CD11b⁻ (bottom left panel). Lymphocytes were categorised based on their CD11b and CD19 staining (top middle panel), and T cells were defined as CD5⁺ CD11b⁻ CD19⁻ (bottom middle panel). Doublets of B and T cells were excluded from the B cell gate (top right panel) and B cells (CD5^{neg/int} CD11b^{neg/int} CD19⁺) were defined as B1a, B1b, B1c or B2 cells based on their CD5 and CD11b staining.

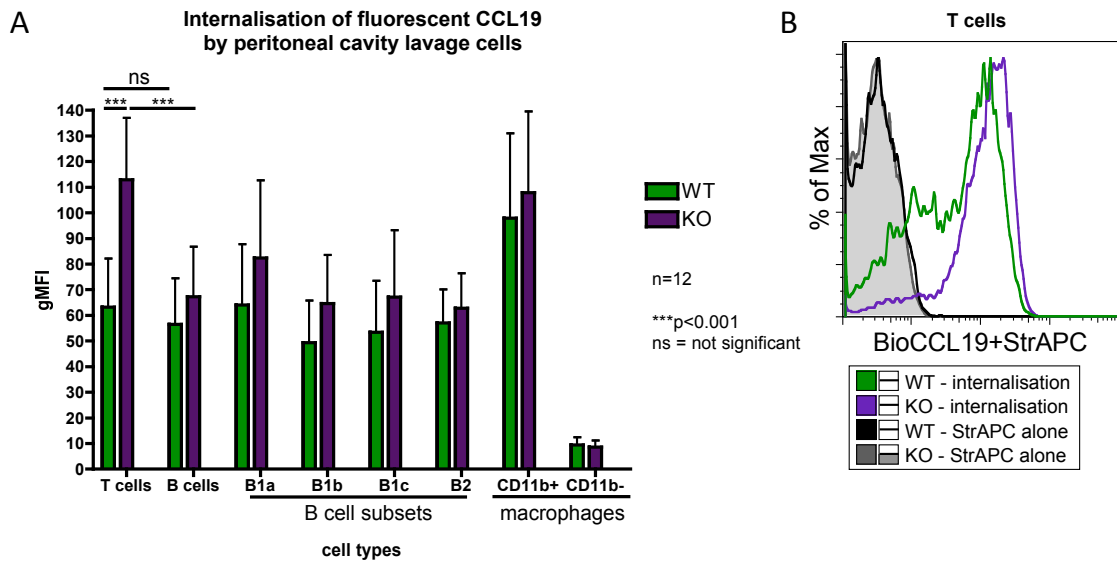


Figure 3.18: Cells isolated from peritoneal lavage do not exhibit CCX-CKR-dependent internalisation of fluorescent CCL19. Cells were gated as per Figure 3.17. Wild-type (WT) and CCX-CKR deficient (KO) cells were incubated with fluorescent CCL19 (BioCCL19 + StrAPC; WT = green line, KO = purple line) or StrAPC alone (WT = black line, KO = grey fill) for 30 minutes, stained with fluorescent antibodies for lineage markers and then analysed for internalisation by flow cytometry. (A) Quantitative representation of data from four pooled experiments, n=3 per experiment. Error bars represent standard deviation from the mean. gMFI = geometric mean fluorescence intensity. Data were analysed by two-way ANOVA with Bonferroni post-test, *** = p<0.001, ns = not significant. (B) Representative histograms of T cell internalisation of CCL19.

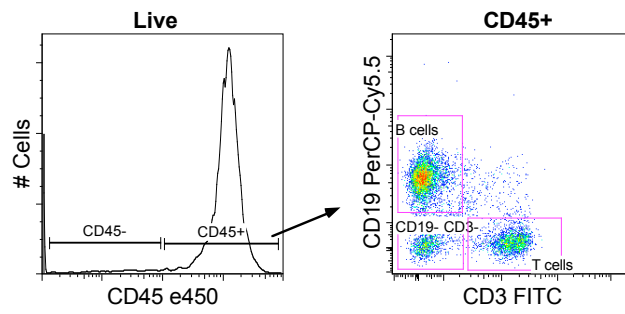


Figure 3.19: Gating strategy for sorting cells from the spleen. Cells were isolated from spleens, stained with antibodies against various lineage markers (CD45, CD3 and CD19) and sorted using a BD FACSAria. Cell populations were defined as CD45⁻ or CD45⁺. The CD45⁺ fraction was further subdivided into CD19⁺ CD3⁻, CD19⁻ CD3⁺ or CD19⁻ CD3⁻ based on surface expression of these markers as shown. Each population was collected in separate tubes, pooled, washed and pelleted, before RNA was extracted.

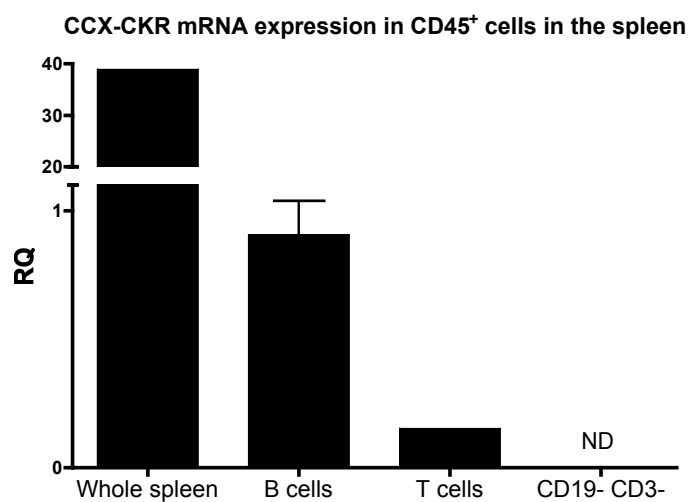


Figure 3.20: Expression of CCX-CKR mRNA by sorted CD45⁺ cells in the spleen. Whole spleen was used as a control. Cells were isolated, antibody-stained and sorted as described in Materials and Methods. RNA was extracted and used to make cDNA, which was analysed by QPCR. B cells are CD45⁺ CD19⁺ CD3⁻, T cells are CD45⁺ CD19⁻ CD3⁺. ND = not detected. n = 1 except for B cells, n = 2.

Sample	Treatment
1	Mashed through nitex
2	Remaining on nitex
3	Chopped, incubated in collagenase for 30 min
4	3, remaining on filter
5	3, passed through filter
6	5, incubated with FACS buffer on ice for 20 mins
7	5, red blood cells lysed
8	7, incubated with FACS buffer on ice for 20 mins

Table 3.1: Stages of spleen disruption. Whole spleens were harvested into ice-cold complete media. Half of one spleen was mashed through nitex, and the isolate that passed through the nitex collected (sample 1) as well as the capsule etc that remained on the nitex (sample 2). All other spleen samples were minced and incubated in HBSS containing 1 mg/ml collagenase D for 30 minutes. A sample was taken after this (sample 3) and the rest passed through a 50 μ m cell strainer (BD). Capsule and cells remaining on the filter were collected (sample 4), as was a sample of the cells that had passed through (sample 5). Of the cells remaining that had passed through the strainer, one sample was incubated with FACS buffer on ice for 20 minutes, to mimic antibody staining (sample 6). The rest of the fraction was incubated with red blood cell lysis buffer for 1 minute to remove erythrocytes. A sample was taken after this treatment (sample 7) and the rest of the cells were incubated with FACS buffer on ice for 20 minutes (sample 8). RNA was extracted from each sample and used to make cDNA, which was subsequently analysed by QPCR.

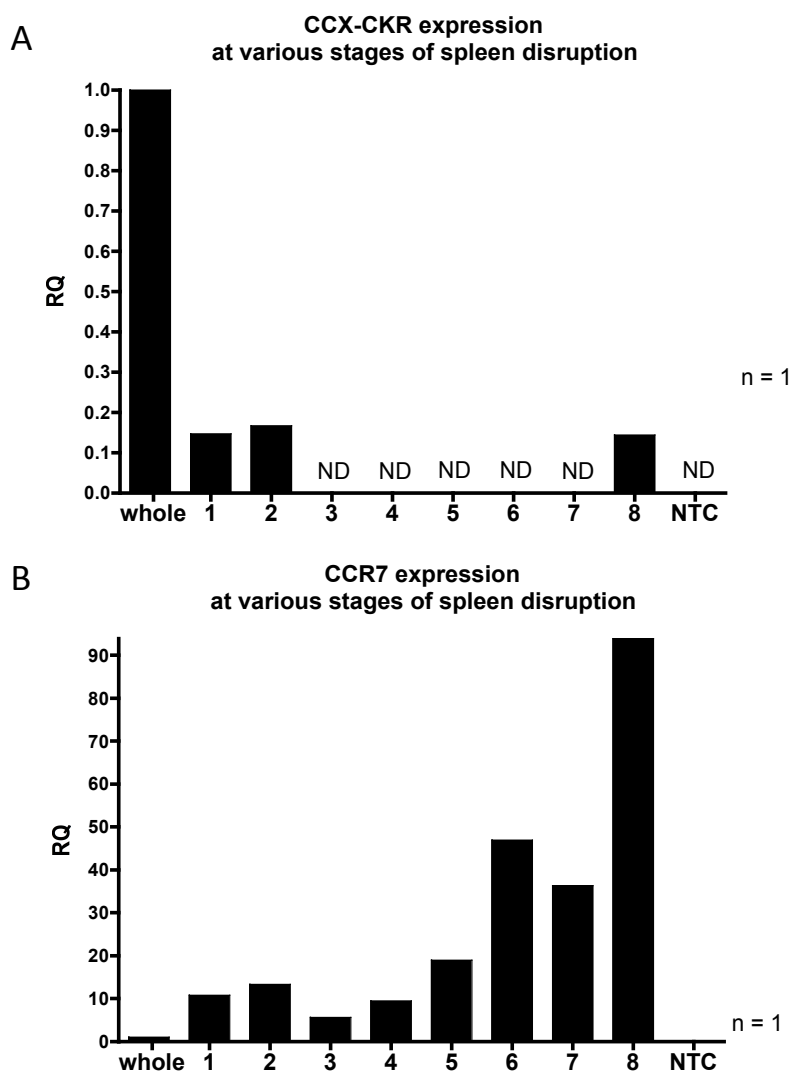


Figure 3.21: Expression of CCX-CKR and CCR7 mRNA in disrupted spleen. Samples were taken at various stages of spleen disruption (see Table 3.1). RNA was isolated and used to synthesise cDNA, which was analysed by QPCR using Taqman assays for CCX-CKR (A) and CCR7 (B). Whole spleen (whole) was used as a positive control, and expression levels in each sample are expressed relative to whole spleen, which is given an RQ value of 1. Water was used as a negative/no template control (NTC). n = 1.

4 Effect of CCX-CKR deletion on expression of its ligands and related receptors

Experiments detailed in the previous chapter have provided insight into which tissues and cell types do, or do not, express CCX-CKR at the mRNA level, although they present only limited indications as to which cells express the protein. They have also provided some interesting information about CCR7 and how its “activity” varies between tissues as well as cell types, verifying data already published about this receptor and providing further information about its expression and activity throughout the immune system. Additionally, internalisation experiments in the previous section have shown that CCX-CKR influences internalisation of fluorescent CCL19 tetramers by peritoneal T cells, probably through CCR7. This may be through affecting expression at the mRNA and/or protein level or through altering the activity of the receptor.

In this chapter, expression of CCR7, as well as CCR9, at the mRNA level is analysed, in an attempt to clarify how deletion of CCX-CKR impacts these receptors. Additionally, the effect of deletion of CCX-CKR on the abundance of some of its ligands in various tissues is investigated. This was done to test the hypothesis that CCX-CKR is acting as a chemokine scavenger *in vivo*. This has been investigated at the protein level, but mRNA for these chemokines has also been quantified in tissues from WT and CCX-CKR deficient mice to control for possible differences in chemokine production between these strains.

4.1 Expression of CCR7 and CCR9 mRNA in the CCX-CKR deficient mouse

At the time these experiments were performed, information about phenotypic differences in the CCX-CKR deficient animal was scarce, with only subtle alterations in cellularity reported in some tissues (Heinzel et al., 2007). It was hypothesised that other related receptors, such as CCR7 and CCR9, might be altered to compensate for the deletion. This has been shown to occur for other chemokine/receptor deletion mutants (see Introduction, section 1.7). Indications that CCR7 expression and/or activity are altered on some cells in the absence of CCX-CKR were provided in the previous section, where T cell internalisation of fluorescent CCL19 tetramers increased in the CCX-CKR deficient ILN compared to WT (see chapter 3). It is also possible that, in the absence of CCX-CKR, migration of leukocytes is disrupted, possibly through altered chemokine levels or

chemokine receptor expression. Again, data from the peritoneal cavity suggests that T cell migration to/from the peritoneal cavity may be aberrant in the absence of CCX-CKR, with loss of a CCL19^{low} population from CCX-CKR deficient peritoneal cavity lavage compared to WT. Therefore, CCR7 and CCR9 expression was investigated by QPCR in whole tissue to assess whether deletion of CCX-CKR, which shares these receptors' ligands, affected these receptors at the level of mRNA expression.

CCR7 mRNA is expressed in lymphoid tissues such as spleen, lymph nodes and thymus. CCX-CKR mRNA is also expressed in these tissues (Figure 3.2), as well as in some non-lymphoid "barrier" tissues, i.e. skin and small intestine. It was hypothesised that CCX-CKR may be involved in the regulation of CCR7, possibly through indirect effects, e.g by altering extracellular chemokine levels. Deletion of CCX-CKR might therefore affect CCR7 mRNA levels in these tissues. CCR7 mRNA expression in WT and CCX-CKR deficient tissues was measured by QPCR. In Figure 4.1, each tissue is calibrated to the same WT spleen sample, except for ILNs, which were analysed in a separate experiment and are calibrated to a WT lymph node sample. Interestingly, CCR7 mRNA was found to be significantly increased in the spleen in the absence of CCX-CKR (Figure 4.1).

Conversely, CCR7 expression was reduced in the ILN in the absence of CCX-CKR, but unchanged in the mesenteric lymph nodes (Figure 4.1). Expression in the thymus and Peyer's patches was also unaffected (Figure 4.1). The expression pattern observed, where CCR7 mRNA expression is highest in MLN and spleen and lower in thymus and Peyer's patches, is likely due to the composition of these tissues. T cells, which typically express high levels of CCR7, constitute a high proportion of cells in the spleen and MLN, whereas Peyer's patches contain a relatively low proportion of T cells and have more B cells, which typically have lower CCR7 in comparison to T cells (see Introduction, section 1.7). Clean dissection of Peyer's patches is technically demanding, thus epithelium and lamina propria from the small intestine could potentially be present in the samples analysed, diluting the number of CCR7⁺ cells in the sample. In the thymus, while CCR7 is expressed on some thymocytes the vast majority are CCR7-negative (Worbs and Förster, 2007).

The effect of CCX-CKR deletion on CCR7 expression at the mRNA level was also examined in skin and in small intestine (from which Peyer's patches had been removed) (Figure 4.2). As described in the Introduction (section 1.7), CCR7 is expressed by DCs in the skin and small intestine to facilitate trafficking to the draining lymph node under both resting and inflamed conditions (Förster et al., 2008, Gunn et al., 1999, Ohl et al., 2004). Interestingly, CCX-CKR is expressed in resting skin (see chapter 3, Figure 3.2), correlating with a report that homing of DCs from the skin of resting CCX-CKR deficient mice to the

lymph node is impaired (Heinzel et al., 2007). Levels of CCX-CKR expression in the small intestine are similar to those of the lymphoid tissues tested (Figure 3.2). In skin and small intestine, the level of CCR7 detected was very low in comparison to spleen ($RQ > 0.02$ for each sample where WT spleen $RQ = 1$, not shown). Therefore, samples were calibrated to a WT skin sample, because using a spleen sample as a calibrator prohibited accurate analysis of potential variation between WT and CCX-CKR deficient tissues. Samples from three WT and three CCX-CKR deficient mice were analysed, with no significant differences in CCR7 mRNA expression observed (Figure 4.2).

CCR9 mRNA expression was also examined by QPCR in these tissues, and in liver, which contains pDCs that can express CCR9 (Figure 4.3 and Figure 4.4). Naïve CD8⁺ T cells and pDCs express CCR9, as described in the Introduction, and gut-homing T cells are “programmed” in the MLN and Peyer’s patches to migrate to the small intestine through induction of CCR9. The expression pattern in WT tissues was consistent with previous reports, with relatively low levels in most tissues but high levels of expression detected in thymus (Carramolino et al., 2001). Most other tissues displayed comparable levels of expression, although some small intestine and Peyer’s patch samples exhibited very high expression of CCR9 mRNA. The reason for this is unclear. Other genes were not affected in this way for the same samples, suggesting the RNA was reliable. Expression of CCR9 in skin and liver was extremely low, as expected (Kunkel et al., 2000, Papadakis et al., 2000). There was no variation in CCR9 expression levels in CCX-CKR deficient tissues compared to WT.

These data suggest that CCX-CKR deletion alters the expression of CCR7, but not CCR9, in some tissues, possibly through disrupted migration of leukocytes. This theory will be investigated in the next chapter.

4.1.1 Expression of CCR7 by peritoneal cavity lavage cells is increased in the absence of CCX-CKR

In light of observed increases in internalisation of fluorescent CCL19 tetramers by CCX-CKR deficient peritoneal T cells compared to WT (see chapter 3, Figure 3.18), CCR7 mRNA expression in cell lysates from peritoneal cavity lavage was also examined by QPCR. Cells were harvested from lavage samples by centrifugation and lysed for RNA extraction. cDNA synthesis and QPCR was carried out as for whole tissue samples (see Materials and Methods). Interestingly, CCR7 mRNA was significantly increased in peritoneal lavage cells when CCX-CKR was absent, $p = 0.0199$ (Figure 4.5). CCR9

expression was also analysed in these samples. Expression was very low, with no CCR9 mRNA detectable in several samples assayed (no amplification was detected above negative control levels; not shown), and there was no difference in expression between WT and CCX-CKR deficient cells with detectable CCR9 mRNA (Figure 4.6).

These data demonstrate that deletion of CCX-CKR leads to increased relative expression of CCR7 mRNA by peritoneal lavage cells, which may be due to loss of a T cell population that exhibit low internalisation of fluorescent CCL19 tetramers (see chapter 3). CCX-CKR mRNA is not expressed by WT peritoneal lavage cells (not shown). Experiments described in the next section explored the impact of CCX-CKR deletion on the cellularity of this body cavity.

4.2 The impact of CCX-CKR deletion on ligand expression and availability

Previous work from our lab showed that, *in vitro*, exogenous CCX-CKR efficiently and constitutively internalises CCL19 into transfected cell lines, supporting the hypothesis that the receptor could act as a scavenger *in vivo* and modulate chemokine levels or distribution within tissues (Comerford et al., 2006). To investigate whether CCX-CKR could be playing a scavenger role *in vivo*, the protein levels of CCL19 and CCL21 were analysed by ELISA in various tissues. An important caveat of these assays was that, in solid tissue samples, they would detect total, rather than just “bioavailable”, chemokine (i.e. the extracellular chemokine available for scavenging), as the samples were homogenised during preparation. Therefore, significant changes in bioavailable chemokine level through CCX-CKR sequestration could be masked due to high levels of intracellular chemokine being released during the processing of samples. This is not the case for serum and peritoneal samples, where chemokines were measured following removal of cells by centrifugation.

The mRNA expression of a CCR7 ligand, CCL19, and the CCR9 ligand, CCL25, were also investigated using QPCR in whole tissue. Work from our lab, in collaboration with Prof. A. Mowat (University of Glasgow), indicated that commercially-available murine CCL25 ELISA kits readily reported high CCL25 protein levels in tissues from CCL25-deficient mice, thus rendering this reagent unreliable. Therefore, this assay was not carried out in this project. Similarly, a Taqman QPCR assay for murine CCL21 was not commercially available during this project and time constraints prevented development and optimisation of a custom-made assay.

4.2.1 Dysregulation of CCL19 protein in CCX-CKR deficient mice

CCL19 has been shown to be efficiently internalised by CCX-CKR *in vitro* (Comerford et al., 2006). Here, spleen and ILNs from WT and CCX-CKR deficient mice were analysed (Figure 4.7), as well as blood and peritoneal lavage (Figure 4.8) and a range of other tissues, both lymphoid (Figure 4.7) and non-lymphoid (Figure 4.9). Although CCL19 is mainly found in lymphoid tissues, some reports have indicated expression of CCL19 mRNA at a number of non-lymphoid sites (Alt et al., 2002, Yoshida et al., 1997). Tissues, serum and peritoneal lavage samples were prepared as described in Materials and Methods.

CCL19 was found to be undetectable in WT serum and peritoneal cavity lavage (Figure 4.8). Peritoneal cavity total protein concentrations were low (0.5-0.71 mg/ml), with only one CCX-CKR deficient peritoneal cavity lavage sample having any detectable CCL19, and this was at a very low level (less than 0.6pg/mg total protein). Further to this, CCL19 was also undetectable in WT serum. Interestingly, however, all serum samples from CCX-CKR deficient mice had significantly elevated CCL19 levels, with more than 5 pg of CCL19 detectable per mg total protein. CCL19 was also found to be elevated in ILNs of CCX-CKR deficient mice (Figure 4.7), although levels of the chemokine were unchanged between WT and CCX-CKR deficient mesenteric lymph nodes, thymus and spleen. Intriguingly, CCL19, which was unexpectedly high in several non-lymphoid tissues, was also elevated in the brain and kidney of CCX-CKR deficient mice (Figure 4.9), while levels in skin and heart samples were unchanged (Figure 4.9).

These data show that there are elevated levels of CCL19 in serum, ILNs, brain and kidney of CCX-CKR deficient mice, with CCL19 levels unchanged in a variety of other tissues. This supports the hypothesis that CCX-CKR can act as a scavenger of chemokine *in vivo* to limit the abundance of CCL19 in some tissues.

4.2.2 Subtle alterations in CCL21 protein levels in CCX-CKR deficient mice

I next investigated the effect of CCX-CKR deletion on CCL21 protein levels in these tissues. CCL21 was undetectable in both serum and peritoneal cavity lavage of WT and CCX-CKR deficient mice (Figure 4.10), and there were no differences in the levels of CCL21 in either spleen or mesenteric lymph nodes (Figure 4.11). CCL21 levels also remained unchanged in kidney, skin, brain and heart homogenates prepared from WT and CCX-CKR deficient mice (Figure 4.12). Intriguingly, CCL21 levels in the CCX-CKR deficient thymus were increased compared to WT, suggesting a role for CCX-CKR in

regulating CCL21 abundance in this tissue (Figure 4.11). In contrast, CCL21 was slightly, but significantly, reduced in ILNs of CCX-CKR deficient mice (Figure 4.11). While this indicates dysregulation of chemokine in the absence of CCX-CKR, it is difficult to reconcile this result with the hypothesised role of CCX-CKR as a scavenger. It is possible that, while acting as a scavenger in some settings, CCX-CKR has a number of functions in the regulation of chemokine in lymphoid tissues.

It is interesting to note that CCL21 was much more abundant in lymphoid tissue than CCL19, with approximately 40-50 fold more CCL21 in LNs, similar to previous reports (Luther et al., 2002), and almost 200-fold more in thymus than CCL19. There was also approximately 10 times more CCL21 than CCL19 in spleen. By contrast, although CCL21 was consistently more abundant in non-lymphoid tissues, the differences were generally not as pronounced. This and other findings presented above are discussed in chapter 7.

4.2.3 Expression of CCL19 and CCL25 mRNA

The increase in ligand seen in a number of disparate tissues supports the idea that, as indicated by *in vitro* data (Comerford et al., 2006), CCX-CKR may act as a scavenger in a variety of locations and situations, with deletion of the receptor leading to an accumulation of chemokine. However, chemokine levels could also be affected at the level of mRNA expression, possibly through dysregulation of signalling events controlling chemokine production. To test this hypothesis, the expression of CCL19 and CCL25 mRNA was investigated in a number of WT and CCX-CKR deficient tissues.

CCL19 protein expression has been shown in various tissues (section 4.2.1 above) and in previous work, and mRNA expression has been demonstrated for various tissues also (Alt et al., 2002, Baekkevold et al., 2001, Bleul and Boehm, 2000, Cyster, 2000, Förster et al., 2008, Luther et al., 2000, Yoshida et al., 1997). There were no differences in expression of CCL19 in any of the tissues analysed (Figure 4.13 and Figure 4.14). Additionally, mRNA for CCL19 could not be detected in peritoneal lavage cells (not shown). CCX-CKR deletion did not affect expression of CCL25 at the mRNA level in various solid tissues (Figure 4.15 and Figure 4.16). Thus, any observed changes in CCL19 protein abundance in CCX-CKR deficient mice cannot be attributed to changes in mRNA levels.

4.3 Summary

In this chapter I investigated the effect of CCX-CKR deletion on the expression of related receptors and ligands, using QPCR and ELISA to investigate mRNA and protein levels respectively. My hypothesis was that, in the absence of CCX-CKR, the expression of CCR7, CCR9 and/or their ligands would be disrupted. This was supported by evidence from internalisation studies (described in chapter 3) that showed that peritoneal cavity T cells from CCX-CKR deficient mice internalised more fluorescent CCL19 tetramers than their WT counterparts. It also built on *in vitro* studies from our group that indicated a scavenging role for CCX-CKR on transfected cells (Comerford et al., 2006). The main findings presented in this chapter are as follows:

1. CCR7 mRNA expression is increased in CCX-CKR deficient whole spleen and peritoneal cavity lavage cells compared to WT, but decreased in CCX-CKR deficient ILNs. It is unchanged in thymus, MLN and Peyer's patches, skin and small intestine. CCR9 mRNA expression is unaffected by the absence of CCX-CKR.
2. CCL19 protein is increased in CCX-CKR deficient serum, ILN, kidney and brain compared to WT; unchanged in spleen, MLN, thymus, skin and heart samples; and undetectable in peritoneal cavity lavage.
3. CCL21 protein is decreased in CCX-CKR deficient ILN and increased in CCX-CKR deficient thymus compared to WT. It is undetectable in serum and peritoneal cavity lavage and unaffected by CCX-CKR deletion in all other tissues investigated.
4. CCL19 and CCL25 mRNA expression is the same in CCX-CKR deficient and WT mice in all tissues investigated.

These data indicate a role for CCX-CKR in regulation of chemokine levels and chemokine receptor expression in various tissues. The implications of these observations are discussed in subsequent chapters, and in detail in chapter 7.

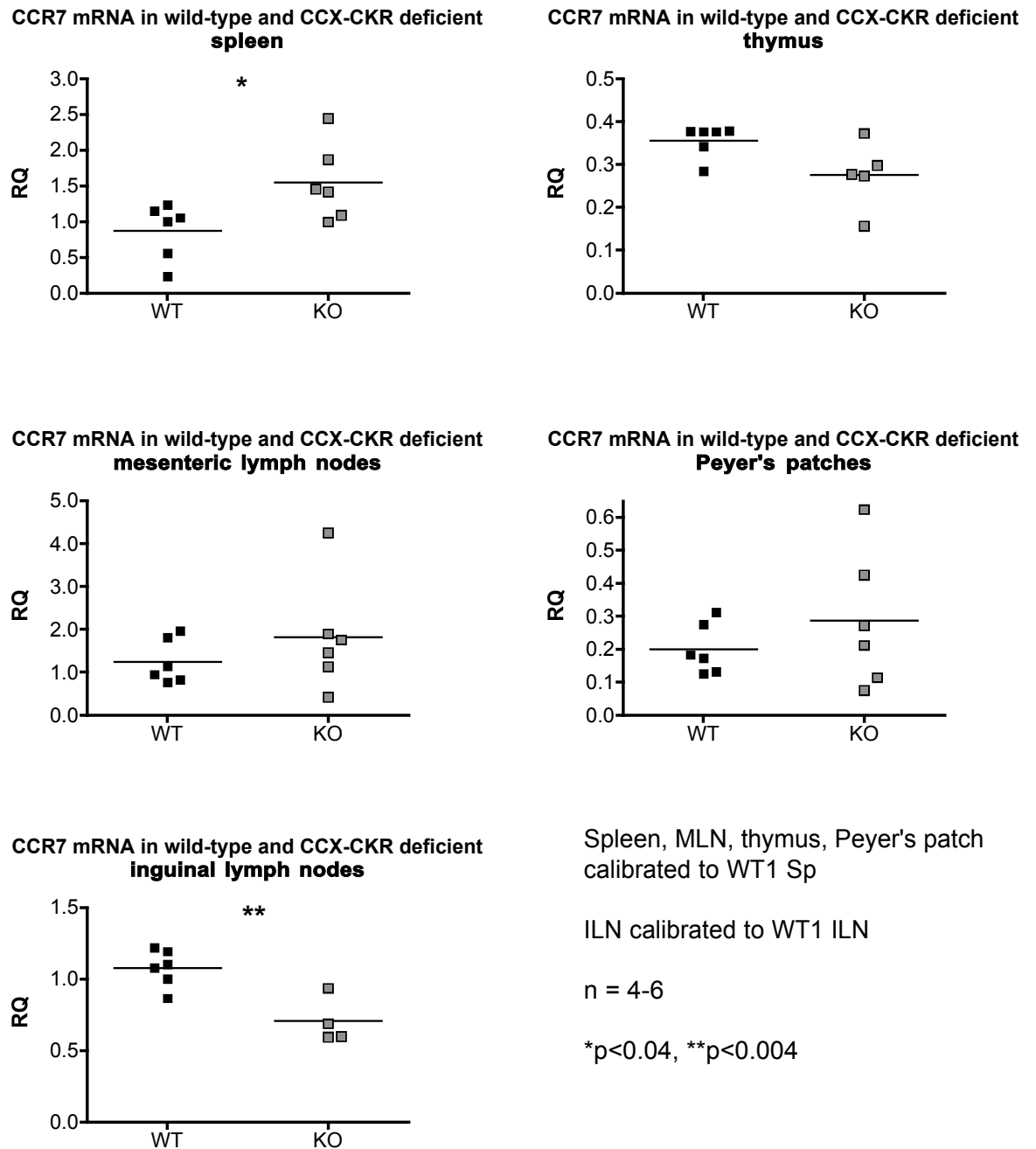


Figure 4.1: Expression of CCR7 mRNA in wild-type and CCX-CKR deficient lymph nodes, spleen, thymus and Peyer's patches. Homogenates of each tissue were analysed by QPCR to determine the level of CCR7 mRNA present in the presence (WT) or absence (KO) of CCX-CKR. Each sample was calibrated to either a wild-type (WT) spleen or WT ILN (LN) sample as indicated. Lines represent the mean, black filled squares represent WT, grey filled squares represent KO. Data were analysed by unpaired t-test, * = p<0.04, ** = p<0.004, n=4-6 per group, RQ = relative quantity.

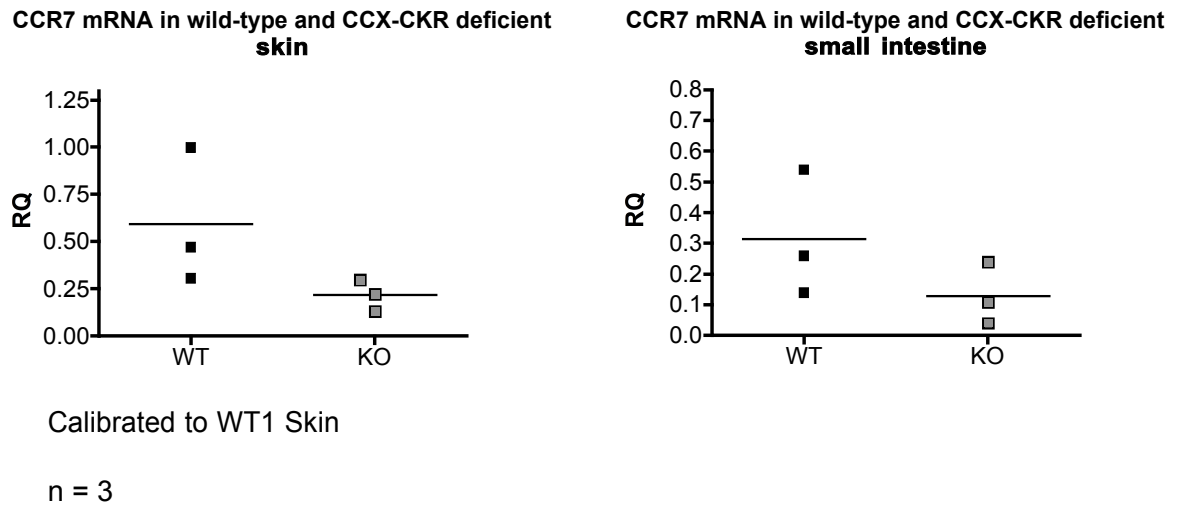


Figure 4.2: Expression of CCR7 mRNA in wild-type and CCX-CKR deficient skin and small intestine. Homogenates of each tissue were analysed by QPCR to determine the level of CCR7 mRNA present in the presence or absence of CCX-CKR. Each sample was calibrated to a wild-type (WT) skin sample. Lines represent the mean, black filled squares represent WT, grey filled squares represent CCX-CKR deficient (KO). n=3 per group, RQ = relative quantity.

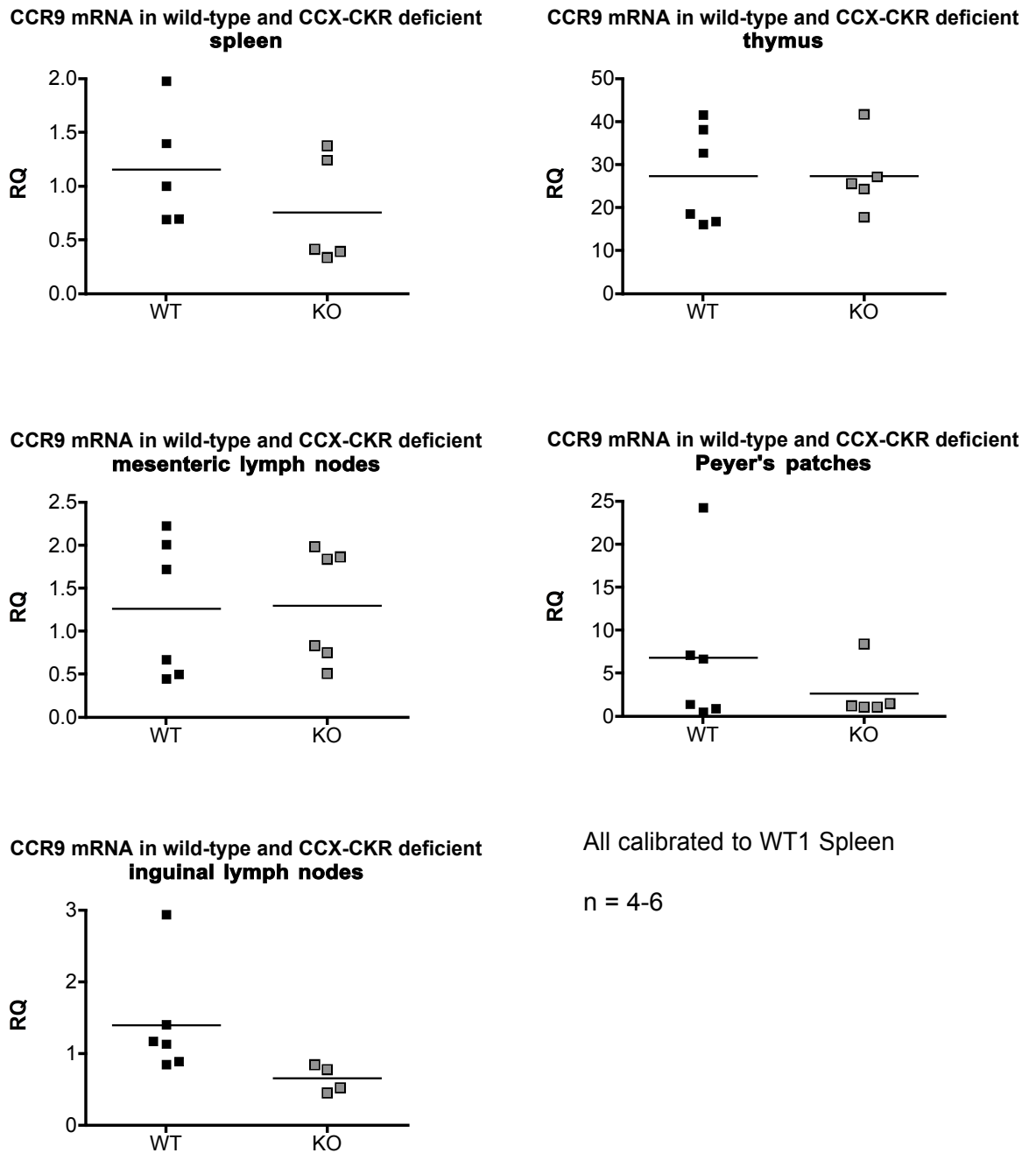
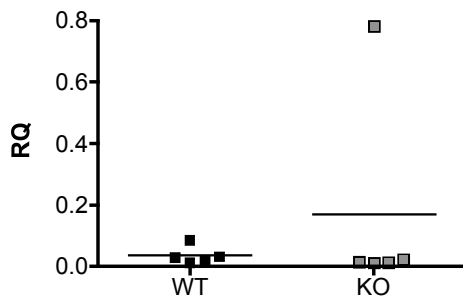
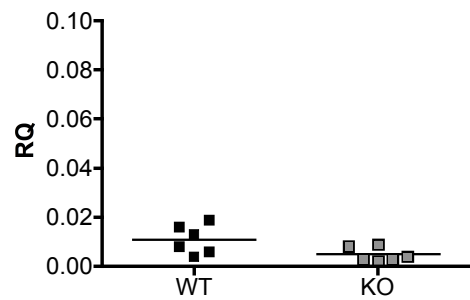


Figure 4.3: Expression of CCR9 mRNA in wild-type and CCX-CKR deficient lymph nodes, spleen and thymus. Homogenates of each tissue were analysed by QPCR to determine the level of CCR9 mRNA present in the presence or absence of CCX-CKR. Each sample was calibrated to a wild-type (WT) spleen sample. Lines represent the mean, black filled squares represent WT, grey filled squares represent CCX-CKR deficient (KO). Data were analysed by unpaired t-test, n=4-6 per group, RQ = relative quantity.

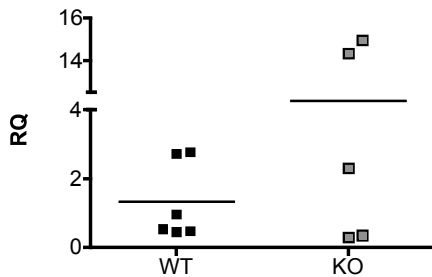
CCR9 mRNA in wild-type and CCX-CKR deficient skin



CCR9 mRNA in wild-type and CCX-CKR deficient liver



CCR9 mRNA in wild-type and CCX-CKR deficient small intestine



All calibrated to WT1 Spleen (see previous figure)

n = 5-6

Figure 4.4: Expression of CCR9 mRNA in wild-type and CCX-CKR deficient skin, liver, Peyer's patches and small intestine. Homogenates of each tissue were analysed by QPCR to determine the level of CCR9 mRNA present in the presence or absence of CCX-CKR. Each sample was calibrated to a wild-type (WT) spleen sample (see **Figure 4.3**). Lines represent the mean, black filled squares represent WT, grey filled squares represent CCX-CKR deficient (KO). Data were analysed by unpaired t-test, n=5-6 per group, RQ = relative quantity.

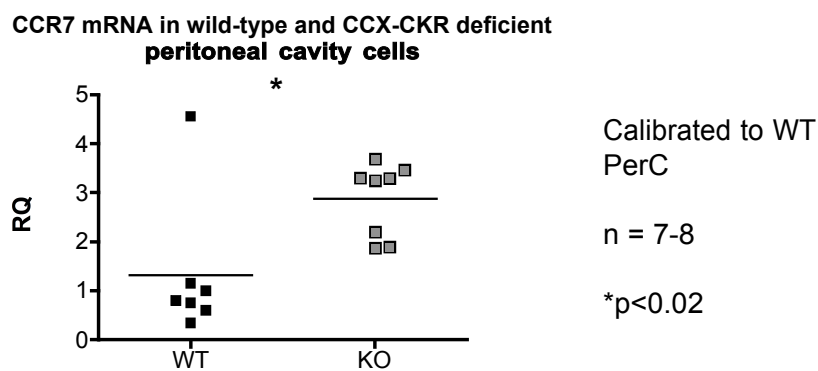


Figure 4.5: Expression of CCR7 mRNA in wild-type and CCX-CKR deficient peritoneal lavage cells. Peritoneal cells were analysed by QPCR to determine the level of CCR7 mRNA present in the presence or absence of CCX-CKR. Each sample was calibrated to a wild-type (WT) sample. Lines represent the mean, black filled squares represent WT, grey filled squares represent CCX-CKR deficient (KO). Data were analysed by unpaired t-test, *p<0.02, n=4-5 per group, RQ = relative quantity.

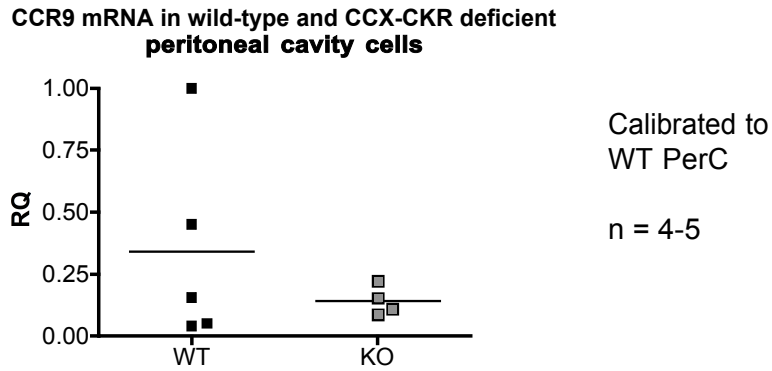


Figure 4.6: Expression of CCR9 mRNA in wild-type and CCX-CKR deficient peritoneal lavage cells. Peritoneal cells were analysed by QPCR to determine the level of CCR9 mRNA present in the presence or absence of CCX-CKR. Each sample was calibrated to a wild-type (WT) sample. Lines represent the mean, black filled squares represent WT, grey filled squares represent CCX-CKR deficient (KO). n=4-5 per group, RQ = relative quantity.

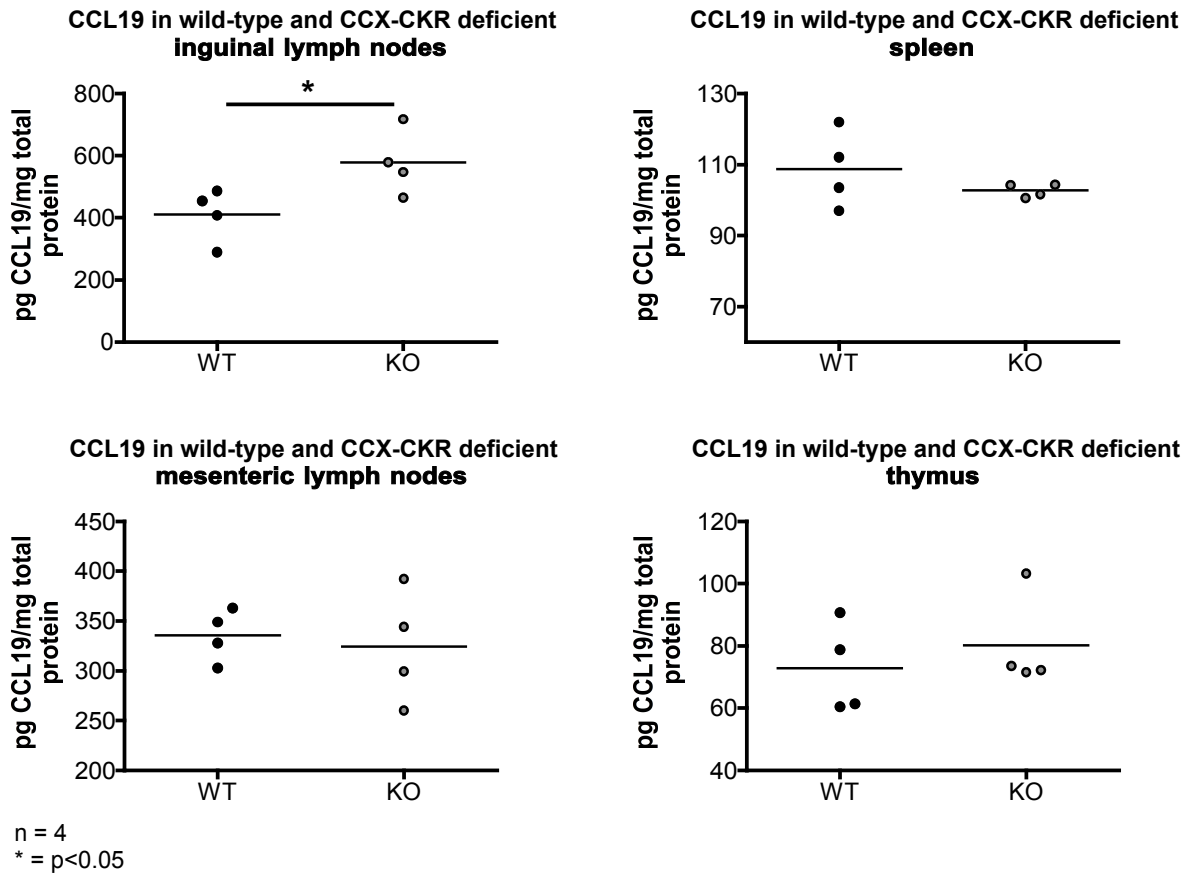


Figure 4.7: CCL19 protein levels in wild-type and CCX-CKR deficient lymph nodes, spleen and thymus. Wild-type (WT) and CCX-CKR deficient (KO) tissues were snap-frozen in liquid nitrogen, homogenised and supernatants recovered as described in Materials and Methods. CCL19 protein levels were determined by ELISA and total protein levels were determined by BCA assay. Data were analysed using unpaired t-tests, n = 4, * = p < 0.05.

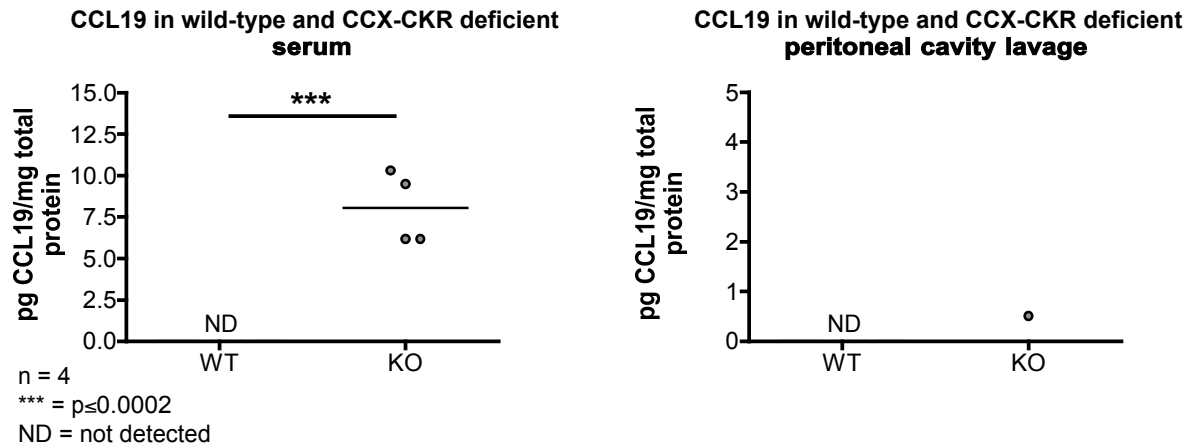


Figure 4.8: CCL19 protein in wild-type and CCX-CKR deficient serum and peritoneal cavity lavage. Wild-type (WT; black filled circles) and CCX-CKR deficient (KO; grey filled circles) peritoneal cavity lavage was retrieved, cells pelleted and supernatant harvested as described in Materials and Methods. Whole blood was harvested from the posterior vena cava, and serum isolated as described in Materials and Methods. CCL19 protein levels were determined by ELISA and total protein levels were determined by BCA assay. Data were analysed using unpaired t-tests, n = 4, *** = $p \leq 0.0002$, ND = not detected. All peritoneal cavity samples but one had undetectable CCL19, making statistical analysis unfeasible.

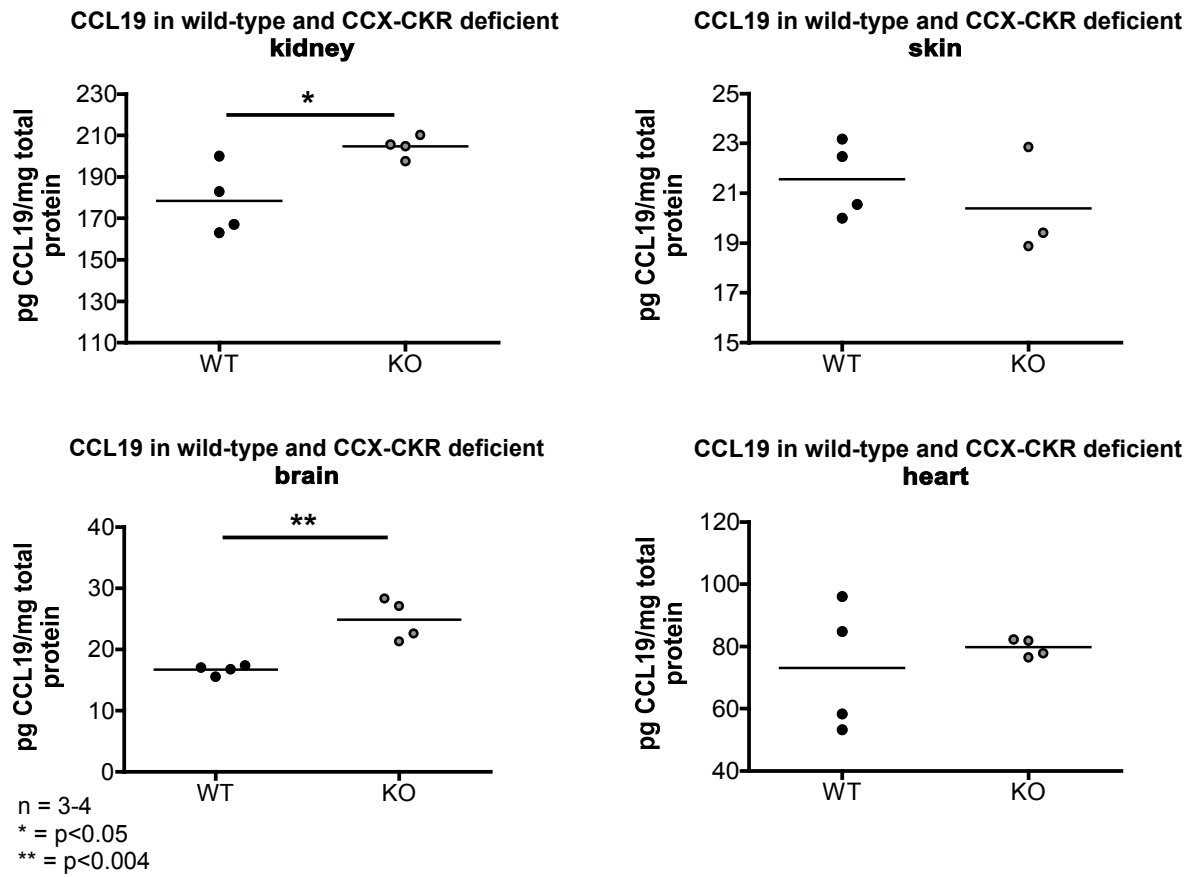


Figure 4.9: CCL19 protein levels in wild-type and CCX-CKR deficient kidney, skin, brain and heart. Wild-type (WT) and CCX-CKR deficient (KO) tissues were snap-frozen in liquid nitrogen, homogenised and supernatants recovered as described in Materials and Methods. CCL19 protein levels were determined by ELISA and total protein levels were determined by BCA assay. Data were analysed using unpaired t-tests, n = 4, * = p < 0.05, ** = p < 0.004.

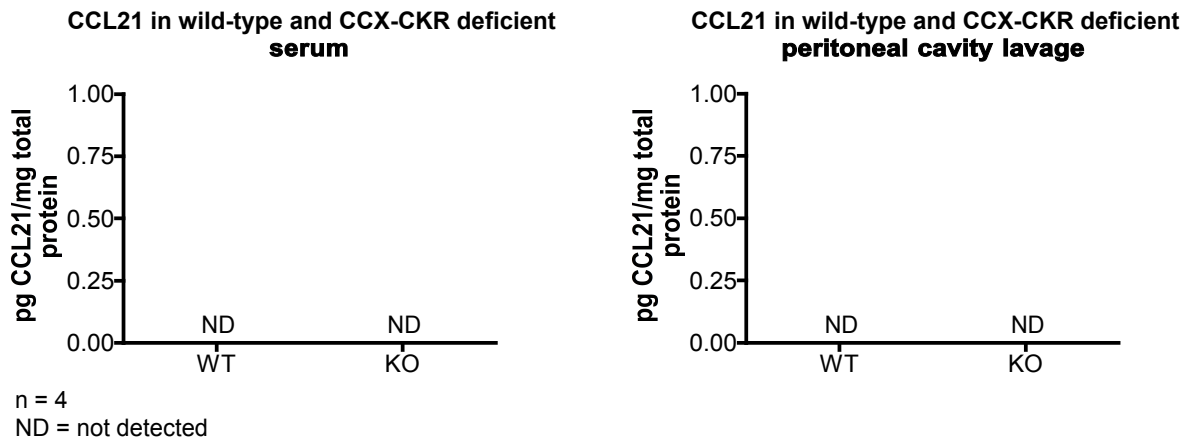


Figure 4.10 CCL21 protein in wild-type and CCX-CKR deficient serum and peritoneal cavity lavage. Wild-type (WT) and CCX-CKR deficient (KO) serum and cells from peritoneal cavity lavage were isolated as before. CCL21 protein levels were determined by ELISA and total protein levels were determined by BCA assay. Statistical analysis was not feasible as CCL21 was not detected in all samples tested, n = 4, ND = not detected.

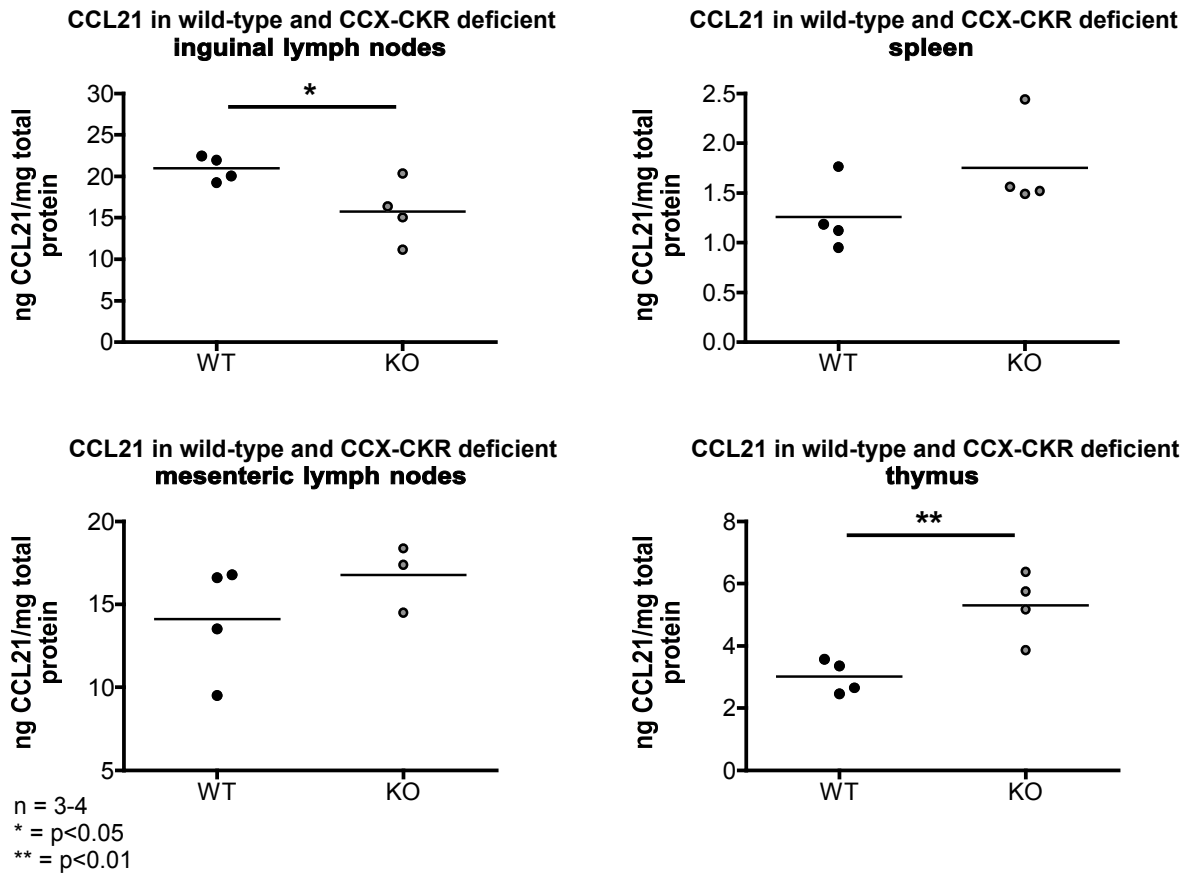


Figure 4.11: CCL21 protein levels in wild-type and CCX-CKR deficient lymph nodes, spleen and thymus. Wild-type (WT) and CCX-CKR deficient (KO) tissues were snap-frozen in liquid nitrogen, homogenised and supernatants recovered as described in Materials and Methods. CCL21 protein levels were determined by ELISA and total protein levels were determined by BCA assay. Data were analysed using unpaired t-tests, n = 3-4, * = p<0.05, ** = p<0.01.

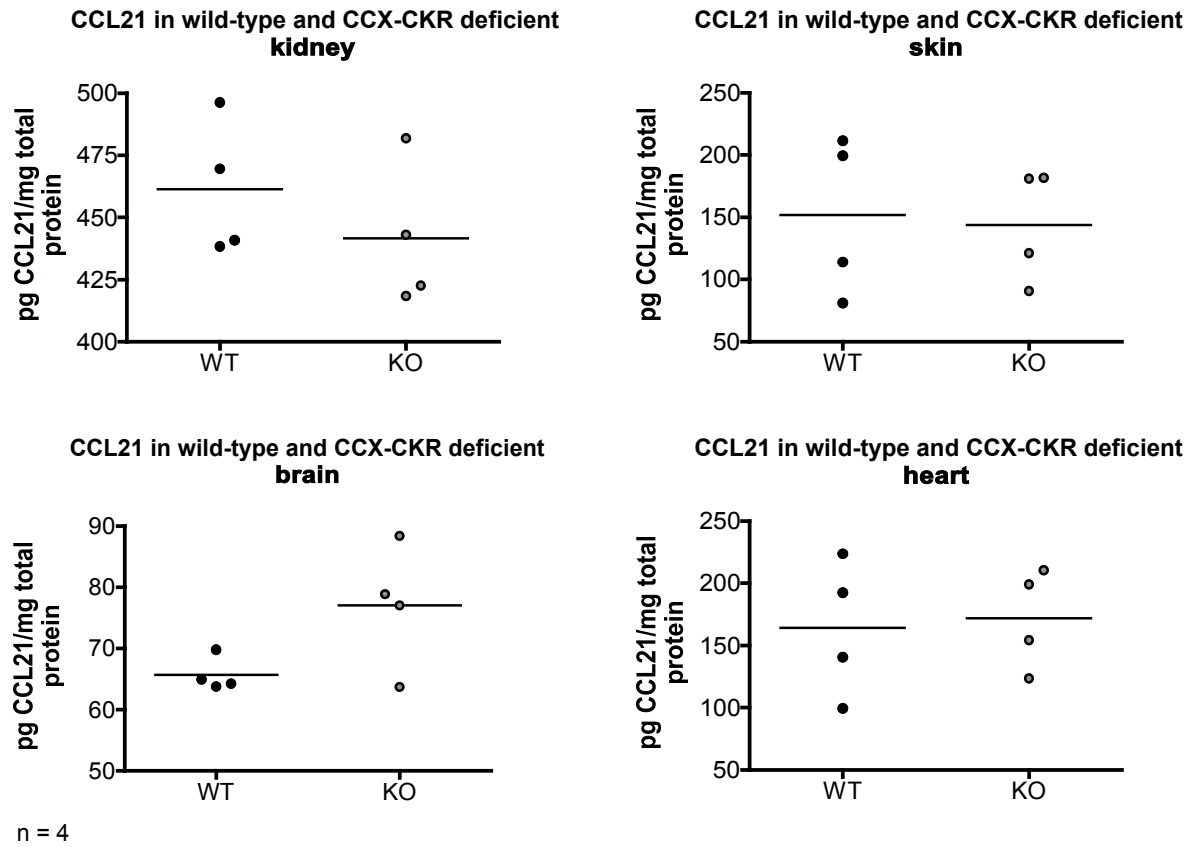
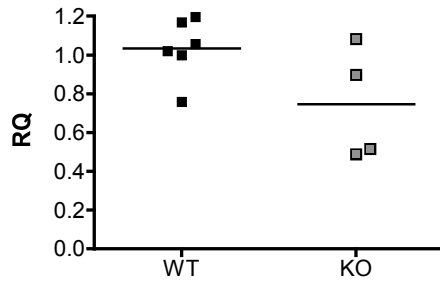
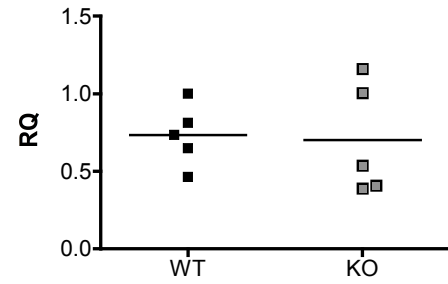


Figure 4.12: CCL21 protein levels in wild-type and CCX-CKR deficient kidney, skin, brain and heart. Wild-type (WT) and CCX-CKR deficient (KO) tissues were snap-frozen in liquid nitrogen, homogenised and supernatants recovered as described in Materials and Methods. CCL21 protein levels were determined by ELISA and total protein levels were determined by BCA assay. Data were analysed using unpaired t-tests, n = 4.

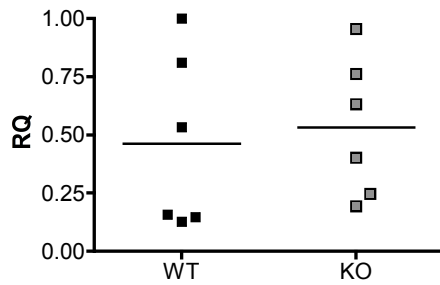
CCL19 mRNA in wild-type and CCX-CKR deficient inguinal lymph nodes



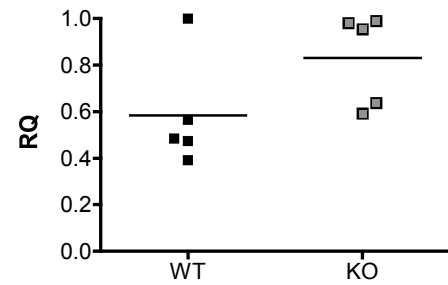
CCL19 mRNA in wild-type and CCX-CKR deficient spleen



CCL19 mRNA in wild-type and CCX-CKR deficient mesenteric lymph nodes



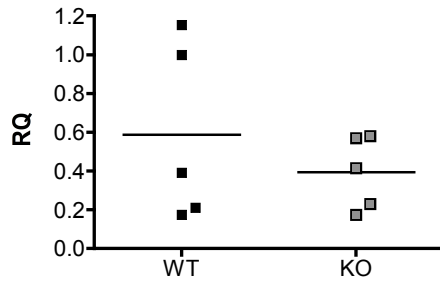
CCL19 mRNA in wild-type and CCX-CKR deficient thymus



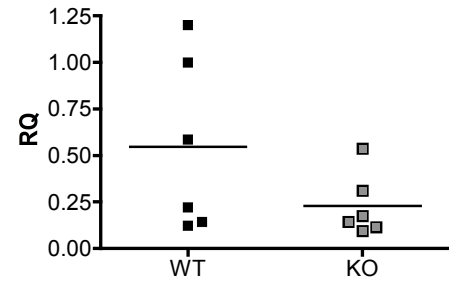
Each tissue calibrated to WT1
n = 5-6

Figure 4.13: Expression of CCL19 mRNA in wild-type and CCX-CKR deficient lymph nodes, spleen and thymus. Homogenates of each tissue were analysed by QPCR to determine the level of CCL19 mRNA present in the presence or absence of CCX-CKR. Each tissue group was calibrated to a wild-type (WT) sample. Lines represent the mean, black filled squares represent WT, grey filled squares represent CCX-CKR deficient (KO). n=5-6 per group, RQ = relative quantity.

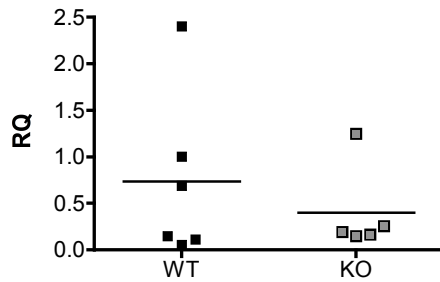
CCL19 mRNA in wild-type and CCX-CKR deficient skin



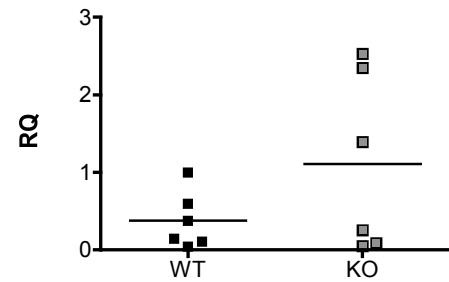
CCL19 mRNA in wild-type and CCX-CKR deficient liver



CCL19 mRNA in wild-type and CCX-CKR deficient Peyer's patches



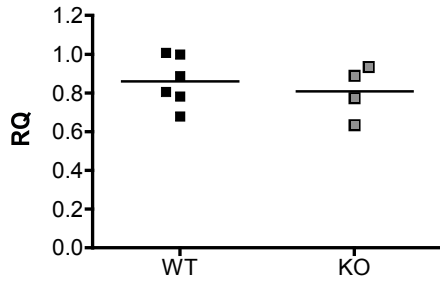
CCL19 mRNA in wild-type and CCX-CKR deficient small intestine



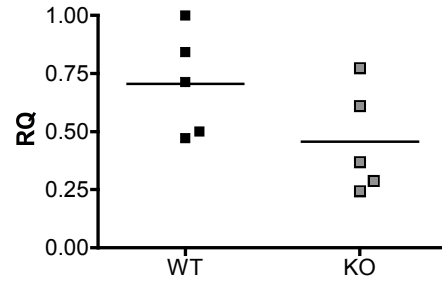
Each tissue calibrated to WT1
n = 5-6

Figure 4.14: Expression of CCL19 mRNA in wild-type and CCX-CKR deficient skin, liver, Peyer's patches and small intestine. Homogenates of each tissue were analysed by QPCR to determine the level of CCL19 mRNA present in the presence or absence of CCX-CKR. Each tissue group was calibrated to a wild-type (WT) sample. Lines represent the mean, black filled squares represent WT, grey filled squares represent CCX-CKR deficient (KO). n=5-6 per group, RQ = relative quantity.

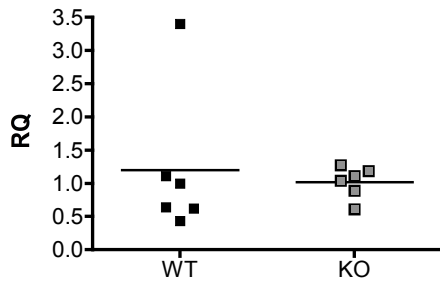
CCL25 mRNA in wild-type and CCX-CKR deficient inguinal lymph nodes



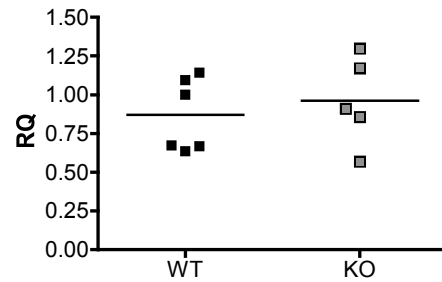
CCL25 mRNA in wild-type and CCX-CKR deficient spleen



CCL25 mRNA in wild-type and CCX-CKR deficient mesenteric lymph nodes



CCL25 mRNA in wild-type and CCX-CKR deficient thymus



Each tissue calibrated to WT1
n = 4-6

Figure 4.15: Expression of CCL25 mRNA in wild-type and CCX-CKR deficient lymph nodes, spleen and thymus. Homogenates of each tissue were analysed by QPCR to determine the level of CCL25 mRNA present in the presence or absence of CCX-CKR. Each tissue group was calibrated to a wild-type (WT) sample. Lines represent the mean, black filled squares represent WT, grey filled squares represent CCX-CKR deficient (KO). n=4-6 per group, RQ = relative quantity.

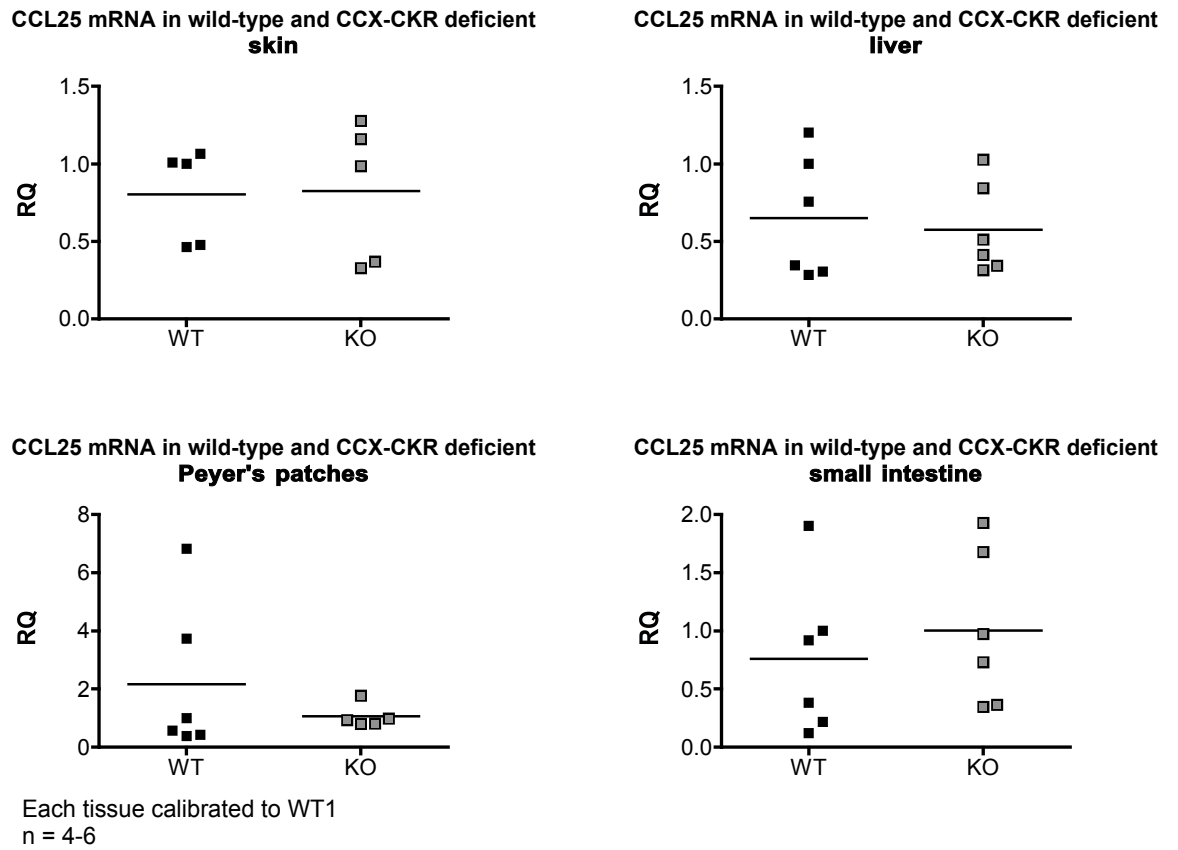


Figure 4.16: Expression of CCL25 mRNA in wild-type and CCX-CKR deficient skin, liver, Peyer's patches and small intestine. Homogenates of each tissue were analysed by QPCR to determine the level of CCL25 mRNA present in the presence or absence of CCX-CKR. Each tissue group was calibrated to a wild-type (WT) sample. Lines represent the mean, black filled squares represent WT, grey filled squares represent CCX-CKR deficient (KO). n=4-6 per group, RQ = relative quantity.

5 Effect of CCX-CKR deletion on cellularity, cell distribution and microarchitecture of resting secondary lymphoid tissues

As described in the Introduction, CCR7 is involved in the development and seeding of lymphoid tissues; the recirculation of leukocytes and homing to lymph nodes; and the positioning of cells within lymphoid tissues. Although CCX-CKR activity was barely detectable on cells from spleen and lymph nodes using the fluorescent CCL19 tetramer internalisation assay, these tissues clearly express CCX-CKR mRNA. Moreover, deletion of CCX-CKR alters the expression of CCR7 in spleen and ILNs, and by peritoneal cavity lavage cells, as well as changing the levels of CCL19 and CCL21 in various tissues and, notably, causing a significant increase in serum CCL19 levels. Therefore, it was hypothesised that deleting CCX-CKR might alter the cellularity and/or structure of immune compartments, either by affecting the ability of cells to enter or exit the site, or by changing the positioning of cells within tissues.

To assess cellularity, cells were isolated as described in Materials and Methods and stained with fluorescent antibodies against various lineage markers to allow identification of different cell types. The abundance of a particular cell type was analysed both as a proportion of the total live cells recovered from each site and, where possible, in absolute numbers of retrieved cells. The total number of cells retrieved from WT and CCX-CKR deficient tissues were also compared to ascertain whether there was any evidence of hypo- or hypercellularity in the absence of CCX-CKR. Spleen, ILN, blood and peritoneal cavity were all investigated, because all displayed alterations in CCR7 mRNA expression and/or chemokine protein levels.

While flow cytometry provides some valuable insights into the effect of CCX-CKR deletion on the cellularity of various immune compartments, it cannot elucidate the role the receptor may play in positioning of cells within tissues. Additionally, some tissues are extremely difficult to examine using flow cytometry – although some attempts were made to analyse the cellularity of skin by this method, this process is technically demanding with a high level of cell death, and the results were not encouraging. Therefore, a histological comparison of WT and CCX-CKR deficient tissues was also carried out and preliminary results from spleen (in this chapter) and skin (chapter 6) are presented. Other tissues, such

as lymph node, thymus and small intestine are under investigation in our lab and elsewhere.

5.1 Cellularity in the spleen

The total number of cells retrieved from WT and CCX-CKR deficient spleens was not significantly different (Figure 5.1). The first cell types analysed were B and T cells. Lymphocytes are the main cell type retrieved from the spleen (see chapter 3) and are known both to express CCR7 and to respond to its ligands (see Introduction). Since CCR7 mRNA expression is increased in the spleen (see previous chapter), it was hypothesised that this might affect the migration of these cells into or out of the spleen. However, T and B cells in the CCX-CKR deficient spleen were present in the same proportions and absolute numbers as in the WT spleen (Figure 5.2). This was also true for B1 cells and marginal zone B cells in this tissue (Figure 5.3). Myeloid cells were then analysed to determine the effect of CCX-CKR deletion on these cells in the spleen. None of the cell types analysed showed any difference in proportion or absolute number between WT and CCX-CKR deficient spleen (Figure 5.4).

5.2 Microarchitecture of the CCX-CKR deficient spleen

The data presented above suggest that CCX-CKR deletion does not significantly influence cell abundance in the spleen, although they do not provide any information on the positioning of cells within the tissue. Therefore, histological analysis of WT and CCX-CKR deficient spleens was carried out to provide some insight into whether CCX-CKR could influence the microarchitecture of this tissue. As detailed in the Introduction, the CCX-CKR ligands CCL19 and CCL21 are crucially important for correct positioning of leukocytes within lymphoid tissues, including the spleen. While previous experiments showed no difference in overall splenic levels of these chemokines, differences in their presentation or availability due to deletion of CCX-CKR cannot be ruled out at this stage.

Initial experiments, using haematoxylin and eosin (H&E) staining, were designed to reveal any gross abnormalities in splenic structure in the CCX-CKR deficient mouse. Frozen spleen sections were stained with H&E to reveal the general architecture of the spleen, with white pulp areas visible as darker, more densely populated areas surrounded by lighter, less cell-rich red pulp regions (Figure 5.5). Using Axiovision software, the area of white pulp present in single fields of view at 100x magnification (i.e. using a 10x objective) was measured from the spleens of four individuals from both groups (WT and

CCX-CKR deficient). Representative images are shown in Figure 5.5, with graphical representation of white pulp area shown below. These data indicate that there is no difference in the general architecture of the spleen in the absence of CCX-CKR.

Following on from this, immunofluorescent staining was carried out to investigate whether there was a defect in the positioning of specific types of cells. Frozen spleen sections were stained with fluorescently-labelled antibodies against IgM and CD3, to identify B and T cells respectively, with sections from at least 4 individuals per group analysed per experiment in two separate experiments. Figure 5.6 shows a representative image from both a WT and a CCX-CKR deficient spleen. B cell localisation appeared intact, as did T cell localisation, with no obvious defects observed. Bright red cells in the red pulp are likely IgM⁺ plasma cells. This supports the flow cytometry data shown above in suggesting that CCX-CKR deletion does not lead to gross abnormalities in the organisation and structure of the spleen.

5.3 Cellularity in the inguinal lymph nodes

ILNs showed decreased CCR7 mRNA expression in the absence of CCX-CKR, as well as altered chemokine protein levels (see previous section). Interestingly, they also had increased total cell numbers compared with WT mice (Figure 5.7). Therefore it was theorised that deletion of CCX-CKR could alter the cellularity of the lymph nodes, either by affecting the ability of cells to migrate to or reside within the nodes. ILN myeloid cells demonstrated CCX-CKR-dependent internalisation of fluorescent CCL19 tetramers (see chapter 3). Additionally, Heinzl and colleagues reported defects in DC homing from the skin to the draining lymph nodes. Therefore, these cells were investigated to determine whether there were any obvious defects in their proportions or numbers in the ILN. Most myeloid cell populations in the ILNs were unaffected by deletion of CCX-CKR (Figure 5.8). However, there was a significant reduction in the proportion of CD11b^{low} F4/80⁻ CD11c⁺ cells (gated as in Figure 3.14, chapter 3) but this did not coincide with any change in absolute numbers of these cells in the tissue (Figure 5.8). These data contrast with reported effects of CCX-CKR deletion on steady-state homing of DCs to the draining lymph node from skin, where CD11c⁺ MHC II^{high} DCs were reduced in the lymph nodes of CCX-CKR deficient mice. However, this may be due to variations between experiments – Heinzl and colleagues investigated the effect of CCX-CKR deletion on CD11c⁺ MHC II^{high} populations in samples pooled from axillary, brachial and ILNs, while my work examined ILNs alone and did not include MHC II staining (Heinzl et al., 2007). Given the

low proportion of ILN cells that are of myeloid lineage, it is unlikely that this compartment is responsible for the increase in total cellularity observed.

As B and T cells are the main populations in ILNs, it was considered likely that the increased cellularity observed was due to alterations in one or both subsets. B cells were not significantly affected by deletion of CCX-CKR (Figure 5.9), either proportionally or in absolute numbers. The proportion of T cells was slightly increased in CCX-CKR deficient ILNs compared to WT, as a percentage of total cells (Figure 5.9). However, absolute numbers of T cells were consistent between WT and CCX-CKR deficient ILNs (Figure 5.9). It is important to note that, due to the level of variation in total cellularity between samples, differences in lymphocyte numbers between individuals may be slight, and differences between strains might only become apparent with analysis of a higher number of individuals. These data were generated from only three individuals from each group, whereas total cellularity data was generated from many more animals.

5.4 Deletion of CCX-CKR increases lymphocyte abundance in the peritoneal cavity

CCR7 expression was increased in some peritoneal cavity lavage cells retrieved from CCX-CKR deficient mice compared with WT. This was apparent in both the fluorescent CCL19 tetramer internalisation assay (see chapter 3, Figure 3.18) and at the mRNA level by QPCR (see chapter 4, Figure 4.5). Given the reported function of this receptor in regulating the migration of leukocytes to and from the peritoneal cavity (Höpken et al., 2004, Höpken et al., 2010), it was hypothesised that the cellularity of the cavity might be altered in the CCX-CKR deficient animal. Indeed, as in the ILNs, the total cell numbers retrieved from the peritoneal cavity were significantly elevated in the absence of CCX-CKR (Figure 5.10). When leukocyte subsets were specifically investigated, it was discovered that there was a significant increase in the proportion of B1b and B2 B cells and T cells in the CCX-CKR deficient peritoneal cavity compared to WT (Figure 5.11). This corresponded to an increase in the absolute number of each of these cell types retrieved from the cavity, and in fact B1a and B1c B cell numbers were also significantly increased (Figure 5.11).

The peritoneal cavity also contains a large population of $FSC^{low} SSC^{med-high}$ cells, mainly macrophages, which can be divided into $CD11b^{+}$ and $CD11b^{-}$ populations (see chapter 3, Figure 3.17). These populations were proportionally decreased in the CCX-CKR deficient peritoneal cavity, although absolute numbers remained consistent with WT (Figure 5.12).

This suggests the decrease in proportion of these cells reflects the overall increase of other cells, i.e. B and T cell populations, rather than a direct effect of CCX-CKR deletion on the macrophage population. These data suggest that CCX-CKR specifically regulates the abundance of lymphocytes in the peritoneal cavity.

5.5 Summary

Previous experiments have shown that CCX-CKR deficient animals have altered chemokine and chemokine receptor expression in a number of tissues. Therefore, experiments in this chapter were designed to assess the impact of deletion of CCX-CKR on cellularity in lymphoid compartments. Cellularity and gross microarchitecture of the CCX-CKR deficient spleen was no different from WT, and lymphocyte proportions in peripheral blood were similarly unchanged (data not shown). Interestingly, total cellularity in both ILNs and peritoneal cavity was increased in the absence of the receptor. The specific cell population affected in the ILN has yet to be uncovered. However, in the peritoneal cavity, there is a clear role for CCX-CKR in regulating the lymphocyte compartment. All major lymphocyte subsets present (i.e. B1a, B1b, B1c and B2 B cells and T cells) were overrepresented. The molecular basis for this phenotype is unclear. Neither CCX-CKR mRNA nor CCL19 tetramer internalisation mediated by this receptor were detected on peritoneal lavage cells, and CCX-CKR was not expressed by the lining of the peritoneal cavity (Figure 3.2). Possible explanations for, and implications of, this phenotype are discussed in Chapter 7.

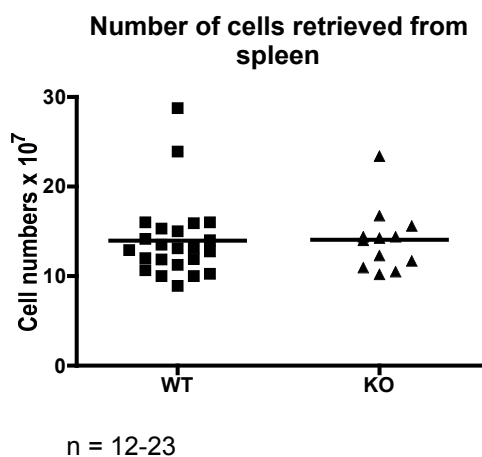


Figure 5.1: Total cell numbers retrieved from wild-type and CCX-CKR deficient spleens. Cells were isolated from wild-type (WT) and CCX-CKR deficient (KO) spleens as described in Materials and Methods and counted using a haemocytometer. Data are pooled from numerous experiments, $n \geq 3$ per group per experiment, line represents the mean.

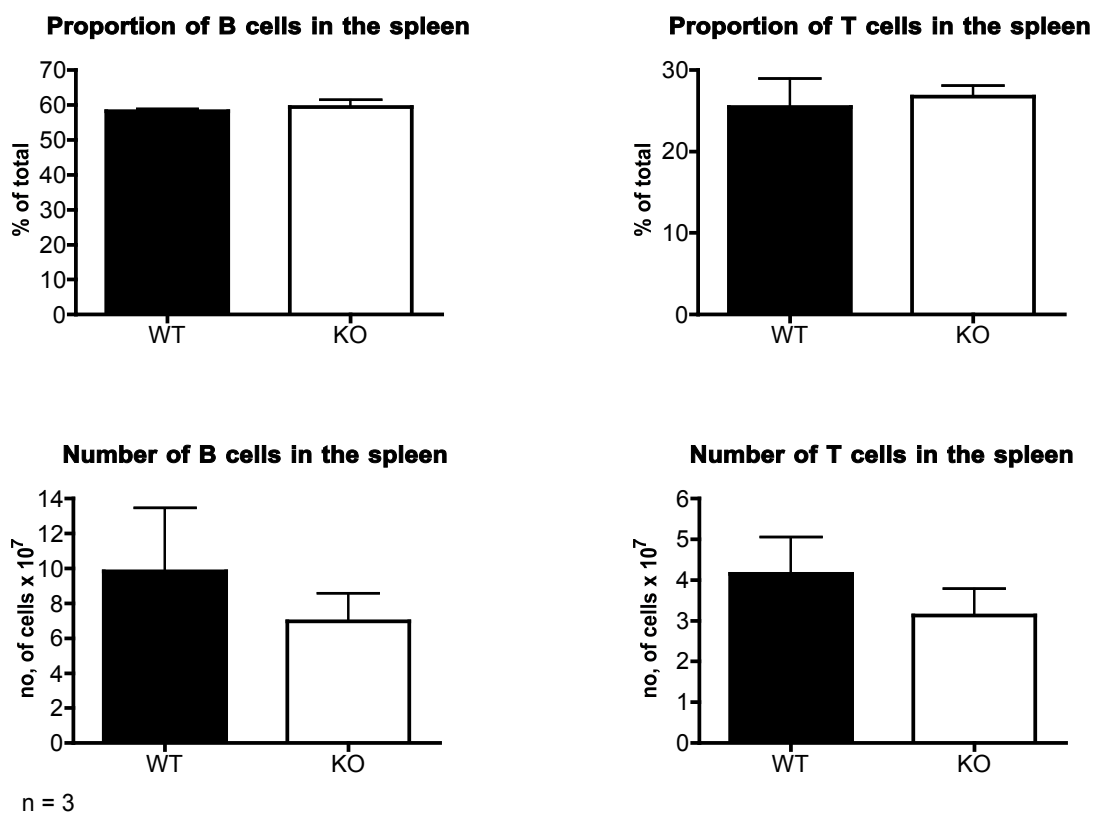


Figure 5.2: B and T cell cellularity in the spleen. Cells from wild-type (WT) and CCX-CKR deficient (KO) spleens were gated as in **Figure 3.6**. B cells are defined as CD19⁺ CD5^{low/-}. T cells are defined as CD5⁺ CD19^{low/-}. Graphs show B and T cells as both a proportion of total cells isolated from the spleen (top panels) and as absolute numbers of cells isolated. Error bars indicate standard deviation, n = 3. Data were analysed by unpaired t-tests, with no significant differences observed.

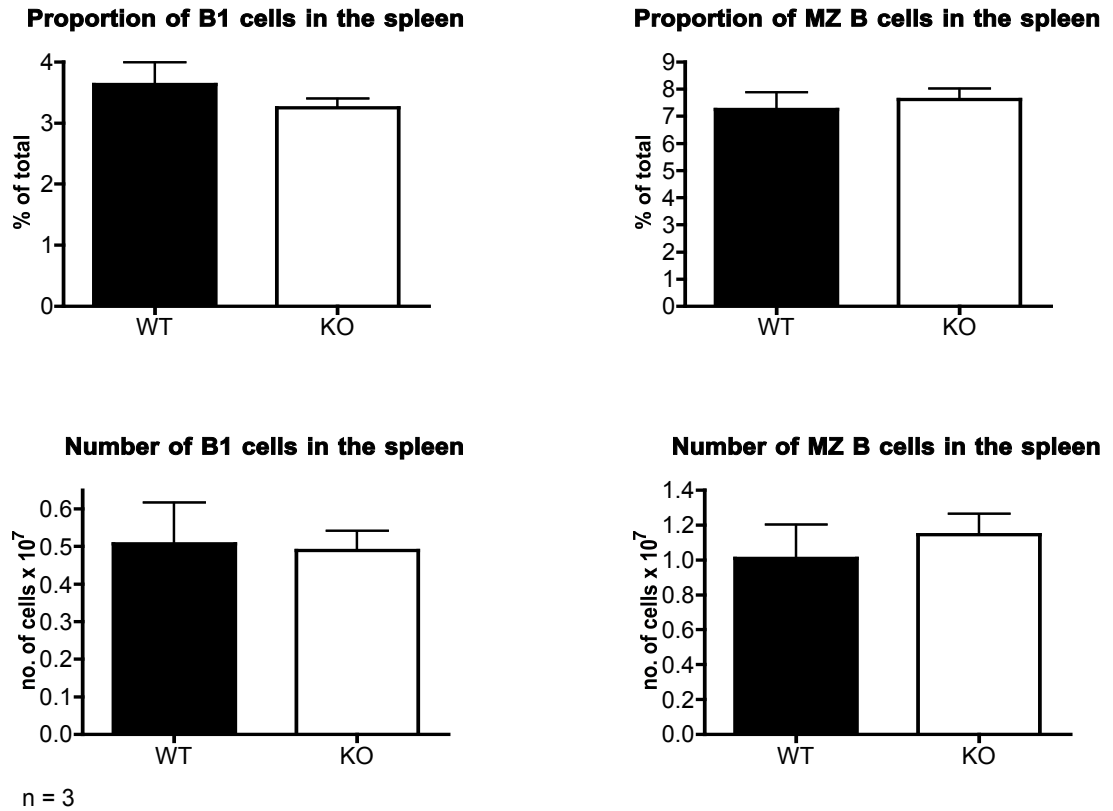
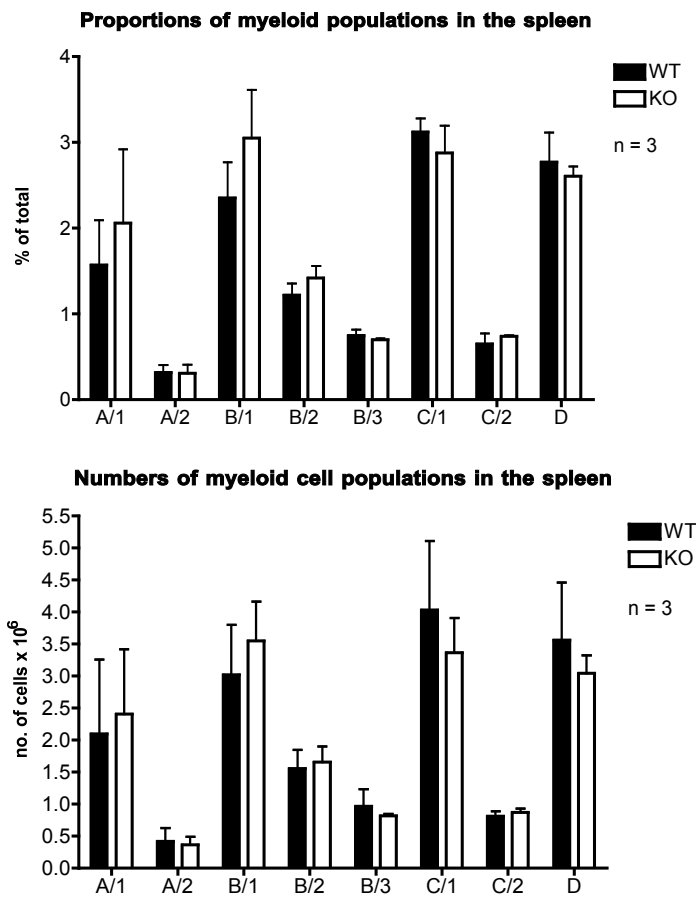


Figure 5.3: Proportions and numbers of B1 and marginal zone B cells in the spleen. Cells from wild-type (WT) and CCX-CKR deficient (KO) spleens were gated as in **Figure 3.8**. B1 B cells were defined as CD19⁺ CD23⁻ CD5^{low}, while marginal zone (MZ) B cells were defined as CD19⁺ CD23⁻ CD21^{low/-}. Graphs show B1 and MZ B cells as both a proportion of total cells isolated from the spleen (top panels) and as absolute numbers of cells isolated. Error bars indicate standard deviation, n = 3. Data were analysed by unpaired t-tests, with no significant differences observed.



Cell type	Marker profile	Cell type	Marker profile
A/1	CD11b high, F4/80 neg, CD11c neg/low	B/3	CD11b high, F4/80 low, CD11c high
A/2	CD11b high, F4/80 neg, CD11c med/high	C/1	CD11b low, F4/80 neg, CD11c low
B/1	CD11b high, F4/80 low, CD11c neg/low	C/2	CD11b low, F4/80 neg, CD11c high
B/2	CD11b high, F4/80 low, CD11c med	D	CD11b low/med, F4/80+, CD11c+

Figure 5.4: Proportions and numbers of myeloid cells in the spleen. Cells from wild-type (WT) and CCX-CKR deficient (KO) spleens were gated as in **Figure 3.9** and defined as detailed in the table (bottom panel). Graphs show myeloid cells as both a proportion of total cells isolated from the spleen (top panel) and as absolute numbers of cells isolated (middle panel). Error bars indicate standard deviation, n = 3. Data were analysed by unpaired t-tests, with no significant differences observed.

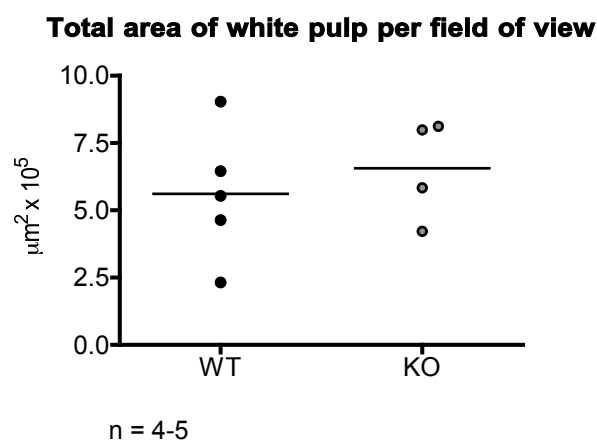
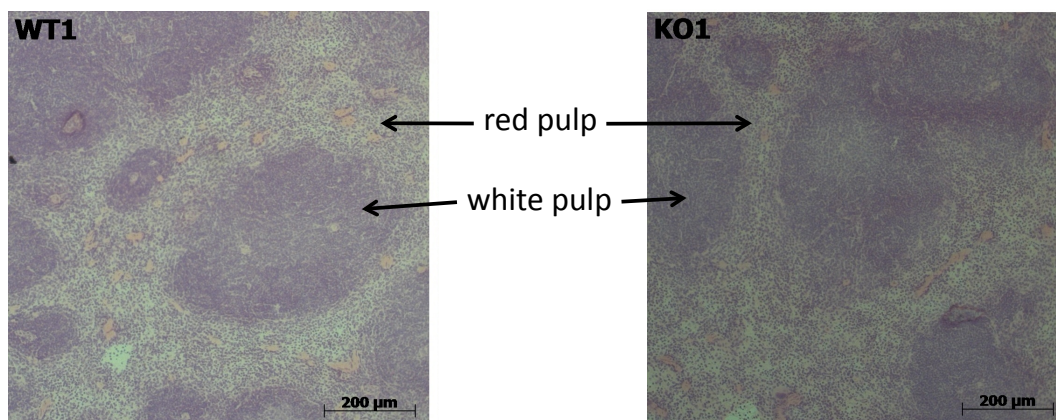


Figure 5.5: Area of white pulp in wild-type and CCX-CKR deficient spleens. Paraffin-embedded sections from wild-type (WT) and CCX-CKR deficient (KO) spleens were prepared and stained with haematoxylin and eosin as described in Materials and Methods. Slides were visualised using an AxioStar Plus microscope with 10x objective. Analysis was carried out using Axiovision software. Graph (bottom panel) shows area of white-pulp (indicated in images, top panel) for WT and KO sections. Line represents the mean, n = 4-5. Data were analysed by unpaired t-test, with no significant differences observed.

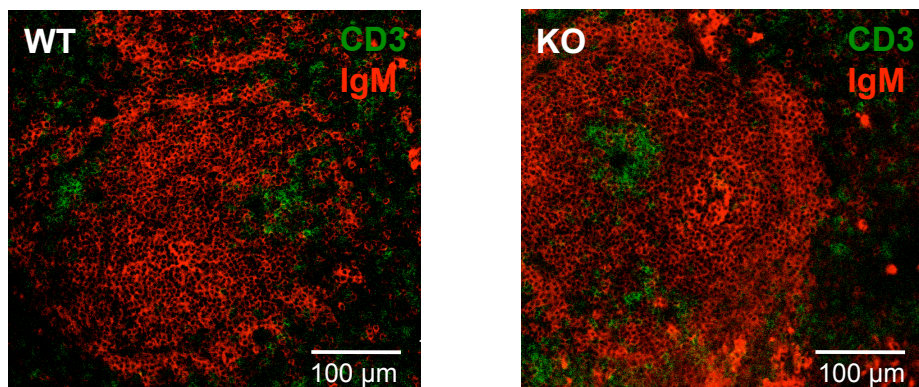
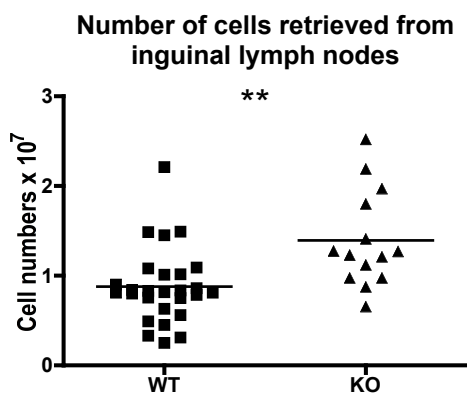


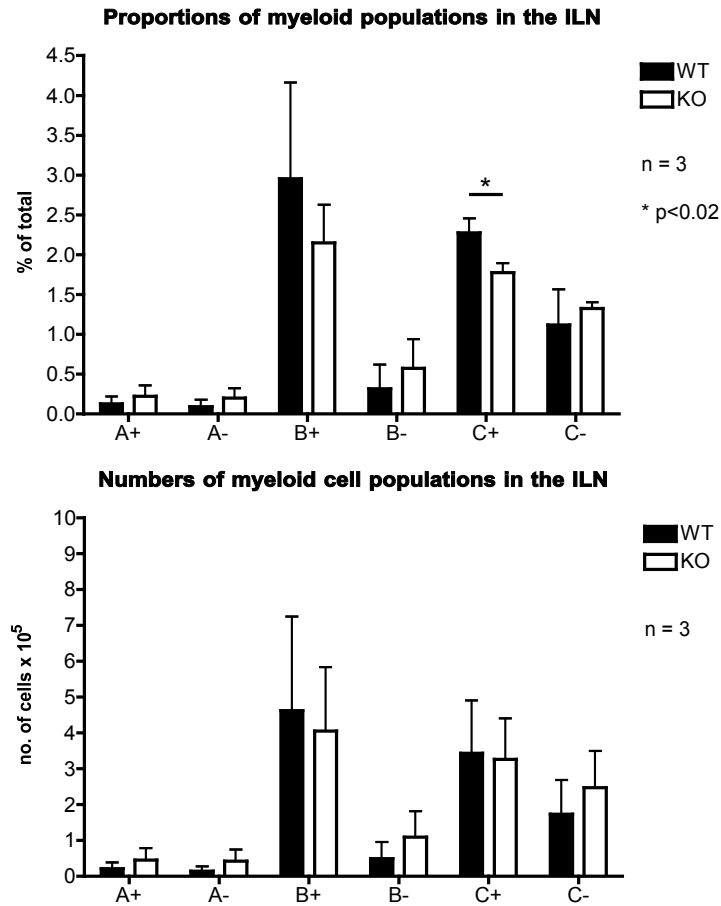
Figure 5.6: Immunofluorescent staining of B and T cells in wild-type and CCX-CKR deficient spleen. Sections from wild-type (WT) and CCX-CKR deficient (KO) spleens were processed as described in Materials and Methods. Images are representative of at least 4 replicates per group per experiment, and of 2 separate experiments. Sections were stained with anti-mouse IgM AF555 (red; to label B cells) and anti-mouse CD3 FITC (green; to label T cells). Sections were visualised using a Zeiss LSM 510 Confocal microscope with 20x objective and analysed using Carl Zeiss AIM software. White line indicates scale.



n = 14-27

** p = 0.0016

Figure 5.7: Total cell numbers retrieved from wild-type and CCX-CKR deficient inguinal lymph nodes. Cells were isolated from wild-type (WT) and CCX-CKR deficient (KO) ILNs as described in Materials and Methods and counted using a haemocytometer. Data are pooled from numerous experiments, n \geq 3 per group per experiment, line represents the mean. Data were analysed using an unpaired t-test, **p=0.0016.



Cell type	Marker profile	Cell type	Marker profile
A+	CD11b high F4/80- CD11c+	A-	CD11b high F4/80- CD11c-
B+	CD11b int/high F4/80 low CD11c+	B-	CD11b int/high F4/80 low CD11c-
C+	CD11b low F4/80- CD11c+	C-	CD11b low F4/80- CD11c-

Figure 5.8: Proportions and numbers of myeloid cells in the inguinal lymph nodes. Cells from wild-type (WT) and CCX-CKR deficient (KO) ILNs were gated as in **Figure 3.14** and defined as in the table shown (bottom panel). Graphs show myeloid cells as both a proportion of total cells isolated from the ILNs (top panel) and as absolute numbers of cells isolated (middle panel). Error bars indicate standard deviation, n = 3. Data were analysed by unpaired t-tests, *p<0.02.

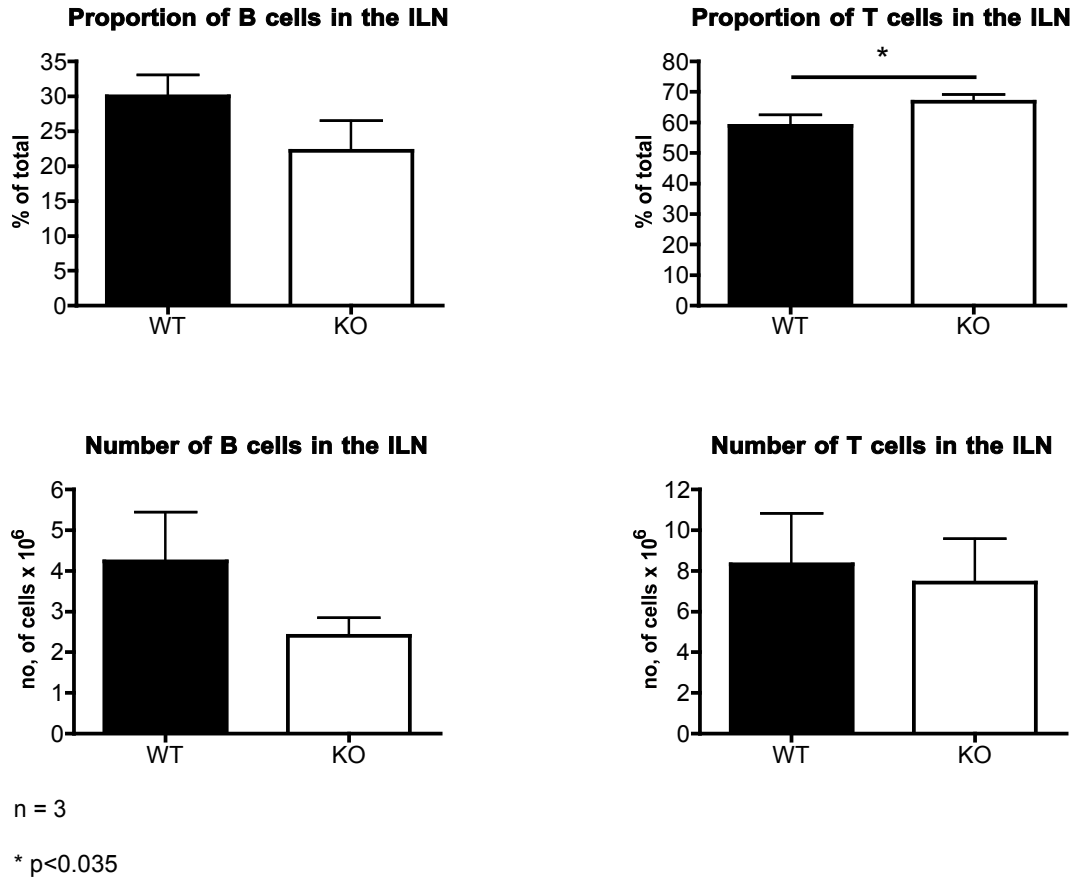


Figure 5.9: B and T cell cellularity in the inguinal lymph nodes. Cells from wild-type (WT) and CCX-CKR deficient (KO) ILNs were gated as in **Figure 3.13**. B cells are defined as CD19⁺ CD5^{low/-}. T cells are defined as CD5⁺ CD19⁻. Graphs show B and T cells as both a proportion of total cells isolated from the ILNs (top panels) and as absolute numbers of cells isolated. Error bars indicate standard deviation, n = 3. Data were analysed by unpaired t-tests, *p < 0.035.

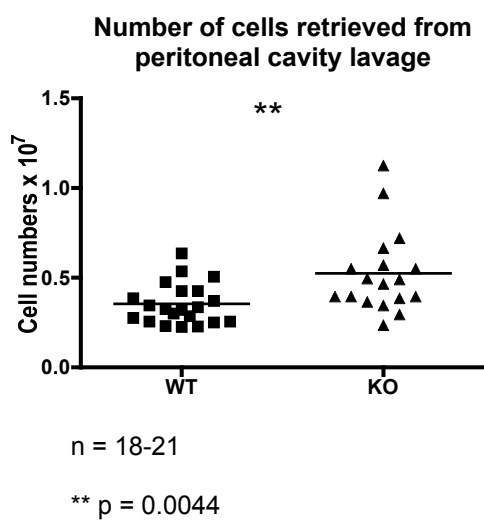


Figure 5.10: Total cell numbers retrieved from wild-type and CCX-CKR deficient peritoneal cavity lavage. Cells were isolated from wild-type (WT) and CCX-CKR deficient (KO) peritoneal cavity as described in Materials and Methods and counted using a haemocytometer. Data are pooled from numerous experiments, $n \geq 3$ per group per experiment, line represents the mean. Data were analysed using an unpaired t-test, ** $p=0.0044$.

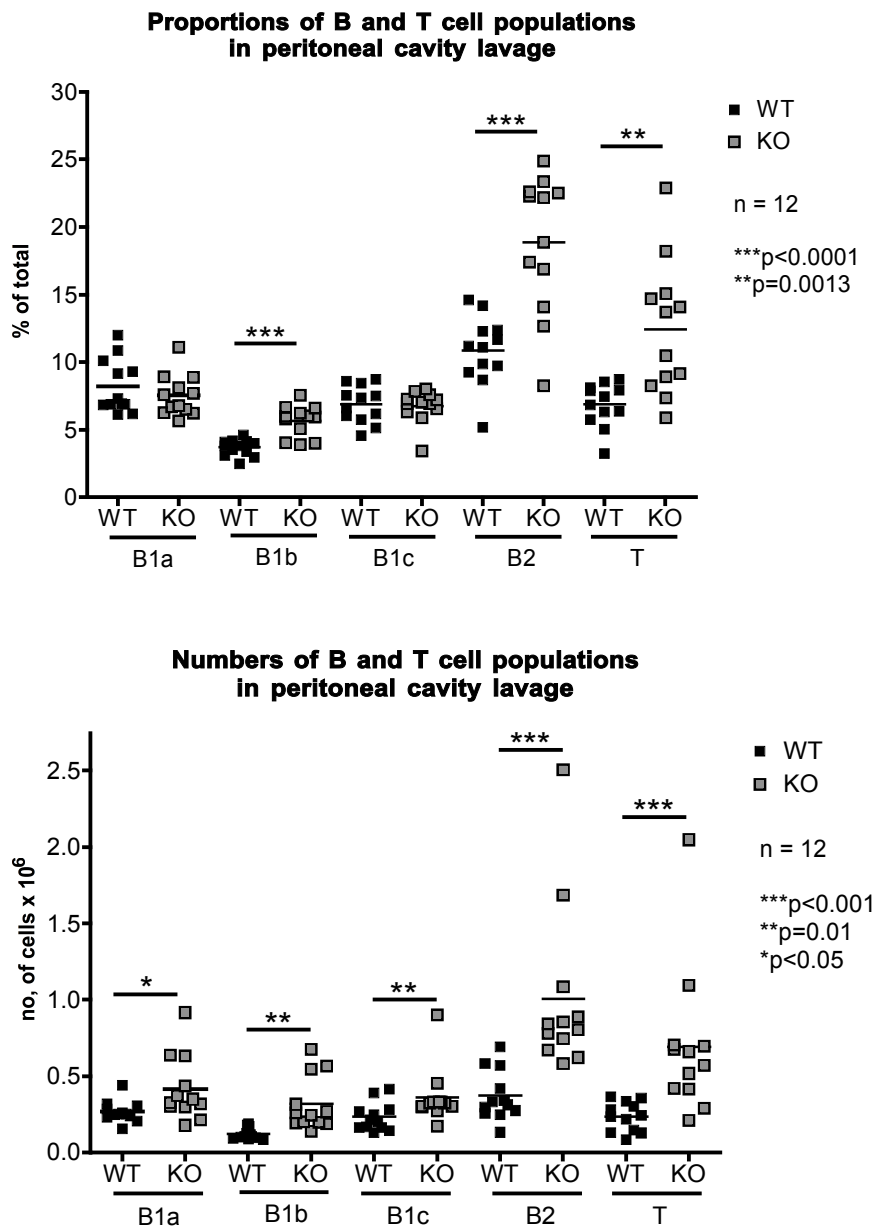


Figure 5.11: B and T cell cellularity in the peritoneal cavity. Cells from wild-type (WT) and CCX-CKR deficient (KO) peritoneal cavity were gated as in **Figure 3.17**. B1a cells are defined as CD19⁺ CD5^{low} CD11b⁺. B1b cells are defined as CD19⁺ CD5⁻ CD11b⁺. B1c cells are defined as CD19⁺ CD5^{low} CD11b⁻. B2 cells are defined as CD19⁺ CD5⁻ CD11b⁻. T cells are defined as CD5⁺ CD11b⁻ CD19⁻. Graphs show B1a, B1b, B1c, B2 and T cells as both a proportion of total cells isolated from the peritoneal cavity (top panels) and as absolute numbers of cells isolated. Error bars indicate standard deviation, n = 12, pooled from 4 separate experiments where n = 3 per experiment. Data were analysed by unpaired t-tests (top panel B1a, B1b, B2 and T populations; B1b population in bottom panel) or Mann-Whitney test (top panel, B1c population; bottom panel, B1a, B1c, B2 and T populations), based on results from D'Agostino and Pearson omnibus normality test, stars indicate p values as shown.

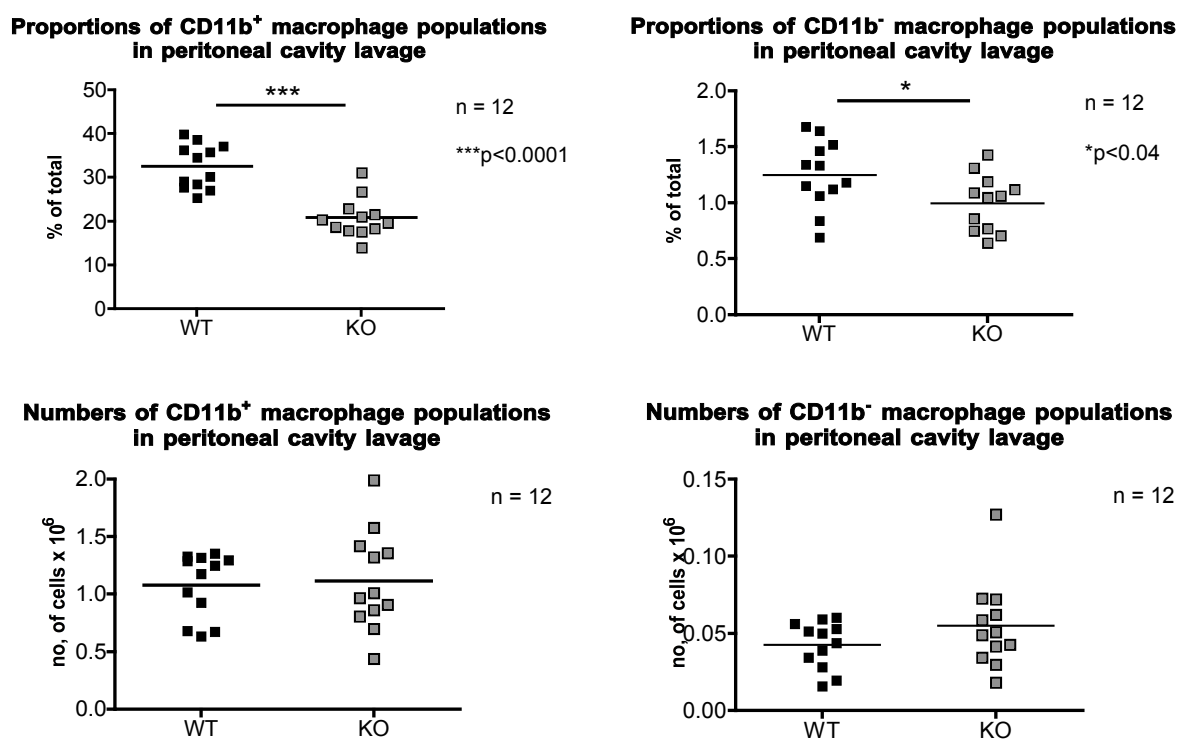


Figure 5.12: Macrophage cellularity in the peritoneal cavity. Cells from wild-type (WT) and CCX-CKR deficient (KO) peritoneal cavity were gated as in **Figure 3.17**. Graphs show myeloid cell subsets as both a proportion of total cells isolated from the peritoneal cavity (top panels) and as absolute numbers of cells isolated. . Error bars indicate standard deviation, n = 12, pooled from 4 separate experiments where n = 3 per experiment. Data were analysed by unpaired t-tests except bottom right panel, analysed by Mann-Whitney test.

6 Effect of CCX-CKR deletion on the inflammatory response

Previous chapters have shown that CCX-CKR mRNA can be detected in a range of tissues, although identifying the cells responsible for this expression has proven very difficult (see chapter 3). In addition, deletion of the receptor has been shown to affect expression of CCR7 mRNA in various tissues and lead to the dysregulation of chemokine protein levels (see chapter 4). Of particular interest are the skin-draining ILNs. CCX-CKR mRNA was readily detectable in both skin and ILNs of resting WT mice (see chapter 3). Expression of CCR7 and its ligands were affected by CCX-CKR deletion, and there was a small increase in cell number observed in CCX-CKR deficient ILNs. Data from Heinzel and colleagues also suggested that these lymph nodes might contain altered numbers of DCs (Heinzel et al., 2007), although this was not apparent in my analysis of mice housed in our animal facility. As described in the Introduction, CCR7 and its ligands are intimately linked to leukocyte homing to and within lymph nodes, under both resting and inflamed conditions. Upon induction of cutaneous inflammation in WT mice, DCs are driven from the skin in a CCR7-dependent fashion, and there are substantial increases in the size and cellularity of the ILNs through CCR7-dependent recruitment of lymphocytes from the blood and decreased lymphocyte departure through inhibition of S1P₁-mediated egress (see Introduction). In fact, DC migration from the periphery may directly influence lymph node size and cellularity (Martín-Fontecha et al., 2003).

Thus, it was hypothesised that, through its regulation of CCR7 and its ligands, the impact of CCX-CKR on lymph node cellularity may become more apparent during the induction of cutaneous inflammation. In addition, since DC migration into lymphatic vessels requires CCR7, it was possible that the cutaneous inflammatory response might be aberrant in the absence of CCX-CKR. Moreover, since inflammation can be used to drive the development of papillomas from mutagenised skin (Kinoshita and Gelboin, 1972), it was considered that CCX-CKR deletion might affect susceptibility to these tumours. The next series of experiments were designed to explore these possibilities. Throughout these experiments, we were also interested in examining how the expression of CCX-CKR was modulated.

A model of skin inflammation was chosen in which 12-O-tetradecanoylphorbol-13-acetate (TPA) is applied to shaved dorsal skin for three consecutive days, as described in Materials

and Methods and outlined in Figure 6.1 (Jamieson et al., 2005). Jamieson and colleagues showed that TPA-induced inflammation in WT skin is driven by production of inflammatory chemokines, which peaks at around 12 hours following a single application of the irritant. Using this protocol, chemokines are typically cleared by about 24 hours post-TPA application. Multiple applications of TPA (on 2 or 3 consecutive days) lead to increased and protracted production of inflammatory chemokines. Following triple application of TPA (i.e. on three consecutive days) the characteristic moderate infiltration of inflammatory cells to WT skin peaks around day 3 and subsides rapidly. By day 6 post-TPA application, skin appears histologically normal in WT animals (Jamieson et al., 2005). In the absence of the atypical chemokine receptor D6, TPA-induced inflammation is protracted and exaggerated, and D6-deficient mice show increased susceptibility to papilloma formation (Jamieson et al., 2005, Nibbs et al., 2007). Additionally, work by a previous student in our lab showed that this protocol led to epidermal thickening by day 3 post-TPA application in female WT C57BL/6 mice, which had begun to resolve by day 5 and had fully resolved by day 7 post-TPA (Comerford, 2005). This work also showed that WT ILNs were enlarged at day 3 and day 5 post-TPA application, but had returned to near normal size and cellularity by day 7 (Comerford, 2005). Therefore, day 3 post-TPA application was chosen to represent the peak of skin inflammation in WT mice and day 6 post-TPA application was chosen to represent the point of resolution of skin inflammation in these animals. It was hypothesised that these timepoints would allow distinction of any lag in either development or resolution of skin inflammation in CCX-CKR deficient mice compared to WT, and would allow any differences in ILN cellularity to be defined. In parallel, expression of CCX-CKR and related genes was investigated at the site of inflammation (i.e. the dorsal skin) and in the draining ILNs at the mRNA level. In collaboration with Dr Clarke in the Nibbs group, we also explored CCX-CKR expression in TPA-promoted skin tumours, and the impact of CCX-CKR deletion on the development of these tumours. CCR7 has been linked to tumour formation, lymph node metastasis and cancer progression in a number of studies (Fang et al., 2008, Wang et al., 2005a, Zlotnik, 2006).

6.1 CCX-CKR in a model of cutaneous inflammation

6.1.1 Histology of wild-type and CCX-CKR deficient inflamed skin

WT and CCX-CKR deficient animals were shaved and treated dorsally with TPA as per Figure 6.1. Paraffin-embedded skin sections were stained with haematoxylin and eosin as described in Materials and Methods to allow visualisation of skin architecture (Figure 6.2).

No obvious structural differences were observed between WT and CCX-CKR deficient skin under resting (i.e. skin untreated after shaving) or inflamed conditions or at the resolution of inflammation. Epidermal thickness was measured in these sections as an indicator of the proliferative status of the epidermis and the level of inflammatory infiltrate into the skin. In resting skin, as well as at day 3 and day 6 post-TPA application, there were no significant differences in epidermal thickness observed between WT and CCX-CKR deficient samples (Figure 6.2). At day 3, the skin of both WT and CCX-CKR deficient mice was clearly inflamed, with a significant increase in epidermal thickness in both strains. By day 6, both WT and CCX-CKR deficient skin had resolved and was similar to untreated controls, indicating that CCX-CKR deletion was not associated with a protracted period of inflammation.

6.1.2 Expression of CCX-CKR and related receptors in inflamed skin

Samples of treated and resting skin were isolated into RNALater and processed to isolate RNA for cDNA synthesis, as described in Materials and Methods. CCX-CKR mRNA expression was assessed by QPCR, with no dramatic or statistically significant changes found over the course of the inflammatory model (Figure 6.3). It should be noted that, in the first experiment, statistical comparison of resting levels of expression compared to inflamed or resolving skin was not possible as the resting group only contained 2 individuals. In the second experiment, statistical analysis was possible but increased variation between samples compared to the first experiment weakened the statistical power of the analysis. Therefore, while there may be a non-significant trend towards reduced expression of CCX-CKR in inflamed skin compared to non-inflamed, further analysis with increased sample sizes would be required to clarify this.

Expression of CCR7 and CCR9 mRNA was also assessed to determine the impact of CCX-CKR deletion on these receptors in resting and inflamed skin during a cutaneous inflammatory response. Both receptors were detectable at low levels, as before (see chapter 4), and although sample size was low, no significant effect of CCX-CKR deletion on the expression of these receptors was observed (Figure 6.4). CCR7 expression was unchanged over time and CCR9 expression likewise showed no significant changes throughout the model.

These data demonstrate that the induction and resolution of TPA-induced cutaneous inflammation in the skin is not substantially affected by CCX-CKR deletion, although

increased group sizes would be desirable in a repetition of this model, to allow detection of potential minor changes masked by sample variability.

6.1.3 No impact of CCX-CKR deletion on the draining lymph node cellularity during skin inflammation

CCX-CKR mRNA is present in ILNs (chapter 3, Figure 3.2), and previous chapters have shown that deletion of CCX-CKR alters chemokine and chemokine receptor expression in resting ILNs. It was hypothesised that deletion of CCX-CKR might disrupt the migration of cells to and/or from the tissue and therefore impact the cellularity of the draining lymph nodes. It was also theorised that CCX-CKR-deficient ILNs might exhibit altered chemokine receptor expression compared to WT, as is found in resting ILNs.

Cellularity data for resting ILN has already been presented (chapter 5), with a slight increase in cellularity of CCX-CKR deficient ILNs compared to WT. In contrast to resting mice, no significant difference in the total number of cells retrieved was observed between WT and CCX-CKR deficient tissues (Figure 6.5). However, the numbers of cells retrieved were approximately three-fold higher than those retrieved from resting WT ILNs (see chapter 5, Figure 5.7), at both day 3 and day 6.

ILNs from resting and treated mice were processed for QPCR as described in Materials and Methods. CCX-CKR mRNA expression was reduced in the inflamed WT ILN relative to resting ILNs, and appeared to be returning to resting levels by day 6 post-TPA application, with expression at this time point not found to be significantly different from expression seen in either resting or inflamed ILNs (Figure 6.6). The level of expression at day 3 post-TPA treatment is approximately half that of resting ILNs. In light of the three-fold increase in cellularity (see above), it is possible that this is masking an increase in the absolute quantity of CCX-CKR mRNA being produced in the inflamed ILN. If the cells entering do not express CCX-CKR they will dilute the relative quantity of CCX-CKR mRNA in the tissue, and in the absence of increased CCX-CKR expression the level of “dilution” seen should match the increase in cellularity observed. As this is not the case, it is likely that either cells resident in the ILN increase their expression of CCX-CKR mRNA or that cells entering the ILN are expressing the receptor, or both. Absolute quantification could be used to confirm this hypothesis, preferably using both whole tissue and purified cell populations. CCR7 and CCR9 mRNA abundance was also analysed in these tissues. CCR7 mRNA expression in the ILN was not significantly altered in this experiment (Figure 6.7, top panel), either by induction of inflammation or by deletion of CCX-CKR.

Previous experiments showed a significant decrease in CCR7 mRNA expression in resting CCX-CKR deficient ILNs compared to WT (see chapter 4, Figure 4.1). Variation within the small number of resting CCX-CKR deficient ILN samples in this experiment may have been responsible for the lack of statistically significant difference observed in this instance. CCR9 mRNA was present at the same level in WT and CCX-CKR deficient ILNs throughout this model (Figure 6.7, bottom panel). However, there was a significantly lower amount of CCR9 mRNA present in both WT and CCX-CKR deficient ILNs at day 3 post-TPA application compared to resting control samples (Figure 6.7, bottom panel). There was also significantly lower expression of CCR9 in CCX-CKR deficient samples at day 6 post-TPA treatment compared to resting control CCX-CKR deficient samples, a difference not seen between equivalent WT samples.

6.1.3.1 Lymphocytes in the draining lymph node of CCX-CKR deficient mice

Single cell suspensions from ILNs of treated animals (i.e. at day 3 and day 6) were stained with lineage markers and analysed by flow cytometry, as described in Materials and Methods. The proportion of B and T cells remained constant between WT and CCX-CKR deficient lymph nodes at both day 3 post-TPA and day 6 post-TPA (Figure 6.8, top panels). There was also no difference in absolute numbers of B or T cells retrieved (Figure 6.8, bottom panels). The proportion of B cells increased in inflamed ILNs compared to resting tissue, from about 30% of total cells in resting WT ILNs to approximately 45% at day 3 post-TPA application. The total number of B cells was approximately three-fold higher in inflamed ILNs compared to resting numbers (see chapter 5, Figure 5.9, and Figure 6.8). Concurrently, the proportion of T cells dropped from approximately 60% of total cells in the resting WT ILNs to about 50% in the inflamed ILN, although absolute numbers were almost doubled in the inflamed ILN compared to resting. By day 6, the proportional difference between B and T cells in the ILN was returning, with T cells comprising just over 50% of the total cellularity, and B cells comprising just over 40% (see chapter 5, Figure 5.9, and Figure 6.8). As shown in Figure 6.9, T and B cells did not display any CCX-CKR dependent internalisation of fluorescent CCL19 tetramers, nor did the level of CCR7 activity appear to be affected by cutaneous inflammation, with levels of internalisation remaining comparable to cells from resting ILNs. These data, together with the cellularity data above, indicate that CCX-CKR deletion does not affect the cellularity, or CCR7 expression and “activity”, of skin-draining ILNs during cutaneous inflammation.

6.1.3.2 Myeloid cells in the draining lymph node of CCX-CKR deficient mice

Internalisation experiments detailed in chapter 3 indicated that CCX-CKR is expressed by some myeloid subsets in WT ILNs, specifically CD11b^{high} F4/80^{neg} CD11c⁺ cells and CD11b^{int/high} F4/80^{low} CD11c⁺ cells, although CCX-CKR deletion had no significant impact on their abundance (see chapter 3, Figure 3.14). In addition, as mentioned previously, chemokine and receptor expression is altered in resting CCX-CKR deficient ILN compared to WT. Therefore, it was hypothesised that migration of myeloid cells to the ILN, and/or their internalisation of chemokine would be altered by the absence of CCX-CKR during inflammation. Supporting this hypothesis, analysis of myeloid cell subsets revealed a number of defects in cellularity in the absence of CCX-CKR. CD11b^{high} F4/80^{neg} cells, both CD11c⁺ and CD11c⁻, were proportionally increased in the CCX-CKR deficient ILN compared to WT at day 3 post-TPA application (Figure 6.10, top left). CD11c^{int/high} F4/80^{low} CD11c⁻ cells also constituted a significantly increased proportion of total cells at this timepoint, while CD11b^{low} F4/80^{neg} CD11c⁺ were significantly decreased in the knock-out (Figure 6.10, top left). There were, however, no differences in absolute numbers of these cells at this timepoint (Figure 6.10, bottom left). The reason for this disparity is unclear. Some of the populations that showed a difference in proportion, including CD11b^{high} F4/80^{neg} CD11c⁺ cells, CD11b^{high} F4/80^{neg} CD11c⁻ cells and CD11b^{int/high} F4/80^{low} CD11c⁻ cells showed a trend towards a similar difference in absolute number, so it is possible that increased replicates would bring these potential differences to statistical significance.

At day 6 post-TPA application, the differences in myeloid cell populations between WT and CCX-CKR deficient ILNs became more apparent. At this time point, CD11b^{high} F4/80^{neg} CD11c⁺ cells were still significantly increased in proportion, as were CD11b^{int/high} F4/80^{low} CD11c⁻ cells (Figure 6.10, top right), but notably, both of these populations were present in significantly elevated absolute numbers as well (Figure 6.10, bottom right). Specifically, there were nearly three-fold more CD11b^{high} F4/80^{neg} CD11c⁺ cells in the CCX-CKR deficient ILNs compared with WT, and CD11b^{int/high} F4/80^{low} CD11c⁻ cells were increased about two-fold. CD11b^{low} F4/80^{neg} CD11c⁺ cells were also proportionally increased and CD11b^{low} F4/80^{neg} CD11c⁻ cells were decreased (Figure 6.10, top right), although neither was significantly altered in terms of absolute numbers at day 6 post-TPA application (Figure 6.10, bottom right).

In light of these subtle, but intriguing, effects observed in myeloid cellularity in the absence of CCX-CKR, as well as the CCX-CKR mediated internalisation observed in

resting ILN cells, we were eager to assess the ability of myeloid ILN cells to internalise fluorescent CCL19 tetramers during inflammation in the absence of CCX-CKR. At day 3 post TPA application, there was a significant decrease in fluorescent CCL19 tetramer internalisation by CCX-CKR deficient $CD11b^{high} F4/80^{neg} CD11c^{+}$ cells and $CD11b^{int/high} F4/80^{low} CD11c^{+}$ cells when compared with WT counterparts (Figure 6.11b, left panel). These are the same cell types that displayed significantly reduced internalisation of fluorescent CCL19 tetramers under resting conditions (see chapter 3, Figure 3.14), suggesting these cells may express CCX-CKR both under resting conditions and during cutaneous inflammation. It is also interesting to note that, compared to WT, one of these cell types, $CD11b^{high} F4/80^{neg} CD11c^{+}$, was consistently over-represented in the CCX-CKR deficient ILN draining TPA-inflamed skin (Figure 6.10). All other myeloid cells showed no significant difference in internalisation of fluorescent CCL19 at day 3 post-TPA application and at day 6 post-TPA application there was no observed impact of CCX-CKR deletion on the ability of myeloid cells to internalise fluorescent CCL19 tetramers in the draining lymph node (Figure 6.11b, right panel).

Collectively, these data indicate a role for CCX-CKR in regulating the abundance of certain populations of myeloid cells in the ILN during inflammation, as well as suggesting that these cells are a site of expression of CCX-CKR in the inflamed WT ILN. A further in depth discussion of these findings can be found in chapter 7.

6.2 CCX-CKR in a model of tumour formation

The tumorigenesis model described at the beginning of this chapter (and in detail in Materials and Methods) explores the impact of chronic inflammation in promoting skin papilloma formation. C57Bl6 mice, which are used in all other experiments throughout this thesis, are highly resistant to papilloma formation, making them unsuitable for this type of study. Instead, WT and CCX-CKR deficient mice backcrossed onto an FVB background for 6 generations were used in this study. As noted above, CCR7 has been implicated in tumour development and lymph node metastasis. Taking into account the effect of CCX-CKR on ILN cellularity and its expression in both skin and ILNs, it was hypothesised that CCX-CKR might alter the development of papillomas and metastasis to LNs. This model, which involved a single topical application of the carcinogen DMBA, followed by a twice-weekly schedule of TPA application for up to 26 weeks, was optimised from a widely used protocol (Stenbäck, 1978). A fuller description of the protocol can be found in Materials and Methods. The protocol was established in our lab by one of the post-doctoral researchers (Dr. Mairi Clarke) who carried out the protocol on my behalf, with assistance

from me. Interestingly, as shown in Figure 6.12, CCX-CKR deletion was associated with a significant reduction in the average number of papillomas that form on the dorsal skin of treated animals. The papillomas that form on WT animals showed reduced expression of CCX-CKR mRNA, relative to unaffected adjacent skin, but increased expression of CCR7 mRNA (Figure 6.13 and Figure 6.14). This increase in CCR7 expression was also seen in CCX-CKR deficient papillomas. Notably, CCX-CKR deletion also had a significant effect on the size of ILNs draining the DMBA/TPA-induced papillomas (Figure 6.15), such that they were approximately two-fold larger in WT mice than CCX-CKR deficient mice by the end of the protocol.

Unfortunately, time constraints meant it was not possible to undertake further experiments. Clearly, a more detailed analysis is required to clarify the precise nature of the skin and ILN phenotypes apparent in this model, and to dissect the mechanisms responsible. Nonetheless, the existing data do suggest that CCX-CKR plays a role in enhancing skin tumour formation, and may enhance the ability of cells from these tumours to metastasise to local draining lymph nodes.

6.3 Summary

Previous chapters have shown that, in resting mice, CCX-CKR deletion produces a number of subtle but significant changes in chemokine levels, chemokine receptor expression and activity, and cellularity in various tissues. In particular, the ILN is altered in terms of chemokine and chemokine expression and activity. In this chapter, I tested the hypothesis that CCX-CKR plays a role in the response to cutaneous inflammation induced by TPA, as well as in the development and progression of DMBA/TPA-induced papilloma formation. The results of this work are summarised below:

1. CCX-CKR mRNA expression in the skin was not altered during TPA-induced inflammation. However, it was significantly reduced in ILN at day 3 post-TPA treatment. Epidermal thickening in response to TPA was unaffected by CCX-CKR deletion.
2. CCR7 and CCR9 mRNA expression in skin was not significantly altered either by CCX-CKR deletion or by induction of inflammation. CCR7 expression in the ILN was unchanged throughout the induced inflammatory response. CCR9 was reduced at day 3 post-TPA compared to resting controls, in both CCX-CKR deficient and WT ILN, and remained reduced at day 6 post-TPA treatment

compared to resting controls in CCX-CKR deficient samples, but not in equivalent WT samples.

3. Total numbers of cells retrieved from ILNs, and the lymphocyte populations within these organs, were unaffected by CCX-CKR deletion.
4. Proportions of several myeloid cell subsets were altered between WT and CCX-CKR deficient ILNs at both day 3 and day 6 post-TPA treatment. More significantly, compared to WT, the absolute numbers of CD11b^{high} F4/80⁻ CD11c⁺ and CD11b^{int/high} F4/80^{low} CD11c⁻ cells were substantially increased in CCX-CKR deficient ILNs at day 6 post-TPA treatment.
5. As observed for resting mice, internalisation of fluorescent CCL19 tetramers by CD11b^{high} F4/80⁻ CD11c⁺ cells and CD11b^{int/high} F4/80^{low} CD11c⁺ cells was reduced in CCX-CKR deficient samples compared to WT at day 3 post-TPA application.
6. In a model of inflammation-driven tumorigenesis, CCX-CKR deletion was associated with a reduction in papilloma susceptibility, and a marked reduction in the size of ILNs draining tumour-bearing skin. WT papillomas had less CCX-CKR mRNA than normal adjacent skin. In both WT and CCX-CKR deficient samples, CCR7 expression was increased in papillomas compared to normal adjacent skin.

Although further studies are required, these data indicate that CCX-CKR (i) regulates myeloid subsets in LNs during TPA-induced cutaneous inflammation, (ii) enhances inflammation-driven papilloma formation, and (iii) may promote metastasis of skin tumour cells to draining ILNs. The implications of these results, along with data from previous chapters, are discussed in depth in Chapter 7.

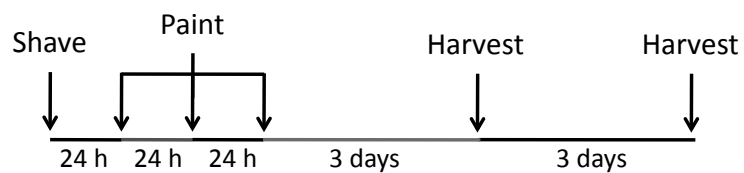


Figure 6.1: Induction of skin inflammation. Mice were shaved dorsally 24 hours prior to initial application of 150 μ l of 50 μ M TPA. This application ("Paint") was repeated at 24 hour intervals for a total of three applications. Mice were sacrificed and tissues harvested at day 3 and day 6 after the final application.

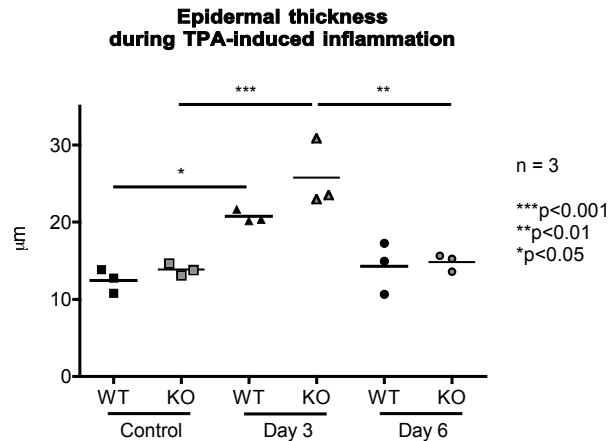
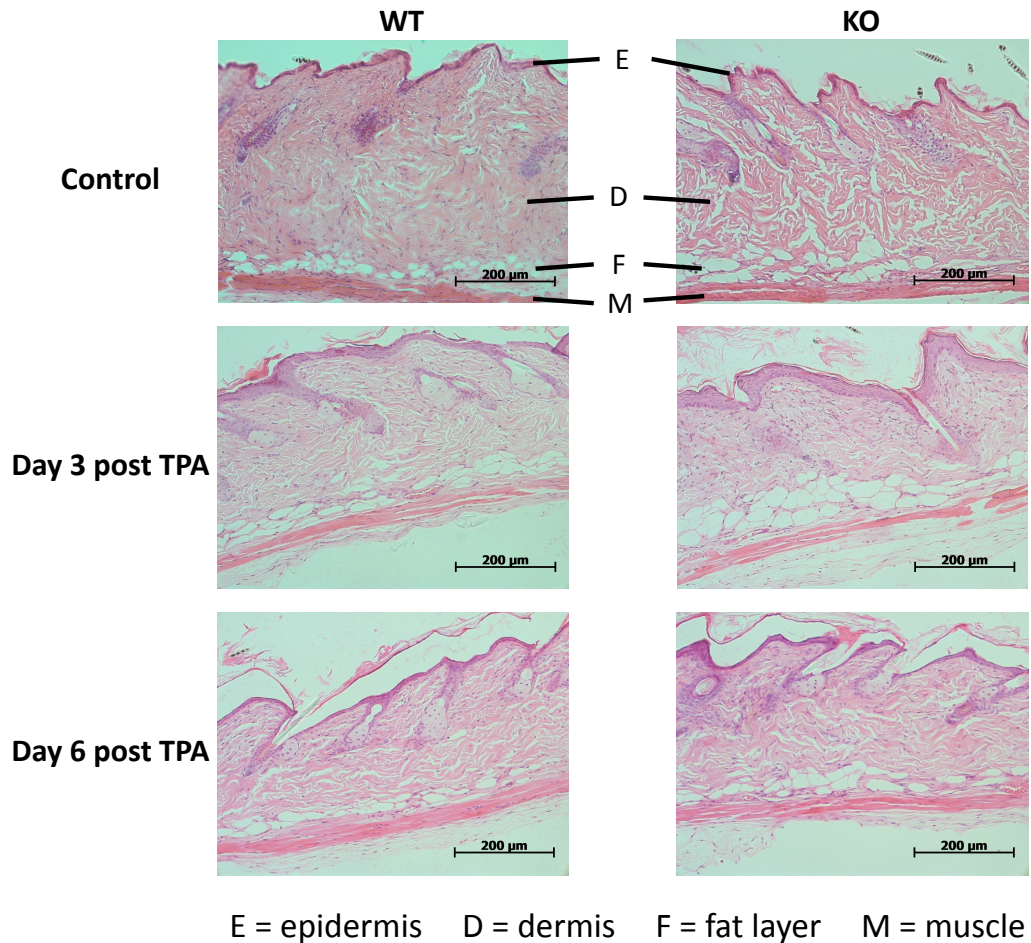


Figure 6.2: Epidermal thickness of wild-type and CCX-CKR deficient skin during TPA-induced inflammation. Wild-type (WT) and CCX-CKR deficient (KO) mice were shaved dorsally and TPA applied to the skin as described in Materials and Methods (see **Figure 6.1**), with skin removed to formalin at harvest. Skin samples were then embedded in paraffin wax and H&E stained as described in Materials and Methods. Images were taken with a 20x objective using an Axiostar plus microscope and Axiovision software. Epidermal thickness was determined by taking 5 random measurements of epidermis (E) in a single field of view per sample and plotting the average of each sample on the graph shown. Lines represent the mean, n = 3. Data were analysed using 2-way ANOVA with Bonferroni post-test, ***p<0.001, **p<0.01, *p<0.05.

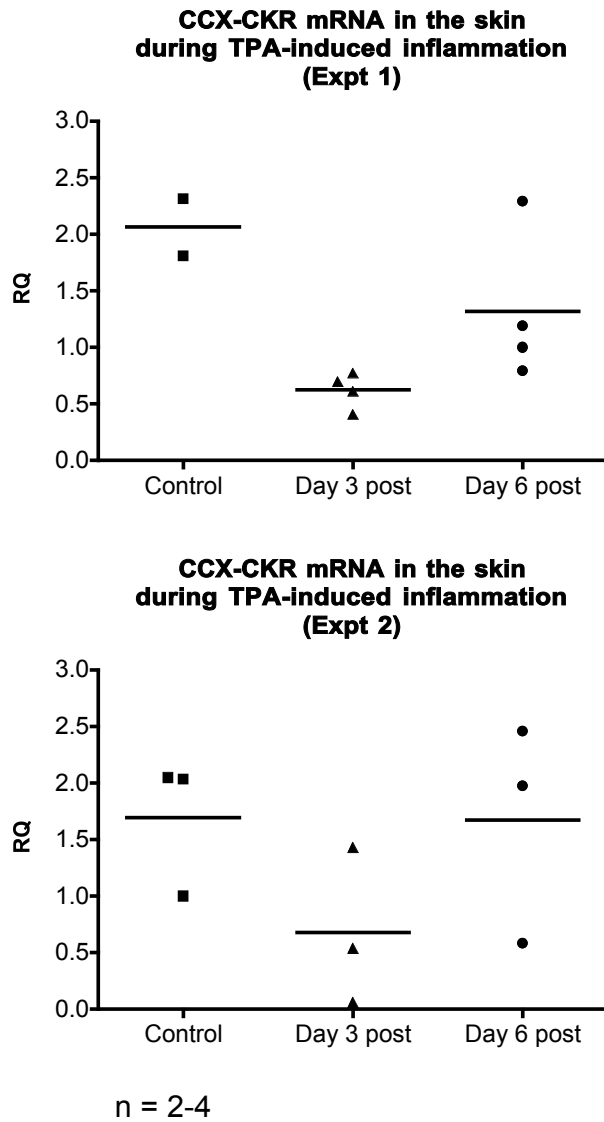


Figure 6.3: Expression of CCX-CKR in the skin during TPA-induced inflammation. Mice were shaved dorsally and TPA applied to the skin as described in Materials and Methods. mRNA was extracted from the skin of resting control mice (“Control”), mice at day 3 after the final application (“Day 3 post”) and mice at day 6 after the final application (“Day 6 post”). This was used to generate cDNA and analysed by QPCR. Graphs represent data from two separate experiments, where n = 2-4 per group. Lines represent the mean RQ (relative quantity). Data were analysed by one-way ANOVA with Bonferroni post-test with no significant differences observed.

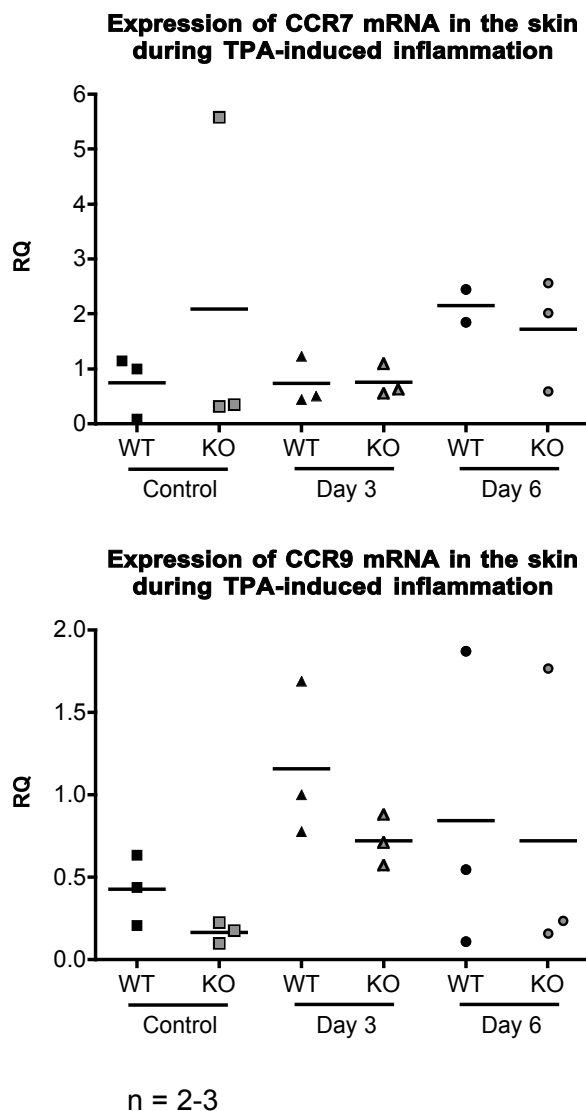


Figure 6.4: Expression of CCR7 and CCR9 in the skin during TPA-induced inflammation. Wild-type (WT) and CCX-CKR deficient (KO) mice were shaved dorsally and TPA applied to the skin as described in Materials and Methods. mRNA was extracted from the skin of resting control mice ("Control"), mice at day 3 after the final application ("Day 3") and mice at day 6 after the final application ("Day 6"). This was used to generate cDNA and analysed by QPCR. Graphs represent data from individual experiments where n = 2-3 per group. Lines represent the mean RQ (relative quantity). Data were analysed by 2-way ANOVA with Bonferroni post-test, with no significant differences observed.

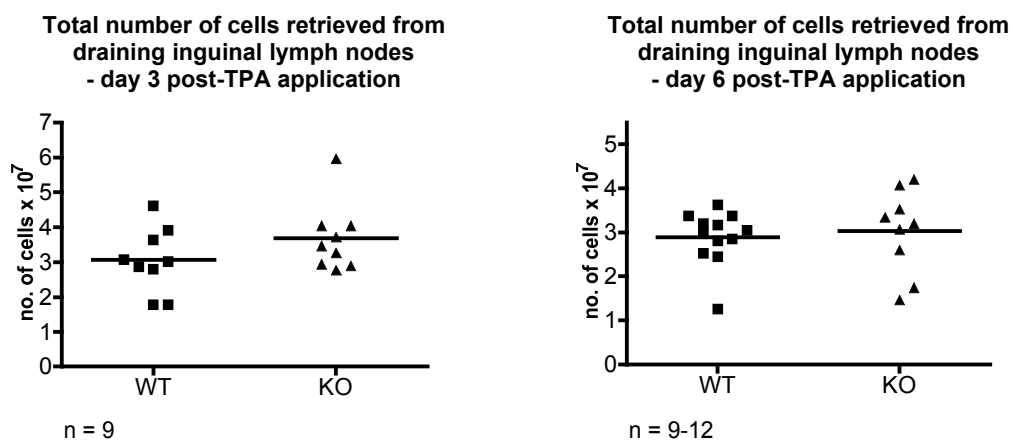


Figure 6.5: Total numbers retrieved from wild-type and CCX-CKR deficient draining inguinal lymph nodes during a model of skin inflammation. Wild-type (WT) and CCX-CKR deficient (KO) mice were shaved dorsally and TPA applied over 3 consecutive days as described in Materials and Methods. Draining ILNs were harvested at day 3 or day 6 post-TPA application. Cells were isolated and counted using a haemocytometer before use in internalisation or cellularity assays. Line represents the mean, n = 9-12, data were analysed by unpaired t-tests with no significant differences observed.

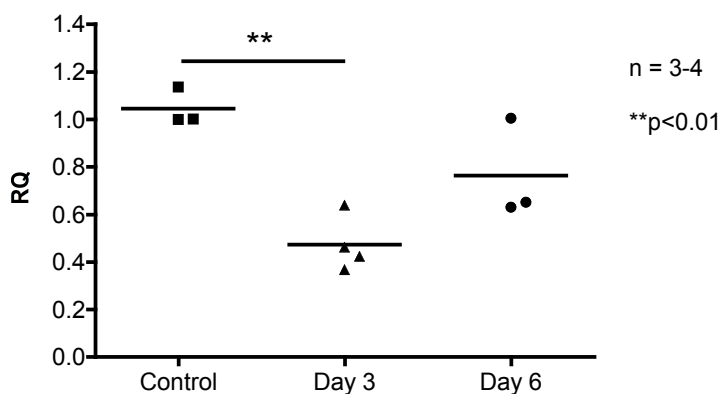
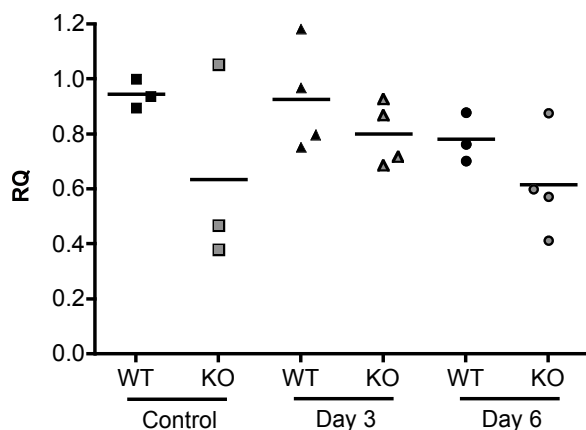
Expression of CCX-CKR mRNA in the inguinal lymph nodes during TPA-induced inflammation

Figure 6.6: Expression of CCX-CKR in the inguinal lymph node during TPA-induced inflammation. Mice were shaved dorsally and TPA applied to the skin as described in Materials and Methods. mRNA was extracted from the ILNs of resting control mice ("Control"), mice at day 3 after the final application ("Day 3") and mice at day 6 after the final application ("Day 6"). This was used to generate cDNA and analysed by QPCR. Data are representative of two separate experiments, n = 3-4 per group. Lines represent the mean RQ (relative quantity). Data were analysed by one-way ANOVA with Bonferroni post-test, **p<0.01.

Expression of CCR7 mRNA in the inguinal lymph nodes during TPA-induced inflammation



Expression of CCR9 mRNA in the inguinal lymph nodes during TPA-induced inflammation

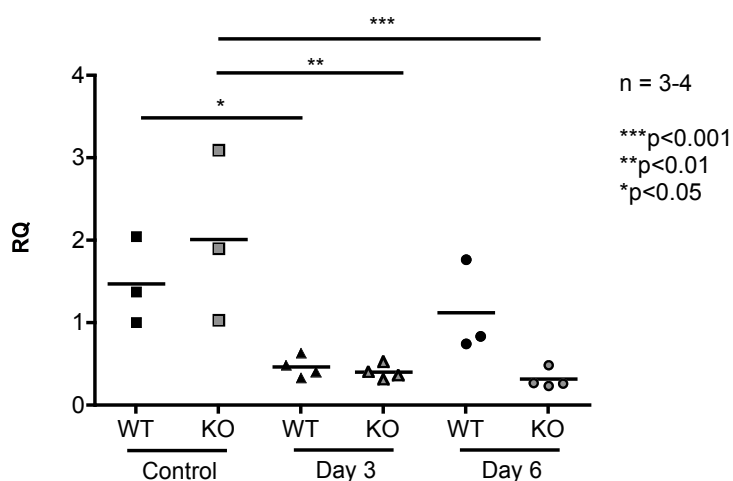


Figure 6.7: Expression of CCR7 and CCR9 in the draining inguinal lymph node during TPA-induced inflammation. Wild-type (WT) and CCX-CKR deficient (KO) mice were shaved dorsally and TPA applied to the skin as described in Materials and Methods. mRNA was extracted from the ILNs of resting control mice ("Control"), mice at day 3 after the final application ("Day 3") and mice at day 6 after the final application ("Day 6"). This was used to generate cDNA and analysed by QPCR. Graphs represent data from individual experiments where n = 3-4 per group. Lines represent the mean RQ (relative quantity). Data were analysed by 2-way ANOVA with Bonferroni post-test, ***p<0.001, **p<0.01, *p<0.05.

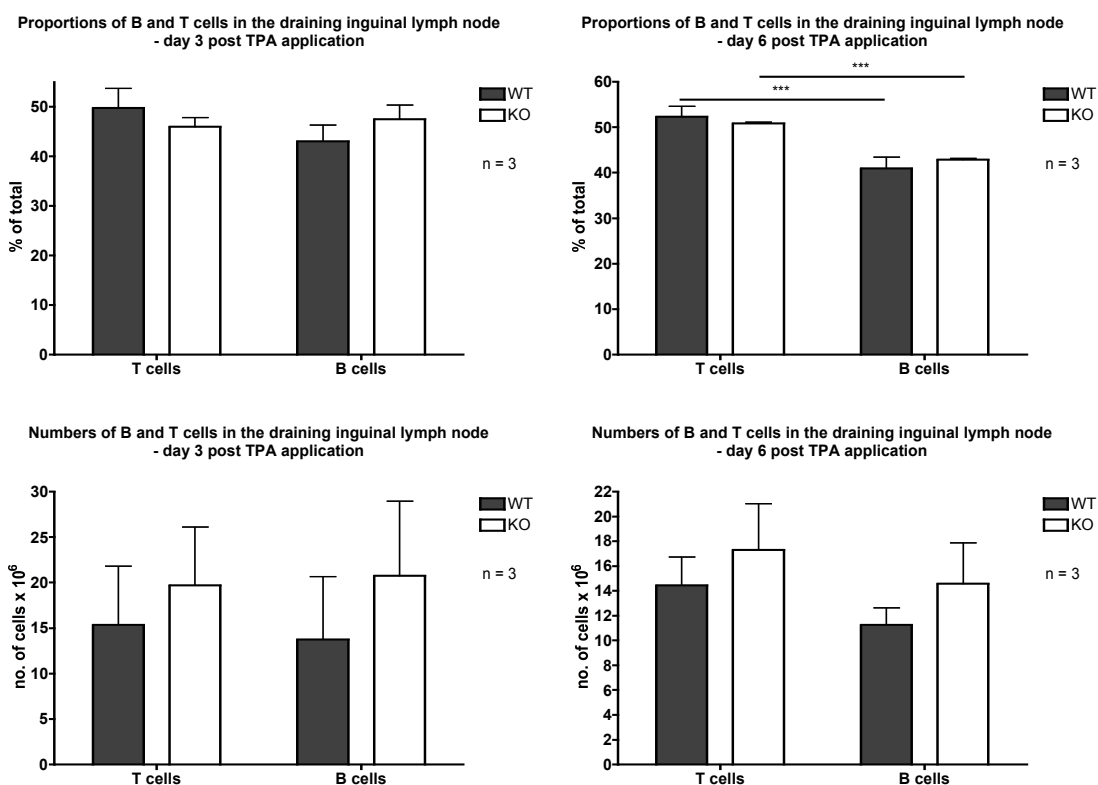


Figure 6.8: Proportions and numbers of B and T cells in the draining inguinal lymph node during a model of skin inflammation. Wild-type (WT) and CCX-CKR deficient (KO) mice were shaved dorsally and TPA applied over 3 consecutive days as described in Materials and Methods. Draining ILNs were harvested at day 3 or day 6 post-TPA application. Cell isolates were stained at 4°C with antibodies against lineage markers. Cells were defined as B or T cells based on anti-CD3 and anti-CD19 staining as shown in **Figure 6.9A**. Graphs show T and B cells as both a proportion of total cells isolated from the draining ILN (top panels) and as absolute numbers of cells isolated, at day 3 (left) and day 6 (right) post-TPA application. Error bars indicate standard deviation, n = 3. Data were analysed by 2-way ANOVA with Bonferroni post-test, ***p<0.001.

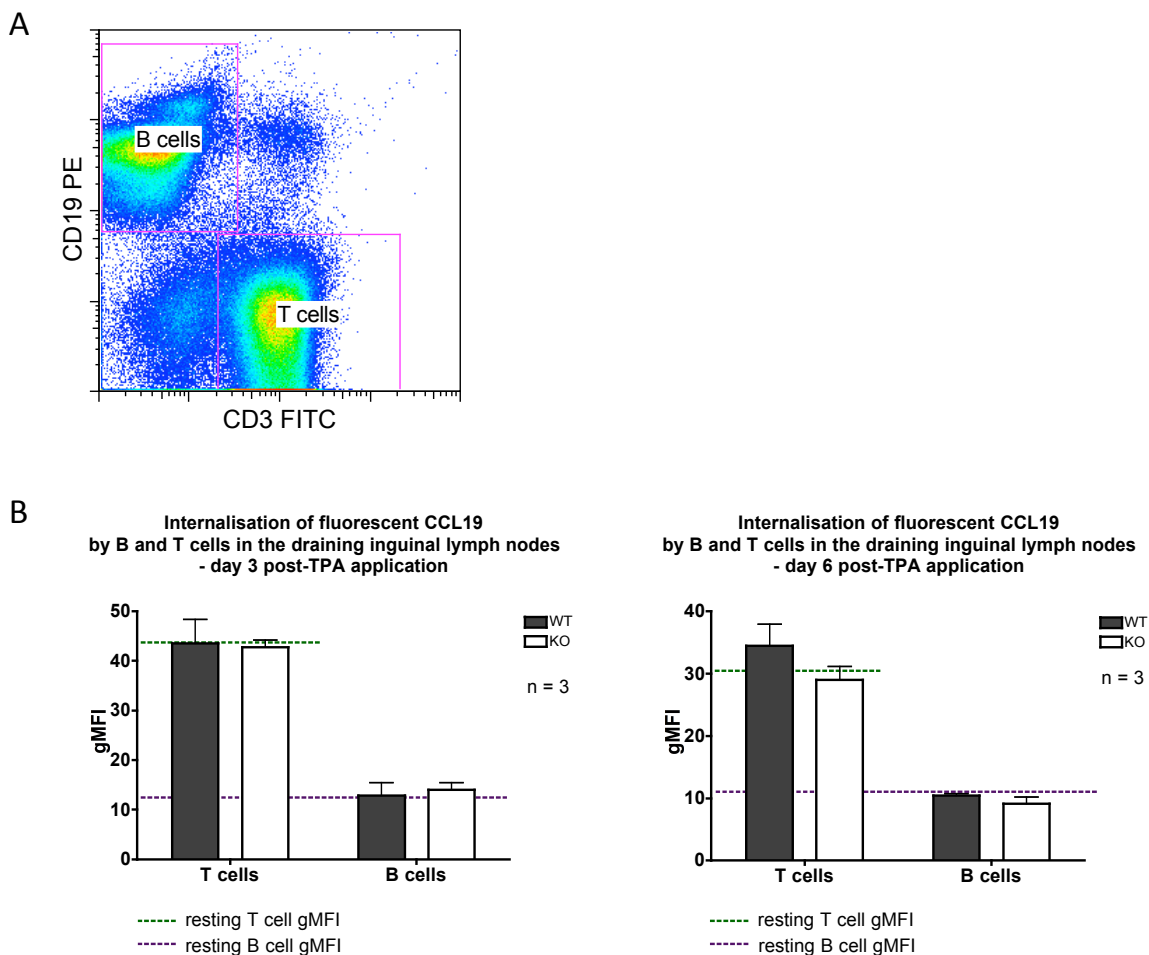


Figure 6.9: Internalisation of CCL19 by wild-type and CCX-CKR deficient T and B cells in the draining lymph node in a model of skin inflammation. Wild-type (WT) and CCX-CKR deficient (KO) mice were shaved dorsally and TPA applied over 3 consecutive days as described in Materials and Methods. Draining ILNs were harvested at day 3 or day 6 post-TPA application. Cell isolates were incubated at 37°C with fluorescent CCL19 tetramers followed by staining at 4°C with antibodies against lineage markers. (A) Cells were defined as B or T cells based on anti-CD3 and anti-CD19 staining as shown. (B) Graphs show gMFI (geometric fluorescence intensity) values for fluorescent CCL19 in WT and KO lymphocytes at day 3 (left panel) and day 6 (right panel), which were analysed in separate experiments. Bars indicate standard deviation, n = 3. Dashed lines indicate average gMFI for combined WT and KO resting samples (n = 1) that were included in each experiment as a control. Green dashed line indicates resting T cell gMFI, purple dashed line indicates resting B cell gMFI. Data are representative of two separate experiments for each timepoint.

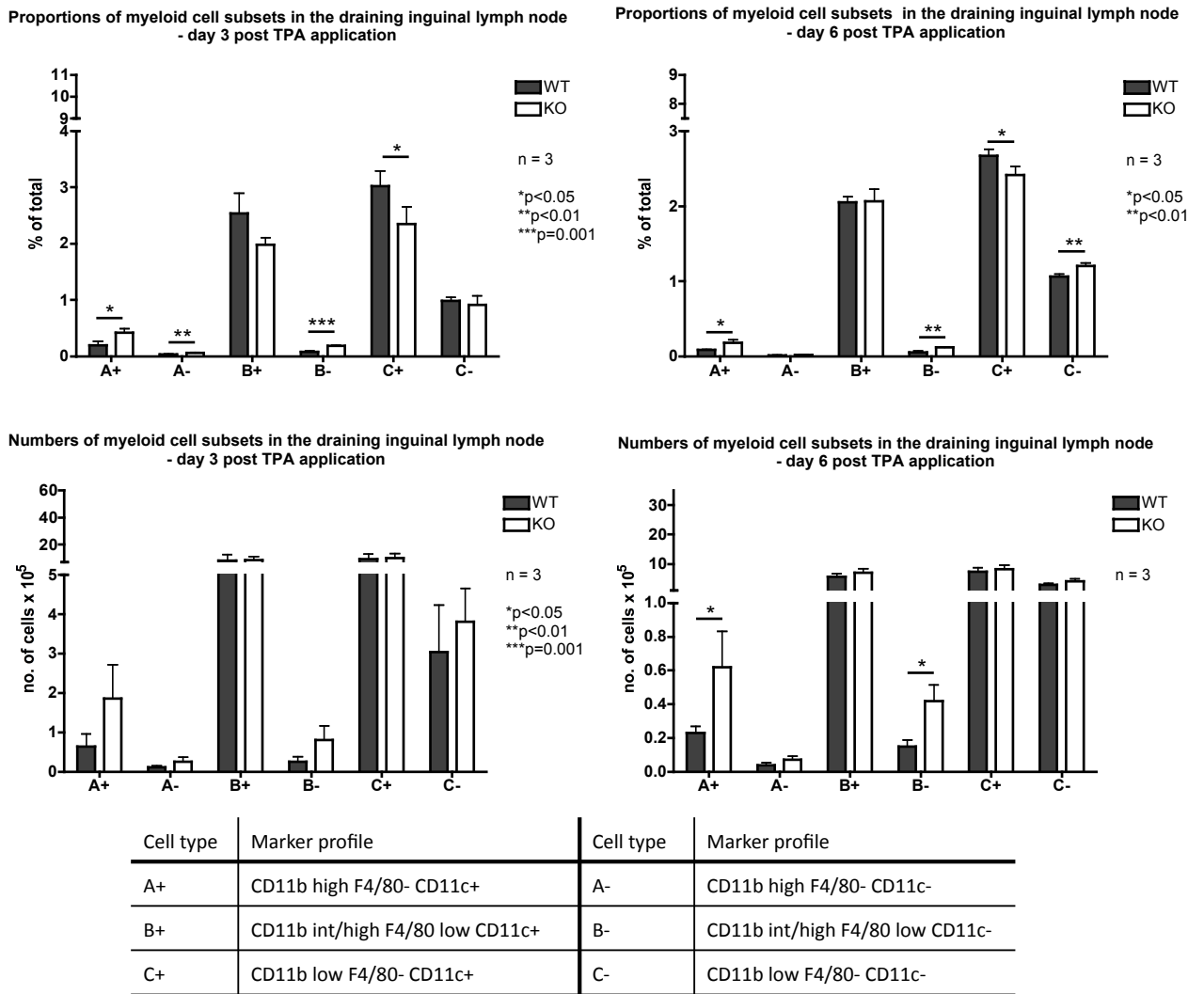


Figure 6.10: Proportions and numbers of myeloid cell subsets in the draining inguinal lymph node during a model of skin inflammation. Wild-type (WT) and CCX-CKR deficient (KO) mice were shaved dorsally and TPA applied over 3 consecutive days as described in Materials and Methods. Draining ILNs were harvested at day 3 or day 6 post-TPA application. Cell isolates were stained at 4°C with antibodies against lineage markers. Cells were defined as shown in **Figure 6.11** using anti-CD11b, anti-F4/80 and anti-CD11c antibodies. Graphs show myeloid cell subsets as both a proportion of total cells isolated from the draining ILN (top panels) and as absolute numbers of cells isolated, at day 3 (left) and day 6 (right) post-TPA application. Error bars indicate standard deviation, n = 3. Data were analysed by unpaired t-tests, *p<0.05, **p<0.01, ***p≤0.001.

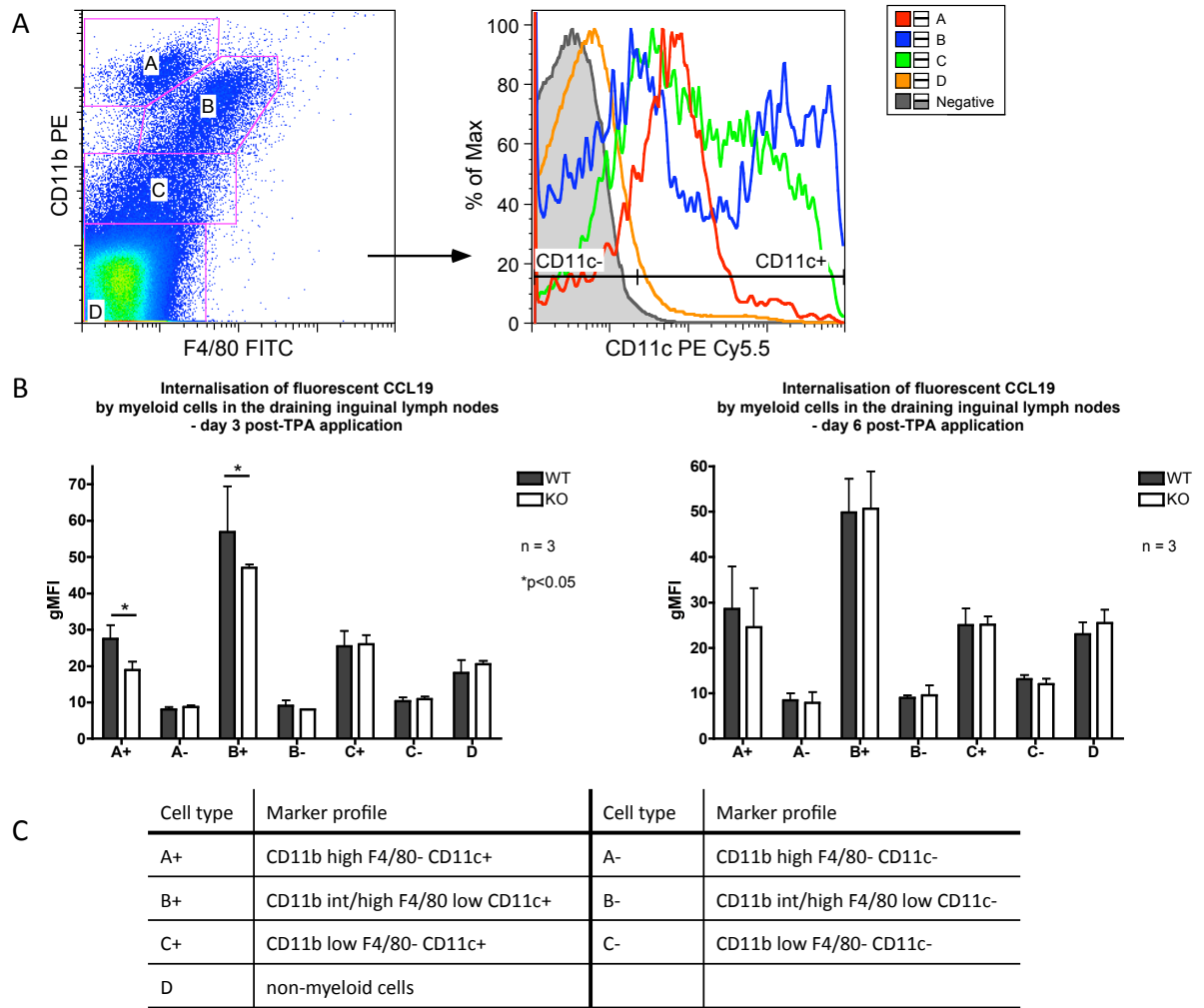
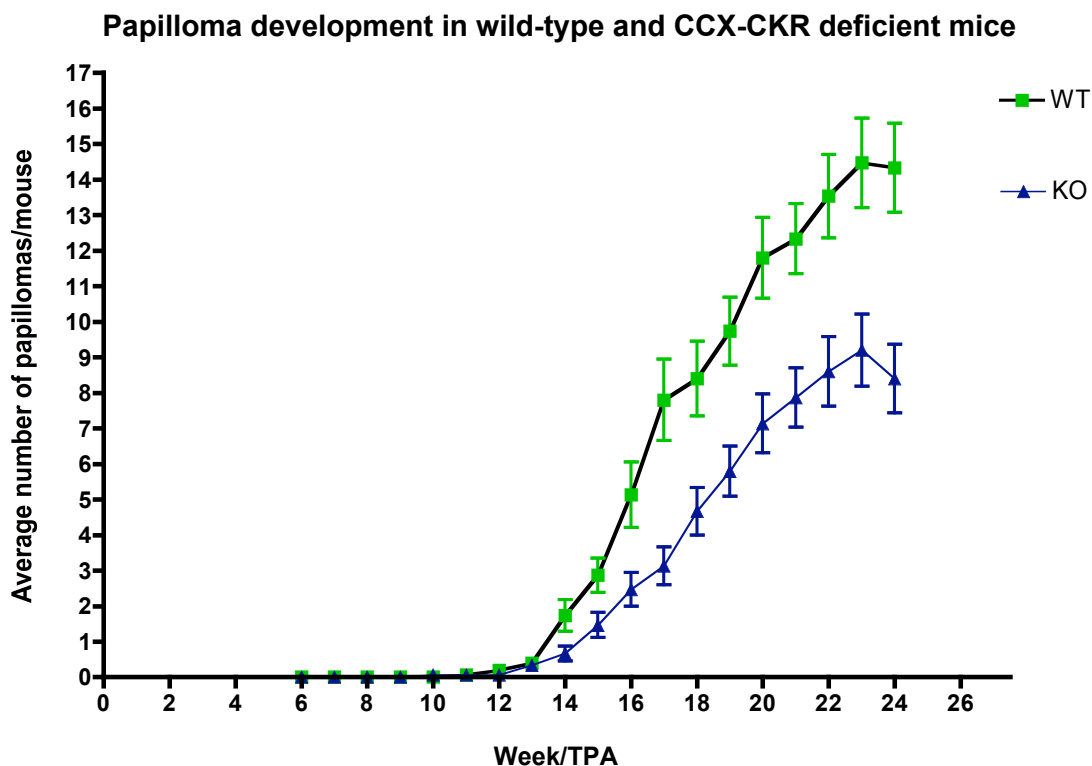


Figure 6.11: Internalisation of fluorescent CCL19 by myeloid cells in the draining lymph node in a model of skin inflammation. Wild-type (WT) and CCX-CKR deficient (KO) mice were shaved dorsally and TPA applied over 3 consecutive days as described in Materials and Methods. Draining ILNs were harvested at day 3 or day 6 post-TPA application. Cell isolates were incubated at 37°C with fluorescent CCL19 tetramers followed by staining at 4°C with antibodies against lineage markers. (A) Cells were defined as shown using anti-CD11b, anti-F4/80 and anti-CD11c antibodies. (B) Graphs show gMFI (geometric fluorescence intensity) values for fluorescent CCL19 in WT and KO myeloid cells at day 3 (left panel) and day 6 (right panel), which were analysed in separate experiments. Bars indicate standard deviation, $n = 3$. Data were analysed by unpaired t-tests, $*p < 0.05$. (C) Marker profile of myeloid subsets.



n = 15

p=0.0003

graph provided by M. Clarke

Figure 6.12: Development of papillomas by wild-type and CCX-CKR deficient mice during a model of tumorigenesis. Wild-type (WT) and CCX-CKR deficient (KO) mice were shaved dorsally and DMBA and TPA applied to the skin as described in Materials and Methods. Mice were monitored and papillomas measured and counted throughout the protocol. Graph shows average numbers of papillomas greater than 3mm in diameter formed during treatment. Green boxes indicate WT and blue triangles indicate KO, n = 15. Error bars indicate standard error of the mean. Data were analysed by 2-way repeated measures ANOVA, p=0.0003. Graph provided by M. Clarke.

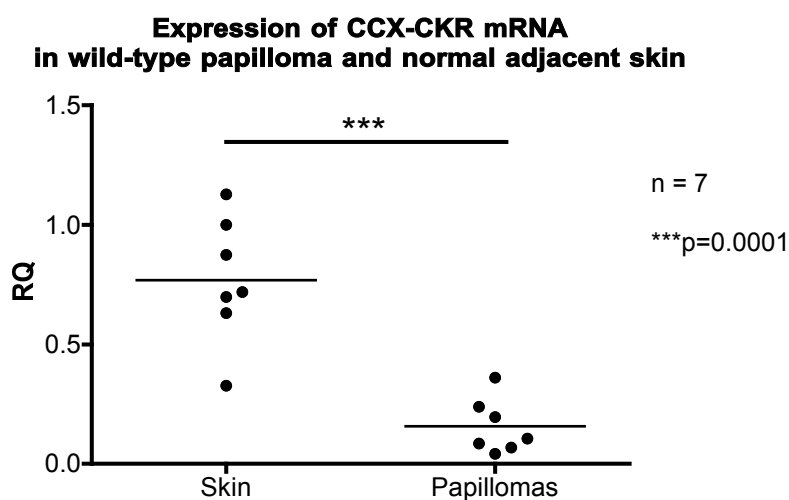


Figure 6.13: Expression of CCX-CKR in papillomas and normal adjacent skin during a model of tumourigenesis. Mice were shaved dorsally and DMBA and TPA applied to the skin as described in Materials and Methods. mRNA was extracted from papillomas and normal adjacent skin of treated mice. This was used to generate cDNA and analysed by QPCR. Lines represent the mean RQ (relative quantity), n = 7. Data were analysed by unpaired t-tests, ***p=0.0001.

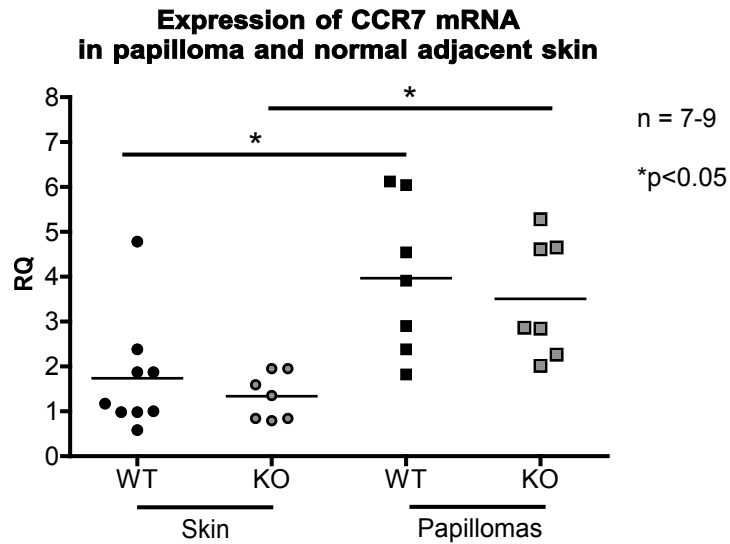


Figure 6.14: Expression of CCR7 in papillomas and normal adjacent skin during a model of tumorigenesis. Wild-type (WT) and CCX-CKR deficient (KO) mice were shaved dorsally and DMBA and TPA applied to the skin as described in Materials and Methods. mRNA was extracted from papillomas and normal adjacent skin of treated mice. This was used to generate cDNA and analysed by QPCR. Lines represent the mean RQ (relative quantity), n = 7-9. Data were analysed by 2-way ANOVA with Bonferroni post-test, *p<0.05.

Weight of ILN in WT and CCX-CKR deficient mice following DMBA/TPA-induced papilloma formation

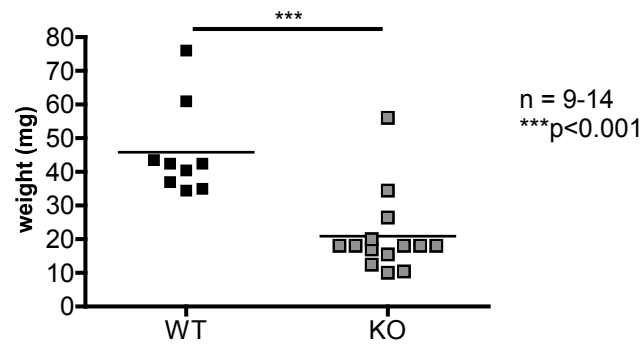


Figure 6.15: CCX-CKR deficient mice exhibit reduced inguinal lymph node size compared to WT following DMBA/TPA-induced papilloma formation. Wild-type (WT) and CCX-CKR deficient (KO) mice were treated with DMBA and TPA as described in Materials and Methods. At the end of the protocol, animals were sacrificed and their ILNs removed and weighed. Data were analysed by Mann-Whitney test, n = 9-14, line represents the mean, ***p<0.001. Graph provided by M. Clarke.

7 Discussion

7.1 Introduction

Chemokines and their receptors are critically important in the development, maintenance and function of the immune system. For some homeostatic chemokines and receptors, the relative faithfulness of their pairing suggests that the role they play in the body is not one that can easily be reprised in their absence. For example, some of the ligands and receptors that form the focus of this thesis, such as CCL19, CCL21 and CCR7, or CCL25 and CCR9, are known to be absolutely crucial for the correct development of the immune system, particularly in the thymus, and are essential in promoting and facilitating a rapid and effective immune response to infection or injury. Their specialisation and proven importance in the immune system makes the discovery and ligand specificity of the related receptor CCX-CKR all the more intriguing. Based primarily on *in vitro* studies, the starting point for this project was the hypothesis that the principal function of cells expressing CCX-CKR is to rapidly internalise its ligands (CCL19, CCL21 and CCL25) *in vivo* and that this scavenging activity regulates the microenvironment of lymphoid and non-lymphoid tissues to ensure optimal migration of leukocytes into, within and/or from these tissues. However, prior to this project, very little was known about when or where CCX-CKR was expressed *in vivo* or how it might function to influence CCR7- and CCR9-mediated migration. Identifying CCX-CKR-expressing cells *in vivo* was considered an important objective because it was hoped that this would not only provide a source of primary cells that could be used to explore the true function of this receptor, but would also help determine when, where and how CCX-CKR might be functionally significant.

7.2 Expression of CCX-CKR in resting tissues

Prior to this project, there were very few published reports detailing CCX-CKR expression, in either human or mouse. Those that did provide information on mRNA expression of the receptor did not provide quantification of expression to indicate the relative level of expression in tissues, nor did they indicate which cells might be responsible for the expression detected. There was also some conflict as to which tissues expressed mRNA for the receptor. Therefore, as detailed in chapter 3, I investigated where CCX-CKR is expressed at the mRNA level using a QPCR approach. This revealed that CCX-CKR is readily detectable in spleen, inguinal and mesenteric LN, thymus, PP, skin and small intestine, but not in liver. Thus, all lymphoid tissues displayed robust expression of the

receptor while the “barrier tissues” investigated, i.e. skin and small intestine, also displayed similar levels of CCX-CKR mRNA expression. CCL19 and CCL21 are both involved in the migration of leukocytes to and within thymus, spleen, LN and PP, with CCL25 also involved in regulating leukocyte movement into and within thymus, and from MLN and PP to the small intestine. Additionally, CCR7 is critical for the steady-state and inflammation-driven migration of DCs from skin to LN. Therefore, all the tissues that express CCX-CKR have been shown to rely on signals from one or more of its ligands for normal immune function. The leukocyte populations in the liver have not been reported to be disrupted in resting CCR7 or CCR9 deficient mice, suggesting that these receptors are dispensable for homeostatic leukocyte trafficking to this tissue. Clearly, these data do not exclude the possibility that the receptor is expressed elsewhere in the body in other non-lymphoid tissues, and published data suggests that the heart may surprisingly be a source of CCX-CKR transcripts. However, having established that all lymphoid tissues examined contained readily detectable CCX-CKR mRNA, and bearing in mind the critical roles played by CCR7 and/or CCR9 in these tissues, I decided that they would be ideal organs in which to attempt to identify CCX-CKR-expressing cells and provide an indication of how and where CCX-CKR functioned within lymphoid tissues.

7.2.1 Detecting CCL19 receptors with CCL19 tetramers

Most studies reporting on the location and level of protein expression of a chemokine receptor make use of monoclonal antibodies, investigating expression by either immunohistochemistry or by flow cytometry. However, at the time of these experiments, no such antibody was commercially available for murine (or human) CCX-CKR, and those produced subsequently were unable to detect exogenous CCX-CKR on transfected cells (R. Nibbs, pers. comm.), rendering them unsuitable for this type of analysis. Therefore, a novel approach was required to allow investigation of this receptor on primary mouse cells. Building on experiments from our lab investigating D6 expression on primary cells (Hansell et al., 2011b) and CCX-CKR activity *in vitro* (Comerford et al., 2006), I established and optimised a protocol to assess CCL19 receptor activity, as defined by internalisation of fluorescent CCL19 tetramers, on primary cells. Theoretically, this assay allowed assessment of not only CCX-CKR expression by primary cells, but also their CCR7 expression and activity on these cells, which could potentially be disrupted by CCX-CKR deletion. I will first discuss how I optimised the assay and the information gained from this process, before discussing the implications of results pertaining to CCX-CKR expression/activity. I will also discuss the potential for further modification of the assay to increase stringency and improve detection of low-level chemokine internalisation. In

section 7.3, I will discuss the analysis of CCR7 expression as determined both by the internalisation assay and by QPCR.

The assay was optimised using splenocytes and, as expected, lymphocytes efficiently internalised the fluorescent CCL19 tetramers. To demonstrate specificity, and eliminate the possibility that this internalisation was by pinocytosis or some other mechanism not involving a CCL19 receptor, unlabelled competitor chemokines were included in incubations. Only CCL19 and CCL21 could block CCL19 tetramer internalisation. This was much more pronounced in the presence of excess unlabelled CCL19 than in the presence of excess unlabelled CCL21. There are a number of potential explanations for this. First, CCL19 is known to bind human CCR7 with slightly higher affinity than CCL21 (Britschgi et al., 2008), so internalisation of fluorescent CCL19 might occur preferentially to internalisation of CCL21. Second, CCL21 is a much “stickier” protein than CCL19, due to its extended C-terminus. This may have limited its ability to gain access to CCL19 receptors in the assays. Third, CCL19 is a more potent stimulator of CCR7 internalisation than CCL21, in both human leukocytes and in cells transfected with CCR7, and binding of CCL19, but not CCL21, causes desensitisation of CCR7, preventing further internalisation (Britschgi et al., 2008). This agreed with titrated timecourse analysis of internalisation of the CCL19 tetramers by primary murine splenocytes, which showed that while increased starting concentrations of the fluorescent CCL19 tetramers led to a marked increase in fluorescence, increasing incubation times had a much less remarkable effect. Thus, it appears as though most tetramer internalisation into lymphocytes occurs within the first 5-15 minutes of exposure to tetramers. It is likely that the reduction in fluorescence seen in samples co-incubated with excess CCL21 is due to some level of CCL21 bound to receptor at the point of internalisation, blocking complete occupancy of receptors by the fluorescent chemokine. Subsequent internalisation of fluorescent CCL19 tetramers could then cause desensitisation of CCR7 and prevent the “competed” samples from reaching similar levels of fluorescence to “uncompeted” samples. Notwithstanding these differences between CCL19 and CCL21, the ability of both these chemokines to diminish internalisation of the fluorescent CCL19 tetramers suggested that the majority of internalisation was CCR7- or CCX-CKR-dependent. The inclusion of CCL25 as a competitor was also considered. CCL25 should only be able to compete with CCL19 for binding to CCX-CKR, but not CCR7, so theoretically it could have helped identify CCX-CKR-expressing cells. However, assays using recombinant CCL25 are technically challenging (pers. comm. E. Anderson), and the extended C-terminus makes it “sticky” and prone to aggregation. Instead, comparisons of fluorescent CCL19 tetramer internalisation between equivalent

populations of WT and CCX-CKR deficient cells were undertaken, making use of CCX-CKR deficient mice generated by a previous student in the lab (Comerford et al., 2010).

A caveat of this experimental design is that it may not be possible to distinguish between specific binding or internalisation of chemokine tetramers and non-specific binding of biotinylated protein linked to streptavidin. As discussed below, some fluorescence is detected, particularly by myeloid cells, that is not diminished using excess unlabelled competitor chemokine, but is also not observed in StrAPC only controls. Therefore, inclusion of an “irrelevant” biotinylated protein linked in the same way to StrAPC as the BioCCL19 may allow distinction of chemokine specific versus biotinylation-dependent binding. However, care must be taken to ensure that this protein does not itself bind specifically to the cells and thus cause background or yield false positive results.

7.2.2 Which cells express CCX-CKR in lymphoid tissues?

Using fluorescent CCL19 tetramers, I carried out a detailed analysis of resting lymphoid compartments, including spleen, inguinal lymph nodes, peritoneal cavity lavage and whole blood, investigating various leukocyte subsets as well as stromal cells where appropriate. I have clearly shown that splenic leukocytes and stromal cells do not internalise fluorescent CCL19 tetramers in a CCX-CKR-dependent manner in this assay, presumably due to either a lack of CCX-CKR expression by these cells or an undetectable level of CCL19 internalisation through this receptor. Peripheral blood lymphocytes did not display CCX-CKR dependent internalisation of fluorescent CCL19 tetramers, although they did exhibit some internalisation of the chemokine, presumably through CCR7. This suggests that CCX-CKR is unlikely to be expressed by these cells. In the peritoneal cavity, none of the leukocyte populations investigated demonstrated CCX-CKR dependent internalisation of fluorescent CCL19 tetramers. Likewise, inguinal lymph node lymphocytes, which require CCR7 for appropriate migration to and within the lymph node, do not exhibit any CCX-CKR dependent internalisation of fluorescent CCL19 tetramers, nor do CD45⁻ cells of the ILN or most myeloid subsets in this tissue. Interestingly, however, CD11b^{high} F4/80⁻ CD11c⁺ and CD11b^{int/high} F4/80^{low} CD11c⁺ cells do demonstrate some CCX-CKR-dependent internalisation of the chemokine, suggesting that either all cells within these populations express the receptor under resting conditions, or a subset of CCX-CKR⁺ or CCR7⁺ cells is lost from both populations in the CCX-CKR deficient animal. Heinzl and colleagues reported that DC populations in the resting LN were disrupted in the absence of CCX-CKR, so lack of CCX-CKR may exclude a subset of DCs from the LN or prohibit their retention there. It is also possible that CCR7 expression or activity is altered on these cells in the absence of CCX-CKR. However, I found no such defect in resting CCX-CKR

deficient ILNs. Effects of CCX-CKR deletion on cellularity will be discussed later. Heinzl and colleagues also reported that CCX-CKR was expressed on cells that line the subcapsular region of the inguinal lymph nodes (Heinzl et al., 2007), concluding, apparently based on their positioning, that this expression was stromal rather than hematopoietic. However, a population of macrophages called SCMs are known to reside just below the capsule of the lymph node, lining the SCS (Phan et al., 2009). These SCMs are believed to be involved in the capture of antigen from draining lymph and its presentation to B cells just underneath the subcapsular sinus, as well as the transfer of antigen to FDCs for presentation to B cells (Phan et al., 2009). Phan and colleagues have identified these cells as being $CD11b^+ F4/80^{neg} CD11c^{low}$, as well as expressing CD169. It is therefore possible that the cells I have identified as potentially being $CCX-CKR^+$ include SCMs. This presents an intriguing possibility as to the identity of CCX-CKR-expressing cells in the LN and the function of the receptor on these cells. CCX-CKR expressed by SCMs might modulate the chemokine environment to allow efficient interactions between SCMs and B cells, control the migration of SCMs between the outer subcapsular sinus and the border of the B cell follicle, or regulate leukocyte survival and/or interaction within the LN cortex. A model showing how CCX-CKR might modulate the LN chemokine environment is shown in Figure 7.1.

SCMs are also believed to be capable of migration into the follicle to deliver immune complexes to FDCs (Phan et al., 2007) and CCX-CKR could promote this activity by “scavenging” CCR7 ligands from the SCM microenvironment, rendering the cells more responsive to CXCL13 or other cues. It would be interesting to examine the kinetics of CCL19 accumulation and eventual dispersal or depletion from this area in WT and CCX-CKR deficient mice, perhaps by employing the same model of footpad or subcutaneous injection of fluorescent chemokine as has been used previously (Baekkevold et al., 2001) and using two-photon microscopy to follow the accumulation and depletion of the chemokine in the draining LN SCS over time. It is worth noting that SCM from the LN and MZ metallophilic macrophages of the spleen are thought to play similar roles, with SCM “filtering” the lymph that enters the LN and MZ metallophilic macrophages doing the same for blood flowing through the spleen (Bajénoff and Germain, 2009). I did not identify any cells exhibiting CCX-CKR dependent internalisation of the fluorescent CCL19 tetramers in the spleen and preliminary confocal staining of WT and CCX-CKR deficient spleen with MOMA-1 (a marker for MZ metallophilic macrophages) did not uncover any obvious aberrations in positioning of the cells (data not shown). However, more detailed and specific analysis of macrophage subsets from the spleen should provide a more

definitive answer as to the possibility of their expressing CCX-CKR, and may yield interesting insights into the *in vivo* function of this receptor.

An alternative possibility is that CCX-CKR is expressed by some DC subsets entering the LN via the lymph. DCs entering from the periphery are known to rely on CCR7, using CCL21 expressed in lymphatics to guide them from peripheral tissue to LNs during both resting and inflamed states. CCL19 and CCL21 also facilitate the migration of arriving DC within the lymph node to the T cell zone, enabling DC/T cell antigen-specific interactions. CCX-CKR might be present on DCs to regulate migration to and/or residence time within the lymph node. It could also influence the localisation of DCs within the ILN. As mentioned above, Heinzl and colleagues have reported a reduction in the number of CD11c⁺ MHCII^{high} DCs in peripheral LN of CCX-CKR-deficient mice (Heinzl et al., 2007), so it is possible that a subset of these cells express CCX-CKR and in its absence cannot migrate to or reside within the LN as normal. Again, it must be noted that my analysis revealed no defect in DC cellularity in the ILN, so further investigation of this phenomenon would be desirable. More advanced multicolour flow cytometry equipment now available in the lab could facilitate a more detailed analysis of LN cellularity in future projects, allowing investigation of specific subsets of LN DCs using markers such as CD8, CD11b, CD11c and MHCII as well as fluorescent CCL19 tetramer internalisation. This, in combination with confocal microscopy of LN sections from WT and CCX-CKR deficient mice, could provide a more complete set of data relating to the specific impact of CCX-CKR deletion on LN DC populations.

Given the paucity of functional CCX-CKR detectable in most cell populations examined using the internalisation assay, I attempted to identify cells from the spleen that expressed CCX-CKR mRNA by purifying various populations by FACS sorting and isolating RNA from these populations for QPCR. However, isolating RNA from primary cells proved technically challenging, with only a small RNA yield from most samples. The preliminary data I was able to generate suggests that leukocytes do not express the receptor. This would point towards stromal cells as the main CCX-CKR⁺ population in the spleen. However, I further investigated the effect of cell isolation on the expression of CCX-CKR mRNA by spleen samples and found that any mechanical disruption of the tissue seemed to severely reduce the level of CCX-CKR mRNA recovered. It is unclear why this might occur, since CCR7 mRNA was not affected in this way in the same samples. While it might be expected from the preliminary data above that removal of stromal cells would decrease the relative amount of CCX-CKR mRNA in a sample, one would then expect that samples where stromal cells were not removed (e.g. samples consisting of debris remaining on

nitex/cell strainers, or unmashed collagenase-treated samples) should retain expression and in fact exhibit a relative increase in mRNA level, but this was not the case. It is possible that CCX-CKR is downregulated on stromal cells during an inflammatory response, which may be induced in cells during the isolation process. This might be designed to alter chemokine levels or bioavailability in the presence of inflammatory signals. However, this data is very preliminary and requires further investigation to reveal the cause of this apparent downregulation of CCX-CKR mRNA expression.

These data have shown that most cells in the tissues analysed do not express CCX-CKR capable of mediating CCL19 internalisation. However, I have identified subpopulations of myeloid cells in the ILN that do exhibit CCX-CKR dependent internalisation, with some intriguing possibilities as to the nature and function of these cells. However, further analysis will be required to define the source of CCX-CKR mRNA expression in lymphoid tissues, and development of a protocol to do the same in “barrier” tissues may provide some further clues as to the role of the receptor at these sites. Continued optimisation of RNA isolation from sorted cell populations may yield some clues, and *in situ* hybridisation could be used to show the distribution of CCX-CKR mRNA expression within tissues. Additionally, recent work by our collaborators has shown that a recently described antibody against human CCX-CKR (Takatsuka et al., 2010) also detects the murine receptor (I. Comerford, pers. comm.), which may allow more conventional analysis of tissues by immunofluorescence, flow cytometry and immunohistochemistry. The CCX-CKR deficient mouse represents an excellent control for false positive detection of the receptor in WT tissues, both in *in situ* hybridisation and with use of anti-CCX-CKR antibodies.

7.3 CCX-CKR influences the expression and activity of CCR7 in resting tissues

As alluded to previously, the internalisation assay, while designed with the purpose of identifying CCX-CKR-expressing cells, also provides insights into the expression and internalising activity of CCR7 on primary leukocytes. As one might expect, splenic T cells internalised the fluorescent CCL19 tetramers more readily than B cells, likely through CCR7. This feature was shared by lymphocytes from blood and ILN but not by lymphocytes from the peritoneal cavity, where CCL19 internalisation was similar between T cells and the various B cell populations found there. This might reflect differing requirements for CCR7 in B and/or T cell migration to and from these sites, or might be

related to the unique nature of the B cell population in the peritoneal cavity compared to other tissues (discussed below). Internalisation of fluorescent CCL19 tetramers by T cells from the spleen was completely abolished by pre- and co-incubation with excess unlabelled CCL19, consistent with reports that CCL19 down-regulates surface expression of CCR7 (Britschgi et al., 2008). Internalisation by splenic B cells was also significantly reduced under these conditions. Investigation of B cell subsets in the spleen revealed that within the B cell compartment there are further distinctions to be made based on the capacity for CCL19 internalisation. In a resting WT mouse, B1 cells internalise more fluorescent CCL19 tetramers than MZ B cells (see chapter 3) and splenic follicular B cells (not shown), while MZ B cell internalisation is equivalent to that of follicular B cells (not shown). This may be due to the different roles played by these subsets, and/or their positioning within the spleen. MZ B cells are resident in the marginal zone of the spleen, where their positioning is dependent on receptors for S1P (S1P₁ and S1P₃) and CXCL13 (CXCR5) (Cinamon et al., 2004, Cinamon et al., 2008), and follicular B cells, which make up the majority of total splenic B cells, rely mainly on CXCR5 for positional cues, although they have been suggested to be prompted by CCR7 to “pause” in the PALS after entry into the spleen before entering the follicle (Förster et al., 1999). B1 cells may use CCR7 to remain in the PALS, and interestingly they are known to have the capacity to act as antigen presenting cells for activation of naïve T cells, at least *in vitro* (Cinamon et al., 2008, Martin and Kearney, 2001). Splenic B1 cells also appear to be less dependent on CXCR5 than other B1 cells and unlike B1 cells in the peritoneal cavity, splenic B1 cell numbers are unaffected by CXCL13 deletion (Ansel et al., 2002). However, detecting B1 cells as they move through the body is difficult due to their inconstant immunophenotype. Most publications identify them by multi-colour flow cytometry rather than immunohistochemistry, and information about their likely position within tissues is scarce. It is interesting to note that in the WT peritoneal cavity, where T and B cells display a similar capacity to internalise CCL19, the “B2” cell compartment, which would correspond most closely to splenic follicular B cells, is likely to contain substantial numbers of B1 cells that cannot be distinguished by the markers used in this study (Hansell et al., 2011b). Therefore it is possible that in fact true B2 cells in this cavity have a low CCL19 internalisation capacity similar to classical B2 cells from other tissues, but that this is masked by the high level of internalisation of fluorescent CCL19 tetramers by these B1 cells. Alternatively, the peritoneal lymphocyte requirement for CCR7 expression to mediate egress, as described below, could potentially explain uniformly high levels of expression suggested by the observed internalisation profile.

Myeloid cells in the spleen displayed varied capacity to internalise the fluorescent CCL19 tetramers. While this may reflect differences in CCR7 expression, pre- and co-incubation experiments showed that internalisation of the chemokine by many of these cells is only slightly reduced, if at all, in the presence of unlabelled CCL19. This indicates a potential method of receptor-independent internalisation of CCL19 by these cells. Strangely, however, internalisation did seem dependent on the presence of chemokine in the tetramers, as exposure to StrAPC alone did not lead to the same level of cell-associated fluorescence, and it is currently unclear how CCL19 tetramers are internalised by these cells. It is interesting to note the difference in effect of pre- versus co-incubation of these cells with unlabelled CCL19. Internalisation of fluorescent CCL19 tetramers by CD11b^{high} F4/80^{low} cells was not altered by co-incubation with unlabelled CCL19, but does decrease slightly following pre-incubation with the unlabelled chemokine. This could suggest that CCR7 acts differently on these cells to other cell types, perhaps being more resistant to desensitisation, although eventually being down-regulated after continuous ligand exposure. Alternatively, it could suggest CCL19-induced down-regulation of non-specific chemokine uptake, or that prolonged CCL19 exposure is inducing other cells in the sample to produce factors that trigger downregulation of CCL19 internalisation by these cells. CCX-CKR deficient samples appear more sensitive to this difference, with some cell types exhibiting significant differences in internalisation between pre- and co-incubated samples from CCX-CKR deficient but not WT spleen. Further examination of this effect could provide interesting insights into how CCR7 activity and/or CCL19 internalisation is controlled on these cells. Splenic CD45⁻ cells, which are mainly stromal, do not internalise fluorescent CCL19 tetramers, regardless of incubation with or without unlabelled CCL19. Likewise, CD45⁻ cells in the inguinal lymph node do not display CCR7-dependent internalisation of fluorescent CCL19 tetramers. Since CCR7 is not known to be expressed by stromal cells, this is unsurprising.

In the absence of CCX-CKR, B cells from the ILN appeared to slightly increase their ability to internalise fluorescent CCL19 tetramers, perhaps due to aberrant CCR7 expression or activity on these cells in the CCX-CKR deficient animal. However the observed increase is very small and, with only a small number of samples analysed, interpretation of this difference is difficult. The relative level of CCR7 mRNA expression was also analysed to try to elucidate whether observed changes in CCL19 internalisation could be due to altered expression of the receptor at the mRNA level. Surprisingly, in the spleen, CCR7 mRNA levels were significantly increased in the absence of CCX-CKR, although no difference in CCL19 internalisation had been observed. In the ILN of CCX-CKR deficient mice, where a slight increase in B cell internalisation of CCL19 and a

decrease in internalisation by some myeloid subsets were observed, CCR7 mRNA levels were slightly decreased. This may mean that the drop in internalisation of CCL19 by myeloid subsets was due to altered CCR7 expression rather than CCX-CKR expression by these cells. Alternatively, changes in CCR7 mRNA expression may be due to altered ligand levels within these tissues – an increase or decrease in CCR7 ligands caused by deletion of CCX-CKR could influence the level of CCR7 mRNA expressed by cells via signalling through CCR7 itself. This possibility will be examined later in this section. The reason for the contrasting effects on CCR7 mRNA expression in spleen and ILN is unclear, but may be due to the different requirement for CCR7 in these tissues. In CCR7 deficient mice, T cells are significantly impaired in their ability to enter lymph nodes, while they maintain the ability to enter the spleen but are not properly localised within it (Förster et al., 1999). If CCX-CKR is an important factor in facilitating the entry of cells into lymphoid organs, for example via its hypothesised function of presentation of chemokine on high endothelial venules (HEVs) and/or lymphatics, its absence may alter the cellularity of the tissues. This potential for altered cellularity is addressed in section 7.5 below.

T cells from the peritoneal cavity displayed a higher capacity to internalise CCL19 tetramers in CCX-CKR deficient samples compared to WT. Absence of a CCL19^{low} population of T cells (which may therefore be CCR7^{low}) appears to be the cause of this disparity between the two strains. CCR7 mRNA expression by peritoneal cavity cells was also significantly increased in CCX-CKR deficient mice, which may in part be caused by this shift in T cell phenotype. However, as discussed below, there are more lymphocytes in the CCX-CKR deficient peritoneal cavity: this may account for the elevated CCR7 mRNA. It is unclear what has happened to the CCL19^{low} T cells. They may represent a subset of T cells that are absent from the CCX-CKR deficient peritoneal cavity, or they may have somehow increased their CCR7 expression in the absence of CCX-CKR. Interestingly, CCR7 has recently been shown to be involved in egress of lymphocytes from the peritoneal cavity. Höpken and colleagues have shown that T cells and B2 cells accumulate in the peritoneal cavity in the absence of CCR7, while B1 cell numbers are reduced (Höpken et al., 2004, Höpken et al., 2010). By comparing the ability of adoptively transferred biotinylated splenocytes from WT and CCR7 deficient animals to traffic from the peritoneal cavity (where they were introduced) to peripheral LNs, Höpken and colleagues showed that CCR7 was required for lymphocytes to recirculate from the peritoneal cavity to LNs. They further showed that the observed defect in recirculation was caused by an inability of CCR7 deficient lymphocytes to exit the peritoneal cavity by carrying out a competitive adoptive transfer. In this experiment, differentially labelled splenocytes from WT and CCR7 deficient mice were introduced into the peritoneal cavity

in a 1:1 ratio. Subsequent analysis of the peritoneal cavity showed that, at 2.5 days post-transfer, there was a four- to five-fold increase in the proportion of CCR7 deficient splenocytes present in the peritoneal cavity compared to transferred WT splenocytes (Höpken et al., 2010). It is possible that CCX-CKR is involved in regulating the lymphocyte cellularity of the peritoneal cavity by influencing CCR7-mediated responses. This could occur by limiting or inducing influx of cells or controlling the rate of egress, and similar adoptive transfer experiments in CCX-CKR deficient mice could verify or refute such a role for the receptor. The effect of CCX-CKR deletion on peritoneal cavity cellularity is discussed further below.

7.4 Regulation of chemokine levels in resting tissue by CCX-CKR

In addition to the possibility that CCR7 expression was being affected by CCX-CKR dependent changes in chemokine levels, work from our lab has shown that, *in vitro*, CCX-CKR that is exogenously expressed on HEK cells efficiently scavenges CCL19 from the media, while CCR7 is downregulated by exposure to its ligand (Comerford et al., 2006). Therefore, it was hypothesised that CCX-CKR might have a scavenging function *in vivo*, and that deletion of the receptor would lead to altered chemokine levels in the mouse. Strikingly, while CCL19 could not be detected in WT serum, it was consistently detected in serum from CCX-CKR deficient mice. This suggests that CCX-CKR is involved in controlling serum levels of this chemokine, although the exact mechanism is unclear. CCX-CKR has also been reported to suppress serum levels of CCL21 (Comerford et al., 2010), but this could not be repeated in our lab, by myself or others. Also in contrast to my findings, this study failed to detect CCL19 in either WT or CCX-CKR deficient serum. The reason for these differing results is unclear but may reflect slight variation in the assays performed, although the antibodies used in both studies came from the same supplier. Nonetheless, serum chemokine dysregulation is a consistent feature of CCX-CKR deficient mice.

Compared to WT, CCL19 was also elevated in CCX-CKR deficient ILN, in agreement with Comerford and colleagues who found elevated CCL19 in pooled homogenates of inguinal, axillary and brachial LNs (Comerford et al., 2010). However, I found CCL21 to be slightly decreased in the ILN in the absence of CCX-CKR, with a previous student finding a similar, though not significant trend (Anderson, 2011). In contrast, Comerford and colleagues found a significant increase in the level of this chemokine in pooled

peripheral LNs. Again, it is unclear why these results are not in agreement, although it is possible that they reflect the variation in samples assessed. It is also possible that the CCL21 detected by one study differs slightly from the other – for example, one study may detect both cleaved and full-length CCL21 (Schumann et al., 2010) while the other detects only the full-length form. Also, the numbers of samples investigated by Comerford and colleagues were consistently greater than 10 per group, while my data was generated from groups of four animals. Therefore, higher sample numbers might alter the trend observed. In any case, CCX-CKR seems to influence the level of chemokine within the ILN, although its mode of action is unclear. A possible explanation for the results presented in this thesis is depicted in Figure 7.1.

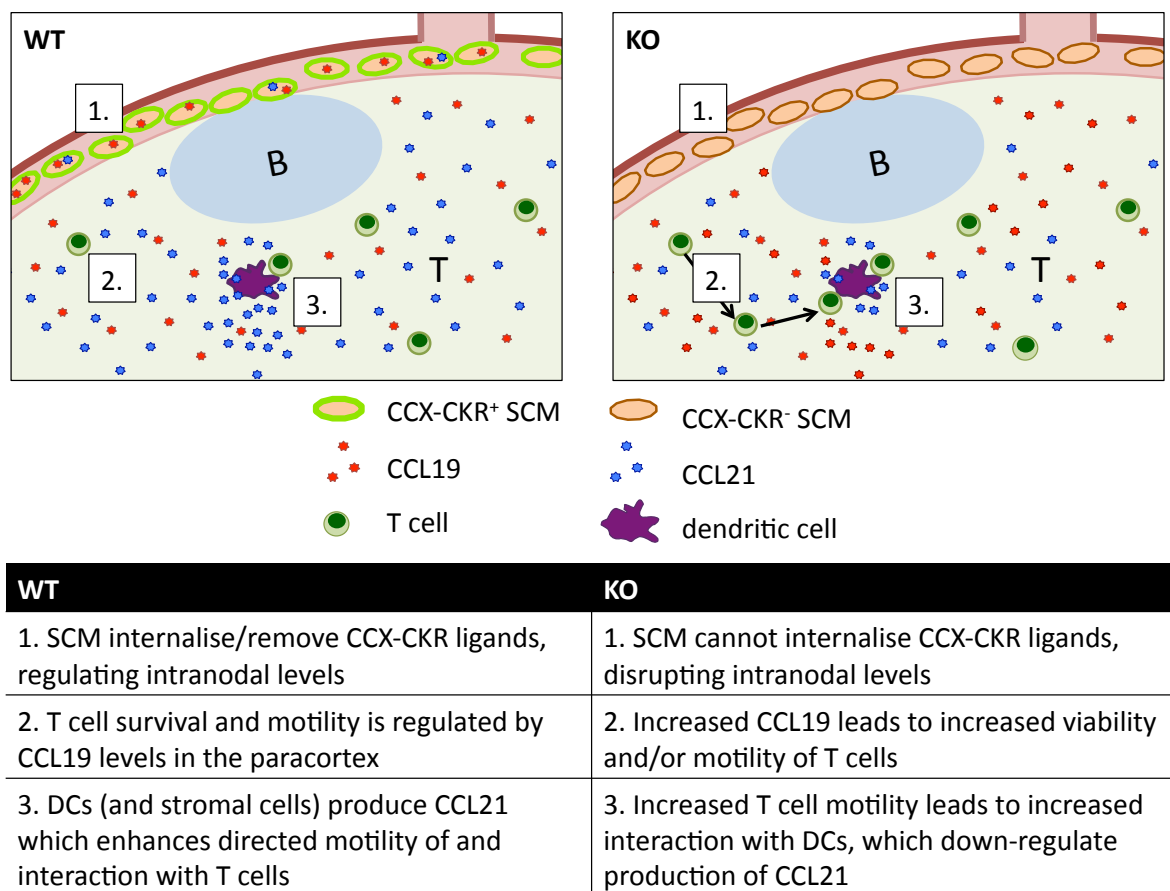


Figure 7.1: A model for CCX-CKR function in the resting lymph node. (1) CCX-CKR expressed by cells lining the subcapsular sinus of the LN (such as subcapsular macrophages; SCM) binds CCL19 and CCL21, either degrading them or transporting them to the afferent lymphatics for presentation to entering leukocytes. (2) In the absence of CCX-CKR, CCL19 levels within the LN rise, leading to increased motility, and possibly increased viability, of T cells, increasing their interaction with DCs. (3) DCs are then prompted to reduce their production of CCL21, causing a drop in intranodal levels of this chemokine.

CCL21 protein levels were also elevated in the thymus of CCX-CKR deficient mice, although CCL19 was unaffected. As described in the Introduction, CCR7 and CCL21 are involved in controlling the directed migration of maturing thymocytes and CCX-CKR may play a role in regulating the localised expression of the chemokine to facilitate this

migration. It is possible that CCX-CKR is expressed by strategically positioned cells to scavenge CCL21 and prevent its attraction of thymocytes. It would be very interesting to assess whether thymocytes development or migration is perturbed in the thymus, or if thymic architecture is disrupted in the absence of CCX-CKR. Indeed, unpublished work by our collaborators has indicated that the structure of the thymus is perturbed in CCX-CKR deficient mice and the numbers of all thymocytes subsets analysed are altered (I. Comerford, pers. comm.). This indicates an important role for CCX-CKR in the development of T cells. It remains to be seen whether these disruptions have any effect on the development of central tolerance or T_{reg} generation. A previous student in the lab has shown that tolerance to orally administered antigen is defective in the absence of CCX-CKR, as measured by DTH and antibody responses, suggesting a role for CCX-CKR in the development of peripheral tolerance (Anderson, 2011). CCR7 has already been shown to have an important role in the development of both central and peripheral tolerance (see Introduction), and it would be interesting to learn whether CCX-CKR could be involved in regulating these critical elements of the immune response.

Interestingly, CCL19 and CCL21 protein were both easily detectable in non-lymphoid tissues, including heart, liver, kidney and brain. The reason for this is unclear. While CCL21 is likely to be expressed in lymphatic vessels in some non-lymphoid tissues, CCL19 is usually expressed by stromal cells in T cell areas of lymphoid tissues, although it can also be expressed by DCs. As there is no evidence of naïve lymphocyte influx into non-lymphoid tissues, it is unlikely that the chemokine detected is functioning to attract these cells, as is the case in LNs. CCL19 is also believed to be involved in promoting survival and proliferation of T cells within the LN, so it may have been co-opted to play a similar role for other cells in non-lymphoid tissue. Expression of CCL19 mRNA has previously been reported in the kidney (Yoshida et al., 1997), and it may be involved in regulating kidney function. Such a role has been postulated for CCR7 and CCL21, which are expressed in the glomeruli of the kidney and have been proposed to be involved in the homeostasis and proliferation of cells within these structures (Banas et al., 2002, Banas et al., 2004). CCL19 protein was elevated in the kidney in the absence of CCX-CKR while CCL21 protein levels were unchanged. CCX-CKR mRNA has been detected in the kidney (Townson and Nibbs, 2002), and may be involved in regulating chemokine levels to modulate cell proliferation or activity. Further work characterising the function of CCX-CKR and CCL19 in the kidney is required to clarify the potential role or roles for these molecules in this tissue.

CCL19 protein levels are also slightly elevated in the CCX-CKR deficient brain. CCL19 has been shown to be expressed in normal resting brain at the blood-brain barrier, and it, along with CCL21 and their receptor CCR7, has been shown to be involved in development of experimental autoimmune encephalitis (EAE), an animal model resembling multiple sclerosis (Alt et al., 2002). Comerford and colleagues have recently reported a role for CCX-CKR in delaying the onset of EAE, with elevation of CCL21 in the CNS during EAE much greater in the CCX-CKR deficient mouse than WT (Comerford et al., 2010). Therefore, CCX-CKR may be linked to the maintenance of an appropriate chemokine milieu in the brain, both under resting and challenged conditions, helping to prevent aberrant inflammatory responses at this immunologically privileged site.

7.5 CCX-CKR influences lymph node and peritoneal cavity cellularity

An interesting finding of this project was that CCX-CKR deletion significantly alters the cellularity of both the ILN and the peritoneal cavity. The spleen was unaffected, both in cellularity and in gross microarchitecture. By contrast, total cell numbers in both ILNs and peritoneal cavity were slightly increased in the CCX-CKR deficient mouse compared to WT. While fractionation of leukocyte subsets in the ILN failed to reveal the affected cell type (or types), it is likely that this was due to insufficient sample numbers. Lymphocytes are the most probable candidates for causing an increase in ILN cellularity, as they comprise the vast majority of cell retrieved from this organ. The cause of such an increase is unclear. The elevated CCL19 levels seen in the absence of CCX-CKR could increase the proliferation and/or survival of T cells in the ILN, since CCL19 is known to be important in these processes (Link et al., 2007). It is possible that a defect in a DC or macrophage subset in the ILN, as suggested by the reduction in internalisation of CCL19 by two myeloid subsets described above, might lead to knock-on effects in terms of the ability to provide survival signals to lymphocytes upon priming, but again the exact cell types likely to be involved are unclear. Notably, in female mice on the same genetic background as those primarily used in this study (i.e. C57Bl6) no significant difference in cellularity of MLN, ILN or spleen was observed by a previous student (E. Anderson, pers. comm.), while another student found that female CCX-CKR deficient mice on an FVB background showed a small but significant decrease in total ILN cellularity compared to WT (Comerford, 2005). Additionally, Comerford and colleagues reported no difference in cellularity between ILNs from resting WT and CCX-CKR deficient resting female C57Bl6 mice (Comerford et al., 2010). These conflicting results may reflect gender or strain-

specific differences in the activity of CCX-CKR, albeit differences currently without explanation. Alternatively, it is possible that variation between samples causes the slight differences observed – all three studies found varying degrees of overlap in total cell number between WT and CCX-CKR deficient mice, regardless of genetic background or gender. Thus, this defect in ILN cellularity requires further investigation before we will have a clear understanding of the role played by CCX-CKR in its regulation.

One of the most striking effects of CCX-CKR deletion uncovered by my work is the effect on peritoneal cavity lymphocyte cellularity. Intriguingly, total cellularity of the peritoneal cavity was slightly elevated in the CCX-CKR deficient peritoneal cavity compared to that of the WT. When analysed further it transpired that this corresponded to a significant and highly reproducible defect in lymphocyte cellularity in particular. All lymphocyte subsets examined (B1a-c and B2 B cells, and T cells) were significantly elevated in number in the CCX-CKR deficient peritoneal cavity. Myeloid cell subsets examined were unaffected in terms of absolute numbers, although proportions were skewed, presumably due to the lymphocyte defect. CCR7 and CXCR5 have been shown to play an important role in regulating the lymphocytic cellularity of the peritoneal cavity, with CCR7 being specifically involved in egress, as discussed above. Interestingly, B1 B cells and B2 B cells of the peritoneal cavity are differently affected by deletion of CCR7, with B1 B cell numbers decreased in the CCR7 deficient cavity while B2 cells are increased in number. Overall, total peritoneal cavity cellularity is increased in the absence of CCR7 and decreased in the absence of CXCR5 (Ansel et al., 2002, Höpken et al., 2004, Höpken et al., 2010). In light of these findings, therefore, what could CCX-CKR be doing that its absence causes a significant increase in all subsets examined? It is possible that B1 cells (and perhaps T cells), which express high levels of CCR7, use both CCR7 and CXCR5 for entry into the peritoneal cavity and CCR7 for egress, while B2 cells rely mainly on CXCR5 for entry and CCR7 for egress. The absence of CCR7 would lead to a reduction in B1 cells (through failure to enter the peritoneal cavity) but an increase of B2 cells that remain capable of entering but failing to leave. Interestingly, in the absence of CCX-CKR, the most substantial difference in cellularity is observed in the B2 B cell population. Therefore, perhaps CCX-CKR reduces the ability of peritoneal leukocytes to respond to CCR7 ligands, either through affecting the availability of these ligands or through direct effects on the cell signalling induced through CCR7. This might lead to a slight defect in B1 B cell (and perhaps T cell) entry into the peritoneal cavity that is nevertheless still intact to the point that a failure to exit the cavity leads to an overall increase in the presence of these subpopulations within the cavity. B2 cells on the other hand would have no such defect in entry, making a failure to exit result in a much more pronounced increase in

cellularity. Again, it must be noted that work carried out subsequent to these experiments has shown that due to the limited number of surface markers used in this analysis, the “B2” cell population identified in this thesis may in fact include a substantial number of B1 B cells (Hansell et al., 2011b). Therefore, the difference in effect on B1 and B2 B cells may be even more pronounced than this analysis shows. A more in depth analysis of this phenotype would be very interesting. The effects of CCX-CKR deletion on the production of natural IgM (a product of B1a B cells), responses to intraperitoneal challenge, responses to bacterial infection, and other markers of B1 B cell activity have yet to be carried out and may uncover a role for CCX-CKR in regulating the innate-like B cell compartment in immune responses.

7.6 CCX-CKR during the induction of cutaneous inflammation

Experiments investigating the role of CCX-CKR in the resting murine immune system showed that its deletion alters chemokine levels in a variety of tissues, including ILNs, thymus and serum, as well as cellularity at these sites, most strikingly in the peritoneal cavity but also in the ILN. In addition, subsets of myeloid cells were also identified that exhibited CCX-CKR-dependent internalisation in the WT ILN. These findings, combined with QPCR expression analysis demonstrating mRNA expression of the receptor in the skin and ILNs, suggested CCX-CKR might be involved in the response to cutaneous inflammation. A short-term model of TPA-induced skin inflammation routinely used in the lab was employed to investigate a possible role for CCX-CKR in cutaneous inflammatory responses. Furthermore, a model of DMBA/TPA-induced tumorigenesis, where papilloma formation is triggered by mutagen application and promoted by induction of chronic inflammation, was used to assess the possible role of CCX-CKR in long-term inflammation and tumour development and progression.

A number of potential roles for CCX-CKR were considered. First, as discussed above, the phenotype of the myeloid subsets identified as displaying CCX-CKR dependent internalisation of CCL19 led to speculation that they might in fact be SCMs. These cells line the inside of the LN, lying just below the capsule and acting as “gatekeepers”, monitoring cells and lymph-borne antigens and proteins entering the LN. This would provide an alternative interpretation for the expression pattern reported by Heinzl and colleagues, which they attributed to stromal cells (Heinzl et al., 2007). Expression of CCX-CKR by these cells could have a number of functions. As proposed above, CCX-CKR expression could control subcapsular movement of cells, including SCMs themselves, by regulating chemokine levels in the SCS. Chemokine from the periphery

drains to LNs via the lymph, while CCR7 ligands are highly expressed within the paracortex of the LN. SCMs line the boundary of the SCS and the B cell follicle, presenting or transferring antigen arriving from the lymph to B cells or FDCs respectively. Migration of SCMs themselves into the follicle is rare, with antigen delivery believed to be mediated by projection of long processes into the B cell follicle (Phan et al., 2009). This localisation could be controlled by tight regulation of the microenvironment of these cells. CCX-CKR expression on SCMs could be used to limit responsiveness to CCR7 ligands either from lymph or from T cell zones. DCs migrating to LNs via the lymph are trapped in the SCS in *plt/plt* mice, due to a lack of LN-expressed CCR7 ligands. Therefore, SCM could use CCX-CKR to locally regulate their chemokine environment and prevent aberrant migration from the SCS. Interestingly, at day 3 post-TPA application, the same subsets of cells displayed CCX-CKR-dependent internalisation of CCL19 as those in the resting ILN, but this was not apparent at day 6 post-TPA. This would suggest that, whatever the role of this putative CCX-CKR on these cells, it is involved at rest and during early stages of the inflammatory response but does not function in the same way at later stages. Figure 7.2 presents a model of CCX-CKR function during an immune response.

Intriguingly, the abundance of one of the affected subsets ($CD11b^{high} F4/80^{neg} CD11c^{+}$) was substantially increased in the CCX-CKR deficient ILN at day 6 post-TPA treatment, with a similar, but not statistically significant trend observed at day 3 post-TPA. This population generally has lower CD11c expression than the other myeloid population exhibiting CCX-CKR dependent internalisation of CCL19 ($CD11b^{int/high} F4/80^{low} CD11c^{+}$ cells) and is therefore more likely to include SCMs (defined as $CD11b^{+} F4/80^{neg} CD11c^{low}$, see above). However, it is important to note that this population may also include migratory DCs. It would be interesting to dissect this population further, preferably using an increased repertoire of lineage markers, to examine whether a specific subset within this population is responsible for either the CCX-CKR-dependent internalisation or the increased cellularity or both. In the case of migratory DCs, it is possible that CCX-CKR expression in the skin is involved in their retention at this site, possibly by limiting inflammation-driven increases in CCL21 expression, with deletion of the receptor leading to dysregulation of migration upon induction of inflammation.

Another potential role for CCX-CKR expression in the SCS, either by SCM or stroma, could be to control the entry of DCs and other cells from the periphery. As discussed in the Introduction, CCR7 and its ligands are important in the entry of DCs and possibly neutrophils from peripheral tissues into LN via the lymph, as well as having crucial roles in the correct positioning of leukocytes within the LN (Beauvillain et al., 2011, Förster et al.,

2008). By controlling the chemokine environment in the SCS, CCX-CKR may facilitate the directed migration of DCs, for example, into the paracortex to interact with T cells. Notably, the scavenging function of CCX-CKR *in vitro* has only been demonstrated for CCL19, so it is possible that CCX-CKR does not internalise CCL21 in the same way. It is known that full-length CCL21 does not induce the same rate of receptor internalisation and level of desensitisation through CCR7 as the more soluble CCL19. Additionally, recent work has shown that DCs can cleave full-length CCL21 into a soluble form that acts much like CCL19 through CCR7 (Schumann et al., 2010). Perhaps CCX-CKR in the SCS removes soluble CCL19 (and potentially cleaved CCL21) while full-length immobilised CCL21 remains available to CCR7⁺ cells, thus allowing random motility of entering DCs that only becomes directed once soluble CCR7 ligand from the paracortex is detected. My finding that CCL19 is increased in the CCX-CKR deficient ILN while CCL21 is slightly decreased suggests that CCX-CKR may respond to these two chemokines differently (although it should be noted that Comerford and colleagues found both chemokines to be elevated in the ILN in the absence of CCX-CKR (Comerford et al., 2010)). If CCX-CKR does indeed function to scavenge soluble CCL19 (and CCL21), in its absence the ubiquitous presence of these chemokines in both the SCS and the paracortex could impair the directional migration of these cells and decrease the efficiency of their interaction with T cells. It would be interesting to investigate whether DC localisation within the LN is perturbed in resting and/or inflamed LNs of CCX-CKR deficient animals. Histological analysis of these tissues should provide some clarity in this matter by allowing visualisation of cell positioning, and adoptive transfer of labelled DCs from WT or CCX-CKR deficient mice into WT or CCX-CKR deficient recipients would provide a useful method of investigating the effect of CCX-CKR deletion on their behaviour and localisation.

As I have observed above, CD11b^{int/high} F4/80^{low} CD11c⁺ cells were also identified as displaying CCX-CKR dependent internalisation of CCL19 in WT ILN, both in resting and inflamed ILN, although it was not observed at day 6 post-TPA treatment. This population likely includes DCs entering from the periphery that need to respond to CCR7 ligands to direct their migration into the T cell zone. Why then would these cells express CCX-CKR? Since only a small proportion of CCL19 internalisation appeared to be CCX-CKR dependent, it is possible that only a subset of these DCs express the receptor in the ILN, such as those that have recently entered the ILN. The cellularity of a second subset of myeloid cells was also affected during inflammation, namely CD11b^{int/high} F4/80^{low} CD11c⁻ cells. These cells were present in roughly equivalent proportions and numbers in resting mice, but were significantly increased in proportion in CCX-CKR deficient ILNs at both

day 3 and day 6 post-TPA treatment. More importantly, the absolute number of these cells was significantly increased in CCX-CKR deficient ILNs at day 6 post-TPA treatment, with a similar trend observed at day 3, albeit one that failed to reach statistical significance. This population clearly requires further characterisation but it may include neutrophils, which have been reported to use CCR7 to migrate to draining LNs from peripheral sites (Beauvillain et al., 2011). It is possible that, as suggested for DC subsets above, neutrophils in inflamed skin express CCX-CKR to mediate their retention at the site of inflammation until they receive a signal to downregulate the receptor and migrate to the ILN. In the absence of CCX-CKR they would have no such retention signal and might aberrantly migrate to the ILN upon induction of inflammation. Although there was no gross defect in skin inflammation as assessed by H&E staining, specific enumeration of neutrophils (and indeed DCs) in inflamed skin, either by flow cytometry or by immunohistochemistry could help to verify or refute this hypothesis. The proposed role of CCX-CKR in the inflammatory response in skin and draining LN is illustrated in Figure 7.2.

7.1 CCX-CKR influences papilloma development during a model of inflammation-driven tumorigenesis

With subtle effects of CCX-CKR deletion observed in the short-term model of cutaneous inflammation described above, and in light of the demonstrated role for CCR7 and its ligands in tumour development and metastasis to LNs, it was hypothesised that deletion of CCX-CKR might alter the progression of inflammation-driven papilloma development. Using a model already established in the lab, a post-doctoral researcher (Dr. Mairi Clarke) and I carried out a lengthy protocol to investigate this possibility. Due to time constraints and the prolonged nature of the protocol, the findings presented in this thesis are preliminary, but do provide some interesting insights into a potential role for CCX-CKR in papilloma development. Firstly, CCX-CKR deficient mice developed significantly fewer tumours than WT mice over the course of the experiment, with this difference becoming more pronounced as the model progressed. Papillomas from WT mice had less relative expression of CCX-CKR mRNA than normal adjacent skin, while the relative level of CCR7 mRNA was increased, in line with an increased proportion of leukocytes within papillomas. There was no difference in CCR7 mRNA level between WT and CCX-CKR deficient papillomas nor between WT and CCX-CKR deficient normal adjacent skin. This may be a preliminary indication that the papillomas that do form are likely to contain a similar leukocyte infiltrate in the presence or absence of CCX-CKR, although extensive

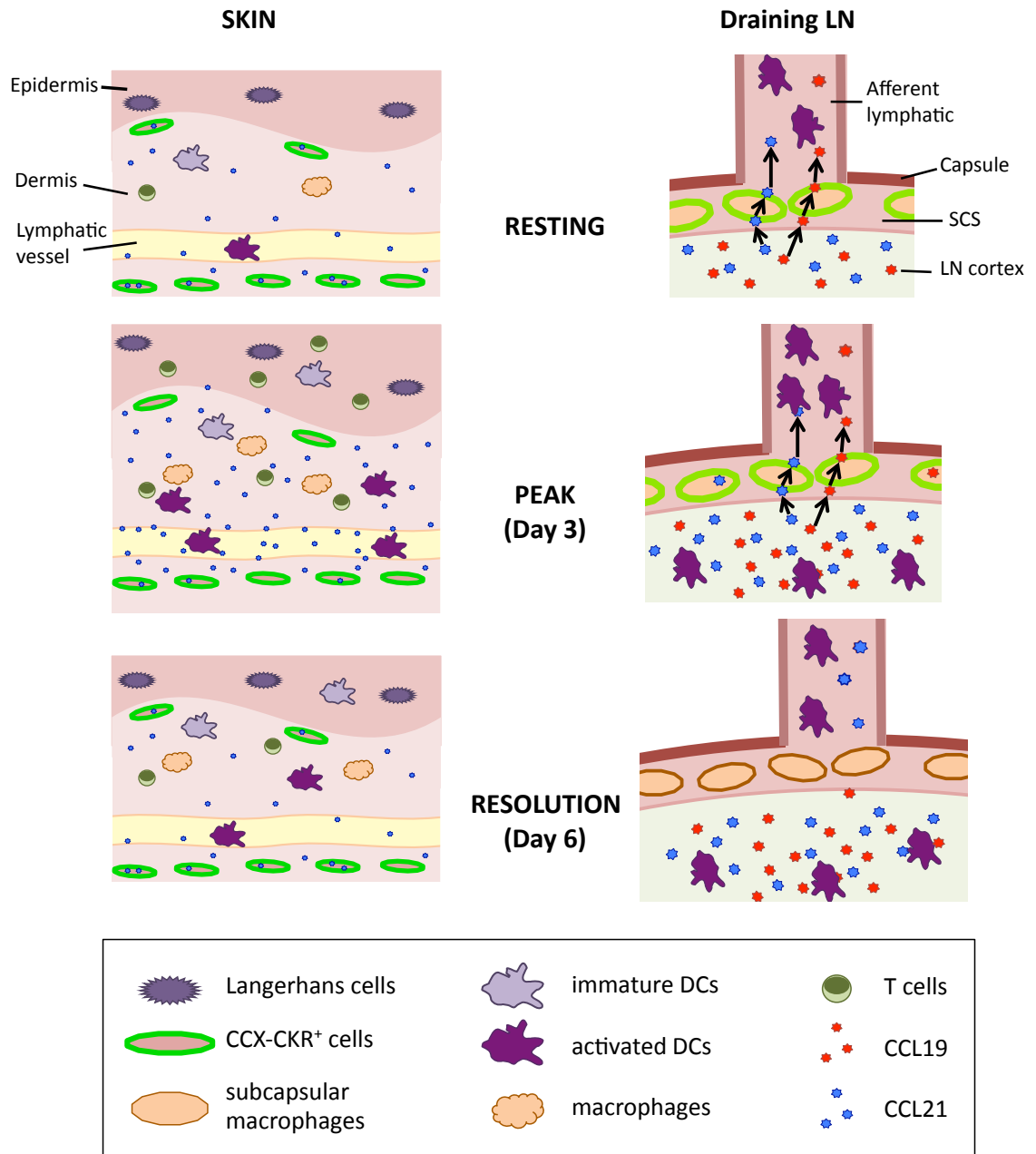


Figure 7.2: A proposed role for CCX-CKR during short-term induced cutaneous inflammation. In the skin, CCX-CKR⁺ cells (currently unidentified) regulate resting levels of CCL21, preventing aberrant migration of DCs to lymph nodes. During inflammation, CCL21 expression is elevated beyond the internalisation limit of the CCX-CKR-expressing cells, allowing rapid directed migration of activated cells to the draining lymph node. As inflammation resolves, CCX-CKR-expressing cells clear excess CCL21 from the skin until resting levels are reached and maintained. In the draining LN, CCL19 (and possibly CCL21) from the LN are presented to entering DCs, increasing directed migration into the T cell zone. During the early stages (day 3) of inflammation, this is maintained, perhaps even increased. By day 6, when skin inflammation is resolving, CCX-CKR expression is downregulated to limit the transfer of chemokine to entering DCs and reduce the level of migration, allowing the immune response to be resolved.

characterisation of papilloma cellularity, either by flow cytometry or immunohistochemistry, or both, would be necessary to confirm this. The decrease in papilloma formation in the CCX-CKR deficient mouse was matched by decreased ILN size and weight in CCX-CKR deficient tumour-burdened mice compared to their WT counterparts. Again, further characterisation of this difference is required, but it may

indicate less metastasis in the absence of CCX-CKR, possibly due to the indirect effect of reduced papilloma numbers. The role of CCX-CKR in papilloma development is uncertain, and with limited data generated thus far, theories as to how it may function are largely speculative. However, based on the subtle influence of CCX-CKR on short-term inflammation, it is possible that alterations in skin cellularity in the absence of the receptor lead to a less tumorigenic environment. See Figure 7.3 for a proposed mechanism by which CCX-CKR deletion might negatively influence papilloma formation. If, in the absence of CCX-CKR, inflammation more readily induces migration of neutrophils and DCs to draining LNs, then over time the deficit of such cells may become more pronounced. Inflammatory chemokines produced by neutrophils and other cells in the skin may be reduced as a result, leading to a decreased rate of inflammatory cell infiltrate and reduced numbers of tumours developing. The smaller size of ILN from CCX-CKR deficient papilloma-bearing mice compared to WT may also reflect not only a reduced response correlating with reduced tumour development, but also reduced capacity for tumour cell migration from skin to LN or a less efficient activation of cells within the LN in response to tumour antigens. These findings are intriguing and require much more extensive and detailed analysis to clarify the role of CCX-CKR during tumorigenesis.

7.1 Conclusions and future directions

What have we learned about the immunological role of CCX-CKR since this project began? The receptor clearly modulates chemokine levels *in vivo*, both in lymphoid and non-lymphoid tissues. The extent of this modulation and the mechanism by which it occurs is as yet unknown, although *in vitro* data provides some interesting suggestions. Cellularity is affected by deletion of CCX-CKR in some, but not all compartments. Particularly, the peritoneal cavity lymphocyte compartment is significantly disrupted. The impact this may have on response to infection, intraperitoneal challenge or natural antibody levels is unclear and experiments to examine this should provide some interesting insights into the role of CCX-CKR in immunity. Work by a previous student, Dr. E. Anderson, has uncovered a defect in intestinal immune responses in the CCX-CKR deficient mouse, which lacks the ability to develop oral tolerance to OVA and has enhanced oral priming following OVA/CT immunisation (Anderson, 2011). As peritoneal B1 cells are believed to be a major source of IgA-producing cells in the small intestine, it would be interesting to see if there could be a link between the altered peritoneal cellularity of the CCX-CKR deficient mouse and its aberrant intestinal immune responses. B cell populations have not

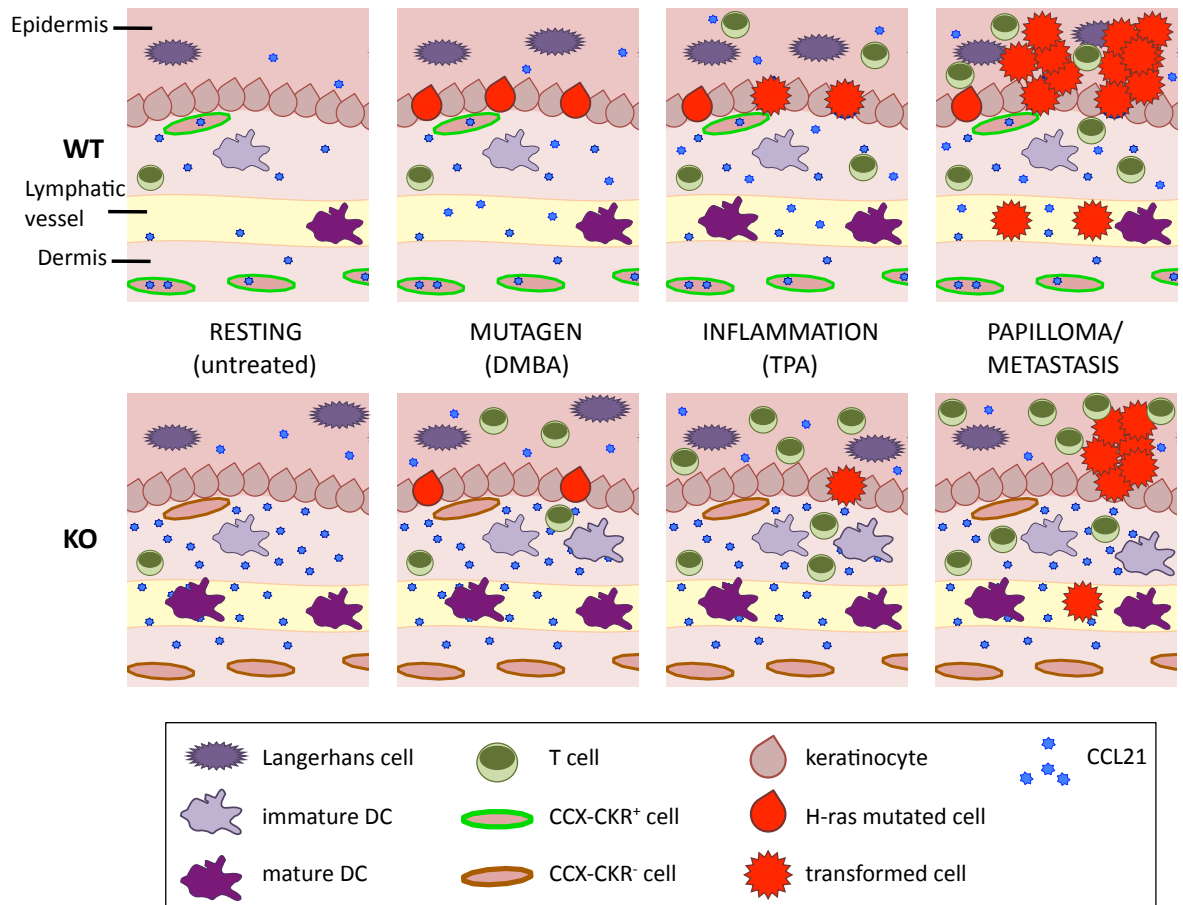


Figure 7.3: A proposed mechanism for reduced papilloma formation in the CCX-CKR deficient mouse. In resting WT skin CCX-CKR regulates the level of CCL21, limiting the steady-state migration of DCs to the draining LN. Treatment with DMBA leads to a mutation in the H-ras oncogene. Subsequent sustained inflammation induced by continuous TPA treatment causes transformation of cells with a H-ras mutation and promotes development of papilloma and metastasis of tumor cells to the draining LN. In the absence of CCX-CKR, CCL21 levels are elevated in the skin, potentially increasing the kinetics of DC immunosurveillance and leading to more rapid response to cell damage/mutation. Inflammation drives papilloma formation but this is reduced, perhaps due to an earlier response to and clearance of some mutated cells. Reduced papilloma formation may lead to reduced metastasis and therefore reduced LN size in the CCX-CKR deficient animal.

been examined in detail in the small intestine of the CCX-CKR deficient mouse and such an analysis might uncover further defects in the B cell compartment in the absence of CCX-CKR. Preliminary reports from Dr. E. Anderson in our lab show a decrease in B cell numbers in the CCX-CKR deficient small intestine (E. Anderson, pers. comm.). Another interesting finding by Anderson was that pDCs were less abundant in the absence of CCX-CKR. Specifically, she found that pDCs were largely absent from the CCX-CKR deficient MLN and reduced in the ILN, with no difference in splenic pDC numbers observed. Adoptively transferred CCX-CKR deficient pDCs appeared less efficient in entering WT MLN than transferred WT pDCs, although this work was preliminary and requires further confirmation (Anderson, 2011). Nonetheless, these findings suggest pDCs as a possible site of expression of the receptor. Alternatively, as pDCs enter LNs via HEVs using CCR7, there may simply be a defect in CCR7 ligand availability in the CCX-CKR deficient mouse

that affects the pDC population, although why it would not similarly affect naïve lymphocytes, which use the same route of LN entry, is unclear. The loss of pDCs could instead indicate a defect in survival of these cells. Further work investigating this phenomenon will hopefully provide some clarity as to its cause.

The influence of CCX-CKR on short-term induced cutaneous inflammation is limited, although there are some indications that it may control leukocyte migration from the skin to the LN. Analysis of chemokine protein levels in skin and LN during this protocol could provide insights into how this might occur. Deletion of the receptor has a more dramatic effect on the progression of inflammation-driven papilloma development, but again, this work needs to be continued and the phenomenon investigated in much more detail before we can understand the role of CCX-CKR in this process. Interestingly, Comerford and colleagues have recently described a role for CCX-CKR in suppressing the development of EAE. They showed that deletion of CCX-CKR leads to an earlier onset of, and more severe disease in EAE (Comerford et al., 2010). This phenotype can be reversed by administering neutralising anti-CCL21 antibodies, indicating that increased levels of CCL21, possibly in the central nervous system, may be responsible for the altered progression of disease (Comerford et al., 2010). The same study also showed that CCX-CKR deficient mice have increased levels of IL-23 in the spleen, corresponding to the observed enhancement of T cell priming in the spleen, and skewing of CD4⁺ T cell responses from Th1 to Th17 (Comerford et al., 2010). CCL19 and CCL21 are reported to be involved in IL-23 production by dendritic cells and expansion of Th17 cells (Kuwabara et al., 2009), and it is reasonable to hypothesise that dysregulation of CCL21 bioavailability by CCX-CKR deletion underpins the observed cytokine and T cell phenotypes. These data strongly support a role for CCX-CKR in fine regulation of the immune response through regulation of chemokine bioavailability.

Together, these studies indicate that CCX-CKR is involved in regulating the immune system, potentially by controlling chemokine levels *in vivo*, but much still needs to be done. The receptor continues to be investigated both by our group and others, and it is hoped that further study of CCX-CKR deficient mice will yield a more complete picture of the role of this receptor in shaping immune responses and pathology.

8 References

- ADDISON, C. L., BELPERIO, J. A., BURDICK, M. D. & STRIETER, R. M. 2004. Overexpression of the duffy antigen receptor for chemokines (DARC) by NSCLC tumor cells results in increased tumor necrosis. *BMC Cancer*, 4, 28.
- AIUTI, A., TAVIAN, M., CIPPONI, A., FICARA, F., ZAPPONE, E., HOXIE, J., PEAULT, B. & BORDIGNON, C. 1999. Expression of CXCR4, the receptor for stromal cell-derived factor-1 on fetal and adult human lympho-hematopoietic progenitors. *Eur J Immunol*, 29, 1823-31.
- AIUTI, A., WEBB, I. J., BLEUL, C., SPRINGER, T. & GUTIERREZ-RAMOS, J. C. 1997. The chemokine SDF-1 is a chemoattractant for human CD34+ hematopoietic progenitor cells and provides a new mechanism to explain the mobilization of CD34+ progenitors to peripheral blood. *J Exp Med*, 185, 111-20.
- AL-AOUKATY, A., SCHALL, T. J. & MAGHAZACHI, A. A. 1996. Differential coupling of CC chemokine receptors to multiple heterotrimeric G proteins in human interleukin-2-activated natural killer cells. *Blood*, 87, 4255-60.
- ALLEN, C. D. C., ANSEL, K. M., LOW, C., LESLEY, R., TAMAMURA, H., FUJII, N. & CYSTER, J. G. 2004. Germinal center dark and light zone organization is mediated by CXCR4 and CXCR5. *Nat Immunol*, 5, 943-52.
- ALLEN, S. J., CROWN, S. E. & HANDEL, T. M. 2007. Chemokine: receptor structure, interactions, and antagonism. *Annu Rev Immunol*, 25, 787-820.
- ALLENDE, M. L., DREIER, J. L., MANDALA, S. & PROIA, R. L. 2004. Expression of the sphingosine 1-phosphate receptor, S1P1, on T-cells controls thymic emigration. *J Biol Chem*, 279, 15396-401.
- ALLMAN, D. & PILLAI, S. 2008. Peripheral B cell subsets. *Curr Opin Immunol*, 20, 149-57.
- ALT, C., LASCHINGER, M. & ENGELHARDT, B. 2002. Functional expression of the lymphoid chemokines CCL19 (ELC) and CCL 21 (SLC) at the blood-brain barrier suggests their involvement in G-protein-dependent lymphocyte recruitment into the central nervous system during experimental autoimmune encephalomyelitis. *Eur J Immunol*, 32, 2133-44.
- ALUGUPALLI, K. R., LEONG, J. M., WOODLAND, R. T., MURAMATSU, M., HONJO, T. & GERSTEIN, R. M. 2004. B1b lymphocytes confer T cell-independent long-lasting immunity. *Immunity*, 21, 379-90.
- ANDERSON, E. J. R. 2011. The Role of the CCX-CKR Chemokine Receptor in Immunity and Tolerance. *PhD thesis, University of Glasgow*.
- ANDREW, D. P., SPELLBERG, J. P., TAKIMOTO, H., SCHMITS, R., MAK, T. W. & ZUKOWSKI, M. M. 1998. Transendothelial migration and trafficking of leukocytes in LFA-1-deficient mice. *Eur J Immunol*, 28, 1959-69.
- ANSEL, K. M., HARRIS, R. B. S. & CYSTER, J. G. 2002. CXCL13 is required for B1 cell homing, natural antibody production, and body cavity immunity. *Immunity*, 16, 67-76.
- ANSEL, K. M., MCHEYZER-WILLIAMS, L. J., NGO, V. N., MCHEYZER-WILLIAMS, M. G. & CYSTER, J. G. 1999. In vivo-activated CD4 T cells upregulate CXC chemokine receptor 5 and reprogram their response to lymphoid chemokines. *J Exp Med*, 190, 1123-34.
- ANSEL, K. M., NGO, V. N., HYMAN, P. L., LUTHER, S. A., FÖRSTER, R., SEDGWICK, J. D., BROWNING, J. L., LIPP, M. & CYSTER, J. G. 2000. A chemokine-driven positive feedback loop organizes lymphoid follicles. *Nature*, 406, 309-14.
- ARAI, H. & CHARO, I. F. 1996. Differential regulation of G-protein-mediated signaling by chemokine receptors. *J Biol Chem*, 271, 21814-9.

- ARBONÉS, M. L., ORD, D. C., LEY, K., RATECH, H., MAYNARD-CURRY, C., OTTEN, G., CAPON, D. J. & TEDDER, T. F. 1994. Lymphocyte homing and leukocyte rolling and migration are impaired in L-selectin-deficient mice. *Immunity*, 1, 247-60.
- ATO, M., NAKANO, H., KAKIUCHI, T. & KAYE, P. M. 2004. Localization of marginal zone macrophages is regulated by C-C chemokine ligands 21/19. *J Immunol*, 173, 4815-20.
- ATTANAVANICH, K. & KEARNEY, J. F. 2004. Marginal zone, but not follicular B cells, are potent activators of naive CD4 T cells. *J Immunol*, 172, 803-11.
- AVECILLA, S. T., HATTORI, K., HEISSIG, B., TEJADA, R., LIAO, F., SHIDO, K., JIN, D. K., DIAS, S., ZHANG, F., HARTMAN, T. E., HACKETT, N. R., CRYSTAL, R. G., WITTE, L., HICKLIN, D. J., BOHLEN, P., EATON, D., LYDEN, D., DE SAUVAGE, F. & RAFII, S. 2004. Chemokine-mediated interaction of hematopoietic progenitors with the bone marrow vascular niche is required for thrombopoiesis. *Nat Med*, 10, 64-71.
- BAEKKEVOLD, E. S., YAMANAKA, T., PALFRAMAN, R. T., CARLSEN, H. S., REINHOLT, F. P., VON ANDRIAN, U. H., BRANDTZAEG, P. & HARALDSEN, G. 2001. The CCR7 ligand elc (CCL19) is transcytosed in high endothelial venules and mediates T cell recruitment. *J Exp Med*, 193, 1105-12.
- BAJÉNOFF, M., EGEN, J. G., KOO, L. Y., LAUGIER, J. P., BRAU, F., GLAICHENHAUS, N. & GERMAIN, R. N. 2006. Stromal cell networks regulate lymphocyte entry, migration, and territoriality in lymph nodes. *Immunity*, 25, 989-1001.
- BAJÉNOFF, M. & GERMAIN, R. N. 2009. B-cell follicle development remodels the conduit system and allows soluble antigen delivery to follicular dendritic cells. *Blood*, 114, 4989-97.
- BANAS, B., WÖRNLE, M., BERGER, T., NELSON, P. J., COHEN, C. D., KRETZLER, M., PFIRSTINGER, J., MACK, M., LIPP, M., GRÖNE, H.-J. & SCHLÖNDORFF, D. 2002. Roles of SLC/CCL21 and CCR7 in human kidney for mesangial proliferation, migration, apoptosis, and tissue homeostasis. *J Immunol*, 168, 4301-7.
- BANAS, B., WÖRNLE, M., MERKLE, M., GONZALEZ-RUBIO, M., SCHMID, H., KRETZLER, M., PIETRZYK, M. C., FINK, M., PEREZ DE LEMA, G. & SCHLÖNDORFF, D. 2004. Binding of the chemokine SLC/CCL21 to its receptor CCR7 increases adhesive properties of human mesangial cells. *Kidney Int*, 66, 2256-63.
- BANCHEREAU, J., BRIERE, F., CAUX, C., DAVOUST, J., LEBECQUE, S., LIU, Y. J., PULENDRAN, B. & PALUCKA, K. 2000. Immunobiology of dendritic cells. *Annu Rev Immunol*, 18, 767-811.
- BANCHEREAU, J. & STEINMAN, R. M. 1998. Dendritic cells and the control of immunity. *Nature*, 392, 245-52.
- BARDI, G., LIPP, M. & BAGGIOLINI, M. 2001. The T cell chemokine receptor CCR7 is internalized on stimulation with ELC, but not with SLC. *European Journal of ...*
- BARGATZE, R. F., JUTILA, M. A. & BUTCHER, E. C. 1995. Distinct roles of L-selectin and integrins alpha 4 beta 7 and LFA-1 in lymphocyte homing to Peyer's patch-HEV in situ: the multistep model confirmed and refined. *Immunity*, 3, 99-108.
- BEAUVILLAIN, C., CUNIN, P., DONI, A., SCOTET, M., JAILLON, S., LOIRY, M.-L., MAGISTRELLI, G., MASTERNAK, K., CHEVAILLER, A., DELNESTE, Y. & JEANNIN, P. 2011. CCR7 is involved in the migration of neutrophils to lymph nodes. *Blood*, 117, 1196-204.
- BELL, D., YOUNG, J. W. & BANCHEREAU, J. 1999. Dendritic cells. *Adv Immunol*, 72, 255-324.
- BENDELAC, A., BONNEVILLE, M. & KEARNEY, J. F. 2001. Autoreactivity by design: innate B and T lymphocytes. *Nat Rev Immunol*, 1, 177-86.

- BENNOUNA, S., BLISS, S. K., CURIEL, T. J. & DENKERS, E. Y. 2003. Cross-talk in the innate immune system: neutrophils instruct recruitment and activation of dendritic cells during microbial infection. *J Immunol*, 171, 6052-8.
- BERAHOVICH, R. D., MIAO, Z., WANG, Y., PREMACK, B., HOWARD, M. C. & SCHALL, T. J. 2005. Proteolytic activation of alternative CCR1 ligands in inflammation. *J Immunol*, 174, 7341-51.
- BERAHOVICH, R. D., ZABEL, B. A., PENFOLD, M. E. T., LEWÉN, S., WANG, Y., MIAO, Z., GAN, L., PEREDA, J., DIAS, J., SLUKVIN, I. I., MCGRATH, K. E., JAEN, J. C. & SCHALL, T. J. 2010. CXCR7 protein is not expressed on human or mouse leukocytes. *J Immunol*, 185, 5130-9.
- BERBERICH, S., FÖRSTER, R. & PABST, O. 2007. The peritoneal microenvironment commits B cells to home to body cavities and the small intestine. *Blood*, 109, 4627-34.
- BERLIN, C., BERG, E. L., BRISKIN, M. J., ANDREW, D. P., KILSHAW, P. J., HOLZMANN, B., WEISSMAN, I. L., HAMANN, A. & BUTCHER, E. C. 1993. Alpha 4 beta 7 integrin mediates lymphocyte binding to the mucosal vascular addressin MAdCAM-1. *Cell*, 74, 185-95.
- BERRES, M.-L., TRAUTWEIN, C., ZALDIVAR, M. M., SCHMITZ, P., PAUELS, K., LIRA, S. A., TACKE, F. & WASMUTH, H. E. 2009. The chemokine scavenging receptor D6 limits acute toxic liver injury in vivo. *Biol Chem*, 390, 1039-45.
- BIRKENBACH, M., JOSEFSEN, K., YALAMANCHILI, R., LENOIR, G. & KIEFF, E. 1993. Epstein-Barr virus-induced genes: first lymphocyte-specific G protein-coupled peptide receptors. *J Virol*, 67, 2209-20.
- BLEUL, C. C. & BOEHM, T. 2000. Chemokines define distinct microenvironments in the developing thymus. *Eur J Immunol*, 30, 3371-9.
- BOLDAJIPOUR, B., MAHABALESHWAR, H., KARDASH, E., REICHMAN-FRIED, M., BLASER, H., MININA, S., WILSON, D., XU, Q. & RAZ, E. 2008. Control of chemokine-guided cell migration by ligand sequestration. *Cell*, 132, 463-73.
- BONECCHI, R., LOCATI, M., GALLIERA, E., VULCANO, M., SIRONI, M., FRA, A. M., GOBBI, M., VECCHI, A., SOZZANI, S., HARIBABU, B., VAN DAMME, J. & MANTOVANI, A. 2004. Differential recognition and scavenging of native and truncated macrophage-derived chemokine (macrophage-derived chemokine/CC chemokine ligand 22) by the D6 decoy receptor. *J Immunol*, 172, 4972-6.
- BOOS, M. D., YOKOTA, Y., EBERL, G. & KEE, B. L. 2007. Mature natural killer cell and lymphoid tissue-inducing cell development requires Id2-mediated suppression of E protein activity. *J Exp Med*, 204, 1119-30.
- BORDON, Y., HANSELL, C. A. H., SESTER, D. P., CLARKE, M., MOWAT, A. M. & NIBBS, R. J. B. 2009. The atypical chemokine receptor D6 contributes to the development of experimental colitis. *J Immunol*, 182, 5032-40.
- BORRONI, E. M., MANTOVANI, A., LOCATI, M. & BONECCHI, R. 2010. Chemokine receptors intracellular trafficking. *Pharmacol Ther*, 127, 1-8.
- BOUNEAUD, C., KOURILSKY, P. & BOUSSO, P. 2000. Impact of negative selection on the T cell repertoire reactive to a self-peptide: a large fraction of T cell clones escapes clonal deletion. *Immunity*, 13, 829-40.
- BOYD, R. L., TUCEK, C. L., GODFREY, D. I., IZON, D. J., WILSON, T. J., DAVIDSON, N. J., BEAN, A. G., LADYMAN, H. M., RITTER, M. A. & HUGO, P. 1993. The thymic microenvironment. *Immunol Today*, 14, 445-59.
- BRANDES, M., WILLIMANN, K., BIOLEY, G., LÉVY, N., EBERL, M., LUO, M., TAMPÉ, R., LÉVY, F., ROMERO, P. & MOSER, B. 2009. Cross-presenting human gammadelta T cells induce robust CD8+ alphabeta T cell responses. *Proc Natl Acad Sci USA*, 106, 2307-12.
- BRANDES, M., WILLIMANN, K. & MOSER, B. 2005. Professional antigen-presentation function by human gammadelta T Cells. *Science*, 309, 264-8.
- BRENDOLAN, A., ROSADO, M. M., CARSETTI, R., SELLERI, L. & DEAR, T. N. 2007. Development and function of the mammalian spleen. *Bioessays*, 29, 166-77.

- BRILES, D. E., NAHM, M., SCHROER, K., DAVIE, J., BAKER, P., KEARNEY, J. & BARLETTA, R. 1981. Antiphosphocholine antibodies found in normal mouse serum are protective against intravenous infection with type 3 streptococcus pneumoniae. *J Exp Med*, 153, 694-705.
- BRINKMANN, V., REICHARD, U., GOOSMANN, C., FAULER, B., UHLEMANN, Y., WEISS, D. S., WEINRAUCH, Y. & ZYCHLINSKY, A. 2004. Neutrophil extracellular traps kill bacteria. *Science*, 303, 1532-5.
- BRITSCHGI, M. R., LINK, A., LISSANDRIN, T. K. A. & LUTHER, S. A. 2008. Dynamic modulation of CCR7 expression and function on naive T lymphocytes in vivo. *J Immunol*, 181, 7681-8.
- BURNS, J. M., SUMMERS, B. C., WANG, Y., MELIKIAN, A., BERAHOVICH, R., MIAO, Z., PENFOLD, M. E. T., SUNSHINE, M. J., LITTMAN, D. R., KUO, C. J., WEI, K., MCMASTER, B. E., WRIGHT, K., HOWARD, M. C. & SCHALL, T. J. 2006. A novel chemokine receptor for SDF-1 and I-TAC involved in cell survival, cell adhesion, and tumor development. *J Exp Med*, 203, 2201-13.
- BYERS, M. A., CALLOWAY, P. A., SHANNON, L., CUNNINGHAM, H. D., SMITH, S., LI, F., FASSOLD, B. C. & VINES, C. M. 2008. Arrestin 3 mediates endocytosis of CCR7 following ligation of CCL19 but not CCL21. *J Immunol*, 181, 4723-32.
- CALVI, L. M., ADAMS, G. B., WEIBRECHT, K. W., WEBER, J. M., OLSON, D. P., KNIGHT, M. C., MARTIN, R. P., SCHIPANI, E., DIVIETI, P., BRINGHURST, F. R., MILNER, L. A., KRONENBERG, H. M. & SCADDEN, D. T. 2003. Osteoblastic cells regulate the haematopoietic stem cell niche. *Nature*, 425, 841-6.
- CAMPANELLA, G. S. V., LEE, E. M. J., SUN, J. & LUSTER, A. D. 2003. CXCR3 and heparin binding sites of the chemokine IP-10 (CXCL10). *J Biol Chem*, 278, 17066-74.
- CAMPBELL, D. J. & BUTCHER, E. C. 2002. Rapid acquisition of tissue-specific homing phenotypes by CD4(+) T cells activated in cutaneous or mucosal lymphoid tissues. *J Exp Med*, 195, 135-41.
- CAMPBELL, D. J., KIM, C. H. & BUTCHER, E. C. 2003. Chemokines in the systemic organization of immunity. *Immunol Rev*, 195, 58-71.
- CAMPBELL, J. J., BOWMAN, E. P., MURPHY, K., YOUNGMAN, K. R., SIANI, M. A., THOMPSON, D. A., WU, L., ZLOTNIK, A. & BUTCHER, E. C. 1998. 6-C-kine (SLC), a lymphocyte adhesion-triggering chemokine expressed by high endothelium, is an agonist for the MIP-3beta receptor CCR7. *J Cell Biol*, 141, 1053-9.
- CARDONA, A. E., SASSE, M. E., LIU, L., CARDONA, S. M., MIZUTANI, M., SAVARIN, C., HU, T. & RANSOHOFF, R. M. 2008. Scavenging roles of chemokine receptors: chemokine receptor deficiency is associated with increased levels of ligand in circulation and tissues. *Blood*, 112, 256-63.
- CARRAMOLINO, L., ZABALLOS, A., KREMER, L., VILLARES, R., MARTÍN, P., ARDAVÍN, C., MARTÍNEZ-A, C. & MÁRQUEZ, G. 2001. Expression of CCR9 beta-chemokine receptor is modulated in thymocyte differentiation and is selectively maintained in CD8(+) T cells from secondary lymphoid organs. *Blood*, 97, 850-7.
- CASAMAYOR-PALLEJÀ, M., MONDIÈRE, P., VERSCHELDE, C., BELLA, C. & DEFRANCE, T. 2002. BCR ligation reprograms B cells for migration to the T zone and B-cell follicle sequentially. *Blood*, 99, 1913-21.
- CHAMPION, S., IMHOF, B. A., SAVAGNER, P. & THIERY, J. P. 1986. The embryonic thymus produces chemotactic peptides involved in the homing of hemopoietic precursors. *Cell*, 44, 781-90.
- CHAN, O. T., MADAIO, M. P. & SHLOMCHIK, M. J. 1999. The central and multiple roles of B cells in lupus pathogenesis. *Immunol Rev*, 169, 107-21.

- CHAPMAN, G. A., MOORES, K. E., GOHIL, J., BERKHOUT, T. A., PATEL, L., GREEN, P., MACPHEE, C. H. & STEWART, B. R. 2000. The role of fractalkine in the recruitment of monocytes to the endothelium. *Eur J Pharmacol*, 392, 189-95.
- CHAUDHURI, A., NIELSEN, S., ELKJAER, M. L., ZBRZEZNA, V., FANG, F. & POGO, A. O. 1997. Detection of Duffy antigen in the plasma membranes and caveolae of vascular endothelial and epithelial cells of nonerythroid organs. *Blood*, 89, 701-12.
- CINAMON, G., MATLOUBIAN, M., LESNESKI, M. J., XU, Y., LOW, C., LU, T., PROIA, R. L. & CYSTER, J. G. 2004. Sphingosine 1-phosphate receptor 1 promotes B cell localization in the splenic marginal zone. *Nat Immunol*, 5, 713-20.
- CINAMON, G., ZACHARIAH, M. A., LAM, O. M., FOSS, F. W. & CYSTER, J. G. 2008. Follicular shuttling of marginal zone B cells facilitates antigen transport. *Nat Immunol*, 9, 54-62.
- CLAING, A., LAPORTE, S. A., CARON, M. G. & LEFKOWITZ, R. J. 2002. Endocytosis of G protein-coupled receptors: roles of G protein-coupled receptor kinases and beta-arrestin proteins. *Prog Neurobiol*, 66, 61-79.
- CLARK, E. A. & LEDBETTER, J. A. 1994. How B and T cells talk to each other. *Nature*, 367, 425-8.
- CLARK-LEWIS, I., KIM, K. S., RAJARATHNAM, K., GONG, J. H., DEWALD, B., MOSER, B., BAGGIOLINI, M. & SYKES, B. D. 1995. Structure-activity relationships of chemokines. *J Leukoc Biol*, 57, 703-11.
- COMERFORD, I. 2005. Functional analysis of the chemokine receptor, CCX-CKR. *PhD thesis, University of Glasgow*.
- COMERFORD, I., LITCHFIELD, W., HARATA-LEE, Y., NIBBS, R. J. B. & MCCOLL, S. R. 2007. Regulation of chemotactic networks by 'atypical' receptors. *Bioessays*, 29, 237-47.
- COMERFORD, I., MILASTA, S., MORROW, V., MILLIGAN, G. & NIBBS, R. 2006. The chemokine receptor CCX-CKR mediates effective scavenging of CCL19 in vitro. *Eur J Immunol*, 36, 1904-16.
- COMERFORD, I., NIBBS, R. J., LITCHFIELD, W., BUNTING, M., HARATA-LEE, Y., HAYLOCK-JACOBS, S., FORROW, S., KORNER, H. & MCCOLL, S. R. 2010. The atypical chemokine receptor CCX-CKR scavenges homeostatic chemokines in circulation and tissues and suppresses Th17 responses. *Blood*.
- COMERFORD, I. & NIBBS, R. J. B. 2005. Post-translational control of chemokines: a role for decoy receptors? *Immunol Lett*, 96, 163-74.
- CONLEY, M. E., PAROLINI, O., ROHRER, J. & CAMPANA, D. 1994. X-linked agammaglobulinemia: new approaches to old questions based on the identification of the defective gene. *Immunol Rev*, 138, 5-21.
- COTTON, M. & CLAING, A. 2009. G protein-coupled receptors stimulation and the control of cell migration. *Cell Signal*, 21, 1045-53.
- COXON, A., TANG, T. & MAYADAS, T. N. 1999. Cytokine-activated endothelial cells delay neutrophil apoptosis in vitro and in vivo. A role for granulocyte/macrophage colony-stimulating factor. *J Exp Med*, 190, 923-34.
- CUFF, C. A., SACCA, R. & RUDDLE, N. H. 1999. Differential induction of adhesion molecule and chemokine expression by LTA α 3 and LTA β in inflammation elucidates potential mechanisms of mesenteric and peripheral lymph node development. *J Immunol*, 162, 5965-72.
- CUPEDO, T., JANSEN, W., KRAAL, G. & MEBIUS, R. E. 2004. Induction of secondary and tertiary lymphoid structures in the skin. *Immunity*, 21, 655-67.
- CURNOCK, A. P., SOTSIOS, Y., WRIGHT, K. L. & WARD, S. G. 2003. Optimal chemotactic responses of leukemic T cells to stromal cell-derived factor-1 requires the activation of both class IA and IB phosphoinositide 3-kinases. *J Immunol*, 170, 4021-30.

- CUTBUSH, M., MOLLISON, P. & PARKIN, D. 1950. A new human blood group. *Nature*.
- CYSTER, J. G. 2000. Leukocyte migration: scent of the T zone. *Curr Biol*, 10, R30-3.
- CYSTER, J. G. 2005. Chemokines, sphingosine-1-phosphate, and cell migration in secondary lymphoid organs. *Annu Rev Immunol*, 23, 127-59.
- CYSTER, J. G., ANSEL, K. M., REIF, K., EKLAND, E. H., HYMAN, P. L., TANG, H. L., LUTHER, S. A. & NGO, V. N. 2000. Follicular stromal cells and lymphocyte homing to follicles. *Immunol Rev*, 176, 181-93.
- D'APUZZO, M., ROLINK, A., LOETSCHER, M., HOXIE, J. A., CLARK-LEWIS, I., MELCHERS, F., BAGGIOLINI, M. & MOSER, B. 1997. The chemokine SDF-1, stromal cell-derived factor 1, attracts early stage B cell precursors via the chemokine receptor CXCR4. *Eur J Immunol*, 27, 1788-93.
- DARBONNE, W. C., RICE, G. C., MOHLER, M. A., APPLE, T., HÉBERT, C. A., VALENTE, A. J. & BAKER, J. B. 1991. Red blood cells are a sink for interleukin 8, a leukocyte chemotaxin. *J Clin Invest*, 88, 1362-9.
- DAVALOS-MISSLITZ, A. C. M., RIECKENBERG, J., WILLENZON, S., WORBS, T., KREMMER, E., BERNHARDT, G. & FÖRSTER, R. 2007a. Generalized multi-organ autoimmunity in CCR7-deficient mice. *Eur J Immunol*, 37, 613-22.
- DAVALOS-MISSLITZ, A. C. M., WORBS, T., WILLENZON, S., BERNHARDT, G. & FÖRSTER, R. 2007b. Impaired responsiveness to T-cell receptor stimulation and defective negative selection of thymocytes in CCR7-deficient mice. *Blood*, 110, 4351-9.
- DAWSON, T. C., LENTSCH, A. B., WANG, Z., COWHIG, J. E., ROT, A., MAEDA, N. & PEIPER, S. C. 2000. Exaggerated response to endotoxin in mice lacking the Duffy antigen/receptor for chemokines (DARC). *Blood*, 96, 1681-4.
- DE JONG, E. K., DIJKSTRA, I. M., HENSENS, M., BROUWER, N., VAN AMERONGEN, M., LIEM, R. S. B., BODDEKE, H. W. G. M. & BIBER, K. 2005. Vesicle-mediated transport and release of CCL21 in endangered neurons: a possible explanation for microglia activation remote from a primary lesion. *J Neurosci*, 25, 7548-57.
- DE PAZ, J. L., MOSEMAN, E. A., NOTI, C., POLITO, L., VON ANDRIAN, U. H. & SEEBERGER, P. H. 2007. Profiling heparin-chemokine interactions using synthetic tools. *ACS Chem Biol*, 2, 735-44.
- DE TOGNI, P., GOELLNER, J., RUDDLE, N. H., STREETER, P. R., FICK, A., MARIATHASAN, S., SMITH, S. C., CARLSON, R., SHORNICK, L. P. & STRAUSS-SCHOENBERGER, J. 1994. Abnormal development of peripheral lymphoid organs in mice deficient in lymphotoxin. *Science*, 264, 703-7.
- DEJARDIN, E., DROIN, N. M., DELHASE, M., HAAS, E., CAO, Y., MAKRIS, C., LI, Z.-W., KARIN, M., WARE, C. F. & GREEN, D. R. 2002. The lymphotoxin-beta receptor induces different patterns of gene expression via two NF-kappaB pathways. *Immunity*, 17, 525-35.
- DEVALARAJA, M. N. & RICHMOND, A. 1999. Multiple chemotactic factors: fine control or redundancy? *Trends Pharmacol Sci*, 20, 151-6.
- DI LIBERTO, D., LOCATI, M., CACCAMO, N., VECCHI, A., MERAVIGLIA, S., SALERNO, A., SIRECI, G., NEBULONI, M., CACERES, N., CARDONA, P.-J., DIELI, F. & MANTOVANI, A. 2008. Role of the chemokine decoy receptor D6 in balancing inflammation, immune activation, and antimicrobial resistance in *Mycobacterium tuberculosis* infection. *J Exp Med*, 205, 2075-84.
- DIJKSTRA, I. M., HULSHOF, S., VAN DER VALK, P., BODDEKE, H. W. G. M. & BIBER, K. 2004. Cutting edge: activity of human adult microglia in response to CC chemokine ligand 21. *J Immunol*, 172, 2744-7.
- DOUGALL, W. C., GLACCUM, M., CHARRIER, K., ROHRBACH, K., BRASEL, K., DE SMEDT, T., DARO, E., SMITH, J., TOMETSKO, M. E., MALISZEWSKI, C. R., ARMSTRONG, A., SHEN, V., BAIN, S., COSMAN, D., ANDERSON, D.,

- MORRISSEY, P. J., PESCHON, J. J. & SCHUH, J. 1999. RANK is essential for osteoclast and lymph node development. *Genes Dev*, 13, 2412-24.
- DUTT, P., WANG, J. F. & GROOPMAN, J. E. 1998. Stromal cell-derived factor-1 alpha and stem cell factor/kit ligand share signaling pathways in hemopoietic progenitors: a potential mechanism for cooperative induction of chemotaxis. *J Immunol*, 161, 3652-8.
- EGAWA, T., KAWABATA, K., KAWAMOTO, H., AMADA, K., OKAMOTO, R., FUJII, N., KISHIMOTO, T., KATSURA, Y. & NAGASAWA, T. 2001. The earliest stages of B cell development require a chemokine stromal cell-derived factor/pre-B cell growth-stimulating factor. *Immunity*, 15, 323-34.
- EHRENSTEIN, M. R. & NOTLEY, C. A. 2010. The importance of natural IgM: scavenger, protector and regulator. *Nat Rev Immunol*, 10, 778-86.
- FANG, L., LEE, V. C., CHA, E., ZHANG, H. & HWANG, S. T. 2008. CCR7 regulates B16 murine melanoma cell tumorigenesis in skin. *J Leukoc Biol*, 84, 965-72.
- FINKE, D., ACHA-ORBEA, H., MATTIS, A., LIPP, M. & KRAEHEBUHL, J. 2002. CD4+CD3- cells induce Peyer's patch development: role of alpha4beta1 integrin activation by CXCR5. *Immunity*, 17, 363-73.
- FINKELMAN, F. D. 2010. Peanut allergy and anaphylaxis. *Curr Opin Immunol*, 22, 783-8.
- FISCHER, A. M., MERCER, J. C., IYER, A., RAGIN, M. J. & AUGUST, A. 2004. Regulation of CXC chemokine receptor 4-mediated migration by the Tec family tyrosine kinase ITK. *J Biol Chem*, 279, 29816-20.
- FLO, T. H., SMITH, K. D., SATO, S., RODRIGUEZ, D. J., HOLMES, M. A., STRONG, R. K., AKIRA, S. & ADEREM, A. 2004. Lipocalin 2 mediates an innate immune response to bacterial infection by sequestering iron. *Nature*, 432, 917-21.
- FÖRSTER, R., DAVALOS-MISLITZ, A. C. & ROT, A. 2008. CCR7 and its ligands: balancing immunity and tolerance. *Nat Rev Immunol*, 8, 362-71.
- FÖRSTER, R., MATTIS, A. E., KREMMER, E., WOLF, E., BREM, G. & LIPP, M. 1996. A putative chemokine receptor, BLR1, directs B cell migration to defined lymphoid organs and specific anatomic compartments of the spleen. *Cell*, 87, 1037-47.
- FÖRSTER, R., SCHUBEL, A., BREITFELD, D., KREMMER, E., RENNER-MÜLLER, I., WOLF, E. & LIPP, M. 1999. CCR7 coordinates the primary immune response by establishing functional microenvironments in secondary lymphoid organs. *Cell*, 99, 23-33.
- FRA, A. M., LOCATI, M., OTERO, K., SIRONI, M., SIGNORELLI, P., MASSARDI, M. L., GOBBI, M., VECCHI, A., SOZZANI, S. & MANTOVANI, A. 2003. Cutting edge: scavenging of inflammatory CC chemokines by the promiscuous putatively silent chemokine receptor D6. *J Immunol*, 170, 2279-82.
- FUKUMA, N., AKIMITSU, N., HAMAMOTO, H., KUSUHARA, H., SUGIYAMA, Y. & SEKIMIZU, K. 2003. A role of the Duffy antigen for the maintenance of plasma chemokine concentrations. *Biochem Biophys Res Commun*, 303, 137-9.
- FÜTTERER, A., MINK, K., LUZ, A., KOSCO-VILBOIS, M. H. & PFEFFER, K. 1998. The lymphotoxin beta receptor controls organogenesis and affinity maturation in peripheral lymphoid tissues. *Immunity*, 9, 59-70.
- GAINETDINOV, R. R., PREMONT, R. T., BOHN, L. M., LEFKOWITZ, R. J. & CARON, M. G. 2004. Desensitization of G protein-coupled receptors and neuronal functions. *Annu Rev Neurosci*, 27, 107-44.
- GALLIERA, E., JALA, V. R., TRENT, J. O., BONECCHI, R., SIGNORELLI, P., LEFKOWITZ, R. J., MANTOVANI, A., LOCATI, M. & HARIBABU, B. 2004. beta-Arrestin-dependent constitutive internalization of the human chemokine decoy receptor D6. *J Biol Chem*, 279, 25590-7.
- GARSIDE, P., INGULLI, E., MERICA, R. R., JOHNSON, J. G., NOELLE, R. J. & JENKINS, M. K. 1998. Visualization of specific B and T lymphocyte interactions in the lymph node. *Science*, 281, 96-9.

- GARTON, K. J., GOUGH, P. J., BLOBEL, C. P., MURPHY, G., GREAVES, D. R., DEMPSEY, P. J. & RAINES, E. W. 2001. Tumor necrosis factor- α -converting enzyme (ADAM17) mediates the cleavage and shedding of fractalkine (CX3CL1). *J Biol Chem*, 276, 37993-8001.
- GAY, D., SAUNDERS, T., CAMPER, S. & WEIGERT, M. 1993. Receptor editing: an approach by autoreactive B cells to escape tolerance. *J Exp Med*, 177, 999-1008.
- GEIJTENBEEK, T. B. H., GROOT, P. C., NOLTE, M. A., VAN VLIET, S. J., GANGARAM-PANDAY, S. T., VAN DUIJNHOFEN, G. C. F., KRAAL, G., VAN OOSTERHOUT, A. J. M. & VAN KOOYK, Y. 2002. Marginal zone macrophages express a murine homologue of DC-SIGN that captures blood-borne antigens in vivo. *Blood*, 100, 2908-16.
- GHOSH, E. E. B., YANG, Y., TUNG, J., HERZENBERG, L. A. & HERZENBERG, L. A. 2008. CD11b expression distinguishes sequential stages of peritoneal B-1 development. *Proc Natl Acad Sci USA*, 105, 5195-200.
- GILL, J., MALIN, M., SUTHERLAND, J., GRAY, D., HOLLANDER, G. & BOYD, R. 2003. Thymic generation and regeneration. *Immunol Rev*, 195, 28-50.
- GIRARD, J. P., BAEKKEVOLD, E. S., YAMANAKA, T., HARALDSEN, G., BRANDTZAEG, P. & AMALRIC, F. 1999. Heterogeneity of endothelial cells: the specialized phenotype of human high endothelial venules characterized by suppression subtractive hybridization. *Am J Pathol*, 155, 2043-55.
- GODIN, I., GARCIA-PORRERO, J. A., DIETERLEN-LIÈVRE, F. & CUMANO, A. 1999. Stem cell emergence and hemopoietic activity are incompatible in mouse intraembryonic sites. *J Exp Med*, 190, 43-52.
- GOMEZ-NICOLA, D., PALLAS-BAZARRA, N., VALLE-ARGOS, B. & NIETO-SAMPEDRO, M. 2010. CCR7 is expressed in astrocytes and upregulated after an inflammatory injury. *J Neuroimmunol*, 227, 87-92.
- GONG, J. H. & CLARK-LEWIS, I. 1995. Antagonists of monocyte chemoattractant protein 1 identified by modification of functionally critical NH₂-terminal residues. *J Exp Med*, 181, 631-40.
- GOSLING, J., DAIRAGHI, D. J., WANG, Y., HANLEY, M., TALBOT, D., MIAO, Z. & SCHALL, T. J. 2000. Cutting edge: identification of a novel chemokine receptor that binds dendritic cell- and T cell-active chemokines including ELC, SLC, and TECK. *J Immunol*, 164, 2851-6.
- GOUGH, P. J., GARTON, K. J., WILLE, P. T., RYCHLEWSKI, M., DEMPSEY, P. J. & RAINES, E. W. 2004. A disintegrin and metalloproteinase 10-mediated cleavage and shedding regulates the cell surface expression of CXC chemokine ligand 16. *J Immunol*, 172, 3678-85.
- GRADY, E. F., BÖHM, S. K. & BUNNETT, N. W. 1997. Turning off the signal: mechanisms that attenuate signaling by G protein-coupled receptors. *Am J Physiol*, 273, G586-601.
- GRAHAM, G. J., MACKENZIE, J., LOWE, S., TSANG, M. L., WEATHERBEE, J. A., ISSACSON, A., MEDICHERLA, J., FANG, F., WILKINSON, P. C. & PRAGNELL, I. B. 1994. Aggregation of the chemokine MIP-1 α is a dynamic and reversible phenomenon. Biochemical and biological analyses. *J Biol Chem*, 269, 4974-8.
- GUAN, E., WANG, J. & NORCROSS, M. A. 2004. Amino-terminal processing of MIP-1 β /CCL4 by CD26/dipeptidyl-peptidase IV. *J Cell Biochem*, 92, 53-64.
- GUAN, E., WANG, J., RODERIQUEZ, G. & NORCROSS, M. A. 2002. Natural truncation of the chemokine MIP-1 β /CCL4 affects receptor specificity but not anti-HIV-1 activity. *J Biol Chem*, 277, 32348-52.
- GUNN, M. D., KYUWA, S., TAM, C., KAKIUCHI, T., MATSUZAWA, A., WILLIAMS, L. T. & NAKANO, H. 1999. Mice lacking expression of secondary lymphoid organ chemokine have defects in lymphocyte homing and dendritic cell localization. *J Exp Med*, 189, 451-60.

- GUNN, M. D., TANGEMANN, K., TAM, C., CYSTER, J. G., ROSEN, S. D. & WILLIAMS, L. T. 1998. A chemokine expressed in lymphoid high endothelial venules promotes the adhesion and chemotaxis of naive T lymphocytes. *Proc Natl Acad Sci USA*, 95, 258-63.
- HA, S.-A., TSUJI, M., SUZUKI, K., MEEK, B., YASUDA, N., KAISHO, T. & FAGARASAN, S. 2006. Regulation of B1 cell migration by signals through Toll-like receptors. *J Exp Med*, 203, 2541-50.
- HAAS, K. M., POE, J. C., STEEBER, D. A. & TEDDER, T. F. 2005. B-1a and B-1b cells exhibit distinct developmental requirements and have unique functional roles in innate and adaptive immunity to *S. pneumoniae*. *Immunity*, 23, 7-18.
- HADLEY, T. J., LU, Z. H., WASNIOWSKA, K., MARTIN, A. W., PEIPER, S. C., HESSELGESSER, J. & HORUK, R. 1994. Postcapillary venule endothelial cells in kidney express a multispecific chemokine receptor that is structurally and functionally identical to the erythroid isoform, which is the Duffy blood group antigen. *J Clin Invest*, 94, 985-91.
- HAMANN, A., JABLONSKI-WESTRICH, D., DUIJVESTIJN, A., BUTCHER, E. C., BAISCH, H., HARDER, R. & THIELE, H. G. 1988. Evidence for an accessory role of LFA-1 in lymphocyte-high endothelium interaction during homing. *J Immunol*, 140, 693-9.
- HANDEL, T. M., JOHNSON, Z., CROWN, S. E., LAU, E. K. & PROUDFOOT, A. E. 2005. Regulation of protein function by glycosaminoglycans--as exemplified by chemokines. *Annu Rev Biochem*, 74, 385-410.
- HANSELL, C. A. H., HURSON, C. E. & NIBBS, R. J. B. 2011a. DARC and D6: silent partners in chemokine regulation? *Immunol Cell Biol*, 89, 197-206.
- HANSELL, C. A. H., SCHIERING, C., KINSTRIE, R., FORD, L., BORDON, Y., MCINNES, I. B., GOODYEAR, C. S. & NIBBS, R. J. B. 2011b. Universal expression and dual function of the atypical chemokine receptor D6 on innate-like B cells in mice. *Blood*.
- HARDY, R. R. & HAYAKAWA, K. 2001. B cell development pathways. *Annu Rev Immunol*, 19, 595-621.
- HARGREAVES, D. C., HYMAN, P. L., LU, T. T., NGO, V. N., BIDGOL, A., SUZUKI, G., ZOU, Y. R., LITTMAN, D. R. & CYSTER, J. G. 2001. A coordinated change in chemokine responsiveness guides plasma cell movements. *J Exp Med*, 194, 45-56.
- HARTMANN, T. N., LEICK, M., EWERS, S., DIEFENBACHER, A., SCHRAUFSTATTER, I., HONCZARENKO, M. & BURGER, M. 2008. Human B cells express the orphan chemokine receptor CRAM-A/B in a maturation-stage-dependent and CCL5-modulated manner. *Immunology*, 125, 252-62.
- HASKELL, C. A., CLEARY, M. D. & CHARO, I. F. 2000. Unique role of the chemokine domain of fractalkine in cell capture. Kinetics of receptor dissociation correlate with cell adhesion. *J Biol Chem*, 275, 34183-9.
- HASTINGS, W. D., GURDAK, S. M., TUMANG, J. R. & ROTHSTEIN, T. L. 2006a. CD5⁺/Mac-1⁻ peritoneal B cells: a novel B cell subset that exhibits characteristics of B-1 cells. *Immunol Lett*, 105, 90-6.
- HASTINGS, W. D., TUMANG, J. R., BEHRENS, T. W. & ROTHSTEIN, T. L. 2006b. Peritoneal B-2 cells comprise a distinct B-2 cell population with B-1b-like characteristics. *Eur J Immunol*, 36, 1114-23.
- HAUSDORFF, W. P., CARON, M. G. & LEFKOWITZ, R. J. 1990. Turning off the signal: desensitization of beta-adrenergic receptor function. *FASEB J*, 4, 2881-9.
- HAWIGER, D., INABA, K., DORSETT, Y., GUO, M., MAHNKE, K., RIVERA, M., RAVETCH, J. V., STEINMAN, R. M. & NUSSENZWEIG, M. C. 2001. Dendritic cells induce peripheral T cell unresponsiveness under steady state conditions in vivo. *J Exp Med*, 194, 769-79.

- HAYAKAWA, K., HARDY, R. R. & HERZENBERG, L. A. 1986. Peritoneal Ly-1 B cells: genetic control, autoantibody production, increased lambda light chain expression. *Eur J Immunol*, 16, 450-6.
- HAYAKAWA, K., HARDY, R. R., HERZENBERG, L. A. & HERZENBERG, L. A. 1985. Progenitors for Ly-1 B cells are distinct from progenitors for other B cells. *J Exp Med*, 161, 1554-68.
- HAYAKAWA, K., HARDY, R. R., PARKS, D. R. & HERZENBERG, L. A. 1983. The "Ly-1 B" cell subpopulation in normal immunodeficient, and autoimmune mice. *J Exp Med*, 157, 202-18.
- HEDRICK, J. A. & ZLOTNIK, A. 1997. Identification and characterization of a novel beta chemokine containing six conserved cysteines. *J Immunol*, 159, 1589-93.
- HEINO, M., PETERSON, P., KUDOH, J., NAGAMINE, K., LAGERSTEDT, A., OVOD, V., RANKI, A., RANTALA, I., NIEMINEN, M., TUUKKANEN, J., SCOTT, H. S., ANTONARAKIS, S. E., SHIMIZU, N. & KROHN, K. 1999. Autoimmune regulator is expressed in the cells regulating immune tolerance in thymus medulla. *Biochem Biophys Res Commun*, 257, 821-5.
- HEINZEL, K., BENZ, C. & BLEUL, C. C. 2007. A silent chemokine receptor regulates steady-state leukocyte homing in vivo. *Proc Natl Acad Sci USA*, 104, 8421-6.
- HEMMERICH, S., PAAVOLA, C., BLOOM, A., BHAKTA, S., FREEDMAN, R., GRUNBERGER, D., KRSTENANSKY, J., LEE, S., MCCARLEY, D., MULKINS, M., WONG, B., PEASE, J., MIZOUE, L., MIRZADEGAN, T., POLSKY, I., THOMPSON, K., HANDEL, T. M. & JARNAGIN, K. 1999. Identification of residues in the monocyte chemoattractant protein-1 that contact the MCP-1 receptor, CCR2. *Biochemistry*, 38, 13013-25.
- HENLEY, J. R., KRUEGER, E. W., OSWALD, B. J. & MCNIVEN, M. A. 1998. Dynamin-mediated internalization of caveolae. *J Cell Biol*, 141, 85-99.
- HERNÁNDEZ-LÓPEZ, C., VARAS, A., SACEDÓN, R., JIMÉNEZ, E., MUÑOZ, J. J., ZAPATA, A. G. & VICENTE, A. 2002. Stromal cell-derived factor 1/CXCR4 signaling is critical for early human T-cell development. *Blood*, 99, 546-54.
- HINTZEN, G., OHL, L., DEL RIO, M.-L., RODRIGUEZ-BARBOSA, J.-I., PABST, O., KOCKS, J. R., KREGE, J., HARDTKE, S. & FÖRSTER, R. 2006. Induction of tolerance to innocuous inhaled antigen relies on a CCR7-dependent dendritic cell-mediated antigen transport to the bronchial lymph node. *J Immunol*, 177, 7346-54.
- HIROSE, J., KAWASHIMA, H., SWOPE WILLIS, M., SPRINGER, T. A., HASEGAWA, H., YOSHIE, O. & MIYASAKA, M. 2002. Chondroitin sulfate B exerts its inhibitory effect on secondary lymphoid tissue chemokine (SLC) by binding to the C-terminus of SLC. *Biochim Biophys Acta*, 1571, 219-24.
- HOGQUIST, K. A., BALDWIN, T. A. & JAMESON, S. C. 2005. Central tolerance: learning self-control in the thymus. *Nat Rev Immunol*, 5, 772-82.
- HOOGWERF, A. J., KUSCHERT, G. S., PROUDFOOT, A. E., BORLAT, F., CLARK-LEWIS, I., POWER, C. A. & WELLS, T. N. 1997. Glycosaminoglycans mediate cell surface oligomerization of chemokines. *Biochemistry*, 36, 13570-8.
- HÖPKEN, U. E., ACHTMAN, A. H., KRÜGER, K. & LIPP, M. 2004. Distinct and overlapping roles of CXCR5 and CCR7 in B-1 cell homing and early immunity against bacterial pathogens. *J Leukoc Biol*, 76, 709-18.
- HÖPKEN, U. E., WINTER, S., ACHTMAN, A. H., KRÜGER, K. & LIPP, M. 2010. CCR7 regulates lymphocyte egress and recirculation through body cavities. *J Leukoc Biol*, 87, 671-82.
- HORUK, R., CHITNIS, C. E., DARBONNE, W. C., COLBY, T. J., RYBICKI, A., HADLEY, T. J. & MILLER, L. H. 1993. A receptor for the malarial parasite *Plasmodium vivax*: the erythrocyte chemokine receptor. *Science*, 261, 1182-4.
- IWATA, M., HIRAKIYAMA, A., ESHIMA, Y., KAGECHIKA, H., KATO, C. & SONG, S.-Y. 2004. Retinoic acid imprints gut-homing specificity on T cells. *Immunity*, 21, 527-38.

- JAMIESON, T., COOK, D. N., NIBBS, R. J. B., ROT, A., NIXON, C., MCLEAN, P., ALCAMI, A., LIRA, S. A., WIEKOWSKI, M. & GRAHAM, G. J. 2005. The chemokine receptor D6 limits the inflammatory response in vivo. *Nat Immunol*, 6, 403-11.
- JANG, M. H., SOUGAWA, N., TANAKA, T., HIRATA, T., HIROI, T., TOHYA, K., GUO, Z., UMEMOTO, E., EBISUNO, Y., YANG, B.-G., SEOH, J.-Y., LIPP, M., KIYONO, H. & MIYASAKA, M. 2006. CCR7 is critically important for migration of dendritic cells in intestinal lamina propria to mesenteric lymph nodes. *J Immunol*, 176, 803-10.
- JARNAGIN, K., GRUNBERGER, D., MULKINS, M., WONG, B., HEMMERICH, S., PAAVOLA, C., BLOOM, A., BHAKTA, S., DIEHL, F., FREEDMAN, R., MCCARLEY, D., POLSKY, I., PING-TSOU, A., KOSAKA, A. & HANDEL, T. M. 1999. Identification of surface residues of the monocyte chemotactic protein 1 that affect signaling through the receptor CCR2. *Biochemistry*, 38, 16167-77.
- JENH, C. H., COX, M. A., KAMINSKI, H., ZHANG, M., BYRNES, H., FINE, J., LUNDELL, D., CHOU, C. C., NARULA, S. K. & ZAVODNY, P. J. 1999. Cutting edge: species specificity of the CC chemokine 6Ckine signaling through the CXC chemokine receptor CXCR3: human 6Ckine is not a ligand for the human or mouse CXCR3 receptors. *J Immunol*, 162, 3765-9.
- JOHNSON, Z., PROUDFOOT, A. E. & HANDEL, T. M. 2005. Interaction of chemokines and glycosaminoglycans: a new twist in the regulation of chemokine function with opportunities for therapeutic intervention. *Cytokine Growth Factor Rev*, 16, 625-36.
- KALUPAHANA, R. S., MASTROENI, P., MASKELL, D. & BLACKLAWS, B. A. 2005. Activation of murine dendritic cells and macrophages induced by *Salmonella enterica* serovar Typhimurium. *Immunology*, 115, 462-72.
- KANG, Y.-S., KIM, J. Y., BRUENING, S. A., PACK, M., CHARALAMBOUS, A., PRITSKER, A., MORAN, T. M., LOEFFLER, J. M., STEINMAN, R. M. & PARK, C. G. 2004. The C-type lectin SIGN-R1 mediates uptake of the capsular polysaccharide of *Streptococcus pneumoniae* in the marginal zone of mouse spleen. *Proc Natl Acad Sci USA*, 101, 215-20.
- KANG, Y.-S., YAMAZAKI, S., IYODA, T., PACK, M., BRUENING, S. A., KIM, J. Y., TAKAHARA, K., INABA, K., STEINMAN, R. M. & PARK, C. G. 2003. SIGN-R1, a novel C-type lectin expressed by marginal zone macrophages in spleen, mediates uptake of the polysaccharide dextran. *Int Immunol*, 15, 177-86.
- KASHIWAZAKI, M., TANAKA, T., KANDA, H., EBISUNO, Y., IZAWA, D., FUKUMA, N., AKIMITSU, N., SEKIMIZU, K., MONDEN, M. & MIYASAKA, M. 2003. A high endothelial venule-expressing promiscuous chemokine receptor DARC can bind inflammatory, but not lymphoid, chemokines and is dispensable for lymphocyte homing under physiological conditions. *Int Immunol*, 15, 1219-27.
- KASLOW, H. R. & BURNS, D. L. 1992. Pertussis toxin and target eukaryotic cells: binding, entry, and activation. *FASEB J*, 6, 2684-90.
- KENNEDY, J., KELNER, G. S., KLEYENSTEUBER, S., SCHALL, T. J., WEISS, M. C., YSSEL, H., SCHNEIDER, P. V., COCKS, B. G., BACON, K. B. & ZLOTNIK, A. 1995. Molecular cloning and functional characterization of human lymphotactin. *J Immunol*, 155, 203-9.
- KHOJA, H., WANG, G., NG, C. T., TUCKER, J., BROWN, T. & SHYAMALA, V. 2000. Cloning of CCRL1, an orphan seven transmembrane receptor related to chemokine receptors, expressed abundantly in the heart. *Gene*, 246, 229-38.
- KIM, D., MEBIUS, R. E., MACMICKING, J. D., JUNG, S., CUPEDO, T., CASTELLANOS, Y., RHO, J., WONG, B. R., JOSIEN, R., KIM, N., RENNERT, P. D. & CHOI, Y. 2000. Regulation of peripheral lymph node genesis by the tumor necrosis factor family member TRANCE. *J Exp Med*, 192, 1467-78.

- KINOSHITA, N. & GELBOIN, H. V. 1972. The role of aryl hydrocarbon hydroxylase in 7,12-dimethylbenz(a)anthracene skin tumorigenesis: on the mechanism of 7,8-benzoflavone inhibition of tumorigenesis. *Cancer Res*, 32, 1329-39.
- KLEIN, U. & DALLA-FAVERA, R. 2008. Germinal centres: role in B-cell physiology and malignancy. *Nat Rev Immunol*, 8, 22-33.
- KOENEN, R. R., VON HUNDELSHAUSEN, P., NESMELOVA, I. V., ZERNECKE, A., LIEHN, E. A., SARABI, A., KRAMP, B. K., PICCININI, A. M., PALUDAN, S. R., KOWALSKA, M. A., KUNGL, A. J., HACKENG, T. M., MAYO, K. H. & WEBER, C. 2009. Disrupting functional interactions between platelet chemokines inhibits atherosclerosis in hyperlipidemic mice. *Nat Med*, 15, 97-103.
- KOHOUT, T. A., NICHOLAS, S. L., PERRY, S. J., REINHART, G., JUNGER, S. & STRUTHERS, R. S. 2004. Differential desensitization, receptor phosphorylation, beta-arrestin recruitment, and ERK1/2 activation by the two endogenous ligands for the CC chemokine receptor 7. *J Biol Chem*, 279, 23214-22.
- KONG, Y. Y., YOSHIDA, H., SAROSI, I., TAN, H. L., TIMMS, E., CAPPARELLI, C., MORONY, S., OLIVEIRA-DOS-SANTOS, A. J., VAN, G., ITIE, A., KHOO, W., WAKEHAM, A., DUNSTAN, C. R., LACEY, D. L., MAK, T. W., BOYLE, W. J. & PENNINGER, J. M. 1999. OPGL is a key regulator of osteoclastogenesis, lymphocyte development and lymph-node organogenesis. *Nature*, 397, 315-23.
- KOPPEL, E. A., LITJENS, M., VAN DEN BERG, V. C., VAN KOOYK, Y. & GEIJTENBEEK, T. B. H. 2008. Interaction of SIGNR1 expressed by marginal zone macrophages with marginal zone B cells is essential to early IgM responses against *Streptococcus pneumoniae*. *Mol Immunol*, 45, 2881-7.
- KROESE, F. G., AMMERLAAN, W. A. & KANTOR, A. B. 1993. Evidence that intestinal IgA plasma cells in mu, kappa transgenic mice are derived from B-1 (Ly-1 B) cells. *Int Immunol*, 5, 1317-27.
- KROESE, F. G., BUTCHER, E. C., STALL, A. M. & HERZENBERG, L. A. 1989a. A major peritoneal reservoir of precursors for intestinal IgA plasma cells. *Immunol Invest*, 18, 47-58.
- KROESE, F. G., BUTCHER, E. C., STALL, A. M., LALOR, P. A., ADAMS, S. & HERZENBERG, L. A. 1989b. Many of the IgA producing plasma cells in murine gut are derived from self-replenishing precursors in the peritoneal cavity. *Int Immunol*, 1, 75-84.
- KRUEGER, A., WILLENZON, S., LYSZKIEWICZ, M., KREMMER, E. & FÖRSTER, R. 2010. CC chemokine receptor 7 and 9 double-deficient hematopoietic progenitors are severely impaired in seeding the adult thymus. *Blood*, 115, 1906-12.
- KRUETZMANN, S., ROSADO, M. M., WEBER, H., GERMING, U., TOURNILHAC, O., PETER, H.-H., BERNER, R., PETERS, A., BOEHM, T., PLEBANI, A., QUINTI, I. & CARSETTI, R. 2003. Human immunoglobulin M memory B cells controlling *Streptococcus pneumoniae* infections are generated in the spleen. *J Exp Med*, 197, 939-45.
- KUNKEL, E. J., CAMPBELL, J. J., HARALDSEN, G., PAN, J., BOISVERT, J., ROBERTS, A. I., EBERT, E. C., VIERRA, M. A., GOODMAN, S. B., GENOVESE, M. C., WARDLAW, A. J., GREENBERG, H. B., PARKER, C. M., BUTCHER, E. C., ANDREW, D. P. & AGACE, W. W. 2000. Lymphocyte CC chemokine receptor 9 and epithelial thymus-expressed chemokine (TECK) expression distinguish the small intestinal immune compartment: Epithelial expression of tissue-specific chemokines as an organizing principle in regional immunity. *J Exp Med*, 192, 761-8.
- KUREBAYASHI, S., UEDA, E., SAKAUE, M., PATEL, D. D., MEDVEDEV, A., ZHANG, F. & JETTEN, A. M. 2000. Retinoid-related orphan receptor gamma (RORgamma) is essential for lymphoid organogenesis and controls apoptosis during thymopoiesis. *Proc Natl Acad Sci USA*, 97, 10132-7.

- KUWABARA, T., ISHIKAWA, F., YASUDA, T., ARITOMI, K., NAKANO, H., TANAKA, Y., OKADA, Y., LIPP, M. & KAKIUCHI, T. 2009. CCR7 ligands are required for development of experimental autoimmune encephalomyelitis through generating IL-23-dependent Th17 cells. *J Immunol*, 183, 2513-21.
- KWAN, J. & KILLEEN, N. 2004. CCR7 directs the migration of thymocytes into the thymic medulla. *J Immunol*, 172, 3999-4007.
- LAAN, M., KISAND, K., KONT, V., MÖLL, K., TSEREL, L., SCOTT, H. S. & PETERSON, P. 2009. Autoimmune regulator deficiency results in decreased expression of CCR4 and CCR7 ligands and in delayed migration of CD4+ thymocytes. *J Immunol*, 183, 7682-91.
- LAPORTE, S. A., OAKLEY, R. H., HOLT, J. A., BARAK, L. S. & CARON, M. G. 2000. The interaction of beta-arrestin with the AP-2 adaptor is required for the clustering of beta 2-adrenergic receptor into clathrin-coated pits. *J Biol Chem*, 275, 23120-6.
- LEE, J.-W., EPARDAUD, M., SUN, J., BECKER, J. E., CHENG, A. C., YONEKURA, A.-R., HEATH, J. K. & TURLEY, S. J. 2007. Peripheral antigen display by lymph node stroma promotes T cell tolerance to intestinal self. *Nat Immunol*, 8, 181-90.
- LEE, J. S., FREVERT, C. W., THORNING, D. R., SEGERER, S., ALPERS, C. E., CARTRON, J.-P., COLIN, Y., WONG, V. A., MARTIN, T. R. & GOODMAN, R. B. 2003. Enhanced expression of Duffy antigen in the lungs during suppurative pneumonia. *J Histochem Cytochem*, 51, 159-66.
- LEE, K. Y., FONG, B. S. P., TSANG, K. S., LAU, T. K., NG, P. C., LAM, A. C., CHAN, K. Y. Y., WANG, C. C., KUNG, H. F., LI, C. K. & LI, K. 2011. Fetal stromal niches enhance human embryonic stem cell-derived hematopoietic differentiation and globin switch. *Stem Cells Dev*, 20, 31-8.
- LEFKOWITZ, R. J. & SHENOY, S. K. 2005. Transduction of receptor signals by beta-arrestins. *Science*, 308, 512-7.
- LEICK, M., CATUSSE, J., FOLLO, M., NIBBS, R. J., HARTMANN, T. N., VEELKEN, H. & BURGER, M. 2010. CCL19 is a specific ligand of the constitutively recycling atypical human chemokine receptor CCR4. *Immunology*, 129, 536-46.
- LEY, K., LAUDANNA, C., CYBULSKY, M. I. & NOURSHARGH, S. 2007. Getting to the site of inflammation: the leukocyte adhesion cascade updated. *Nat Rev Immunol*, 7, 678-89.
- LINK, A., VOGT, T. K., FAVRE, S., BRITSCHGI, M. R., ACHA-ORBEA, H., HINZ, B., CYSTER, J. G. & LUTHER, S. A. 2007. Fibroblastic reticular cells in lymph nodes regulate the homeostasis of naive T cells. *Nat Immunol*, 8, 1255-65.
- LIU, C., SAITO, F., LIU, Z., LEI, Y., UEHARA, S., LOVE, P., LIPP, M., KONDO, S., MANLEY, N. & TAKAHAMA, Y. 2006. Coordination between CCR7- and CCR9-mediated chemokine signals in prevascular fetal thymus colonization. *Blood*, 108, 2531-9.
- LIU, C., UENO, T., KUSE, S., SAITO, F., NITTA, T., PIALI, L., NAKANO, H., KAKIUCHI, T., LIPP, M., HOLLANDER, G. A. & TAKAHAMA, Y. 2005. The role of CCL21 in recruitment of T-precursor cells to fetal thymus. *Blood*, 105, 31-9.
- LIU, K. D., GAFFEN, S. L. & GOLDSMITH, M. A. 1998. JAK/STAT signaling by cytokine receptors. *Curr Opin Immunol*, 10, 271-8.
- LOETSCHER, P., PELLEGRINO, A., GONG, J. H., MATTIOLI, I., LOETSCHER, M., BARDI, G., BAGGIOLINI, M. & CLARK-LEWIS, I. 2001. The ligands of CXC chemokine receptor 3, I-TAC, Mig, and IP10, are natural antagonists for CCR3. *J Biol Chem*, 276, 2986-91.
- LOPES-CARVALHO, T. & KEARNEY, J. F. 2004. Development and selection of marginal zone B cells. *Immunol Rev*, 197, 192-205.
- LUKACS, N. W. & TEKKANAT, K. K. 2000. Role of chemokines in asthmatic airway inflammation. *Immunol Rev*, 177, 21-30.

- LUO, H., CHAUDHURI, A., ZBRZEZNA, V., HE, Y. & POGO, A. O. 2000. Deletion of the murine Duffy gene (Dfy) reveals that the Duffy receptor is functionally redundant. *Mol Cell Biol*, 20, 3097-101.
- LUSTER, A. D. 1998. Chemokines--chemotactic cytokines that mediate inflammation. *N Engl J Med*, 338, 436-45.
- LUTHER, S. A., ANSEL, K. M. & CYSTER, J. G. 2003. Overlapping roles of CXCL13, interleukin 7 receptor alpha, and CCR7 ligands in lymph node development. *J Exp Med*, 197, 1191-8.
- LUTHER, S. A., BIDGOL, A., HARGREAVES, D. C., SCHMIDT, A., XU, Y., PANIYADI, J., MATLOUBIAN, M. & CYSTER, J. G. 2002. Differing activities of homeostatic chemokines CCL19, CCL21, and CXCL12 in lymphocyte and dendritic cell recruitment and lymphoid neogenesis. *J Immunol*, 169, 424-33.
- LUTHER, S. A., TANG, H. L., HYMAN, P. L., FARR, A. G. & CYSTER, J. G. 2000. Coexpression of the chemokines ELC and SLC by T zone stromal cells and deletion of the ELC gene in the plt/plt mouse. *Proc Natl Acad Sci USA*, 97, 12694-9.
- LUTZ, M. B. & SCHULER, G. 2002. Immature, semi-mature and fully mature dendritic cells: which signals induce tolerance or immunity? *Trends Immunol*, 23, 445-9.
- MA, Q., JONES, D., BORGHESANI, P. R., SEGAL, R. A., NAGASAWA, T., KISHIMOTO, T., BRONSON, R. T. & SPRINGER, T. A. 1998. Impaired B-lymphopoiesis, myelopoiesis, and derailed cerebellar neuron migration in CXCR4- and SDF-1-deficient mice. *Proc Natl Acad Sci USA*, 95, 9448-53.
- MADIGAN, J., FREEMAN, D. J., MENZIES, F., FORROW, S., NELSON, S. M., YOUNG, A., SHARKEY, A., MOFFETT, A., GRAHAM, G. J., GREER, I. A., ROT, A. & NIBBS, R. J. B. 2010. Chemokine scavenger D6 is expressed by trophoblasts and aids the survival of mouse embryos transferred into allogeneic recipients. *J Immunol*, 184, 3202-12.
- MANDALA, S., HAJDU, R., BERGSTROM, J., QUACKENBUSH, E., XIE, J., MILLIGAN, J., THORNTON, R., SHEI, G.-J., CARD, D., KEOHANE, C., ROSENBAACH, M., HALE, J., LYNCH, C. L., RUPPRECHT, K., PARSONS, W. & ROSEN, H. 2002. Alteration of lymphocyte trafficking by sphingosine-1-phosphate receptor agonists. *Science*, 296, 346-9.
- MANLEY, N. R. 2000. Thymus organogenesis and molecular mechanisms of thymic epithelial cell differentiation. *Semin Immunol*, 12, 421-8.
- MANLEY, N. R. & BLACKBURN, C. C. 2003. A developmental look at thymus organogenesis: where do the non-hematopoietic cells in the thymus come from? *Curr Opin Immunol*, 15, 225-32.
- MANTOVANI, A. 1999. The chemokine system: redundancy for robust outputs. *Immunol Today*, 20, 254-7.
- MANZ, R. A., THIEL, A. & RADBRUCH, A. 1997. Lifetime of plasma cells in the bone marrow. *Nature*, 388, 133-4.
- MARSHALL, J. D., HEEKE, D. S., ABBATE, C., YEE, P. & VAN NEST, G. 2006. Induction of interferon-gamma from natural killer cells by immunostimulatory CpG DNA is mediated through plasmacytoid-dendritic-cell-produced interferon-alpha and tumour necrosis factor-alpha. *Immunology*, 117, 38-46.
- MARSLAND, B. J., BÄTTIG, P., BAUER, M., RUEDL, C., LÄSSING, U., BEERLI, R. R., DIETMEIER, K., IVANOVA, L., PFISTER, T., VOGT, L., NAKANO, H., NEMBRINI, C., SAUDAN, P., KOPF, M. & BACHMANN, M. F. 2005. CCL19 and CCL21 induce a potent proinflammatory differentiation program in licensed dendritic cells. *Immunity*, 22, 493-505.
- MARTIN, F. & KEARNEY, J. F. 2001. B1 cells: similarities and differences with other B cell subsets. *Curr Opin Immunol*, 13, 195-201.
- MARTIN, F. & KEARNEY, J. F. 2002. Marginal-zone B cells. *Nat Rev Immunol*, 2, 323-35.

- MARTÍN-FONTECHA, A., SEBASTIANI, S., HÖPKEN, U. E., UGUCCIONI, M., LIPP, M., LANZAVECCHIA, A. & SALLUSTO, F. 2003. Regulation of dendritic cell migration to the draining lymph node: impact on T lymphocyte traffic and priming. *J Exp Med*, 198, 615-21.
- MARTINEZ DE LA TORRE, Y., BURACCHI, C., BORRONI, E. M., DUPOR, J., BONECCHI, R., NEBULONI, M., PASQUALINI, F., DONI, A., LAURI, E., AGOSTINIS, C., BULLA, R., COOK, D. N., HARIBABU, B., MERONI, P., RUKAVINA, D., VAGO, L., TEDESCO, F., VECCHI, A., LIRA, S. A., LOCATI, M. & MANTOVANI, A. 2007. Protection against inflammation- and autoantibody-caused fetal loss by the chemokine decoy receptor D6. *Proc Natl Acad Sci USA*, 104, 2319-24.
- MARTINEZ DE LA TORRE, Y., LOCATI, M., BURACCHI, C., DUPOR, J., COOK, D. N., BONECCHI, R., NEBULONI, M., RUKAVINA, D., VAGO, L., VECCHI, A., LIRA, S. A. & MANTOVANI, A. 2005. Increased inflammation in mice deficient for the chemokine decoy receptor D6. *Eur J Immunol*, 35, 1342-6.
- MATLOUBIAN, M., LO, C. G., CINAMON, G., LESNESKI, M. J., XU, Y., BRINKMANN, V., ALLENDE, M. L., PROIA, R. L. & CYSTER, J. G. 2004. Lymphocyte egress from thymus and peripheral lymphoid organs is dependent on S1P receptor 1. *Nature*, 427, 355-60.
- MATTA, B. M., CASTELLANETA, A. & THOMSON, A. W. 2010. Tolerogenic plasmacytoid DC. *Eur J Immunol*, 40, 2667-76.
- MAYR, F. B., SPIEL, A. O., LEITNER, J. M., FIRBAS, C., KLIEGEL, T., JILMA-STOHLAWETZ, P., DERENDORF, H. & JILMA, B. 2008. Duffy antigen modifies the chemokine response in human endotoxemia. *Crit Care Med*, 36, 159-65.
- MCCULLOCH, C. V., MORROW, V., MILASTA, S., COMERFORD, I., MILLIGAN, G., GRAHAM, G. J., ISAACS, N. W. & NIBBS, R. J. B. 2008. Multiple roles for the C-terminal tail of the chemokine scavenger D6. *J Biol Chem*, 283, 7972-82.
- MCDERMOTT, M. R., MARK, D. A., BEFUS, A. D., BALIGA, B. S., SUSKIND, R. M. & BIENENSTOCK, J. 1982. Impaired intestinal localization of mesenteric lymphoblasts associated with vitamin A deficiency and protein-calorie malnutrition. *Immunology*, 45, 1-5.
- MCKENNA, K., BEIGNON, A.-S. & BHARDWAJ, N. 2005. Plasmacytoid dendritic cells: linking innate and adaptive immunity. *J Virol*, 79, 17-27.
- MCQUIBBAN, G. A., BUTLER, G. S., GONG, J. H., BENDALL, L., POWER, C., CLARK-LEWIS, I. & OVERALL, C. M. 2001. Matrix metalloproteinase activity inactivates the CXC chemokine stromal cell-derived factor-1. *J Biol Chem*, 276, 43503-8.
- MCQUIBBAN, G. A., GONG, J.-H., WONG, J. P., WALLACE, J. L., CLARK-LEWIS, I. & OVERALL, C. M. 2002. Matrix metalloproteinase processing of monocyte chemoattractant proteins generates CC chemokine receptor antagonists with anti-inflammatory properties in vivo. *Blood*, 100, 1160-7.
- MCQUIBBAN, G. A., GONG, J. H., TAM, E. M., MCCULLOCH, C. A., CLARK-LEWIS, I. & OVERALL, C. M. 2000. Inflammation dampened by gelatinase A cleavage of monocyte chemoattractant protein-3. *Science*, 289, 1202-6.
- MEBIUS, R. E. 2003. Organogenesis of lymphoid tissues. *Nat Rev Immunol*, 3, 292-303.
- MEBIUS, R. E. & KRAAL, G. 2005. Structure and function of the spleen. *Nat Rev Immunol*, 5, 606-16.
- MEBIUS, R. E., MIYAMOTO, T., CHRISTENSEN, J., DOMEN, J., CUPEDO, T., WEISSMAN, I. L. & AKASHI, K. 2001. The fetal liver counterpart of adult common lymphoid progenitors gives rise to all lymphoid lineages, CD45⁺CD4⁺CD3⁻ cells, as well as macrophages. *J Immunol*, 166, 6593-601.

- MEBIUS, R. E., RENNERT, P. & WEISSMAN, I. L. 1997. Developing lymph nodes collect CD4+CD3- LTbeta+ cells that can differentiate to APC, NK cells, and follicular cells but not T or B cells. *Immunity*, 7, 493-504.
- MELLADO, M., RODRÍGUEZ-FRADE, J. M., ARAGAY, A., DEL REAL, G., MARTÍN, A. M., VILA-CORO, A. J., SERRANO, A., MAYOR, F. & MARTÍNEZ-A, C. 1998. The chemokine monocyte chemotactic protein 1 triggers Janus kinase 2 activation and tyrosine phosphorylation of the CCR2B receptor. *J Immunol*, 161, 805-13.
- MELLADO, M., RODRÍGUEZ-FRADE, J. M., MAÑES, S. & MARTÍNEZ-A, C. 2001. Chemokine signaling and functional responses: the role of receptor dimerization and TK pathway activation. *Annu Rev Immunol*, 19, 397-421.
- METZGER, T. C. & ANDERSON, M. S. 2011. Control of central and peripheral tolerance by Aire. *Immunol Rev*, 241, 89-103.
- MIDDLETON, J., NEIL, S., WINTLE, J., CLARK-LEWIS, I., MOORE, H., LAM, C., AUER, M., HUB, E. & ROT, A. 1997. Transcytosis and surface presentation of IL-8 by venular endothelial cells. *Cell*, 91, 385-95.
- MILLER, L. H., MASON, S. J., DVORAK, J. A., MCGINNISS, M. H. & ROTHMAN, I. K. 1975. Erythrocyte receptors for (*Plasmodium knowlesi*) malaria: Duffy blood group determinants. *Science*, 189, 561-3.
- MILLER, M. J., HEJAZI, A. S., WEI, S. H., CAHALAN, M. D. & PARKER, I. 2004. T cell repertoire scanning is promoted by dynamic dendritic cell behavior and random T cell motility in the lymph node. *Proc Natl Acad Sci USA*, 101, 998-1003.
- MILLIGAN, G. 2004. G protein-coupled receptor dimerization: function and ligand pharmacology. *Mol Pharmacol*, 66, 1-7.
- MISSLITZ, A., PABST, O., HINTZEN, G., OHL, L., KREMMER, E., PETRIE, H. T. & FÖRSTER, R. 2004. Thymic T cell development and progenitor localization depend on CCR7. *J Exp Med*, 200, 481-91.
- MONTECINO-RODRIGUEZ, E., LEATHERS, H. & DORSHKIND, K. 2006. Identification of a B-1 B cell-specified progenitor. *Nat Immunol*, 7, 293-301.
- MORA, J. R., BONO, M. R., MANJUNATH, N., WENINGER, W., CAVANAGH, L. L., ROSEMBLATT, M. & VON ANDRIAN, U. H. 2003. Selective imprinting of gut-homing T cells by Peyer's patch dendritic cells. *Nature*, 424, 88-93.
- MORA, J. R., IWATA, M., EKSTEEN, B., SONG, S.-Y., JUNT, T., SENMAN, B., OTIPOBY, K. L., YOKOTA, A., TAKEUCHI, H., RICCIARDI-CASTAGNOLI, P., RAJEWSKY, K., ADAMS, D. H. & VON ANDRIAN, U. H. 2006. Generation of gut-homing IgA-secreting B cells by intestinal dendritic cells. *Science*, 314, 1157-60.
- MORA, J. R. & VON ANDRIAN, U. H. 2009. Role of retinoic acid in the imprinting of gut-homing IgA-secreting cells. *Semin Immunol*, 21, 28-35.
- MOWAT, A. M. 2003. Anatomical basis of tolerance and immunity to intestinal antigens. *Nat Rev Immunol*, 3, 331-41.
- MUELLER, D. L. 2010. Mechanisms maintaining peripheral tolerance. *Nat Immunol*, 11, 21-7.
- MURPHY, K., TRAVERS, P. & WALPORT, M. 2010. Janeway's Immunobiology†.
- MURPHY, P. M., BAGGIOLINI, M., CHARO, I. F., HÉBERT, C. A., HORUK, R., MATSUSHIMA, K., MILLER, L. H., OPPENHEIM, J. J. & POWER, C. A. 2000. International union of pharmacology. XXII. Nomenclature for chemokine receptors. *Pharmacol Rev*, 52, 145-76.
- NAGASAWA, T., HIROTA, S., TACHIBANA, K., TAKAKURA, N., NISHIKAWA, S., KITAMURA, Y., YOSHIDA, N., KIKUTANI, H. & KISHIMOTO, T. 1996. Defects of B-cell lymphopoiesis and bone-marrow myelopoiesis in mice lacking the CXC chemokine PBSF/SDF-1. *Nature*, 382, 635-8.
- NAGIRA, M., IMAI, T., HIESHIMA, K., KUSUDA, J., RIDANPÄÄ, M., TAKAGI, S., NISHIMURA, M., KAKIZAKI, M., NOMIYAMA, H. & YOSHIE, O. 1997.

- Molecular cloning of a novel human CC chemokine secondary lymphoid-tissue chemokine that is a potent chemoattractant for lymphocytes and mapped to chromosome 9p13. *J Biol Chem*, 272, 19518-24.
- NAITO, A., AZUMA, S., TANAKA, S., MIYAZAKI, T., TAKAKI, S., TAKATSU, K., NAKAO, K., NAKAMURA, K., KATSUKI, M., YAMAMOTO, T. & INOUE, J. 1999. Severe osteopetrosis, defective interleukin-1 signalling and lymph node organogenesis in TRAF6-deficient mice. *Genes Cells*, 4, 353-62.
- NAKANO, H., TAMURA, T., YOSHIMOTO, T., YAGITA, H., MIYASAKA, M., BUTCHER, E. C., NARIUCHI, H., KAKIUCHI, T. & MATSUZAWA, A. 1997. Genetic defect in T lymphocyte-specific homing into peripheral lymph nodes. *Eur J Immunol*, 27, 215-21.
- NAKANO, H., YOSHIMOTO, T., KAKIUCHI, T. & MATSUZAWA, A. 1993. Nonspecific augmentation of lymph node T cells and I-E-independent selective deletion of V beta 14+ T cells by Mtv-2 in the DDD mouse. *Eur J Immunol*, 23, 2434-9.
- NAKAYAMA, T., WATANABE, Y., OISO, N., HIGUCHI, T., SHIGETA, A., MIZUGUCHI, N., KATOU, F., HASHIMOTO, K., KAWADA, A. & YOSHIE, O. 2010. Eotaxin-3/CC chemokine ligand 26 is a functional ligand for CX3CR1. *J Immunol*, 185, 6472-9.
- NAMEN, A. E., LUPTON, S., HJERRILD, K., WIGNALL, J., MOCHIZUKI, D. Y., SCHMIERER, A., MOSLEY, B., MARCH, C. J., URDAL, D. & GILLIS, S. 1988. Stimulation of B-cell progenitors by cloned murine interleukin-7. *Nature*, 333, 571-3.
- NATHAN, C. 2006. Neutrophils and immunity: challenges and opportunities. *Nat Rev Immunol*, 6, 173-82.
- NAUMANN, U., CAMERONI, E., PRUENSTER, M., MAHABALESHWAR, H., RAZ, E., ZERWES, H.-G., ROT, A. & THELEN, M. 2010. CXCR7 functions as a scavenger for CXCL12 and CXCL11. *PLoS ONE*, 5, e9175.
- NEOTE, K., DARBONNE, W., OGEZ, J., HORUK, R. & SCHALL, T. J. 1993. Identification of a promiscuous inflammatory peptide receptor on the surface of red blood cells. *J Biol Chem*, 268, 12247-9.
- NESMELOVA, I. V., SHAM, Y., GAO, J. & MAYO, K. H. 2008. CXC and CC chemokines form mixed heterodimers: association free energies from molecular dynamics simulations and experimental correlations. *J Biol Chem*, 283, 24155-66.
- NEWBERRY, R. D. & LORENZ, R. G. 2005. Organizing a mucosal defense. *Immunol Rev*, 206, 6-21.
- NGO, V. N., TANG, H. L. & CYSTER, J. G. 1998. Epstein-Barr virus-induced molecule 1 ligand chemokine is expressed by dendritic cells in lymphoid tissues and strongly attracts naive T cells and activated B cells. *J Exp Med*, 188, 181-91.
- NIBBS, R. J., KRIEHLER, E., PONATH, P. D., PARENT, D., QIN, S., CAMPBELL, J. D., HENDERSON, A., KERJASCHKI, D., MAURER, D., GRAHAM, G. J. & ROT, A. 2001. The beta-chemokine receptor D6 is expressed by lymphatic endothelium and a subset of vascular tumors. *Am J Pathol*, 158, 867-77.
- NIBBS, R. J., WYLIE, S. M., PRAGNELL, I. B. & GRAHAM, G. J. 1997a. Cloning and characterization of a novel murine beta chemokine receptor, D6. Comparison to three other related macrophage inflammatory protein-1alpha receptors, CCR-1, CCR-3, and CCR-5. *J Biol Chem*, 272, 12495-504.
- NIBBS, R. J., WYLIE, S. M., YANG, J., LANDAU, N. R. & GRAHAM, G. J. 1997b. Cloning and characterization of a novel promiscuous human beta-chemokine receptor D6. *J Biol Chem*, 272, 32078-83.
- NIBBS, R. J. B., GILCHRIST, D. S., KING, V., FERRA, A., FORROW, S., HUNTER, K. D. & GRAHAM, G. J. 2007. The atypical chemokine receptor D6 suppresses the development of chemically induced skin tumors. *J Clin Invest*, 117, 1884-92.

- NICHOLS, B. J. & LIPPINCOTT-SCHWARTZ, J. 2001. Endocytosis without clathrin coats. *Trends Cell Biol*, 11, 406-12.
- NITTA, T., MURATA, S., UENO, T., TANAKA, K. & TAKAHAMA, Y. 2008. Thymic microenvironments for T-cell repertoire formation. *Adv Immunol*, 99, 59-94.
- NOLTE, M. A., ARENS, R., KRAUS, M., VAN OERS, M. H. J., KRAAL, G., VAN LIER, R. A. W. & MEBIUS, R. E. 2004. B cells are crucial for both development and maintenance of the splenic marginal zone. *J Immunol*, 172, 3620-7.
- OEHEN, S., ODERMATT, B., KARRER, U., HENGARTNER, H., ZINKERNAGEL, R. & LÓPEZ-MACÍAS, C. 2002. Marginal zone macrophages and immune responses against viruses. *J Immunol*, 169, 1453-8.
- OHL, L., HENNING, G., KRAUTWALD, S., LIPP, M., HARDTKE, S., BERNHARDT, G., PABST, O. & FÖRSTER, R. 2003. Cooperating mechanisms of CXCR5 and CCR7 in development and organization of secondary lymphoid organs. *J Exp Med*, 197, 1199-204.
- OHL, L., MOHAUPT, M., CZELOTH, N., HINTZEN, G., KIAFARD, Z., ZWIRNER, J., BLANKENSTEIN, T., HENNING, G. & FÖRSTER, R. 2004. CCR7 governs skin dendritic cell migration under inflammatory and steady-state conditions. *Immunity*, 21, 279-88.
- OKADA, T., MILLER, M. J., PARKER, I., KRUMMEL, M. F., NEIGHBORS, M., HARTLEY, S. B., O'GARRA, A., CAHALAN, M. D. & CYSTER, J. G. 2005. Antigen-engaged B cells undergo chemotaxis toward the T zone and form motile conjugates with helper T cells. *PLoS Biol*, 3, e150.
- OKADA, T., NGO, V. N., EKLAND, E. H., FÖRSTER, R., LIPP, M., LITTMAN, D. R. & CYSTER, J. G. 2002. Chemokine requirements for B cell entry to lymph nodes and Peyer's patches. *J Exp Med*, 196, 65-75.
- OLDHAM, W. M. & HAMM, H. E. 2008. Heterotrimeric G protein activation by G-protein-coupled receptors. *Nat Rev Mol Cell Biol*, 9, 60-71.
- OLSON, T. S. & LEY, K. 2002. Chemokines and chemokine receptors in leukocyte trafficking. *Am J Physiol Regul Integr Comp Physiol*, 283, R7-28.
- OTERO, C., GROETTRUP, M. & LEGLER, D. F. 2006. Opposite fate of endocytosed CCR7 and its ligands: recycling versus degradation. *J Immunol*, 177, 2314-23.
- OTT, T. R., LIO, F. M., OLSHEFSKI, D., LIU, X.-J., LING, N. & STRUTHERS, R. S. 2006. The N-terminal domain of CCL21 reconstitutes high affinity binding, G protein activation, and chemotactic activity, to the C-terminal domain of CCL19. *Biochem Biophys Res Commun*, 348, 1089-93.
- PABST, O., OHL, L., WENDLAND, M., WURBEL, M.-A., KREMMER, E., MALISSEN, B. & FÖRSTER, R. 2004. Chemokine receptor CCR9 contributes to the localization of plasma cells to the small intestine. *J Exp Med*, 199, 411-6.
- PAKIANATHAN, D. R., KUTA, E. G., ARTIS, D. R., SKELTON, N. J. & HÉBERT, C. A. 1997. Distinct but overlapping epitopes for the interaction of a CC-chemokine with CCR1, CCR3 and CCR5. *Biochemistry*, 36, 9642-8.
- PALFRAMAN, R. T., JUNG, S., CHENG, G., WENINGER, W., LUO, Y., DORF, M., LITTMAN, D. R., ROLLINS, B. J., ZWEERINK, H., ROT, A. & VON ANDRIAN, U. H. 2001. Inflammatory chemokine transport and presentation in HEV: a remote control mechanism for monocyte recruitment to lymph nodes in inflamed tissues. *J Exp Med*, 194, 1361-73.
- PALMER, E. 2003. Negative selection--clearing out the bad apples from the T-cell repertoire. *Nat Rev Immunol*, 3, 383-91.
- PAN, J., KUNKEL, E. J., GOSSLAR, U., LAZARUS, N., LANGDON, P., BROADWELL, K., VIERRA, M. A., GENOVESE, M. C., BUTCHER, E. C. & SOLER, D. 2000. A novel chemokine ligand for CCR10 and CCR3 expressed by epithelial cells in mucosal tissues. *J Immunol*, 165, 2943-9.
- PAPADAKIS, K. A., PREHN, J., NELSON, V., CHENG, L., BINDER, S. W., PONATH, P. D., ANDREW, D. P. & TARGAN, S. R. 2000. The role of thymus-expressed

- chemokine and its receptor CCR9 on lymphocytes in the regional specialization of the mucosal immune system. *J Immunol*, 165, 5069-76.
- PARISH, C. R. 2006. The role of heparan sulphate in inflammation. *Nat Rev Immunol*, 6, 633-43.
- PARKS, W. C., WILSON, C. L. & LÓPEZ-BOADO, Y. S. 2004. Matrix metalloproteinases as modulators of inflammation and innate immunity. *Nat Rev Immunol*, 4, 617-29.
- PARTON, R. G. & SIMONS, K. 2007. The multiple faces of caveolae. *Nat Rev Mol Cell Biol*, 8, 185-94.
- PATTERSON, A. M., SIDDALL, H., CHAMBERLAIN, G., GARDNER, L. & MIDDLETON, J. 2002. Expression of the duffy antigen/receptor for chemokines (DARC) by the inflamed synovial endothelium. *J Pathol*, 197, 108-16.
- PAWLOWSKI, N. 2010. Dynamin self-assembly and the vesicle scission mechanism: how dynamin oligomers cleave the membrane neck of clathrin-coated pits during endocytosis. *Bioessays*, 32, 1033-9.
- PELKMANS, L., BÜRLLI, T., ZERIAL, M. & HELENIUS, A. 2004. Caveolin-stabilized membrane domains as multifunctional transport and sorting devices in endocytic membrane traffic. *Cell*, 118, 767-80.
- PELKMANS, L. & HELENIUS, A. 2002. Endocytosis via caveolae. *Traffic*, 3, 311-20.
- PHAN, T. G., GREEN, J. A., GRAY, E. E., XU, Y. & CYSTER, J. G. 2009. Immune complex relay by subcapsular sinus macrophages and noncognate B cells drives antibody affinity maturation. *Nat Immunol*, 10, 786-93.
- PHAN, T. G., GRIGOROVA, I., OKADA, T. & CYSTER, J. G. 2007. Subcapsular encounter and complement-dependent transport of immune complexes by lymph node B cells. *Nat Immunol*, 8, 992-1000.
- PRATTEN, M. K. & LLOYD, J. B. 1986. Pinocytosis and phagocytosis: the effect of size of a particulate substrate on its mode of capture by rat peritoneal macrophages cultured in vitro. *Biochim Biophys Acta*, 881, 307-13.
- PROCKOP, S. & PETRIE, H. T. 2000. Cell migration and the anatomic control of thymocyte precursor differentiation. *Semin Immunol*, 12, 435-44.
- PROUDFOOT, A. E. I., HANDEL, T. M., JOHNSON, Z., LAU, E. K., LIWANG, P., CLARK-LEWIS, I., BORLAT, F., WELLS, T. N. C. & KOSCO-VILBOIS, M. H. 2003. Glycosaminoglycan binding and oligomerization are essential for the in vivo activity of certain chemokines. *Proc Natl Acad Sci USA*, 100, 1885-90.
- PRUENSTER, M., MUDDE, L., BOMBOSI, P., DIMITROVA, S., ZSAK, M., MIDDLETON, J., RICHMOND, A., GRAHAM, G. J., SEGERER, S., NIBBS, R. J. B. & ROT, A. 2009. The Duffy antigen receptor for chemokines transports chemokines and supports their promigratory activity. *Nat Immunol*, 10, 101-8.
- RAFII, S., MOHLE, R., SHAPIRO, F., FREY, B. M. & MOORE, M. A. 1997. Regulation of hematopoiesis by microvascular endothelium. *Leuk Lymphoma*, 27, 375-86.
- RAJAGOPAL, S., KIM, J., AHN, S., CRAIG, S., LAM, C. M., GERARD, N. P., GERARD, C. & LEFKOWITZ, R. J. 2010. Beta-arrestin- but not G protein-mediated signaling by the "decoy" receptor CXCR7. *Proc Natl Acad Sci USA*, 107, 628-32.
- RAMAN, D., SOBOLIK-DELMARE, T. & RICHMOND, A. 2011. Chemokines in health and disease. *Exp Cell Res*, 317, 575-89.
- RANDOLPH, G. J., BEAULIEU, S., LEBECQUE, S., STEINMAN, R. M. & MULLER, W. A. 1998. Differentiation of monocytes into dendritic cells in a model of transendothelial trafficking. *Science*, 282, 480-3.
- RAPPERT, A., BIBER, K., NOLTE, C., LIPP, M., SCHUBEL, A., LU, B., GERARD, N. P., GERARD, C., BODDEKE, H. W. G. M. & KETTENMANN, H. 2002. Secondary lymphoid tissue chemokine (CCL21) activates CXCR3 to trigger a Cl-current and chemotaxis in murine microglia. *J Immunol*, 168, 3221-6.

- REIF, K., EKLAND, E. H., OHL, L., NAKANO, H., LIPP, M., FÖRSTER, R. & CYSTER, J. G. 2002. Balanced responsiveness to chemoattractants from adjacent zones determines B-cell position. *Nature*, 416, 94-9.
- RENNERT, P. D., BROWNING, J. L., MEBIUS, R., MACKAY, F. & HOCHMAN, P. S. 1996. Surface lymphotoxin alpha/beta complex is required for the development of peripheral lymphoid organs. *J Exp Med*, 184, 1999-2006.
- RICKERT, P., WEINER, O. D., WANG, F., BOURNE, H. R. & SERVANT, G. 2000. Leukocytes navigate by compass: roles of PI3Kgamma and its lipid products. *Trends Cell Biol*, 10, 466-73.
- RIVAS-CAICEDO, A., SOLDEVILA, G., FORTOUL, T. I., CASTELL-RODRÍGUEZ, A., FLORES-ROMO, L. & GARCÍA-ZEPEDA, E. A. 2009. Jak3 is involved in dendritic cell maturation and CCR7-dependent migration. *PLoS ONE*, 4, e7066.
- ROBERTS, C. W., SHUTTER, J. R. & KORSMEYER, S. J. 1994. Hox11 controls the genesis of the spleen. *Nature*, 368, 747-9.
- RODRÍGUEZ-FRADE, J. M., MELLADO, M. & MARTÍNEZ-A, C. 2001. Chemokine receptor dimerization: two are better than one. *Trends Immunol*, 22, 612-7.
- RODRÍGUEZ-FRADE, J. M., VILA-CORO, A. J., MARTÍN, A., NIETO, M., SÁNCHEZ-MADRID, F., PROUDFOOT, A. E., WELLS, T. N., MARTÍNEZ-A, C. & MELLADO, M. 1999. Similarities and differences in RANTES- and (AOP)-RANTES-triggered signals: implications for chemotaxis. *J Cell Biol*, 144, 755-65.
- ROGERS, W. J. & BASU, P. 2005. Factors regulating macrophage endocytosis of nanoparticles: implications for targeted magnetic resonance plaque imaging. *Atherosclerosis*, 178, 67-73.
- ROSSI, D. & ZLOTNIK, A. 2000. The biology of chemokines and their receptors. *Annu Rev Immunol*, 18, 217-42.
- ROSSI, D. L., VICARI, A. P., FRANZ-BACON, K., MCCLANAHAN, T. K. & ZLOTNIK, A. 1997. Identification through bioinformatics of two new macrophage proinflammatory human chemokines: MIP-3alpha and MIP-3beta. *J Immunol*, 158, 1033-6.
- ROT, A. 2005. Contribution of Duffy antigen to chemokine function. *Cytokine Growth Factor Rev*, 16, 687-94.
- SAINTE-MARIE, G. & PENG, F. S. 1986. Diffusion of a lymph-carried antigen in the fiber network of the lymph node of the rat. *Cell Tissue Res*, 245, 481-6.
- SALANGA, C. L. & HANDEL, T. M. 2011. Chemokine oligomerization and interactions with receptors and glycosaminoglycans: The role of structural dynamics in function. *Exp Cell Res*.
- SALLUSTO, F., LENIG, D., FÖRSTER, R., LIPP, M. & LANZAVECCHIA, A. 1999a. Two subsets of memory T lymphocytes with distinct homing potentials and effector functions. *Nature*, 401, 708-12.
- SALLUSTO, F., PALERMO, B., LENIG, D., MIETTINEN, M., MATIKAINEN, S., JULKUNEN, I., FORSTER, R., BURGSTHALER, R., LIPP, M. & LANZAVECCHIA, A. 1999b. Distinct patterns and kinetics of chemokine production regulate dendritic cell function. *Eur J Immunol*, 29, 1617-25.
- SALLUSTO, F., SCHAERLI, P., LOETSCHER, P., SCHANIEL, C., LENIG, D., MACKAY, C. R., QIN, S. & LANZAVECCHIA, A. 1998. Rapid and coordinated switch in chemokine receptor expression during dendritic cell maturation. *Eur J Immunol*, 28, 2760-9.
- SÁNCHEZ-SÁNCHEZ, N., RIOL-BLANCO, L. & RODRÍGUEZ-FERNÁNDEZ, J. L. 2006. The multiple personalities of the chemokine receptor CCR7 in dendritic cells. *J Immunol*, 176, 5153-9.
- SASAKI, K. & MATSUMURA, G. 1988. Spleen lymphocytes and haemopoiesis in the mouse embryo. *J Anat*, 160, 27-37.
- SCHEU, S., ALFERINK, J., PÖTZEL, T., BARCET, W., KALINKE, U. & PFEFFER, K. 2002. Targeted disruption of LIGHT causes defects in costimulatory T cell

- activation and reveals cooperation with lymphotoxin beta in mesenteric lymph node genesis. *J Exp Med*, 195, 1613-24.
- SCHUMANN, K., LÄMMERMANN, T., BRUCKNER, M., LEGLER, D. F., POLLEUX, J., SPATZ, J. P., SCHULER, G., FÖRSTER, R., LUTZ, M. B., SOROKIN, L. & SIXT, M. 2010. Immobilized chemokine fields and soluble chemokine gradients cooperatively shape migration patterns of dendritic cells. *Immunity*, 32, 703-13.
- SCHWAB, S. R. & CYSTER, J. G. 2007. Finding a way out: lymphocyte egress from lymphoid organs. *Nat Immunol*, 8, 1295-301.
- SCHWAB, S. R., PEREIRA, J. P., MATLOUBIAN, M., XU, Y., HUANG, Y. & CYSTER, J. G. 2005. Lymphocyte sequestration through S1P lyase inhibition and disruption of S1P gradients. *Science*, 309, 1735-9.
- SCHWARZ, B. A., SAMBANDAM, A., MAILLARD, I., HARMAN, B. C., LOVE, P. E. & BHANDoola, A. 2007. Selective thymus settling regulated by cytokine and chemokine receptors. *J Immunol*, 178, 2008-17.
- SCHWEICKART, V., EPP, A., RAPORT, C. & GRAY, P. 2001. CCR11 is a functional receptor for the monocyte chemoattractant protein family of chemokines. *J Biol Chem*, 276, 856.
- SCHWEICKART, V. L., EPP, A., RAPORT, C. J. & GRAY, P. W. 2000. CCR11 is a functional receptor for the monocyte chemoattractant protein family of chemokines. *J Biol Chem*, 275, 9550-6.
- SCHWEICKART, V. L., RAPORT, C. J., GODISKA, R., BYERS, M. G., EDDY, R. L., SHOWS, T. B. & GRAY, P. W. 1994. Cloning of human and mouse EB11, a lymphoid-specific G-protein-coupled receptor encoded on human chromosome 17q12-q21.2. *Genomics*, 23, 643-50.
- SCIMONE, M. L., AIFANTIS, I., APOSTOLOU, I., VON BOEHMER, H. & VON ANDRIAN, U. H. 2006. A multistep adhesion cascade for lymphoid progenitor cell homing to the thymus. *Proc Natl Acad Sci USA*, 103, 7006-11.
- SEVERIN, I. C., GAUDRY, J.-P., JOHNSON, Z., KUNGL, A., JANSMA, A., GESSLBAUER, B., MULLOY, B., POWER, C., PROUDFOOT, A. E. I. & HANDEL, T. 2010. Characterization of the chemokine CXCL11-heparin interaction suggests two different affinities for glycosaminoglycans. *J Biol Chem*, 285, 17713-24.
- SHEN, H., SCHUSTER, R., STRINGER, K. F., WALTZ, S. E. & LENTSCH, A. B. 2006. The Duffy antigen/receptor for chemokines (DARC) regulates prostate tumor growth. *FASEB J*, 20, 59-64.
- SHIELDS, J. D., FLEURY, M. E., YONG, C., TOMEI, A. A., RANDOLPH, G. J. & SWARTZ, M. A. 2007. Autologous chemotaxis as a mechanism of tumor cell homing to lymphatics via interstitial flow and autocrine CCR7 signaling. *Cancer Cell*, 11, 526-38.
- SIERRO, F., BIBEN, C., MARTÍNEZ-MUÑOZ, L., MELLADO, M., RANSOHOFF, R. M., LI, M., WOEHL, B., LEUNG, H., GROOM, J., BATTEN, M., HARVEY, R. P., MARTÍNEZ-A, C., MACKAY, C. R. & MACKAY, F. 2007. Disrupted cardiac development but normal hematopoiesis in mice deficient in the second CXCL12/SDF-1 receptor, CXCR7. *Proc Natl Acad Sci USA*, 104, 14759-64.
- SITNICKA, E., BRAKEBUSCH, C., MARTENSSON, I.-L., SVENSSON, M., AGACE, W. W., SIGVARDSSON, M., BUZA-VIDAS, N., BRYDER, D., CILIO, C. M., AHLENIUS, H., MARASKOVSKY, E., PESCHON, J. J. & JACOBSEN, S. E. W. 2003. Complementary signaling through flt3 and interleukin-7 receptor alpha is indispensable for fetal and adult B cell genesis. *J Exp Med*, 198, 1495-506.
- SITNICKA, E., BRYDER, D., THEILGAARD-MÖNCH, K., BUZA-VIDAS, N., ADOLFSSON, J. & JACOBSEN, S. E. W. 2002. Key role of flt3 ligand in regulation of the common lymphoid progenitor but not in maintenance of the hematopoietic stem cell pool. *Immunity*, 17, 463-72.

- SKELTON, N. J., QUAN, C., REILLY, D. & LOWMAN, H. 1999. Structure of a CXC chemokine-receptor fragment in complex with interleukin-8. *Structure*, 7, 157-68.
- SMITH, H., CHEN, I. M., KUBO, R. & TUNG, K. S. 1989. Neonatal thymectomy results in a repertoire enriched in T cells deleted in adult thymus. *Science*, 245, 749-52.
- SOEHNLEIN, O. & LINDBOM, L. 2010. Phagocyte partnership during the onset and resolution of inflammation. *Nat Rev Immunol*, 10, 427-39.
- SOEHNLEIN, O., LINDBOM, L. & WEBER, C. 2009. Mechanisms underlying neutrophil-mediated monocyte recruitment. *Blood*, 114, 4613-23.
- SORIANO, S. F., HERNANZ-FALCÓN, P., RODRÍGUEZ-FRADE, J. M., DE ANA, A. M., GARZÓN, R., CARVALHO-PINTO, C., VILA-CORO, A. J., ZABALLOS, A., BALOMENOS, D., MARTÍNEZ-A, C. & MELLADO, M. 2002. Functional inactivation of CXC chemokine receptor 4-mediated responses through SOCS3 up-regulation. *J Exp Med*, 196, 311-21.
- SORIANO, S. F., SERRANO, A., HERNANZ-FALCÓN, P., MARTÍN DE ANA, A., MONTEERRUBIO, M., MARTÍNEZ, C., RODRÍGUEZ-FRADE, J. M. & MELLADO, M. 2003. Chemokines integrate JAK/STAT and G-protein pathways during chemotaxis and calcium flux responses. *Eur J Immunol*, 33, 1328-33.
- SOTO, H., WANG, W., STRIETER, R. M., COPELAND, N. G., GILBERT, D. J., JENKINS, N. A., HEDRICK, J. & ZLOTNIK, A. 1998. The CC chemokine 6Ckine binds the CXC chemokine receptor CXCR3. *Proc Natl Acad Sci USA*, 95, 8205-10.
- SOTSIOS, Y., WHITTAKER, G. C., WESTWICK, J. & WARD, S. G. 1999. The CXC chemokine stromal cell-derived factor activates a Gi-coupled phosphoinositide 3-kinase in T lymphocytes. *J Immunol*, 163, 5954-63.
- SOZZANI, S., ALLAVENA, P., VECCHI, A. & MANTOVANI, A. 2000. Chemokines and dendritic cell traffic. *J Clin Immunol*, 20, 151-60.
- SOZZANI, S., SALLUSTO, F., LUINI, W., ZHOU, D., PIEMONTE, L., ALLAVENA, P., VAN DAMME, J., VALITUTTI, S., LANZAVECCHIA, A. & MANTOVANI, A. 1995. Migration of dendritic cells in response to formyl peptides, C5a, and a distinct set of chemokines. *J Immunol*, 155, 3292-5.
- STALL, A. M., ADAMS, S., HERZENBERG, L. A. & KANTOR, A. B. 1992. Characteristics and development of the murine B-1b (Ly-1 B sister) cell population. *Ann N Y Acad Sci*, 651, 33-43.
- STEIN, J. V., ROT, A., LUO, Y., NARASIMHASWAMY, M., NAKANO, H., GUNN, M. D., MATSUZAWA, A., QUACKENBUSH, E. J., DORF, M. E. & VON ANDRIAN, U. H. 2000. The CC chemokine thymus-derived chemotactic agent 4 (TCA-4, secondary lymphoid tissue chemokine, 6Ckine, exodus-2) triggers lymphocyte function-associated antigen 1-mediated arrest of rolling T lymphocytes in peripheral lymph node high endothelial venules. *J Exp Med*, 191, 61-76.
- STEIN, J. V., SORIANO, S. F., M'RINI, C., NOMBELA-ARRIETA, C., DE BUITRAGO, G. G., RODRÍGUEZ-FRADE, J. M., MELLADO, M., GIRARD, J.-P. & MARTÍNEZ-A, C. 2003. CCR7-mediated physiological lymphocyte homing involves activation of a tyrosine kinase pathway. *Blood*, 101, 38-44.
- STEINMAN, R. M., HAWIGER, D. & NUSSENZWEIG, M. C. 2003. Tolerogenic dendritic cells. *Annu Rev Immunol*, 21, 685-711.
- STEINMAN, R. M. & NUSSENZWEIG, M. C. 2002. Avoiding horror autotoxicus: the importance of dendritic cells in peripheral T cell tolerance. *Proc Natl Acad Sci USA*, 99, 351-8.
- STENBÄCK, F. 1978. Tumor persistence and regression in skin carcinogenesis. *Journal of Cancer Research and Clinical Oncology*.
- STENSTAD, H., ERICSSON, A., JOHANSSON-LINDBOM, B., SVENSSON, M., MARSAL, J., MACK, M., PICARELLA, D., SOLER, D., MARQUEZ, G., BRISKIN, M. & AGACE, W. W. 2006. Gut-associated lymphoid tissue-primed CD4+ T cells display CCR9-dependent and -independent homing to the small intestine. *Blood*, 107, 3447-54.

- STREETER, P. R., BERG, E. L., ROUSE, B. T., BARGATZE, R. F. & BUTCHER, E. C. 1988a. A tissue-specific endothelial cell molecule involved in lymphocyte homing. *Nature*, 331, 41-6.
- STREETER, P. R., ROUSE, B. T. & BUTCHER, E. C. 1988b. Immunohistologic and functional characterization of a vascular addressin involved in lymphocyte homing into peripheral lymph nodes. *J Cell Biol*, 107, 1853-62.
- SUN, Z., UNUTMAZ, D., ZOU, Y. R., SUNSHINE, M. J., PIERANI, A., BRENNER-MORTON, S., MEBIUS, R. E. & LITTMAN, D. R. 2000. Requirement for ROR γ in thymocyte survival and lymphoid organ development. *Science*, 288, 2369-73.
- SVENSSON, M., MARSAL, J., ERICSSON, A., CARRAMOLINO, L., BRODÉN, T., MÁRQUEZ, G. & AGACE, W. W. 2002. CCL25 mediates the localization of recently activated CD8 α beta(+) lymphocytes to the small-intestinal mucosa. *J Clin Invest*, 110, 1113-21.
- SVENSSON, M., MARSAL, J., URONEN-HANSSON, H., CHENG, M., JENKINSON, W., CILIO, C., JACOBSEN, S. E. W., SITNICKA, E., ANDERSON, G. & AGACE, W. W. 2008. Involvement of CCR9 at multiple stages of adult T lymphopoiesis. *J Leukoc Biol*, 83, 156-64.
- SZAKAL, A. K., HOLMES, K. L. & TEW, J. G. 1983. Transport of immune complexes from the subcapsular sinus to lymph node follicles on the surface of nonphagocytic cells, including cells with dendritic morphology. *J Immunol*, 131, 1714-27.
- SZANYA, V., ERMANN, J., TAYLOR, C., HOLNESS, C. & FATHMAN, C. G. 2002. The subpopulation of CD4+CD25+ splenocytes that delays adoptive transfer of diabetes expresses L-selectin and high levels of CCR7. *J Immunol*, 169, 2461-5.
- TACHIBANA, K., HIROTA, S., IIZASA, H., YOSHIDA, H., KAWABATA, K., KATAOKA, Y., KITAMURA, Y., MATSUSHIMA, K., YOSHIDA, N., NISHIKAWA, S., KISHIMOTO, T. & NAGASAWA, T. 1998. The chemokine receptor CXCR4 is essential for vascularization of the gastrointestinal tract. *Nature*, 393, 591-4.
- TAICHMAN, R. S. & EMERSON, S. G. 1998. The role of osteoblasts in the hematopoietic microenvironment. *Stem Cells*, 16, 7-15.
- TAKATSUKA, S., SEKIGUCHI, A., TOKUNAGA, M., FUJIMOTO, A. & CHIBA, J. 2010. Generation of a panel of monoclonal antibodies against atypical chemokine receptor CCX-CKR by DNA immunization. *Journal of pharmacological and toxicological methods*.
- TAN, W., MARTIN, D. & GUTKIND, J. S. 2006. The Galpha13-Rho signaling axis is required for SDF-1-induced migration through CXCR4. *J Biol Chem*, 281, 39542-9.
- TANABE, S., LU, Z., LUO, Y., QUACKENBUSH, E. J., BERMAN, M. A., COLLINS-RACIE, L. A., MI, S., REILLY, C., LO, D., JACOBS, K. A. & DORF, M. E. 1997. Identification of a new mouse beta-chemokine, thymus-derived chemotactic agent 4, with activity on T lymphocytes and mesangial cells. *J Immunol*, 159, 5671-9.
- TANG, M. L., STEEBER, D. A., ZHANG, X. Q. & TEDDER, T. F. 1998. Intrinsic differences in L-selectin expression levels affect T and B lymphocyte subset-specific recirculation pathways. *J Immunol*, 160, 5113-21.
- TESTER, A. M., COX, J. H., CONNOR, A. R., STARR, A. E., DEAN, R. A., PUENTE, X. S., LÓPEZ-OTÍN, C. & OVERALL, C. M. 2007. LPS responsiveness and neutrophil chemotaxis in vivo require PMN MMP-8 activity. *PLoS ONE*, 2, e312.
- THELEN, M., MUÑOZ, L. M., RODRÍGUEZ-FRADE, J. M. & MELLADO, M. 2010. Chemokine receptor oligomerization: functional considerations. *Curr Opin Pharmacol*, 10, 38-43.
- THOMPSON, B. D., JIN, Y., WU, K. H., COLVIN, R. A., LUSTER, A. D., BIRNBAUMER, L. & WU, M. X. 2007. Inhibition of G α i2 activation by G α i3 in CXCR3-mediated signaling. *J Biol Chem*, 282, 9547-55.

- THOMSEN, P., ROEPSTORFF, K., STAHLHUT, M. & VAN DEURS, B. 2002. Caveolae are highly immobile plasma membrane microdomains, which are not involved in constitutive endocytic trafficking. *Mol Biol Cell*, 13, 238-50.
- TIEGS, S. L., RUSSELL, D. M. & NEMAZEE, D. 1993. Receptor editing in self-reactive bone marrow B cells. *J Exp Med*, 177, 1009-20.
- TOWNSON, J. R. & NIBBS, R. J. B. 2002. Characterization of mouse CCX-CKR, a receptor for the lymphocyte-attracting chemokines TECK/mCCL25, SLC/mCCL21 and MIP-3beta/mCCL19: comparison to human CCX-CKR. *Eur J Immunol*, 32, 1230-41.
- TUMANG, J. R., HASTINGS, W. D., BAI, C. & ROTHSTEIN, T. L. 2004. Peritoneal and splenic B-1 cells are separable by phenotypic, functional, and transcriptomic characteristics. *Eur J Immunol*, 34, 2158-67.
- UENO, H. & WEISSMAN, I. L. 2010. The origin and fate of yolk sac hematopoiesis: application of chimera analyses to developmental studies. *Int J Dev Biol*, 54, 1019-31.
- UENO, T., HARA, K., WILLIS, M. S., MALIN, M. A., HÖPKEN, U. E., GRAY, D. H. D., MATSUSHIMA, K., LIPP, M., SPRINGER, T. A., BOYD, R. L., YOSHIE, O. & TAKAHAMA, Y. 2002. Role for CCR7 ligands in the emigration of newly generated T lymphocytes from the neonatal thymus. *Immunity*, 16, 205-18.
- UENO, T., SAITO, F., GRAY, D. H. D., KUSE, S., HIESHIMA, K., NAKANO, H., KAKIUCHI, T., LIPP, M., BOYD, R. L. & TAKAHAMA, Y. 2004. CCR7 signals are essential for cortex-medulla migration of developing thymocytes. *J Exp Med*, 200, 493-505.
- VAN DAMME, J., STRUYF, S., WUYTS, A., VAN COILLIE, E., MENTEN, P., SCHOLS, D., SOZZANI, S., DE MEESTER, I. & PROOST, P. 1999. The role of CD26/DPP IV in chemokine processing. *Chem Immunol*, 72, 42-56.
- VAN DE PAVERT, S. A. & MEBIUS, R. E. 2010. New insights into the development of lymphoid tissues. *Nat Rev Immunol*, 10, 664-74.
- VAN DE PAVERT, S. A., OLIVIER, B. J., GOVERSE, G., VONDENHOFF, M. F., GREUTER, M., BEKE, P., KUSSER, K., HÖPKEN, U. E., LIPP, M., NIEDERREITHER, K., BLOMHOFF, R., SITNIK, K., AGACE, W. W., RANDALL, T. D., DE JONGE, W. J. & MEBIUS, R. E. 2009. Chemokine CXCL13 is essential for lymph node initiation and is induced by retinoic acid and neuronal stimulation. *Nat Immunol*, 10, 1193-9.
- VAN DEN STEEN, P. E., PROOST, P., WUYTS, A., VAN DAMME, J. & OPDENAKKER, G. 2000. Neutrophil gelatinase B potentiates interleukin-8 tenfold by aminoterminal processing, whereas it degrades CTAP-III, PF-4, and GRO-alpha and leaves RANTES and MCP-2 intact. *Blood*, 96, 2673-81.
- VAN WEERING, H. R. J., DE JONG, A. P. H., DE HAAS, A. H., BIBER, K. P. H. & BODDEKE, H. W. G. M. 2010. CCL21-induced calcium transients and proliferation in primary mouse astrocytes: CXCR3-dependent and independent responses. *Brain Behav Immun*, 24, 768-75.
- VASSILEVA, G., SOTO, H., ZLOTNIK, A., NAKANO, H., KAKIUCHI, T., HEDRICK, J. A. & LIRA, S. A. 1999. The reduced expression of 6Ckine in the plt mouse results from the deletion of one of two 6Ckine genes. *J Exp Med*, 190, 1183-8.
- VEIGA-FERNANDES, H., COLES, M. C., FOSTER, K. E., PATEL, A., WILLIAMS, A., NATARAJAN, D., BARLOW, A., PACHNIS, V. & KIOUSSIS, D. 2007. Tyrosine kinase receptor RET is a key regulator of Peyer's patch organogenesis. *Nature*, 446, 547-51.
- VERMI, W., RIBOLDI, E., WITTAMER, V., GENTILI, F., LUINI, W., MARRELLI, S., VECCHI, A., FRANSSSEN, J.-D., COMMUNI, D., MASSARDI, L., SIRONI, M., MANTOVANI, A., PARMENTIER, M., FACCHETTI, F. & SOZZANI, S. 2005. Role of ChemR23 in directing the migration of myeloid and plasmacytoid dendritic cells to lymphoid organs and inflamed skin. *J Exp Med*, 201, 509-15.

- VETRANO, S., BORRONI, E. M., SARUKHAN, A., SAVINO, B., BONECCHI, R., CORREALE, C., ARENA, V., FANTINI, M., RONCALLI, M., MALESCI, A., MANTOVANI, A., LOCATI, M. & DANESE, S. 2010. The lymphatic system controls intestinal inflammation and inflammation-associated Colon Cancer through the chemokine decoy receptor D6. *Gut*, 59, 197-206.
- VICARI, A. P., FIGUEROA, D. J., HEDRICK, J. A., FOSTER, J. S., SINGH, K. P., MENON, S., COPELAND, N. G., GILBERT, D. J., JENKINS, N. A., BACON, K. B. & ZLOTNIK, A. 1997. TECK: a novel CC chemokine specifically expressed by thymic dendritic cells and potentially involved in T cell development. *Immunity*, 7, 291-301.
- VIGNALI, D. A. A., COLLISON, L. W. & WORKMAN, C. J. 2008. How regulatory T cells work. *Nat Rev Immunol*, 8, 523-32.
- VILA-CORO, A. J., RODRÍGUEZ-FRADE, J. M., MARTÍN DE ANA, A., MORENO-ORTÍZ, M. C., MARTÍNEZ-A, C. & MELLADO, M. 1999. The chemokine SDF-1alpha triggers CXCR4 receptor dimerization and activates the JAK/STAT pathway. *FASEB J*, 13, 1699-710.
- VON ANDRIAN, U. H. & MEMPEL, T. R. 2003. Homing and cellular traffic in lymph nodes. *Nat Rev Immunol*, 3, 867-78.
- VONDENHOFF, M. F., GREUTER, M., GOVERSE, G., ELEWAUT, D., DEWINT, P., WARE, C. F., HOORWEG, K., KRAAL, G. & MEBIUS, R. E. 2009. LTbetaR signaling induces cytokine expression and up-regulates lymphangiogenic factors in lymph node anlagen. *J Immunol*, 182, 5439-45.
- VROON, A., HEIJNEN, C. J. & KAVELAARS, A. 2006. GRKs and arrestins: regulators of migration and inflammation. *J Leukoc Biol*, 80, 1214-21.
- WAGNER, N., LÖHLER, J., KUNKEL, E. J., LEY, K., LEUNG, E., KRISSENSSEN, G., RAJEWSKY, K. & MÜLLER, W. 1996. Critical role for beta7 integrins in formation of the gut-associated lymphoid tissue. *Nature*, 382, 366-70.
- WANG, J., XI, L., GOODING, W., GODFREY, T. E. & FERRIS, R. L. 2005a. Chemokine receptors 6 and 7 identify a metastatic expression pattern in squamous cell carcinoma of the head and neck. *Adv Otorhinolaryngol*, 62, 121-33.
- WANG, L., FUSTER, M., SRIRAMARAO, P. & ESKO, J. D. 2005b. Endothelial heparan sulfate deficiency impairs L-selectin- and chemokine-mediated neutrophil trafficking during inflammatory responses. *Nat Immunol*, 6, 902-10.
- WARDEMANN, H., BOEHM, T., DEAR, N. & CARSETTI, R. 2002. B-1a B cells that link the innate and adaptive immune responses are lacking in the absence of the spleen. *J Exp Med*, 195, 771-80.
- WEBER, M., BLAIR, E., SIMPSON, C. V., O'HARA, M., BLACKBURN, P. E., ROT, A., GRAHAM, G. J. & NIBBS, R. J. B. 2004. The chemokine receptor D6 constitutively traffics to and from the cell surface to internalize and degrade chemokines. *Mol Biol Cell*, 15, 2492-508.
- WELLER, S., BRAUN, M. C., TAN, B. K., ROSENWALD, A., CORDIER, C., CONLEY, M. E., PLEBANI, A., KUMARARATNE, D. S., BONNET, D., TOURNILHAC, O., TCHERNIA, G., STEINIGER, B., STAUDT, L. M., CASANOVA, J.-L., REYNAUD, C.-A. & WEILL, J.-C. 2004. Human blood IgM "memory" B cells are circulating splenic marginal zone B cells harboring a prediversified immunoglobulin repertoire. *Blood*, 104, 3647-54.
- WENDLAND, M., CZELOTH, N., MACH, N., MALISSEN, B., KREMMER, E., PABST, O. & FÖRSTER, R. 2007. CCR9 is a homing receptor for plasmacytoid dendritic cells to the small intestine. *Proc Natl Acad Sci USA*, 104, 6347-52.
- WENINGER, W. & VON ANDRIAN, U. H. 2003. Chemokine regulation of naïve T cell traffic in health and disease. *Semin Immunol*, 15, 257-70.
- WHITEHEAD, G. S., WANG, T., DEGRAFF, L. M., CARD, J. W., LIRA, S. A., GRAHAM, G. J. & COOK, D. N. 2007. The chemokine receptor D6 has opposing

- effects on allergic inflammation and airway reactivity. *Am J Respir Crit Care Med*, 175, 243-9.
- WIGLE, J. T. & OLIVER, G. 1999. Prox1 function is required for the development of the murine lymphatic system. *Cell*, 98, 769-78.
- WILKINSON, B., OWEN, J. J. & JENKINSON, E. J. 1999. Factors regulating stem cell recruitment to the fetal thymus. *J Immunol*, 162, 3873-81.
- WILLIMANN, K., LEGLER, D. F., LOETSCHER, M., ROOS, R. S., DELGADO, M. B., CLARK-LEWIS, I., BAGGIOLINI, M. & MOSER, B. 1998. The chemokine SLC is expressed in T cell areas of lymph nodes and mucosal lymphoid tissues and attracts activated T cells via CCR7. *Eur J Immunol*, 28, 2025-34.
- WILSON, N. S., EL-SUKKARI, D., BELZ, G. T., SMITH, C. M., STEPTOE, R. J., HEATH, W. R., SHORTMAN, K. & VILLADANGOS, J. A. 2003. Most lymphoid organ dendritic cell types are phenotypically and functionally immature. *Blood*, 102, 2187-94.
- WITT, D. P. & LANDER, A. D. 1994. Differential binding of chemokines to glycosaminoglycan subpopulations. *Curr Biol*, 4, 394-400.
- WOLFE, B. L. & TREJO, J. 2007. Clathrin-dependent mechanisms of G protein-coupled receptor endocytosis. *Traffic*, 8, 462-70.
- WONG, M. & FISH, E. N. 1998. RANTES and MIP-1alpha activate stats in T cells. *J Biol Chem*, 273, 309-14.
- WONG, M., UDDIN, S., MAJCHRZAK, B., HUYNH, T., PROUDFOOT, A. E., PLATANIAS, L. C. & FISH, E. N. 2001. Rantes activates Jak2 and Jak3 to regulate engagement of multiple signaling pathways in T cells. *J Biol Chem*, 276, 11427-31.
- WORBS, T., BODE, U., YAN, S., HOFFMANN, M. W., HINTZEN, G., BERNHARDT, G., FÖRSTER, R. & PABST, O. 2006. Oral tolerance originates in the intestinal immune system and relies on antigen carriage by dendritic cells. *J Exp Med*, 203, 519-27.
- WORBS, T. & FÖRSTER, R. 2007. A key role for CCR7 in establishing central and peripheral tolerance. *Trends Immunol*, 28, 274-80.
- WORBS, T., MEMPEL, T. R., BÖLTER, J., VON ANDRIAN, U. H. & FÖRSTER, R. 2007. CCR7 ligands stimulate the intranodal motility of T lymphocytes in vivo. *J Exp Med*, 204, 489-95.
- WORKMAN, C. J., SZYMCZAK-WORKMAN, A. L., COLLISON, L. W., PILLAI, M. R. & VIGNALI, D. A. A. 2009. The development and function of regulatory T cells. *Cell Mol Life Sci*, 66, 2603-22.
- WURBEL, M.-A., MALISSEN, B. & CAMPBELL, J. J. 2006. Complex regulation of CCR9 at multiple discrete stages of T cell development. *Eur J Immunol*, 36, 73-81.
- XANTHOU, G., DUCHESNES, C. E., WILLIAMS, T. J. & PEASE, J. E. 2003. CCR3 functional responses are regulated by both CXCR3 and its ligands CXCL9, CXCL10 and CXCL11. *Eur J Immunol*, 33, 2241-50.
- YAMADA, M., KUBO, H., KOBAYASHI, S., ISHIZAWA, K., HE, M., SUZUKI, T., FUJINO, N., KUNISHIMA, H., HATTA, M., NISHIMAKI, K., AOYAGI, T., TOKUDA, K., KITAGAWA, M., YANO, H., TAMAMURA, H., FUJII, N. & KAKU, M. 2011. The increase in surface CXCR4 expression on lung extravascular neutrophils and its effects on neutrophils during endotoxin-induced lung injury. *Cell Mol Immunol*.
- YANAGAWA, Y. & ONOÉ, K. 2002. CCL19 induces rapid dendritic extension of murine dendritic cells. *Blood*, 100, 1948-56.
- YANAGAWA, Y. & ONOÉ, K. 2003. CCR7 ligands induce rapid endocytosis in mature dendritic cells with concomitant up-regulation of Cdc42 and Rac activities. *Blood*, 101, 4923-9.
- YOSHIDA, H., NAITO, A., INOUE, J.-I., SATOH, M., SANTEE-COOPER, S. M., WARE, C. F., TOGAWA, A., NISHIKAWA, S. & NISHIKAWA, S.-I. 2002.

- Different cytokines induce surface lymphotoxin-alpha on IL-7 receptor-alpha cells that differentially engender lymph nodes and Peyer's patches. *Immunity*, 17, 823-33.
- YOSHIDA, R., IMAI, T., HIESHIMA, K., KUSUDA, J., BABA, M., KITaura, M., NISHIMURA, M., KAKIZAKI, M., NOMIYAMA, H. & YOSHIE, O. 1997. Molecular cloning of a novel human CC chemokine EBI1-ligand chemokine that is a specific functional ligand for EBI1, CCR7. *J Biol Chem*, 272, 13803-9.
- YOSHIDA, R., NAGIRA, M., KITaura, M., IMAGAWA, N., IMAI, T. & YOSHIE, O. 1998. Secondary lymphoid-tissue chemokine is a functional ligand for the CC chemokine receptor CCR7. *J Biol Chem*, 273, 7118-22.
- YOSHIDA, T., IMAI, T., KAKIZAKI, M., NISHIMURA, M. & YOSHIE, O. 1995. Molecular cloning of a novel C or gamma type chemokine, SCM-1. *FEBS Lett*, 360, 155-9.
- ZABALLOS, A., GUTIÉRREZ, J., VARONA, R., ARDAVÍN, C. & MÁRQUEZ, G. 1999. Cutting edge: identification of the orphan chemokine receptor GPR-9-6 as CCR9, the receptor for the chemokine TECK. *J Immunol*, 162, 5671-5.
- ZABEL, B. A., AGACE, W. W., CAMPBELL, J. J., HEATH, H. M., PARENT, D., ROBERTS, A. I., EBERT, E. C., KASSAM, N., QIN, S., ZOVKO, M., LAROSA, G. J., YANG, L. L., SOLER, D., BUTCHER, E. C., PONATH, P. D., PARKER, C. M. & ANDREW, D. P. 1999. Human G protein-coupled receptor GPR-9-6/CC chemokine receptor 9 is selectively expressed on intestinal homing T lymphocytes, mucosal lymphocytes, and thymocytes and is required for thymus-expressed chemokine-mediated chemotaxis. *J Exp Med*, 190, 1241-56.
- ZABEL, B. A., NAKAE, S., ZÚÑIGA, L., KIM, J.-Y., OHYAMA, T., ALT, C., PAN, J., SUTO, H., SOLER, D., ALLEN, S. J., HANDEL, T. M., SONG, C. H., GALLI, S. J. & BUTCHER, E. C. 2008. Mast cell-expressed orphan receptor CCRL2 binds chemerin and is required for optimal induction of IgE-mediated passive cutaneous anaphylaxis. *J Exp Med*, 205, 2207-20.
- ZABEL, B. A., SILVERIO, A. M. & BUTCHER, E. C. 2005. Chemokine-like receptor 1 expression and chemerin-directed chemotaxis distinguish plasmacytoid from myeloid dendritic cells in human blood. *J Immunol*, 174, 244-51.
- ZABEL, B. A., WANG, Y., LEWÉN, S., BERAHOVICH, R. D., PENFOLD, M. E. T., ZHANG, P., POWERS, J., SUMMERS, B. C., MIAO, Z., ZHAO, B., JALILI, A., JANOWSKA-WIECZOREK, A., JAEN, J. C. & SCHALL, T. J. 2009. Elucidation of CXCR7-mediated signaling events and inhibition of CXCR4-mediated tumor cell transendothelial migration by CXCR7 ligands. *J Immunol*, 183, 3204-11.
- ZARBOCK, A., BISHOP, J., MÜLLER, H., SCHMOLKE, M., BUSCHMANN, K., VAN AKEN, H. & SINGBARTL, K. 2010. Chemokine homeostasis vs. chemokine presentation during severe acute lung injury: the other side of the Duffy antigen receptor for chemokines. *Am J Physiol Lung Cell Mol Physiol*, 298, L462-71.
- ZARBOCK, A., SCHMOLKE, M., BOCKHORN, S. G., SCHARTE, M., BUSCHMANN, K., LEY, K. & SINGBARTL, K. 2007. The Duffy antigen receptor for chemokines in acute renal failure: A facilitator of renal chemokine presentation. *Crit Care Med*, 35, 2156-63.
- ZHANG, J., NIU, C., YE, L., HUANG, H., HE, X., TONG, W.-G., ROSS, J., HAUG, J., JOHNSON, T., FENG, J. Q., HARRIS, S., WIEDEMANN, L. M., MISHINA, Y. & LI, L. 2003. Identification of the haematopoietic stem cell niche and control of the niche size. *Nature*, 425, 836-41.
- ZHANG, X. F., WANG, J. F., MATCZAK, E., PROPER, J. A. & GROOPMAN, J. E. 2001. Janus kinase 2 is involved in stromal cell-derived factor-1alpha-induced tyrosine phosphorylation of focal adhesion proteins and migration of hematopoietic progenitor cells. *Blood*, 97, 3342-8.
- ZLOTNIK, A. 2006. Chemokines and cancer. *Int J Cancer*, 119, 2026-9.

- ZLOTOFF, D. A., SAMBANDAM, A., LOGAN, T. D., BELL, J. J., SCHWARZ, B. A. & BHANDoola, A. 2010. CCR7 and CCR9 together recruit hematopoietic progenitors to the adult thymus. *Blood*, 115, 1897-905.
- ZOU, Y. R., KOTTMANN, A. H., KURODA, M., TANIUCHI, I. & LITTMAN, D. R. 1998. Function of the chemokine receptor CXCR4 in haematopoiesis and in cerebellar development. *Nature*, 393, 595-9.